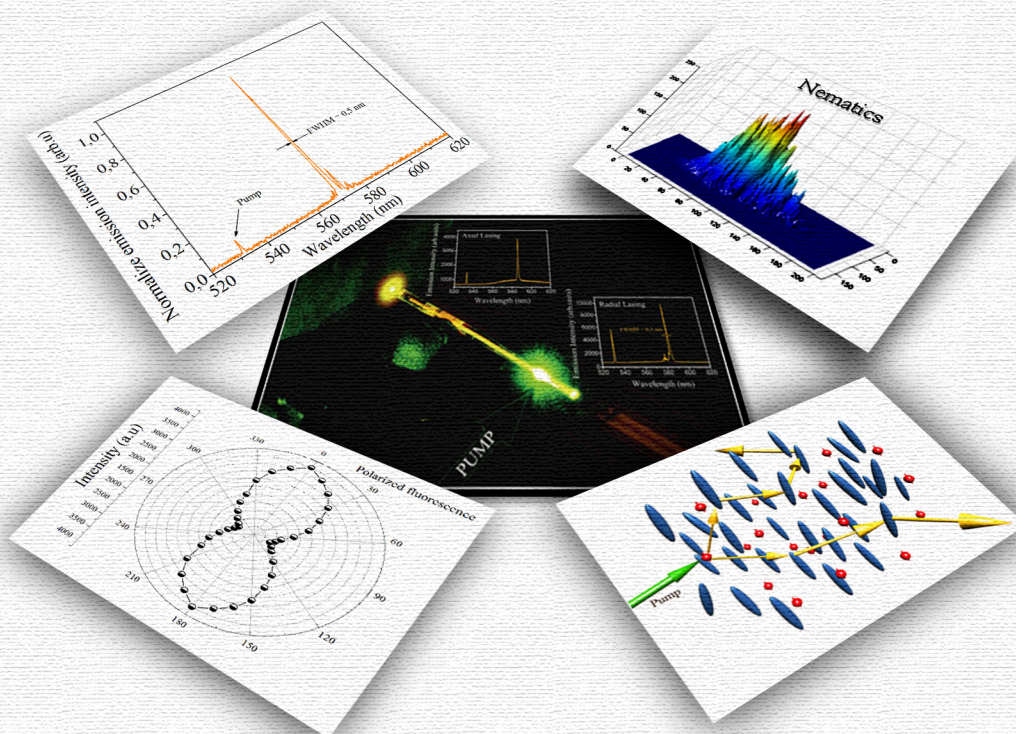Università della Calabria Italy

University Tunis El Manar Tunisia

Science and Technologies of Mesophases and Molecular Materials
STM3 – International Doctorate – XX Cycle

Joint Thesis

Laser Action in Liquid Crystals: from Random to Periodic Systems

Dr. Ferjani Sameh

Supervisor: G. Strangi

Supervisor: A. Gharbi

Coordinator: C. Versace

A.A 2006-2007

University of Calabria - Italy   University Tunis El Manar - Tunisia

Science and Technologies of Mesophases and Molecular Materials
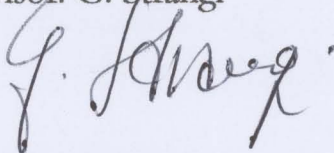
STM^3 – International Doctorate – XX Cycle

Thesis in "cotutelle"

Laser Action in Liquid Crystals: from Random to Periodic Systems

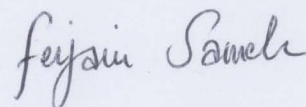Settore disciplinare: FISICA DELLA MATERIA

Supervisor: G. Strangi   Supervisor: A. Gharbi

Coordinator: C. Versace   Candidate: S. Ferjani

Approved by:
Prof. Giancarlo Abbate
Prof. Raouf Ben Naceur
Prof. Lorenzo Marrucci
Prof. Noureddine Meskini

A.A 2006- 2007

To my self

To my mother and my father

To Karim , Mounir and Moetez

To my sister , her husband and her son

To all my teachers and my friends

Acknowledgments

Ritengo molto difficile citare tutte le persone che hanno fatto parte sia della mia vita scientifica che della mia vita sociale durante questi ultimi tre anni e che mi hanno aiutato a portare avanti questo lavoro. Sentiti e doverosi ringraziamenti vanno al mio supervisore Giuseppe Strangi per la sua continua disponibilità sia sul piano scientifico che umano, oltre che per la pazienza dimostrata sopportandomi per tre lunghi anni nel quale mi ha trasmesso tanto entusiasmo e anche tantissime conoscenza in questo campo. Per quanto riguarda i miei colleghi e compagni di lavoro vorrei ringraziare in particolare Valentin Barna, Antonio de Luca, Roberto Caputo e i professori Carlo Versace, Roberto Bartolino e Nicola Scaramazza per il loro supporto scientifico e non vorrei dimenticare i miei compagni di scrivania Stefano d'Elia e Carlo Vena. Continuo con i collaboratori e vorrei ringraziare Luca Sorriso con cui è stata svolta la parte statistica di questo lavoro.

Devo ringraziare anche il dott. Alfredo Pane e sig. Bruno de Nardo per il loro aiuto tecnico e ovviamente ringrazio tutto il resto del gruppo LiCryL.

La mia profonda riconoscenza va anche ai miei cari amici Luigia Pezzi, Luciano de Sio, Alessandro Veltri e Salvatore Marino; in primo luogo per l'aiuto offertomi nell' apprendimento della lingua italiana come primi maestri (e che maestri!!!! Dopo 3 anni non parlo bene l'italiano ma il calabrese si ☺) , Ale sapevo cosa è il delfino anche prima di venire in Italia ☺) e, in secondo luogo, per l'amicizia e l'affetto da loro ricevuto durante la mia permanenza(anche se da te Luciano speravo di più ma abbiamo ancora tempo☺).

Il mio profondo rispetto e ringraziamento vanno al Prof Longeri e sua moglie per la loro accoglienza e l'affetto che mi hanno dato dal mio primo giorno (31 settembre 2004) sul territorio Italiano fino ad ora.

Poi c'è tutto il GMI, in particolare le mie amichette Ella e Rosa (Rosa pensaci bene io sono sempre pronta☺), che meriterebbe di essere ringraziato, con il quale ho condiviso tutti i miei momenti, belli e anche brutti. A questo punto la lista si allunga col ringraziare

Corriamo dei rischi non per fuggire alla vita, bensì per impedirle di fuggire da noi (Sergio Barbarèn. *Max*)

Contents

Introduction

Recently laser is considered as an essential tool in our society. It have found widespread use as well on daily basis, for example in compact disc (CD) and digital versatile disc (DVD) players, as in industry, telecommunications and medicine where the laser is used for high precision surgery. This is why this particular field of physics is being nowadays privileged and it attracted a great interesting in both practical and fundamental point of view and why the ongoing developments in nanotechnology have led to the quest for nanolasers. In a laser, the light is generated by the combination of light amplification by stimulated emission and optical feedback. It has been demonstrated in a variety of materials and more recently the interest has been devoted to organic materials where intensive studies on one- and two-dimensional band-gap materials have been performed. In a one-dimensional (1D) periodic structure, laser action has been demonstrated at the edge of the photonic band-gap, where the photon group velocity approaches zero. Lasing has been explained through the phenomena of distributed feedback. These distributed feedback laser are highly compact because they do not require the use of a mirror cavity to operate. This possibility has been recently exploited with success by different research groups using these organic materials. Several advantages arise from the combination of responsive soft materials and gain media, such as low threshold lasing, tunability, well defined wavelength and directionality. The first part of the research activity performed during the doctoral studies was dedicated to photonic band gap soft materials. A later important phase focused on the experimental investigations of random lasing in partially disordered liquid crystals.

Multiple scattering is invoked as the main responsible for lasing in these systems because its ability to increases the dwell time, or path length, of light inside the gain

medium, enhancing light amplification. Even in this scenario, we no longer need mirrors to trap the light in the gain medium like in regular lasers since scattering can do the job on its own. Since strong light scattering usually occurs in highly disordered media, the word "random" has been used to describe lasers that operate on the basis of these properties.

This thesis explores lasing in liquid crystals from periodic to random, by studying their emission light properties as function several external stimuli and constraints (temperature, geometries, electric and magnetic field etc..). This topics are discussed individually in the following chapters.

Chapter I is an introduction to liquid crystals and some of their main physical properties. In the last part of this chapter a definition of fluorescence and mirror-less laser has been reported.

In chapter II is discussed the propagation and the emission of light in periodic and disordered scattering media. It presents the main physic concepts which govern lasing both in ordered media such as periodic photonic band gap structures and disordered systems which manifest Anderson localization and enhanced back scattering.

The chapter III reports the experimental investigations about the confinement and emission of dye doped chiral liquid crystals in capillary tubes. The light emission properties in such system behave as a fiber-like multidirectional distributed feedback laser. The experiments performed for this confining geometry show that laser action is exhibited both axially and radially, indicating a self-organized three-dimensional blue phase-like configuration. The thermal behavior shows wavelength tunability for both orientations emphasizing two different linear behaviors. The distributed feedback mechanism and the Q factor of the mirrorless resonant cavity result enhanced for axial stimulated emission because of the significant increase in the number of helical periods. In addition, long-lived spectrally narrow defect modes appear within the photonic band gap owing to optical phase jumps which take place in local structural defects.

In the second part of this chapter a new micro-structuring technique based on the combination of a dichroic photoinitiator and polarization holography is reported. By using the polarization holography to polymerize a mixture of both reactive and non reactive liquid crystals and photoinitiator. After the etching process a high aspect ratio grating is created. A low threshold microcavity lasers was created by embedding dye

doped cholesteric liquid crystals in these pre-designed micro channels. The work is still in progress in the framework of a collaborative project between Licryl and Engineering Chemistry group of the University of Eindhoven (The Netherlands).

Chapter IV reported the first observation of random lasing in optically anisotropic dye doped nematic liquid crystals with long range dielectric tensor fluctuations. The unexpected surviving of interference effects in recurrent multiple scattering provide the required optical feedback for lasing in nematics. Coherent backscattering of light waves in partially ordered nematic liquid crystals manifests a weak localization of light which strongly supports diffusive laser action in presence of gain medium. The experimental characterizations demonstrate that above a given pump power the fluorescence curve collapses and discrete sharp peaks appear. The analysis of the emission spectra emphasizes an irregular intensity fluctuations of the speckle–like emission pattern indicating the typical spatio-temporal randomness of diffusive laser emission. To gain further understanding about the mechanism behind this phenomena, it was varied the confinement geometry of the studied systems (wedge cell, capillary tube, freely suspended and free standing films) and the concentration of the nano-powders added to these systems. Also a comparison of the laser action is reported for systems with different order degree: fully disordered semiconductor powders, self-ordered cholesterics and partially ordered nematic liquid crystals is reported in this work. In addition, the role of the thermally modulated order parameter on the lasing in nematics was investigated.

This experimental work is supported by a statistical study carried out in collaboration with theoretical colleagues within LICRYL lab and presented in chapter V.

Introduction
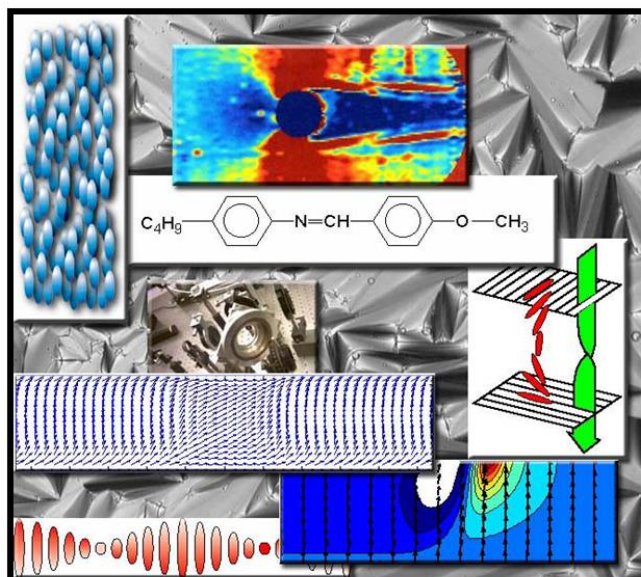
1.   Liquid Crystals: Chiral and Achiral

1. 1 A New Phase of Matter

Between 1850 and 1888, researchers in different fields such as chemistry, biology, medicine and physics found that several materials behaved strangely at temperatures near their melting points. It was observed that the optical properties of these materials changed discontinuously with increasing temperatures. *W. Heintz*, for example, reported in 1850 that stearin melted from a solid to a cloudy liquid at 52°C, changed at 58°C to an opaque and at 62.5°C to a clear liquid. Others reported observing blue colors when compounds synthesized from cholesterol were cooled. Biologists observed anisotropic optical behavior in "liquid" biological materials, a behavior usually expected only in the crystal phase.

In 1888, an Austrian botanist named *Friedrich Reinitzer*, interested in the biological function of cholesterol in plants, was looking at the melting behavior of an organic substance related to cholesterol (The chemical structure of cholesterol was still unknown, today we know that the observed substance was cholesteryl benzoate). He observed, as W. Heintz did with stearin 38 years the substance melted to a cloudy liquid at 145.5°C and became a clear liquid at 178.5°C. He repeated an earlier observation which showed that upon cooling the clear liquid, a brief appearance of blue color could be seen at the transition temperature, and that a blue violet color appeared just before crystallization. Discussion with Lehmann and others led to the identification of a new phase of matter called the *liquid crystal phase*.

1. 2 What are liquid crystals?

The term *"liquid crystal"* refers to materials that possess phases with molecular order that are intermediate of a crystalline solid and an isotropic fluid. A liquid crystal (LC) may flow like a liquid, but have the molecules in the liquid arranged and/or oriented in a crystal-like way.
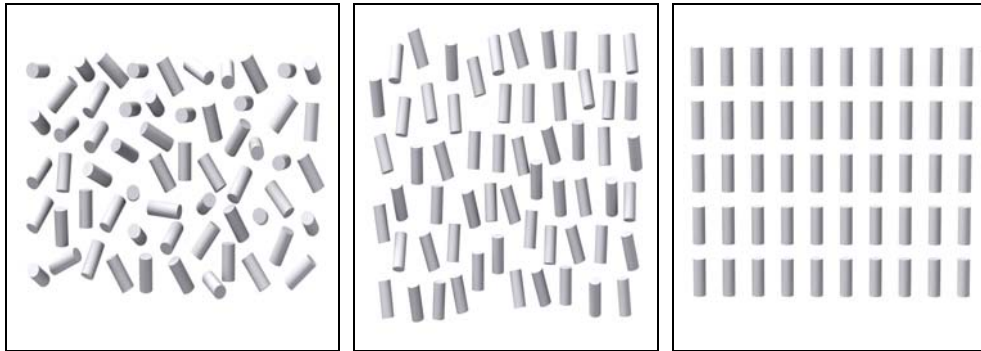
There are many different types of LC phases, which can be distinguished based on their different optical properties (such as birefringence). When viewed under a microscope using a polarized light source, different liquid crystal phases will appear to have a distinct texture. Each "patch" in the texture corresponds to a domain where the LC molecules are oriented in a different direction. Within a domain, however, the molecules are well ordered. Liquid crystal materials may not always be in an LC phase (just as water is not always in the liquid phase: it may also be found in the solid or gas phase). Liquid crystals can be divided into thermotropic and lyotropic LCs. Thermotropic LCs exhibit a phase transition into the LC phase as temperature is changed, whereas lyotropic LCs exhibit phase transitions as a function of concentration of the mesogen in a solvent (typically water) as well as temperature.

1. 3 Liquid crystal phases

The various LC phases (called *mesophases*) can be characterized by the type of ordering that is present. One can distinguish positional order (whether molecules are arranged in any sort of ordered lattice) and orientational order (whether molecules are mostly pointing to the same direction), and moreover order can be either short-range (only between molecules close to each other) or long-range (extending to larger, sometimes macroscopic, dimensions). Most thermotropic LCs will have an isotropic phase at high temperature. That is, heating will eventually drive them into a conventional liquid phase characterized by random and isotropic molecular ordering (little to no long-range order), and fluid-like flow behavior. Under other conditions (for instance, lower temperature), an LC might inhabit one or more phases with significant

anisotropic orientational structure and short-range orientational order while still having the ability to flow.

The ordering of liquid crystalline phases is extensive on the molecular scale. This order extends up to the entire domain size, which may be on the order of micrometers, but usually does not extend to the macroscopic scale as often occurs in classical crystalline solids. However, some techniques (such as the use of boundaries or an applied electric field) can be used to enforce a single ordered domain in a macroscopic liquid crystal sample. The ordering in a liquid crystal might extend along only one dimension, with the material being essentially disordered in the other two directions.

1. 3. 1 Isotropic Phase

In the isotropic phase the moelcules are randomly aligned and exhibit no long range order. The isotropic phase has a low viscosity and will often appear to be very clear. There is no long range positional or orientational order of the molecules, although this sort of order may exist on very short length scales of order tens of Angstroms, corresponding to a few molecular distances. For all practical purposes, the isotropic phase macroscopically appears to be like any other isotropic liquid such as water.

1. 3. 2 Nematic phase

One of the most common LC phases is the nematic, where the molecules have no positional order, but they have long-range orientational order. Thus, the molecules flow and their center of mass positions are randomly distributed as in a liquid, but they all point in the same direction (within each domain). Most nematics are uniaxial: they have one axis that is longer and preferred, with the other two being equivalent (can be approximated as cylinders). Some liquid crystals are biaxial nematics, meaning that in addition to orienting their long axis, they also orient along a secondary axis.

The name of this phase has been given with respect to thread-like textures observed under polarizing microscope. Nematic phase is the first one which is obtained when cooling down from isotropic. The orientations of the molecules are largely "frozen" such that the particles point on average in the same direction. This direction of

preferred alignment can be described by a unit vector, the so-called nematic director $\vec{n}$. The orientation of individual molecules may differ from this direction, so that the director must be more correctly defined as the symmetry axis of the orientational distribution (Fig 1). In nematics the distribution function is rotationally symmetric around the director, i.e. they are uniaxial. Usually, the nematic liquid crystals are invariant for an inversion of $\vec{n}$ [1] (meaning that $\vec{n}$ and $-\vec{n}$ states are indistinguishable). The nematic symmetry is present even when the constituent molecules are polar because the molecules form anti-parallel pairs to minimize the intermolecular interaction energy (usually originating from Van der Waals force). As consequence of the existence of this privileged axis of orientation, there is a macroscopic anisotropy in many material properties, such as dielectric constants and refractive indices
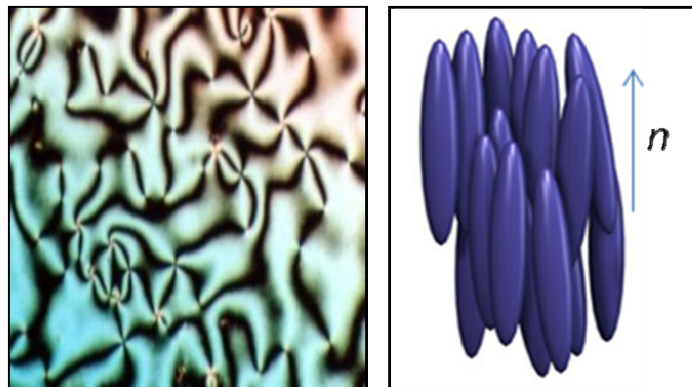
Fig.1: *(a) Picture showing a typical nematic texture with point disclinations, the nuclei of divergent brushes or threads. (b) picture showing the orientation of molecules in the nematic liquid crystalline phase.*

Nematics are (still) the most commonly used phase in liquid crystal displays (LCDs), with many such devices using the twisted nematic geometry.

1. 3. 3 Smectic phase

The word "smectic" is derived from the Greek word for soap. This seemingly ambiguous origin is explained by the fact that the thick, slippery substance often found

at the bottom of a soap dish is actually a type of smectic liquid crystal. The smectic phases, which are found at lower temperatures than the nematic, form well-defined layers that can slide over one another like soap. The smectics are thus positionally ordered along one direction. In the Smectic A phase, the molecules are oriented along the layer normal, while in the Smectic C phase they are tilted away from the layer normal. These phases, which are liquid-like within the layers, are illustrated below. There is a very large number of different smectic phases, all characterized by different types and degrees of positional and orientational order.

In the smectic-A mesophase, the director is perpendicular to the smectic plane, and there is no particular positional order in the layer (Fig 2). Similarly, the smectic-B mesophase orients with the director perpendicular to the smectic plane, but the molecules are arranged into a network of hexagons within the layer. In the smectic-C mesophase, molecules are arranged as in the smectic-A mesophase, but the director is at a constant tilt angle measured normally to the smectic plane (Fig 3).
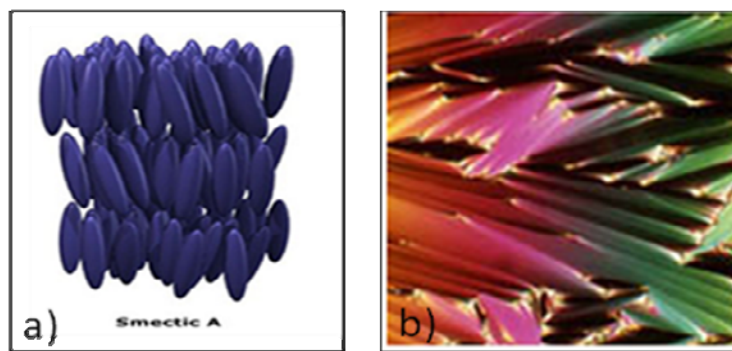
Fig 2: *(a) Diagram showing the orientation of molecules in the Smectic A phase. (b) Typical texture of the Smectic A phase.*
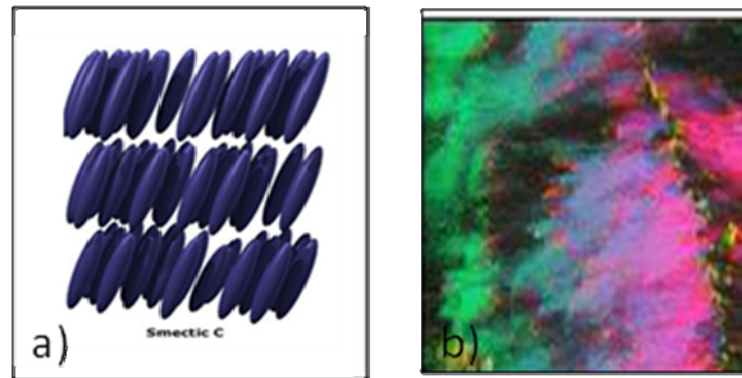
Fig 3: *(a) Diagram showing the orientation of molecules in the Smectic C phase. (b) Typical texture of the Smectic C phase.*

1. 3. 4 Chiral phases

The chiral nematic phase exhibits chirality (handedness). This phase is often called the *cholesteric* phase because it was first observed for cholesterol derivatives[2]. Only chiral molecules (i.e.: those that lack inversion symmetry) can give rise to such a phase. This phase exhibits a twisting of the molecules along the director, with the molecular axis perpendicular to the director. The finite twist angle between adjacent molecules is due to their asymmetric packing, which results in longer-range chiral order.

As in the nematic, the smectic-C mesophase has a chiral state designated C*. Consistent with the smectic-C, the *director* makes a tilt angle with respect to the smectic layer. The difference is that this angle rotates from layer to layer forming a helix. In other words, the director of the smectic-C* mesophase is not parallel or perpendicular to the layers, and it rotates from one layer to the next. Notice the twist of the director, represented by the green arrows, in each layer in the following diagram (Fig 4).
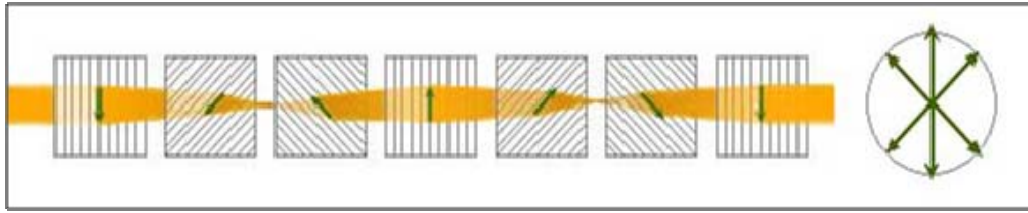
Fig 4: *A schematic representation of a smectic C* phase (left), and a view of the same phase, but along the axis (right).*

In some smectic mesophases, the molecules are affected by the various layers above and below them. Therefore, a small amount of three dimensional order is observed. Smectic-G is an example demonstrating this type of arrangement.

An important characteristic of the cholesteric mesophase is the *pitch* [3]. The pitch, p, is defined as the distance it takes for the director to rotate one full turn in the helix as illustrated in the above figure (Fig 5). A byproduct of the helical structure of the chiral nematic phase, is its ability to selectively reflect light of wavelengths equal to the pitch length, so that a color will be reflected when the pitch is equal to the corresponding wavelength of light in the visible spectrum. The effect is based on the temperature dependence of the gradual change in director orientation between successive layers, which modifies the pitch length resulting in an alteration of the wavelength of reflected light according to the temperature. The angle at which the director changes can be made larger, and thus tighten the pitch, by increasing the temperature of the molecules, hence giving them more thermal energy. Similarly, decreasing the temperature of the molecules increases the pitch length of the chiral nematic liquid crystal. This makes it possible to build a liquid crystal thermometer that displays the temperature of its environment by the reflected color. Mixtures of various types of these liquid crystals are often used to create sensors with a wide variety of responses to temperature change. Such sensors are used for thermometers often in the form of heat sensitive films to detect flaws in circuit board connections, fluid flow patterns, condition of batteries, the presence of radiation, or in novelties such as "mood" rings. In the fabrication of films, since putting chiral nematic liquid crystals directly on a black background would lead to degradation and perhaps contamination, the crystals are micro-encapsulated into particles of very small dimensions. The particles are then treated with a binding material that will contract

upon curing so as to flatten the microcapsules and produce the best alignment for brighter colors. An application of a class of chiral nematic liquid crystals which are less temperature sensitive is to create materials such as clothing, dolls, inks and paints.
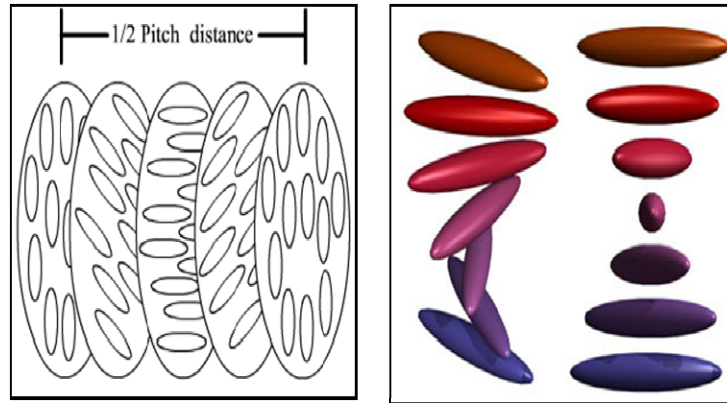
Fig.5: *Diagram showing the typical orientation of molecules in the Cholesteric Phase.*

The wavelength of the reflected light can also be controlled by adjusting the chemical composition, since cholesterics can either consist of exclusively chiral molecules or of nematic molecules with a chiral dopant dispersed throughout. In this case, the dopant concentration is used to adjust the chirality and thus the pitch.

2. The order parameter

In liquid crystals, a local preferred molecular orientation can be always found, its direction being usually indicated by a unit vector called "*director*". It represents the average molecular direction in a volume small enough to make meaningful talking about a molecular direction, and large enough to contain a great number of molecules, which makes meaningful an averaging procedure. The above-mentioned observation that a macroscopic polarization is generally not found even with polar molecules means that the orientations n and $-n$ are equivalent. In the volume where it is defined, in general n does not coincide with the orientation direction ξ of the single molecule. If θ is the angle between ξ and n, the degree of molecular order of the liquid crystal can be given by a parameter which takes into account the distribution $f(\theta)$ describing the alignment of

the molecules with respect to *n*. On the basis of these arguments, a scalar order parameter *S* is defined in the following way [4]:

$$S = \frac{1}{2}\left\langle 3\cos^2 \vartheta - 1 \right\rangle = \int \frac{1}{2}(3\cos^2 \vartheta - 1) f(\vartheta) \, d\Omega \qquad (1.1)$$

where $d\Omega \approx \sin\theta \, d\theta \, d\phi$ is the solid angle (Fig 6). Expression (*1.1*) indicates that the scalar order parameter S is defined as the ensemble average of the second-order Legendre polynomial of $\cos\theta$.

$$S = P_2 \langle \xi.n \rangle$$
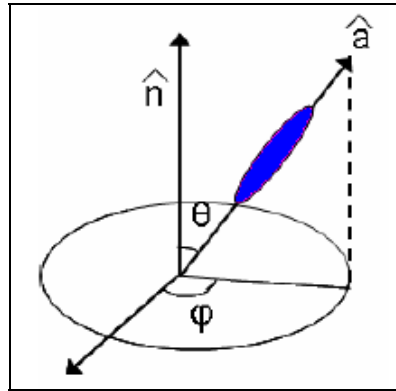
Fig 6: *Geometry used for defining the order parameter.*

According to the mean field theory of R. Mayer and A. Saupe [1], typical values of the order parameter for a nematic liquid crystals, far from the nematic-isotropic transition, are included between 0.3 and 0.9. In this model the scalar order parameter is a universal function of T/T_C, where T_C is the phase transition temperature to the isotropic state. Furthermore, the dependence of *S* slightly decreases by increasing the temperature up to few degrees below T_C, where it starts to become strongly affected by a further temperature increase.

3.   Fluorescence and dye lasers

3.   1 What is fluorescence?

. . . ex arte calcinati,et   *[. . . properly calcinated, and*

illuminato aeri seu solis   *illuminated either by*

radiis,seu flammae   *sunlight or flames, they*

fulgoribus expositi,lucem   *conceive light from*

inde sine calore   *themselves without heat; . . .]*

concipiunt in sese; . . .

Licetus,1640 (about the Bologna stone)

Luminescence is an emission of ultraviolet, visible or infrared photons from an electronically excited species. The word luminescence, which comes from the Latin (lumen = light) was first introduced as luminescent by the physicist and science historian Eilhardt Wiedemann in 1888,to describe 'all those phenomena of light which are not solely conditioned by the rise in temperature', as opposed to incandescence. Luminescence is cold light whereas incandescence is hot light. The various types of luminescence are classified according to the mode of excitation (see Table).

The various types of luminescence

Phenomenon	*Mode of excitation*
Photoluminescence (fluorescence, phosphorescence,delayed fluorescence)	Absorption of light (photons)
Radioluminescence	Ionizing radiation (X-rays, a, b, g)
Cathodoluminescence	Cathode rays (electron beams)
Electroluminescence	Electric field
Thermoluminescence (e.g. radioactive irradiation)	Heating after prior storage of energy
Chemiluminescence	Chemical process (e.g. oxidation)
Bioluminescence	Biochemical process
Triboluminescence	Frictional and electrostatic forces

Sonoluminescence   Ultrasounds

Fluorescence and phosphorescence are particular cases of luminescence (Table)(Fig.7). The mode of excitation is absorption of a photon, which brings the absorbing species into an electronic excited state. The emission of photons accompanying de-excitation is then called photoluminescence (fluorescence, phosphorescence or delayed fluorescence), which is one of the possible physical effects resulting from interaction of light with matter, as shown in Figure[5].
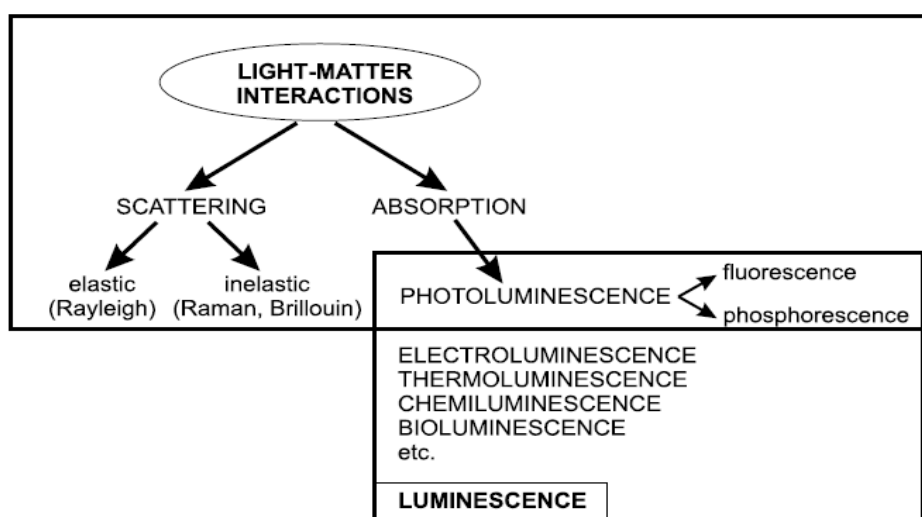
Fig. 7: *Position of fluorescence and phosphorescence in the frame of light–matter interactions.*

Fluorescence is one of the ubiquitous luminescence family of processes in which susceptible molecules emit light from electronically excited states created by either a physical (for example, absorption of light), mechanical (friction), or chemical mechanism. Generation of luminescence through excitation of a molecule by ultraviolet or visible light photons is a phenomenon termed photoluminescence, which is formally divided into two categories, fluorescence and phosphorescence, depending upon the electronic configuration of the excited state and the emission pathway. Fluorescence is the property of some atoms and molecules to absorb light at a particular wavelength and

to subsequently emit light of longer wavelength after a brief interval, termed the fluorescence lifetime. The process of phosphorescence occurs in a manner similar to fluorescence, but with a much longer excited state lifetime.

Fluorescence process is governed by three important events, all of which occur on timescales that are separated by several orders of magnitude (see Fig 8). Excitation of a susceptible molecule by an incoming photon happens in femtoseconds(10^{-15} seconds), while vibrational relaxation of excited state electrons to the lowest energy level is much slower and can be measured in picoseconds(10^{-12}seconds). The final process, emission of a longer wavelength photon and return of the molecule to the ground state, occurs in the relatively long time period of nanoseconds(10^{-9}seconds). Although the entire molecular fluorescence lifetime, from excitation to emission, is measured in only billionths of a second, the phenomenon is a stunning manifestation of the interaction between light and matter that forms the basis for the expansive fields of steady state and time-resolved fluorescence spectroscopy and microscopy.
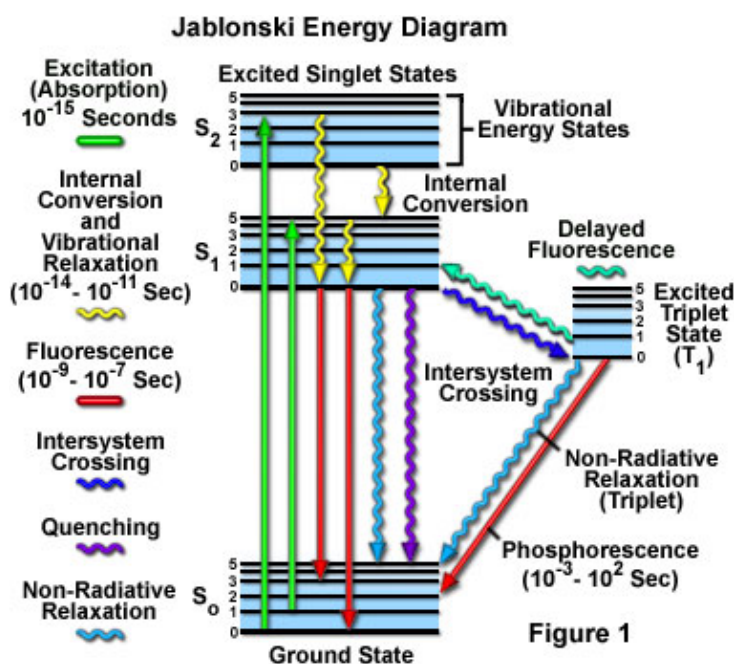
Fig 8: *sketch present Jablonski energy diagram*

Fluorescence is generally studied with highly conjugated polycyclic aromatic molecules that exist at any one of several energy levels in the ground state, each

associated with specific arrangement of electronic molecular orbital. The electronic state of a molecule determines the distribution of negative charge and the overall molecular geometry. For any particular molecule, several different electronic states exist(illustrated as S(0), S(1) and S(2) in the fig)depending on the total electron energy and the symmetry of various electron spin states[6]. Each electronic state is further subdivided into a number of vibrational and rotational energy levels associated with the atomic nuclei and bonding orbitals. The ground state for most organic molecules is an electronic singlet in which all electrons are spin-paired(have opposite spins). At room temperature, very few molecules have enough internal energy to exist in any state other than the lowest vibrational level of the ground state, and thus, excitation processes usually originate from this energy level.

3. 2 Fluorescence polarization

Light is an electromagnetic wave consisting of an electric field $\vec{E}$ and a magnetic field $\vec{B}$ perpendicular both to each other and to the direction of propagation, and oscillating in phase. For natural light, these fields have no preferential orientation, but for linearly polarized light, the electric field oscillates along a given direction; the intermediate case corresponds to partially polarized light. Most chromophores absorb light along a preferred direction depending on the electronic state. In contrast, the emission transition moment is the same whatever the excited state reached by the molecule upon excitation, because of internal conversion towards the first singlet state (Figure 9). If the incident light is linearly polarized, the probability of excitation of a chromophore is proportional to the square of the scalar product $M_A.E$, i.e. $\cos^2 \theta_A$, θ_A being the angle between the electric vector E of the incident light and the absorption transition moment M_A (Figure 9). This probability is maximum when E is parallel to M_A of the molecule; it is zero when the electric vector is perpendicular.
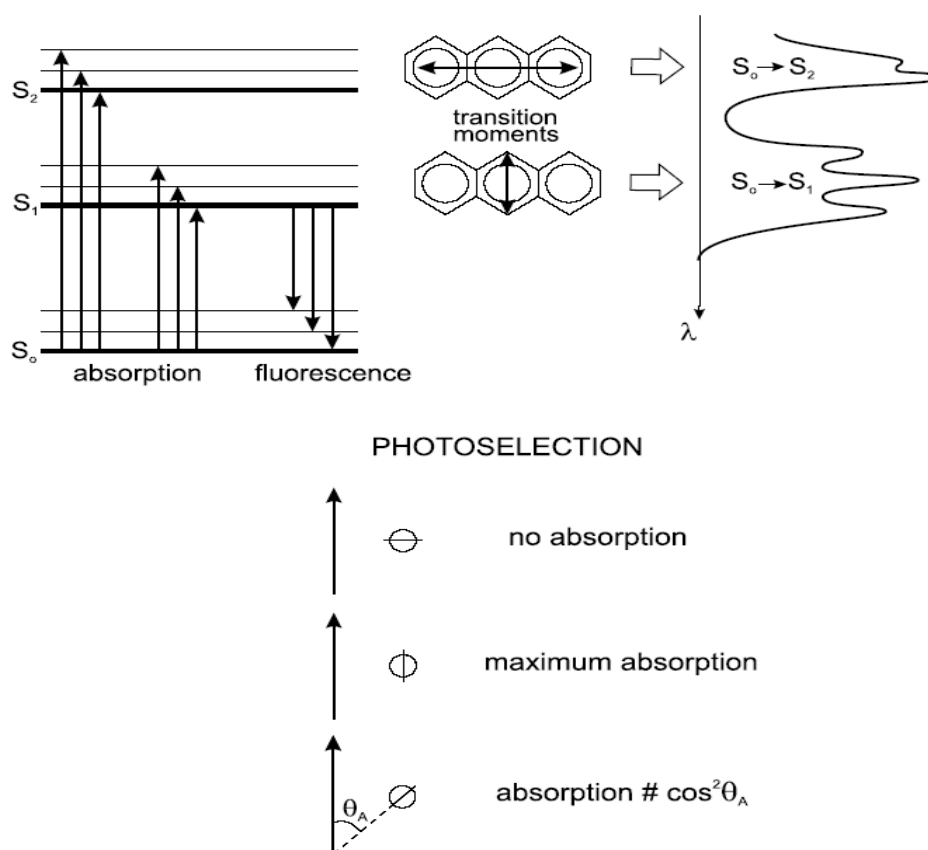
Fig. 9: *Transition moments and photoselection.*

Fluorescence polarization measurements can thus provide useful information on molecular mobility, size, shape and flexibility of molecules, fluidity of a medium, and order parameters.

Consider an XYZ coordinate framework with a fluorescent solution placed at the origin, as shown below, where XZ is in the plane of the page. In this system, the exciting light is traveling along the X direction. If a polarizer is inserted in the beam, one can isolate a unique direction of the electric vector and obtain light polarized parallel to the Z axis which corresponds to the vertical laboratory axis. This exciting light will be absorbed by the fluorophore at the origin and give rise to fluorescence which is typically observed at 90° to the excitation direction, i.e., from along the Y axis.
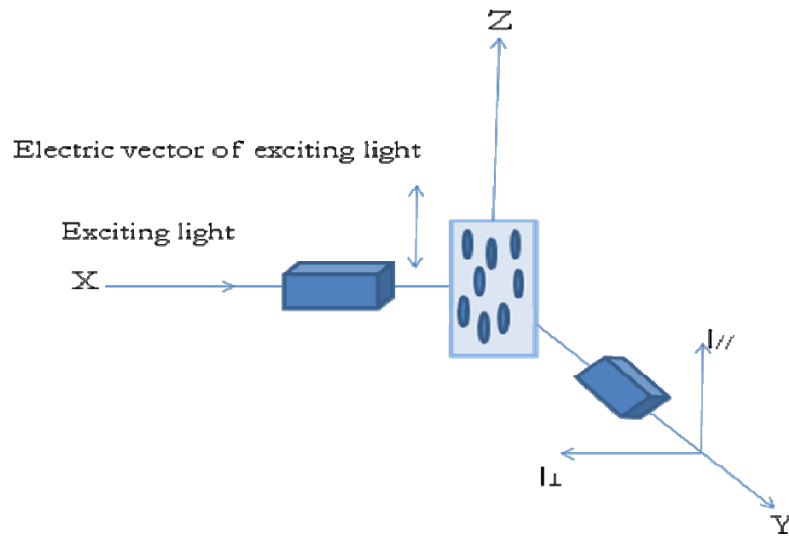
The actual direction of the electric vector of the emission can be determined by viewing the emission through a polarizer which can be oriented alternatively in the parallel or perpendicular direction relative to the Z axis or laboratory vertical direction. Polarization is then defined as a function of the observed parallel (I_{ll}) and perpendicular intensities ($I_\perp$)[7] :

$$P = \frac{I_{II} - I_\perp}{I_{II} + I_\perp}$$

As an example, by studying the polarized fluorescence of the dye doped nematic liquid crystal filled in a wedge cell, the experimental measurements put into evidence a strong dependence of the emission intensity (spontaneous emission) on the pump polarization, as it shown in the polar plot of (Fig 10). By maintaining the pump energy fixed, a four fold increase in the spontaneous emission intensity was recorded by rotating a linear state of polarization from parallel to perpendicular to the nematic director and by analyzing the emitted light along the direction of the excitation polarization[8].
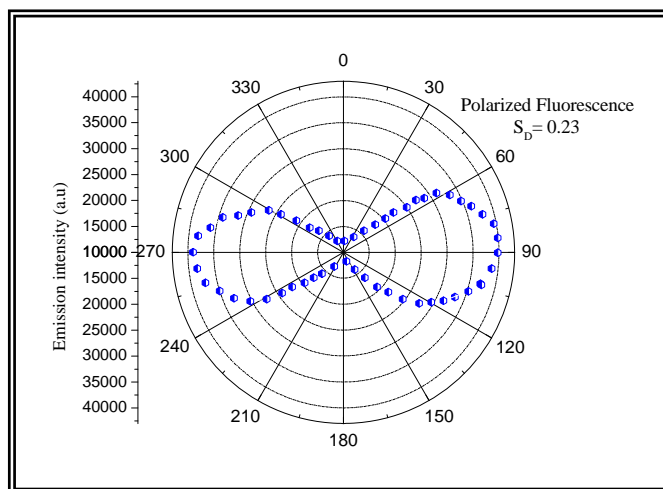
Fig. 10: *Polarized fluorescence measurements suggest an anisotropic orientational distribution for the dye transition dipole moments. Calculated order parameter value is S_D=0.23.*

This suggests that the dye molecules possess an anisotropic orientational distribution of the transition dipole moments because of the strongly anisotropic environment in which has been dissolved, with a calculated dye order parameter S_D = 0.23 .

4. Dye laser

The first human-made (synthetic) organic dye, mauveine, was discovered by William Henry Perkin in 1856. Dyes, either as solutions or vapours, are the active medium in pulsed and continuous-wave dye lasers as well as ultrafast shutters for Q-switching and passive modelocking. They emit in a comparatively narrow spectral region (typically 30 nm); thus a variety of dyes is necessary in order to cover the entire (visible) spectral range.

The optical excitation of dyes corresponds to transitions of molecules in the singlet state, with the absorption S_0 --> S_1 being the strongest (Fig 11), and is specific for each

dye molecule. For optimum pumping ($S_0 \rightarrow S_1$) of the various dyes, one would therefore need a number of pump laser wavelengths.
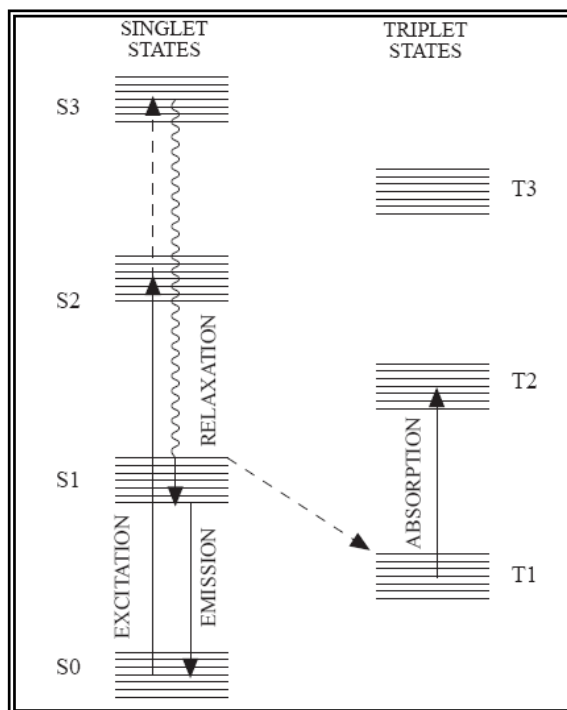
Fig. 11: *Schematic energy levels of a dye molecule.*

Fortunately, nearly all dyes have additional absorption bands in the UV. These absorptions correspond to transitions to higher singlet states, from which fast internal relaxation processes lead to the upper laser level (S_1) with high quantum efficiency the reason most dyes can be pumped by a single UV laser. However, this attractive excitation scheme, one pump laser for all dyes, brings other problems.

(i) The inner efficiency of dye lasers is lower as a result of excitation in higher S-states because a considerable part of the excitation energy is converted into heat (large Stokes shift). This disadvantage is more than compensated for, however, by the high efficiency of pulsed lasers.

(ii) A multiphoton excitation can lead to destruction of the cell and the solvent molecules. In this process, a previously excited molecule absorbs further photons (sequential absorption), or a molecule absorbs several photons "at the same time". In

these absorption processes the molecule can absorb so much energy that the binding energy is surpassed, and the molecule dissociates, or at least changes its structure. This process is more probable during excitation with UV light than with visible light. Thus, one must expect a reduced photostability of the dye when pumping with UV light.

(iii) Another problem results from the small absorption cross section at short wavelengths. To excite as many molecules as possible, a very high pump power density I_p (I_p being inversely proportional to the absorption cross section), or high dye concentrations is required. I_p is limited to values <30 MW/cm^2 due to the stability of most solvents.

The most important dyes used in our experiments are:

DCM: 4-dicyanomethylene-2-methyl-6-(*p*(dimethylamino)styryl)-4H-pyran
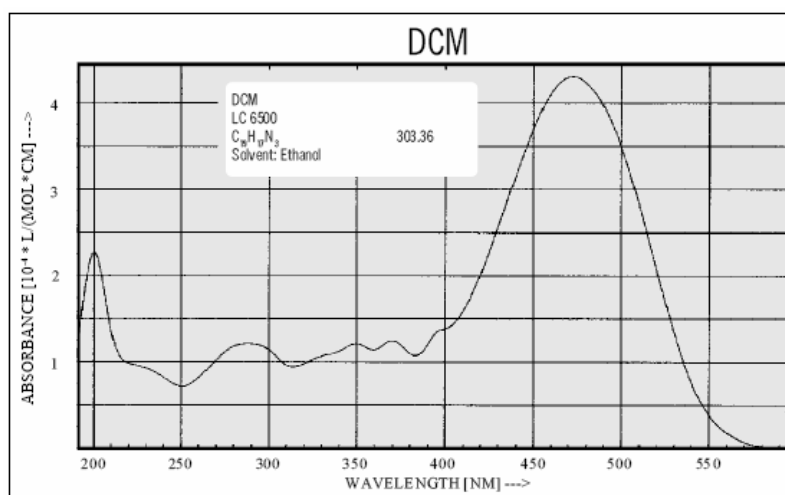
Pyrromethene 597: 4,4-Difluoro-2,6-di-t-butyl-1,3,5,7,8-pentamethyl-4-bora-3a,4a-diaza-s-indacene2,6-Di-t-butyl-1,3,5,7,8-pentamethylpyrromethenedifluoroborate Complex

PM 597
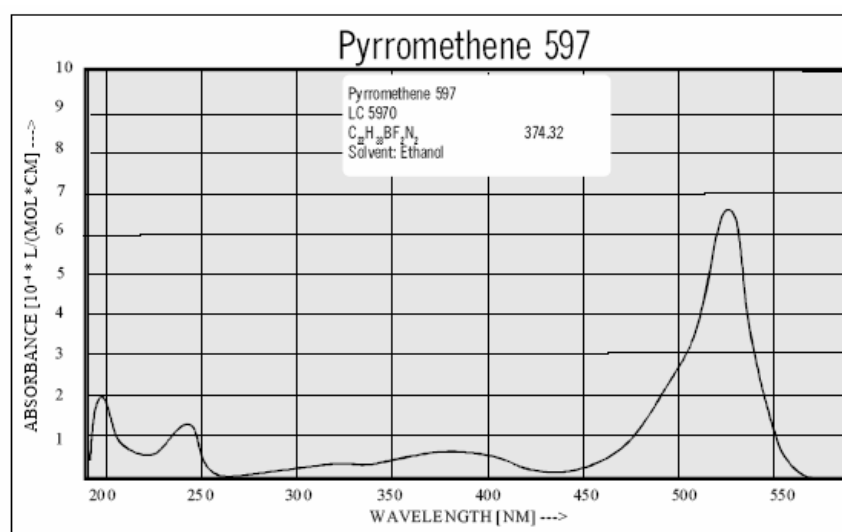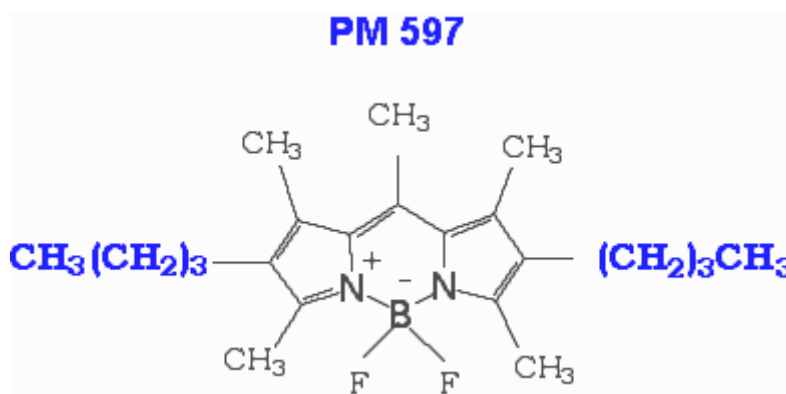
Pyrromethene 650: 1,2,3,5,6,7-hexamethyl-8-cyanopyrromethene-difluoroborate complex

Pyrromethene 650

Chemical Formula: $C_{16}H_{18}BF_2N_3$
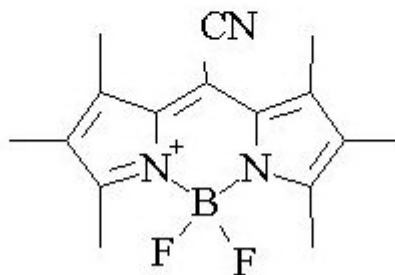
5. Principle of mirror-less laser

Besides the many applications that have been discovered since the first experimental demonstration in 1960 by Theodore Maiman [9], the laser itself has also been subject of intense scientific study. In a laser, light is generated by a combination of light amplification by stimulated emission and optical feedback [10,11]. The practical implementation of both functional laser parts, optical gain and optical feedback, comes in many varieties. For example, laser oscillation has been shown to be possible using solid-state gain media [12] or gaseous media [13], while implementations of laser cavities include, among many others, ring-type cavities [14], chaotic cavities [15] and photonic-crystal cavities [16, 17].

In physics, a laser is a device that emits light through a specific mechanism for which the term laser is an acronym: **l**ight **a**mplification by **s**timulated **e**mission of **r**adiation. As a light source, a laser can have various properties depending on the purpose for which it is designed. A typical laser emits light in a narrow, low-divergence beam and with a well-defined wavelength (corresponding to a particular color if the laser is operating in the visible spectrum). This is in contrast to a light source such as the incandescent light bulb, which emits into a large solid angle and over a wide spectrum of wavelength. These properties can be summarized in the term coherence.

A laser consists of a *gain medium* inside an *optical cavity*, with a means to supply energy to the gain medium. The gain medium is a material (gas, liquid, solid or free electrons) with appropriate optical properties. In its simplest form, a cavity consists of two mirrors arranged such that light bounces back and forth, each time passing through the gain medium. Typically, one of the two mirrors, the output coupler, is partially transparent. The output laser beam is emitted through this mirror as show in Fig 12.

Light of a specific wavelength that passes through the gain medium is amplified (increases in power); the surrounding mirrors ensure that most of the light makes many passes through the gain medium. Part of the light that is between the mirrors (i.e., is in the cavity) passes through the partially transparent mirror and appears as a beam of light. The process of supplying the energy required for the amplification is called pumping and the energy is typically supplied as an electrical current or as light at a

different wavelength. In the latter case, the light source can be a flash lamp or another laser. Most practical lasers contain additional elements that affect properties such as the wavelength of the emitted light and the shape of the beam.
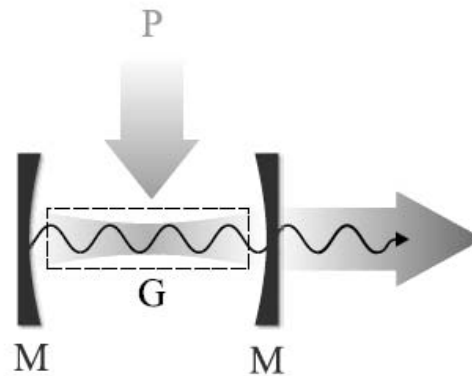
Fig. 12: *Schematical impression of a laser: two mirrors (M) with a gain medium (G) in between. The two mirrors form a cavity, which confines the light and provide the optical feedback. The right mirror is partly transmitting. One of the cavity modes is shown. The gain medium is pumped with an external pump source (PS). The resulting laser light is directional, with a small spectral bandwidth.*

5. 1 Mirror-less lasing

The inclination toward miniaturization in the emerging generation of nanoscale optoelectronic devices leads to a growing interest in morphologically periodic photonic heterostructures like photonic bandgap (PBG)[18]. Photonic crystals having an ordered structure with a periodicity equal to optical wavelengths have attracted considerable attention from both fundamental and practical points of view because novel physical concepts such as the photonic bandgap have been theoretically predicted and various applications of photonic crystals have been proposed[19]. In particular, the study of stimulated emission in the photonic bandgap is one of the most attractive subjects, since, in the bandgap, spontaneous emission is inhibited and low-threshold lasers based

on photonic crystals are expected[20,21]. So far, intensive studies on one- and two-dimensional bandgap materials have been performed. In a one-dimensional (1D) periodic structure, laser action is expected at the photonic band edge, where the photon group velocity approaches zero[22].

Helixed liquid crystals materials are self-organized mesophases which possess all the peculiar optical properties for achieving organic mirror-less optical resonant cavities. The birefringence and natural ability to form periodic structures make chiral liquid crystals interesting one-dimensional photonic bandgap materials. In fact, chiral liquid crystals (CLC) possess a helical superstructure which provides a 1D spatial modulation of the refractive index giving rise to Bragg selective reflection for circularly polarized light having the same handedness as the LC structure. In PBG microstructures light can be confined and manipulated by engineering quasi-ideal distributed feedback (DFB) micro-resonators . In a CLC doped with fluorescent guest molecules, the spontaneous emission is suppressed for the reflection stop band and it is enhanced at the band edges where a series of narrow long-lived transmission modes are expected [19,23]. Within the bandgap, the wave is evanescent and decays exponentially, so that the density of states (DOS) within the gap vanishes in large structures. At the stop band edges the density of states is expected to diverge. The group velocity v_g is real, and at the photonic band edge tends to zero, while the photon dwell time is greatly increased, so that the gain is significantly enhanced at these spectral positions [24]. This gain enhancement together with distributed feedback mechanism can give rise to low threshold mirror-less lasing at the band edge in a variety of liquid crystal materials. In chiral liquid crystals the index modulation is relatively low so that sufficient feedback can be achieved by increasing the length of the resonant cavity (Fig.13). Thousands of periods are needed in order to obtain an optical cavity with a quite high quality factor, Q [25].
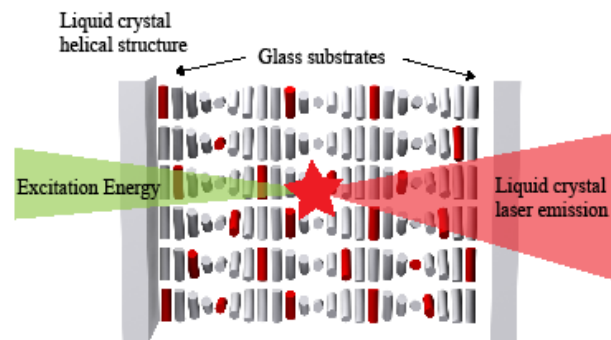
Fig. 13: *schematic mirror-less lasing emission in chiral nematic liquid crystal*

The laser emission study in ordered and periodic systems has known an extraordinary revival in the last years; even because of the remarkable development of experimental techniques which allow to scale the photonic crystal structures down to the nanoscale with the aim to mould the flow of light [26]. Surprisingly, active random media repeatedly proved to be suitable for obtaining mirror-less diffusive laser action, mainly based on the resonant feedback mechanisms in multiple scattering. Light localization and interference effects which survive to multiple scattering events have been invoked to explain the mirror-less lasing observed in many exotic and complex systems [27,28] (Fig 14).
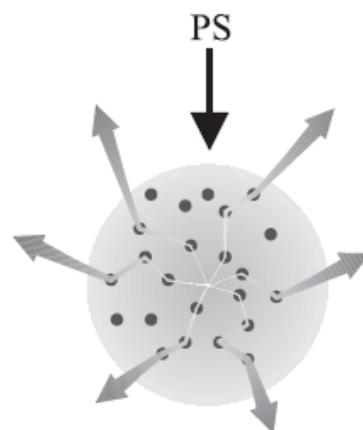
Figure 14: *Schematical impression of a random laser: a gain medium (gray area) with randomly placed scattereres. The gain medium is pumped with an external pump source (PS). The resulting laser light is omnidirectional.*

A random laser is a non-conventional laser whose feedback mechanism is based on disorder-induced light scattering. Depending on whether the feedback supplied by scattering is intensity feedback or amplitude feedback, random lasers are classified into two categories: random lasers with incoherent feedback and random lasers with coherent feedback. This will be discussed with more details in the next chapter.

References

[1] P. G. de Gennes, J. Prost, *The Physics of Liquid Crystals* (Clarendon Press, Oxford, 1993).

[2] R. Podgornik, H.H. Strey, K. Gawrisch, D.C. Rau, A. Rupprecht, V.A. Parsegian, *Proc. Natl. Acad. Sci. USA* **1996**, *93*, 4261.

[3] H.H. Strey, J. Wang, R. Podgornik, A. Rupprecht, L. Yu, V.A. Parsegian, E.B. Sirota, *Phys. Rev. Lett.* **2000**, *84*, 3105.

[4] F. Simoni, "Nonlinear optical properties of liquid crystal and polymer dispersed liquid crystal", World Scientific (1997).

[5] Bernard Valeur *"Molecular Fluorescence: Principles and Applications".* 2001 Wiley-VCH Verlag GmbH

[7] S. T. Wu and D.K. Yang, "*Reflective Liquid Crystal Displays*" (John Wiley & Sons, Chichester, 2001).

[8] G. Strangi, S. Ferjani, V. Barna, A. De Luca, C. Versace, N. Scaramuzza, and R. Bartolino Optics Express, Vol. 14, Issue 17, pp. 7737-7744

[9] T. H. Maiman, *Stimulated Optical Radiation in Ruby*, Nature (London) **187**, 493 (1960).

[10] H. Haken, *Laser Theory* (Springer, Berlin, 1984.

[11] L. Mandel and E. Wolf, *Optical Coherence and Quantum Optics (Cambridge University Press, Cambridge, 1995)* — p.17, 29, 60, 70, 78, and 131.

[12] T. Maiman*, Stimulated Optical Radiation in Ruby*, Nature 187, 493 (1960.

[13] A. Sz¨oke and A. Javan, *Effects of Collisions on Saturation Behavior of the 1.15-μ Transition of Ne Studied with He-Ne laser*, Phys. Rev. 145, 137 (1966).

[14] R. Roy and L. Mandel, *Optical bistability and first order phase transition in a ring dye laser*, Opt. Comm. 34, 133 (1980).

[15] J. N¨ockel and A. Stone, *Ray and wave chaos in asymmetric resonant optical cavities*, Nature 385, 45

(1997).

[16] R. Lee, O. Painter, B. Kitzke, A. Scherer, and A. Yariv, Photonic Bandgap Disk

Laser, Electron. Lett. 35, 569 (1999).

[17] S. Strauf, K. Hennessy, M. Rakher, Y.-S. Choi, A. Badolato, L. Andreani, E. Hu, P.

Petroff, and D. Bouwmeester, Self-Tuned Quantum Dot Gain in Photonic Crystal Lasers, Phys.

Rev. Lett. 96, 127404 (2006) — p.17 and 50.

[18] S. John, Phys. Rev. Lett. 1987, 58, 2486.

[19] E. Yablonovitch, Phys. Rev. Lett. 1987, 58, 2059.

[20] K. Yoshino, S. Tatsuhara, Y. Kawagishi, M. Ozaki, A. A. Zakhidov, Z. V. Vardeny, Appl.

Phys. Lett. 1999, 74, 2590.

[21] K. Yoshino, S. B. Lee, S. Tatsuhara, Y. Kawagishi, M. Ozaki, A. A. Zakhidov, Appl. Phys.
Lett. 1998, 73, 3506.

[22] S. Chandrasekhar, Liquid Crystals, Cambridge University Press, Cambridge 1992.

[23] D. Wiersma, Nature (London) 406,132 (2000)

[24] J. P. Dowling, M. Scalora, M. J. Bloemer, C. M. Bowden, J. Appl. Phys. 1994, 75, 1896.

[25] E. M Purcell, Phys. Rev. 69, 681 (1946)

[26] J. D. Joannopoulos, R. D. Meade, and J. N.Winn, Photonic Crystals: "*Moulding the Flow of*

Light" (Princeton University Press, Princeton, NJ, 1995).

[27] H. Cao, Y. G. Zhao, S. T. Ho, E. W. Seelig, Q. H. Wang, and R. P. H. Chang, "Random

Laser Action in Semiconductor Powder," Phys. Rev. Lett. **82**, 2278 (1999).

[28] D. Wiersma and S. Cavalieri, "A temperature tunable random laser," Nature **414**, 708(2001).

Propagation of Light in Periodic and Disordered Scattering Media
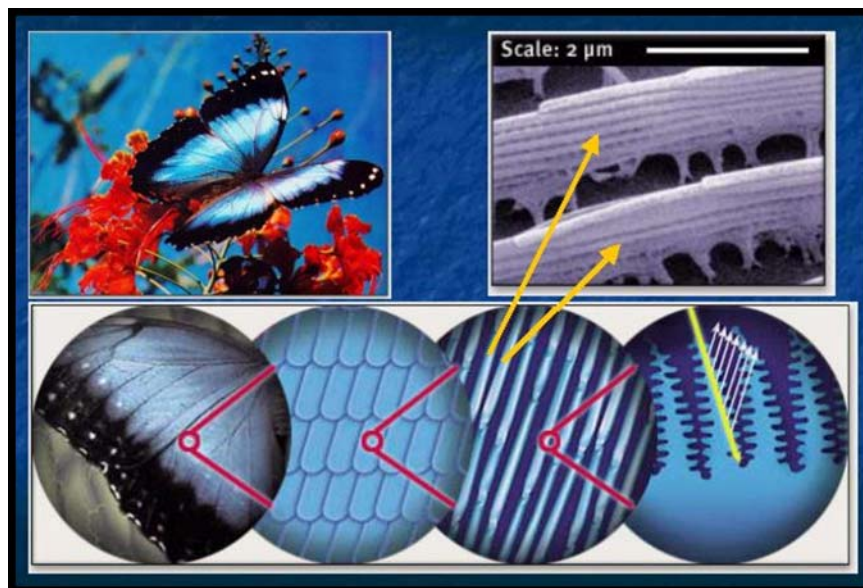
La lumière (. . .) donne la
couleur et l'eclat à toutes
les productions de la
nature et de l'art; elle
multiplie l'univers en le
peignant dans les yeux de
tout ce qui respire.

[Light (. . .) gives color and
brilliance to all works of
nature and of art; it
multiplies the universe by
painting it in the eyes of all
that breathe.]

Abbé Nollet, 1783

1.   Introduction

What we humans perceive as colour is actually light waves that hit our eyes, translated into nerve impulses, and interpreted by our brains as all the various colours around us. We see things because they emit or scatter light that is subsequently absorbed by our eyes. Absorption, emission, reflection and scattering of light of certain distinct wavelengths occur and materialize to the eye as a colour appearance of an object. If a colour appearance of an object is created by absorbance of specific wavelengths, the wavelengths that are not absorbed determine the colour of appearance. Emission of light by substances such as pigments that are present in the material, can also cause the colour appearance of an object.

In nature many examples of absorption and emission are encountered: such a paint is red because the pigment perylene, present inside, absorbs green light and emits red light, a grass is green since the chlorophyll absorbs blue and red light and emits green light.

Another evident phenomenon of light scattering is present in the nature: the appearance of a blue sky. Particles that are smaller than the wavelength of light and present in the sky cause the blue part of the emitted spectrum of the sun to be scattered more than the red part of the spectrum, causing a blue appearance. This phenomenon is also called Rayleigh scattering.

A colour appearance can result also from reflectance of specific colours from a physical structure of the material. Due to constructive interference from a plane, a thin layer, or a collection of ordered lattice planes in the material, light with a certain wavelength is reflected causing appearance of a colour. If such a structure is illuminated with white light, the light is reflected under different angles and the incident white light is split up into its spectral colours. This phenomenon is also known as iridescence. A thin layer of oil on water is a great example of this iridescence, the light is reflected from the front side and the backside of the oil layer since there is a change in refractive index at both sides; from air to oil and from oil to water. The reflected waves interfere constructively and cause a rainbow-like colour appearance. Other examples of iridescence in nature are butterfly wings [1] or

fish-scales (Fig. 1). The following figure shows how the butterfly wings reflecting blue-greenish colours due to the wing structure consisting of discrete multilayer of cuticle (tough but flexible, non-mineral covering of an organism) and air. It also displays a rainbow fish with a hue of colours. Because of a structure of periodically varying refractive index of air and chitine the incident light is Bragg diffracted and the reflected light appears in a rainbow of colours.
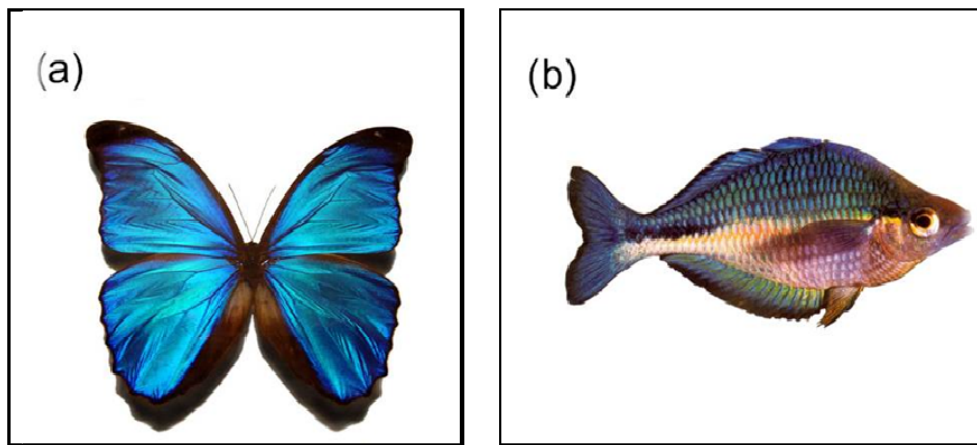
Fig.1: *Examples of iridescence in nature caused by interference from multilayer structures with periodically varying refractive indices.*

If in addition to iridescence, some random scattering takes place due to imperfections for example, the phenomenon is called opalescence. In nature opalescence is known as having the name of the gemstone opal. The shells and the opal gems present great examples of natural opalescence (Fig. 2).
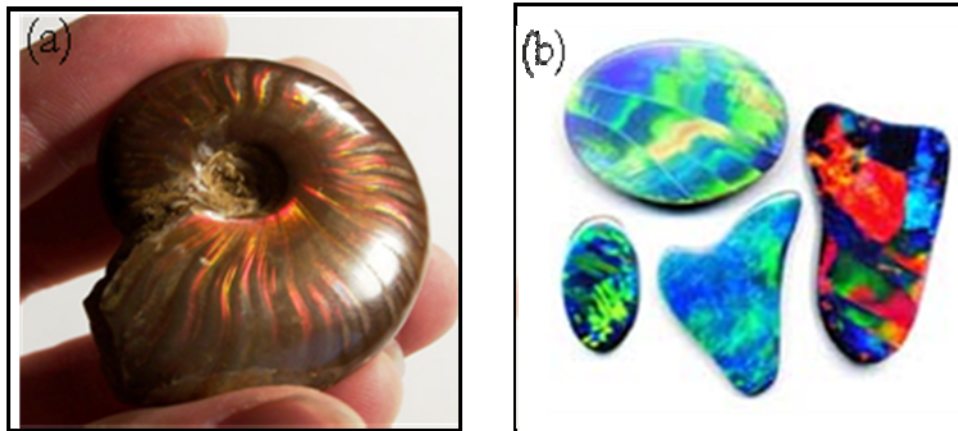
Fig. 2: *Natural opalescence: (a) Shells. (b)Opal gems.*

The microscopic structure of these opals consist of periodically arranged glass spheres, organized in a three-dimensional (3D) ordering. Opal is made of tiny, microscopic spheres of silica. It is these tiny spheres that give opal it's amazing colours, by breaking white light up into rays of different colours. When white light enters a precious opal, it hits the spheres of silica. The spheres split light into rays of different wavelengths, which we see as different colours. The colours and patterns in an opal are determined primarily by the size and arrangement of the silica spheres it contains.

However, this success at explaining natural phenomena came to be tested from an unexpected direction, the behavior of light, whose intangible nature had puzzled philosophers and scientists for centuries. In 1873 the Scottish physicist James Clerk Maxwell showed that light is an electromagnetic wave with oscillating electrical and magnetic components.

Electromagnetic radiation has a dual nature as both particles and waves. One way to look at it is as changing electric and magnetic fields which propagate through space, forming an electromagnetic wave. This wave has amplitude, which is the brightness of the light, wavelength, which is the color of the light, and an angle at which it is vibrating, called

polarization. This was the classical interpretation, crystallized in Maxwell's Equations, which held sway until Planck, Einstein and others came along with quantum theory.

Due to the importance of light in the humans life we will discuss and investigate in this chapter the propagation of light in periodic and aperiodic crystals. We probe the possibility of these structures to manipulate light by investigating the properties of emission.

2. Periodic Structures

2. 1 Photonic crystals and photonic band-gap

The simplest form of a photonic crystal is a one-dimensional periodic structure, such as a multilayer film (a *Bragg mirror*). Electromagnetic wave propagation in such systems was first studied by Lord Rayleigh in 1887 [2], who showed that any such one-dimensional system has a band gap. Almost 100 years after 2D and 3 D photonic crystals were introduced by Yablonovich [3] and John [4] and have attracted a huge interest because of their remarkable potential confirmed in physics and emerging applications.

Originally photonic crystals were proposed as materials that could localize light [4] and completely inhibit spontaneous emission if a light source is embedded in such a crystal [3], an extreme example of the Purcell effect [5]. Analogous to the electronic bandgap in semiconductors such photonic crystals exhibit a certain frequency range where light cannot propagate in any direction in the structure (Fig. 3). This frequency range is known as photonic bandgap. While semiconductors exist by virtue of the periodicity of the underlying crystalline lattice of atoms, photonic crystals are formed by a periodic variation in dielectric constant on a length scale comparable to the wavelength of interest. If an atom is placed inside such a structure, the atom cannot radiate away energy if its transition frequency falls within the photonic bandgap, and thus spontaneous emission can be completely inhibited.
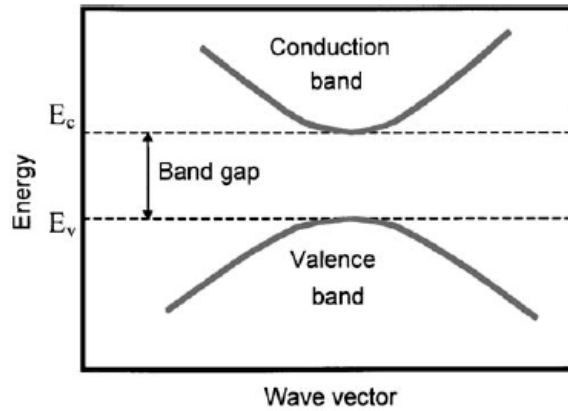
Fig. 3: *Energy-wave vector diagram for semiconductor.*

Photonic band gap materials are expected to play an important role in the development of new optical devices. They consist of a periodically arranged composite of dielectric materials, which influences the propagation of light in a manner analogous to the way crystalline solids influence the flow of electrons.

As described above, photonic crystals are materials that have a periodic arrangement of the dielectric constant on a length scale comparable to the wavelength of interest. Due to this periodicity one can find a frequency band for which the propagation of light in a certain direction is forbidden, this band is called the stop gap in that particular direction. This frequency band is centered around the frequency that fulfills the Bragg condition in that direction. The inhibition of emission is expected to lead to novel phenomenon in optics and quantum optics and may serve as the basis for lasers without threshold and highly efficient emitting diodes.

Photonic crystals are common in nature mentioned before. At the University of Sydney, Parker *et al.* have discovered that photonic crystals exist also in the animal world [6], specifically for the "sea mouse", a small worm. The sea mouse, shown in fig. 4 (a), is covered with long threads and spines that produce a brilliant iridescence.
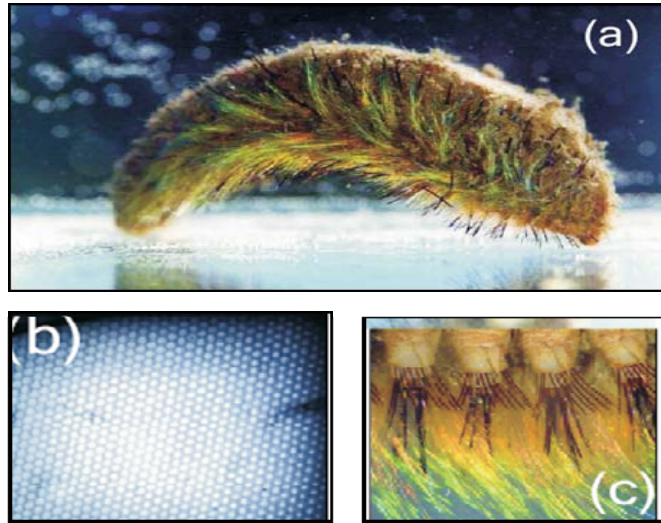
Fig. 4*: (a) Picture of a sea mouse with its iridescent spine (c). In (b) the SEM picture of a spine reveals the photonic crystal nature of iridescence [6].*

A scanning electron microscope (SEM) image for a spine is depicted in figure. 4(b). It reveals a periodic microstructured pattern with hexagonal symmetry. This is an example of a two-dimensional photonic crystal that possesses a pseudo-gap. Other examples of photonic crystals can be found in some butterflies possessing blue iridescence. Blue pigments are, indeed, very rare in nature.

Photonic crystals can be classified into three main groups, that is, one-dimensional (1D), two-dimensional (2D) and three-dimensional (3D) systems, according to the dimensionality of the structure that forms the crystal (Fig. 5). We can have structures that go from the microwave regime to visible wavelengths. Decreasing the wavelength means increasing the difficulties to produce them because precise miniaturization processes have to been involved.
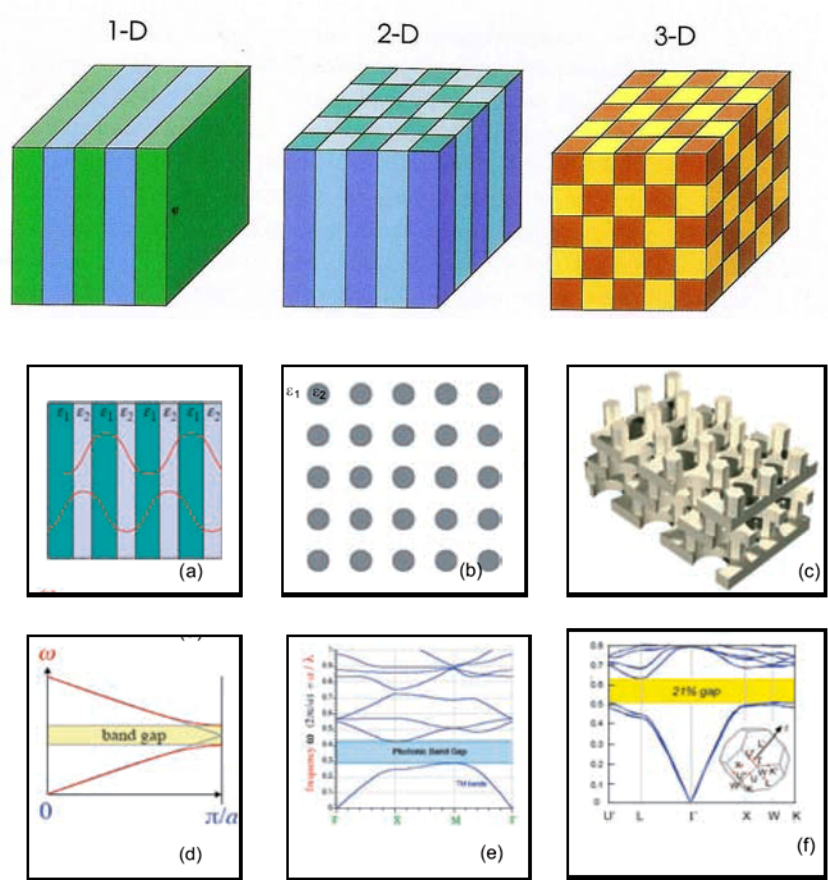
Fig . 5: *Examples (a-c) of 1D, 2D and 3D photonic crystals and (d-f) corresponding band structures.*

2. 1. 1 1D photonic crystal

The simplest possible photonic crystal (Fig. 6) consists of alternating layers of material with different dielectric constants ε_1 and ε_2. This photonic crystal can act as a perfect mirror for light with frequency within a sharply- defined gap, and can localize light modes if there are any defect in its structure.

The traditional approach to an understanding of this system is to allow a plane wave to propagate through the material and to consider the multiple reflections that take place at each interface. A schematic of photonic crystals is presented in the fig. 7. 1 D crystal is obviously the simplest that exists, and relatively easy to fabricate, in its simplest form it is a

dielectric mirror. This structure can be formed by distributed Bragg mirror and by some defects that trap the electromagnetic field inside the sample[7]. Nowadays such multilayer structures are obtained by chemical vapor deposition or by using porous silicon[8], grown by hydrofluoric acid etching.
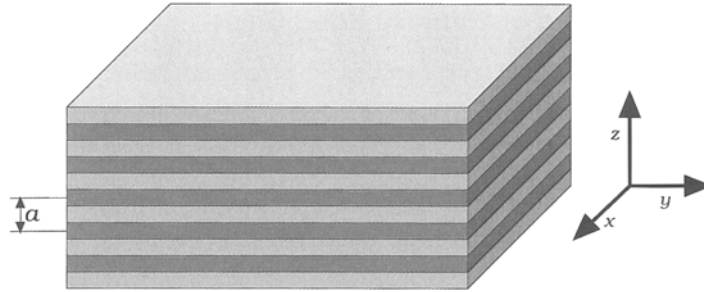
Fig. 6: *a one dimensional photonic crystal, it consists of alternating layers of materials with different dielectric constants, spaced by a distance a*
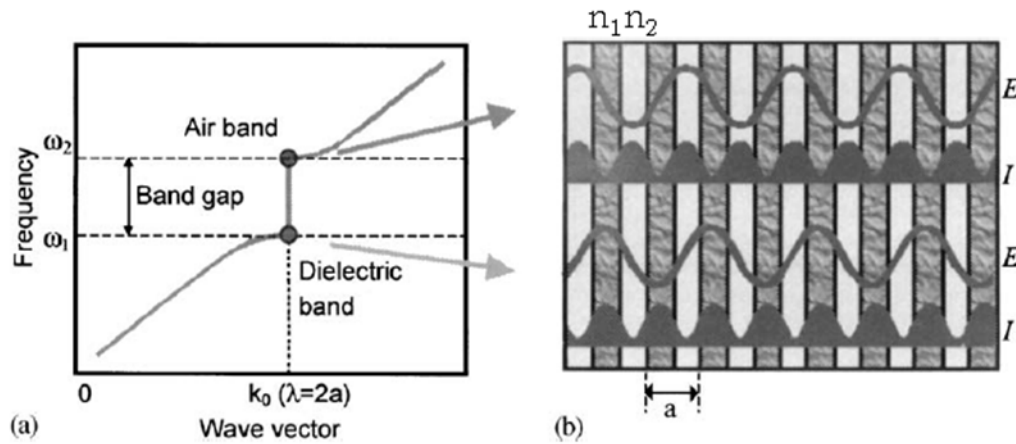
Fig. 7: *(a) Photonic band structure of a layered dielectric system with period a: (b) Dark and light layers correspond to high and low refractive indices, respectively.*

2. 1. 2 2-D and 3-D photonic crystal

A photonic crystals are multi- dimensional periodic structures with a period of the order of optical wavelength. They have many analogies to solid state crystals. The most important one is the *band of photons*, which is a powerful theory for the understanding of light behavior in a complex photonic crystal structure. It enables us to create the *photonic bandgap* and the *localization of light*. They have great potentials for novel applications in optics, optoelectronics, μ-wave technologies, quantum engineering, bio-photonics, acoustics, and so on. In this section, I will outline these fundamental features of photonic crystals with their progress of research.

Since the beginning of research in photonic band gap materials, the main purpose was to design structures exhibiting a complete photonic band gap in three dimensions to achieve a full control over spontaneous emission and light localization. This meant that researchers concentrated on the fabrication and theoretical study of 3D photonic crystals. Calculating the band structure of such devices was not an easy task, also because of the vector nature of Maxwell's equation. The very first problem to solve in order to design the right structure was the development of a suitable numerical method. In fact, except for very special cases, it is not possible to obtain analytical solutions of the eigen value problem. This was proposed in 1989 an 1990 by Yablonovitch [9] and Leung [10], under the name of plane-wave method. It was of course based on plane wave expansion of the electromagnetic field and the diagonalization of the resultant eige nvalue problem. The first geometries with complete band gap proposed were the diamond structure made of dielectric spheres in air [11] and, more important, the yablonovitc structure, shown in figure 8, specially designed to be suitable for micro-fabrication.

In three dimensions the fabrication of photonic crystals for optical frequencies relies mainly on self-assembly techniques. In two dimensions, lithography and anisotropic etching techniques can be used. Two-dimensional (2-D) photonic crystals can be integrated with existing planar optical waveguide technology in which lithography and etching are used

routinely for the fabrication of waveguides and other devices. In two dimensions the only simple structure that offers a full photonic bandgap.
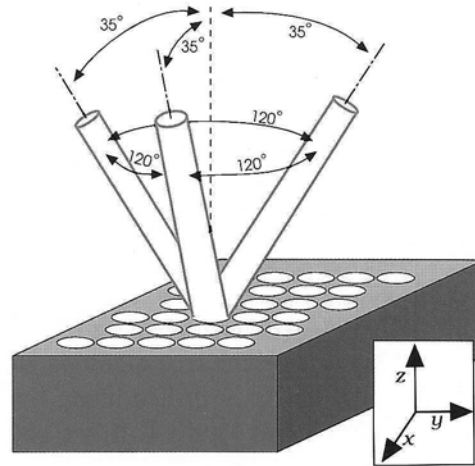
Figure 8: *Yablonovite structure, from the original Yablonovitch work [12]*

2. 2 Photonic band structure

The theoretical description of the propagation of light in photonic crystals is provided by calculating the photonic band structure from Maxwell's equations. Such calculations are done numerically and make use of the periodicity of the lattice by imposing periodic boundary conditions. Based on concepts well known from solid state physics, the solutions to Maxwell's equations are represented in terms of a photonic band structure or dispersion relation $\omega(k)$ (analogous to the electronic band structure $E(k)$ in semiconductor crystals). The optical modes in this structure are Block waves, i. e. functions that have the periodicity of the lattice with an additional phase factor $\exp(ik \cdot r)$(Fig. 9).
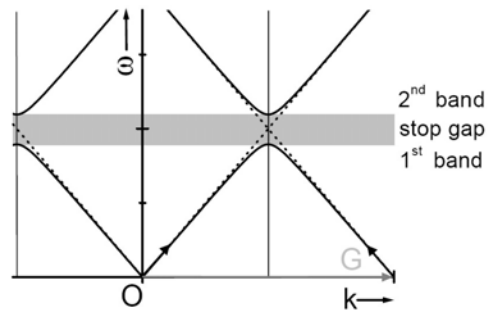
Fig. 9: *The band structure is obtained from a two-band model*

The periodic structure can diffract a wave, thereby shifting the dispersion relation by a reciprocal lattice vector. This implies that for any k-vector in reciprocal space the dispersion relation can always be shifted back to the first Brillouin zone by adding or subtracting an integer number of reciprocal lattice vectors. By making use of all symmetries of the lattice it suffices to specify the band structure in the irreducible part of the Brillouin zone [13] only. In general the band structure is only plotted along the characteristic path of the irreducible part of the Brillouin zone, i. e. a line following all edges of the irreducible part. In practice [13], all maxima and minima of the band structure lie on this characteristic path. Hence the existence and frequency range of a photonic bandgap can be deduced from a plot of the band structure along the characteristic path.

2. 3 Bragg reflection in periodic structures

Bragg reflection plays a prominent role in optical experiments on photonic crystals. It occurs whenever there is constructive interference of waves reflected from a set of lattice planes, as illustrated in Fig. 10.
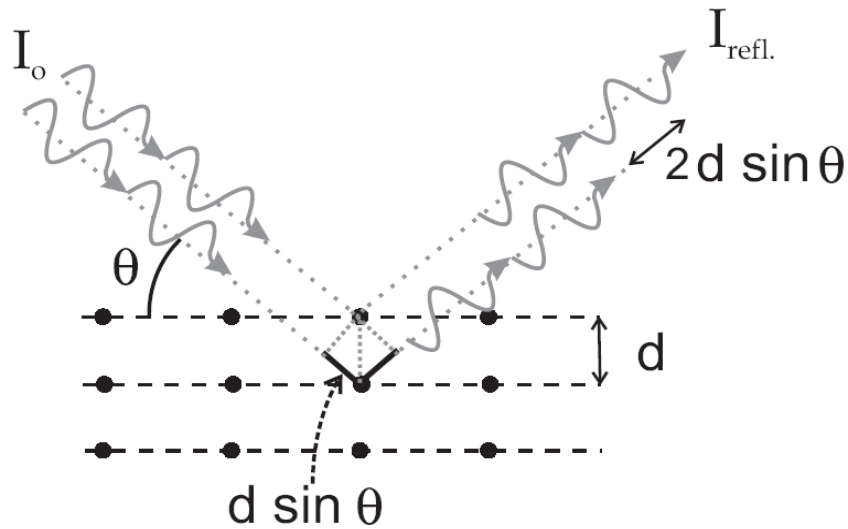
Fig. 10: *Bragg reflection occurs when light reflected from a set of lattice planes interferes constructively, the extra path length indicated by the thick line equals an integral number of wavelengths.*

The reflection appears only for specific wavelengths λ and angles θ, given by Bragg's law:

$$2d \sin\theta = n\lambda$$

Here d denotes the distance between the set of lattice planes responsible for Bragg reflection, θ is the angle of incidence, n is the order of the Bragg reflection and λ denotes the wavelength. The Bragg peak of an infinite photonic crystal designed for optical wavelengths displays a certain spectral width, in contrast to the Bragg peaks observed in ordinary x-ray diffraction. This is due to the fact that only a limited number of lattice planes are involved in the Bragg reflection taking place in a photonic crystal, which is caused by the high index contrast between the materials used.

If a crystal is sufficiently well ordered that the reflections from many lattice planes interfere constructively, then the Bragg reflection will be very strong. The associated extinction will be very large, increasing exponentially with sample thickness. Light cannot

propagate in the direction of Bragg reflection: the Bragg reflections correspond to the stop gaps in the photonic band structure.

If light is strongly diffracted by the scatterers, then a small number of lattice planes suffice to reflect an incident wave. The wavelength λ and angle θ then do not need to conform to Bragg's law exactly: the interference still will be constructive for the limited number of lattice planes involved. As consequence, the Bragg reflections extend over a range of frequencies, corresponding to the width of the stop gaps.

2. 4 Distributed feedback (DFB)

In general, a material can provide such feedback by having either a modulated gain constant or a modulated index of refraction. Figure 11 shows a simplified diagram explaining the functioning of a distributed feedback system. In this figure two arrows are drawn representing light waves, one is travelling to the left and the other to the right. At each point along the structure each wave is receiving energy from the wave travelling in the opposite direction through backwards Bragg scattering. This is distributed feedback. If the material in which the waves are travelling also has gain then the proper conditions for an oscillation, or standing wave, will be present [14]. The reason why this system can output a spectrally narrow beam is that Bragg refection is wavelength sensitive so that only a narrow range of wavelengths will provide feedback to the system.
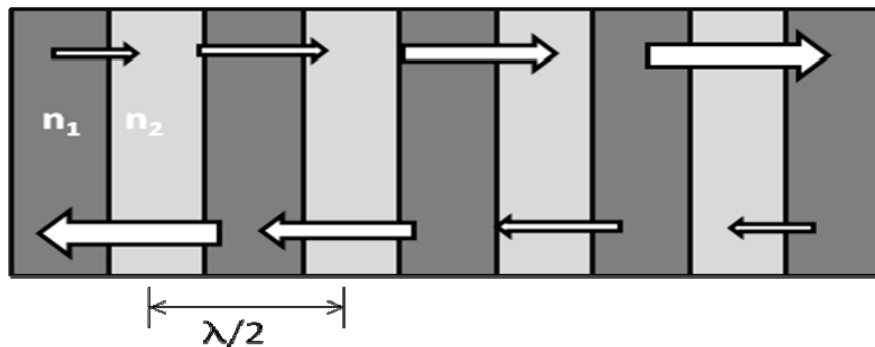
Fig. 11: *Scheme of the DFB mechanism in a 1D periodic structure.*

In order to utilize such a system one must know what the resonant frequencies are and what their corresponding threshold gains are. To answer these questions is not simple task, it involves a lengthy derivation which was completed by Kogelnik and Shank [14] . In this thesis I will discuss a system in which the feedback comes from a modulated index of refraction and not from a modulated gain constant the resonance with the lowest associated gain threshold is expected to be located just outside of the stop band of the material [14]. Also, this theory predicts that the spectral width $\Delta\lambda$ of the laser beam emitted from the system at resonance will be inversely proportional to the length of the device.

Kogelnik and Shank [15] were the first to report laser action in mirrorless periodic Bragg DFB structures. Laser action in chiral liquid crystals was predicted by Goldberg and Schnur in 1973 [16] and firstly observed by Il'chishin et al. in 1981 [17] being explained using the distributed feedback theory [15]. In a distributed feedback (DFB) laser the laser modes receive feedback at one specific wavelength (and to a smaller extent, its harmonics), determined by the grating period of the structure. While the mode is propagating along the structure a small part of its energy is reflected (i.e. coupled into the counter-propagating mode)

2. 5 Cholesteric as 1D photonic crystal

Among many photonic bandgap (PBG) structures, liquid crystals with periodic structures are very attractive as self-assembled photonic crystal[20], leading to optical devices such as dye laser[21,22].

The birefringence and natural ability to form periodic structures make chiral liquid crystals interesting one-dimensional photonic bandgap materials. In fact, chiral liquid crystals (CLC) possess a helical superstructure which provides a 1D spatial modulation of the refractive index giving rise to Bragg selective reflection for circularly polarized light having the same handedness as the LC structure. In PBG microstructures light can be confined and manipulated by engineering quasi-ideal distributed feedback (DFB) micro-resonators [23,24]. In a CLC doped with fluorescent guest molecules, the spontaneous emission is suppressed for the reflection stop band and it is enhanced at the band edges

where a series of narrow long-lived transmission modes are expected [25]. Within the bandgap, the wave is evanescent and decays exponentially, so that the density of states (DOS) within the gap vanishes in large structures. At the stop band edges the density of states is expected to diverge. The group velocity v_g is real, and at the photonic band edge tends to zero, while the photon dwell time is greatly increased, so that the gain is significantly enhanced at these spectral positions [26].
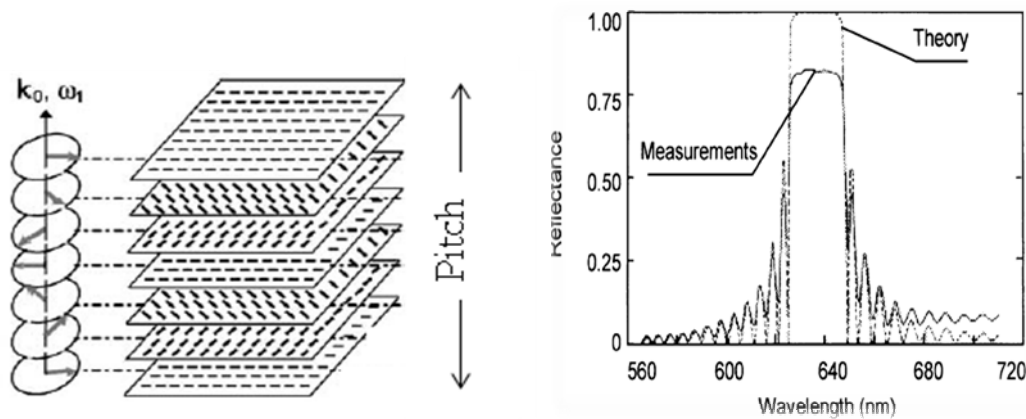
Fig. 12: *Molecular structure and the photonic bandgap structure of cholesteric liquid crystal*

In the next chapter I will present a detailed physical characterization of organic distributed feedback microcavity lasers. This optical microcavity was obtained by confining self-organized cholesteric liquid crystal doped with fluorescent guest molecules into different confinement geometries. The chiral liquid crystal act as mirrorless cavity lasers, where the emitted laser light propagates along the liquid crystal helical axis behaving as Bragg resonator.

3. Disordered scattering media

3. 1 Single scattering

Propagation of light inside a homogeneous material is simple: light propagates in straight trajectories. Eventually, optical absorption may occur and the light intensity decays exponentially as the wave travels in the medium. If the wave encounters an inhomogeneity it is scattered, and changes its direction of propagation. A scatterer can be an atom with polarizability φ, or a particle of refractive index *n*, or a density fluctuation in a liquid or gas. The scattering cross section of the scatterer σ_s is defined as the amount of light removed from the incident beam by scattering.

Depending on the size of the scatterer *r* relative to the wavelength λ_o, the scattering can be classified in three different types: Rayleigh scattering, Mie scattering, and geometrical-optics scattering.

Rayleigh scattering is the scattering by particles much smaller than the optical wavelength, like for instance atoms and molecules. In this regime the scattering is very inefficient and the cross section is given by [27]:

$$\sigma_S = \frac{8}{3}\pi\varphi^2 k_0^4$$

where φ is the polarizability and the wave vector in vacuum is given by $k_o = 2\pi/\lambda_o$.

If the size of the scatterer is of the order of the wavelength then σ_s is maximal. This regime is known as Mie scattering. The determination of the Mie cross section is far from trivial and it was calculated numerically for objects with a high degree of symmetry, as spheres or cylinders [27]. In general, σ_s is larger when the refractive index contrast *m* between the scatterer and the surrounding medium is higher.

If the size of the scatterer is much larger than the wavelength then its scattering cross section is equal to two times its geometrical cross section. This is the geometrical-optics regime, and the scattering is described by Snell's law [28].

3. 2 Multiple scattering and light localization

The scattering mean free path, l_s , in a medium, is defined as the average distance between two consecutive scattering events. If the medium is larger than l_s the single scattering approximation is not valid. Multiple scattering takes place. Depending on the arrangement of the scatterers, two limiting cases of multiple scattering media can be distinguished: crystals on one side and random or disordered media on the other. A disordered medium has a random distribution of scatterers. The photonic or scattering strength in a disordered scattering medium is described by the inverse of the localization parameter kl_s (also known as the Ioffe-Regel parameter [29]):

$$kl_S = \frac{2\pi}{\lambda_0} n_e l_S$$

where k is the wave vector in the medium, and n_e is the effective refractive index of the medium.

The scattering mean free path is, to a first approximation (independent scattering approximation), given by:

$$l_S = \frac{1}{\rho \sigma_S}$$

where ρ is the density of scatterers and σ_s is the average scattering cross section.

In a weakly scattering medium we have $kl_s \gg 1$. The photonic strength can be increased by reducing l_s, which is achieved by maximizing the scattering cross section.

In the weak scattering limit, that is when the scatterers density is low, and/or when the scattering cross section is small, the transport of light is well described by the diffusion

equation. The wave diffuses in the medium as electrons do in a disordered metal. The main approximation of the diffusion approach is to neglect any interference of the wave propagating along different paths. When the scattering becomes strong, interference plays an important role.

By using the diffusion equation a great simplification is achieved in the macroscopic description of the wave propagation [30] (i.e. on length scales larger than l_s). The main approximation that the diffusion approach does is to neglect any interference effect.

The main aspect of the diffusion approximation can be considered by looking at the average intensity I_{AB} in a point Q produced by a source located in a point P, as shown in Figure 13.
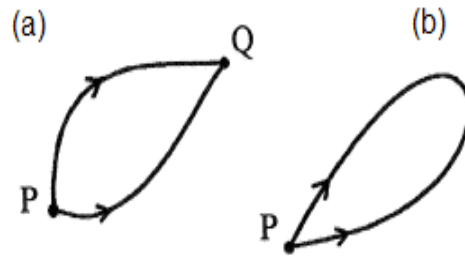
Fig. 13: *(a) The intensity at point Q due to a source in P is given by the sum of intensities of all possible paths leading from P to Q. (b) If Q is overlapped with P an interference contribution appears.*

By average intensity is meant the ensemble average or the intensity averaged over all possible positions of the scatterers.

The wave can propagate along many different optical paths, but for simplicity, only two of these paths are represented. The lines representing the optical paths in Fig.13 correspond to the wave vector of the scattered waves.

Inside any multiple scattering medium, the intensity at the point Q is given by the square of the sum over a suitably normalized amplitudes of waves following all possible scattering paths connecting P to Q

$$I = \left| \sum_i A_i (P \rightarrow Q) \right|^2$$

Since each path gives a different phase shift to the wave, on average, the cross terms in the square will cancel out and the intensity at Q will be given by the sum of the squared amplitudes (meaning that the interference contribution is absent)

$$I = \sum_i \left| A_i (P \rightarrow Q) \right|^2$$

In the case for which Q coincides with P, the scattering path can be crossed in opposite direction. A wave traversing the path in one direction will interfere constructively with a wave crossing the path in the other direction, which doubles the total intensity at P. Thus, the probability to return to the initial position is twice as large as one would expect (without taken into account interference).

In a real system there are many possible optical paths, and the interference term leads to the characteristic speckle pattern that can be observed on the transmitted or reflected light. Speckles are the bright and dark spots formed by the scattered light and they give to the transmission and reflection its granular aspect [31]. If the intensity is averaged over all possible realizations of the disorder, the interference term, or speckle, vanishes. This vanishing of the speckle occurs because on average the interference term cancels out since the contribution of constructive and destructive interference are equal. When neglecting the interference term is the sum of the intensities of the waves diffusing along different paths. Therefore, the diffusion approximation does not make any distinction between diffusing particles or wave intensities. The wave diffuses in a 3D medium with a diffusion constant D_B given by:

$$D_B = \frac{1}{3} v l_B$$

where v is the energy velocity or the rate at which the energy is transported, and l_B is the Boltzman mean free path or the length over which the direction of propagation of the wave is randomized by scattering in the absence of interference.

However, in a random medium there is always an interference contribution that survives (even for weakly scattering media) the averaging over different configurations of the disorder. This interference originates from closed paths (Fig. 13). For each closed path a wave emitted at the source P can return to the same point after propagating along two reversed paths, I and II. These paths are called time-reversed paths. This effect is called weak localization, since it is believed to be the precursor of Anderson localization or strong localization.

Similar to photonic crystals, direct and inverse random media can be realized. A direct medium or disordered opal consists of a powder of particles in air; while an inverse random media is a sponge like material in which air voids are surrounded by the material with high refractive index.

3. 3 Weak localization of light

Interference of light in random dielectric systems influences the transport of light in a way that is similar to the interference that occurs for electrons when they propagate in disordered conducting materials.

One of the most robust interference phenomena that survives multiple scattering is coherent backscattering or weak localization of light [32,33]. In weak localization, interference of the direct and reverse paths leads to a net reduction of light transport in the forward direction, similar to the weak localization phenomenon for electrons in disordered (semi)conductors and often seen as the precursor to Anderson (or strong) localization of light [34]. Weak localization of light can be detected since it is manifest as an enhancement

of light intensity in the backscattering direction. This substantial enhancement is called the cone of coherent backscattering.

Weak localization has been initially studied for electronic systems, in the 1970s, where it has been reported as quantum interference (coherent echo) between electronic waves multiple scattered by impurities in conductors [35]. Weak localization manifests itself as an anomaly of the resistance of a conducting thin film [36]. In electronic systems it has arisen much interest, as it is one of those unique cases where the superposition principle of quantum mechanics leads to observable consequences in the properties of macroscopic systems [37].

At the beginning of the 1980s, this concept based on interference has been successfully exported also to light waves, which instead of electrons show very weak photon to photon interaction, have a much longer coherence time and are extremely sensitive to interference effects. On the other hand in optical experiment, it is hard to measure quantities like the total conductance, but it is possible, due to the long coherence length, to observe its counterpart, i.e. directly the interference-induced increase diffusion in backscattering: the coherent backscattering cone.

Since the first experimental observation of coherent backscattering from colloidal suspensions, the phenomenon has been successfully studied for electromagnetic waves in strongly scattering powders [38], cold atom gases [39], two-dimensional random systems of rods [40], randomized laser materials [41], disordered liquid crystals [42], chaotic cavities [43] photonic crystals [44] and even sea bottom. The phenomenon is typical of any wave which is multiply scattered, and it has indeed been observed also for mechanical waves: acoustic waves in macroscopic disordered systems and even seismic waves propagating in the earth crust.

Weak localization has its origin in the interference between direct and reverse paths in the backscattering direction. When a multiply scattering medium is illuminated by a laser beam, the scattered intensity results from the interference between the amplitudes associated with the various scattering paths; for a disordered medium, the interference terms are washed out when averaged over many sample configurations, except in a narrow

angular range around exact backscattering where the average intensity is enhanced. This phenomenon, is the result of many two-waves interference patterns

$$I(\theta,\phi) = I_0 (1 + \zeta \cos(d \cdot \Delta k))$$

where I_0 is the total intensity forgetting interferences, ζ the contrast of the interference, θ and ϕ the angles with respect to the backscattering direction, and we assume no additional phase difference along the reverse paths exists. The incident and scattered *k*-vector k_i and k_f are written as

$$k_i = (0, 0, k)$$

$$k_f = (- k \sin \theta \cos \phi, - k \sin \theta \sin \phi, - k \cos \theta)$$

This interference is generated by counter-propagating light paths with entering-exiting distance $d = r_1 \_ r_N$ and initial and final *k*-vectors k_i, k_f such that $\Delta k = k_f + k_i$ (see Fig. 14). Maximum interference is obtained when the counter-propagating paths have the same amplitude (and thus $\zeta = 1$), and only at $\theta = 0$.
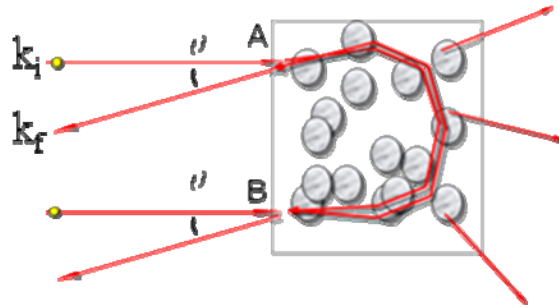
Fig. 14: *counter propagating light paths that give rise to weak localization (coherent back scattering)*

3. 4 Anderson (strong) localization

Anderson predicted in 1958 a transition in the diffusive transport of electrons in metals, in particular, in lattices where disorder was introduced as impurities [45]. The transition changes the electrons transport from classic diffusion (what happens in a copper

wire for example) to the absence of diffusion. Experimental evidence of this prediction was found in the following years when studying this transition in conducting materials. The electric conductivity σ decayed exponentially with the length of the system when the Anderson localization regime was reached [46]. The Anderson transition means that a conductor becomes an insulator, because the wave function of electrons is localized inside the sample, stopping the classic diffusion. The origin of this effect is the multiple scattering of the electrons by defects in solids.

The same effect is present for photons in strongly disordered dielectrics, with the great advantage that no interaction is present for photons with respect to electron-electron interaction in the electronic case. This fact can make photonic systems more suitable for studying Anderson localization than electronic ones. On the contrary obtaining the same scattering efficiency with respect to electronic solids is not so easy in dielectrics. The proposal of John for photonic crystals derived from the necessity to design a strongly scattering dielectric system to study Anderson localization of photons.

Experimental proofs for the existence of localization of light in the near infrared was given in 1997 by Wiersma *et al.* [47], where *GaAs* powder, with particles dimension of $\sim$ 300 nm was used. To obtain localization in a 3D sample, the transport mean free path l_t (the length over which the light has lost its original direction completely) is subject to the Ioffe-Regel condition [48]

$$kl_t \leq 1$$

Localization means that the diffusion mechanism of photons is stopped, and the light is trapped inside the sample. The transmission of the sample (without absorption) will be

$$T = T0 \exp(-L/\xi)$$

where L is the length of sample and ξ is the *localization length*, that represents the critical dimension for a sample to have localized states. Fig. 15 shows schematically what happens to photons in the localized regime. If A is a point source inside a strongly scattering medium, subject to the Ioffe-Regel condition, two waves that propagates in opposite directions along this loop will acquire the same phase shift and so they interfere

constructively. Far from the localization, loops of this type have very low probability to exist and classical diffusion dominates
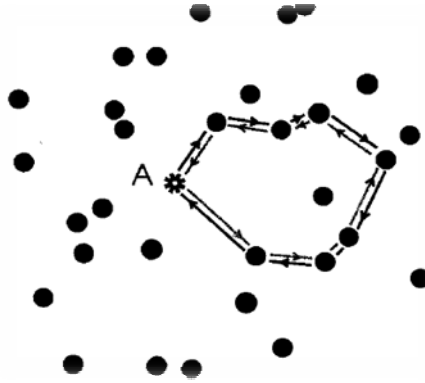
Figure. 15: *Anderson localization is caused by constructive interference of time reversed waves if the Ioffe-Regel criterion is fulfilled in a 3D system. The diffusion is stopped and the light is localized in loops.*

.

3. 5 Anisotropic Coherent Backscattering in Nematic Liquid Crystal

In the last decay, a lot of study has been done in the propagation of light in disordered multiply scattering systems. The physical condition to have light diffusion is simply $\lambda \ll l_t \ll L$, meaning that we have to stay away from Anderson transport and also that the sample dimensions L have to be longer with respect to transport mean free path to be in the multiple scattering regime. From a diffusive sample we can perform measurements from which we extract the transport mean free path, using the coherent backscattering technique [33], or we can measure the diffusion constant D with a time-resolved experiment [49]. These two are related if one supposes to have isotropic diffusion in three dimensions by

$$D(\omega) = 1/3 v_e(\omega) \, l_t(\omega)$$

v_e is called energy velocity (it describes the transport of the electromagnetic energy). It can be of the order of the phase velocity c/n for many dielectric systems, but can be also $10^{-5}c$, as happens for a cold cloud of rubidium atoms.

It was demonstrated that for applications one can add some optical gain to these systems to obtain an optical device. What we have in this way is a *random amplifying medium* or what is called today a *random laser* that will be the mean subject of the forth chapter of this thesis. In this chapter I will present the first observation of random lasing in nematic liquid crystals.

Liquid crystals in the nematic phase are strongly scattering materials. The nematic phase of a liquid crystal is characterized by a global alignment of the molecules in a direction called the nematic director n(r), and an otherwise translational disorder. The strong opacity of the nematic phase comes about from local fluctuations in the nematic director $n(r; t) = n_0 + \delta n(r; t)$, that elastically scatter light [20]. Transmission experiments have shown that light transport in ordered nematic liquid crystals indeed shows anisotropic features, both in static and dynamic experiments, and that diffusive models and radiative transfer theory can describe light transport in such a complex medium [50].

Pioneering experiments on coherent backscattering from nematics have been performed, and the existence of the interference phenomenon could be confirmed. Anisotropy in coherent backscattering due to an anisotropic transport mean free path has been predicted numerically in Monte-Carlo simulations [51]. Recently, Wiersma and his group observed an anisotropic behavior in weak localization from ordered nematic liquid crystals. They demonstrated that the backscattering cone profile exhibits an angular anisotropy dependence on the direction of the nematic director (Fig.16).

This study opens the way for further investigation on light transport in such a complex medium. Multiple light scattering in these media is a recent subject of fundamental investigation as they are suitable candidates to observe anisotropic light transport and to study anisotropic interference phenomena.
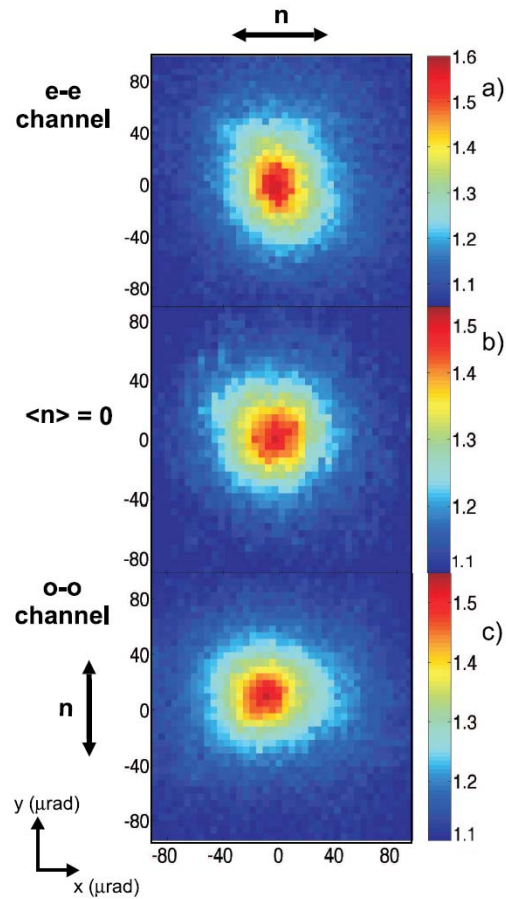
Figure. 16: *Coherent backscattering cones in polar colour plots from nematic liquid crystal for three cases of the nematic director. Top: nematic director in x, bottom: director in y, middle: polydomain phase. The anisotropy in the backscattering cone is clearly visible. The polarization is in the x-direction in all cases.*
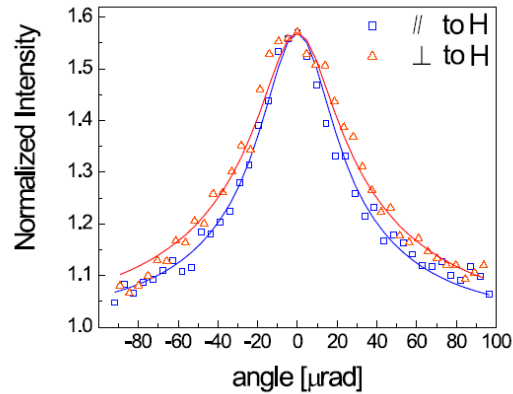
Figure 16: *Coherent backscattering from a monodomain nematic for both orthogonal scanning directions, in a linear plot. Nematic director and polarization in the x-direction[].*

The diffusion and transport of light waves in complex dielectric structures have spurred a vast range of experimental and theoretical work, revealing one of the most challenging and exciting scientific area of the past decade. The propagation of electromagnetic waves in periodically structured dielectric systems, i.e. photonic bandgap materials, and the linear and non-linear optical phenomena in completely disordered systems doped with gain media represent two opposite sides of this promising scientific branch. The literature demonstrates that much has been done in these extreme areas, but the huge intermediate world constituted by the partially ordered systems still remains almost unexplored. In the next chapters I will report about the laser emission in periodic, partially ordered systems and totally disordered media.

References:

[1]http://images.google.it/imgres?imgurl=http://upload.wikimedia.org/wikipedia/commons/thumb/6/65/Blue_morpho_butterfly.jpg/300px

[2] Lord RAYLEIGH, *Math. Soc. Proc.* xi., p. 57, 1880.

[3] E. Yablonovitch, Pys. Rev. Lett. 58, 2059 (1987).

[4] S. John, Pys. Rev. Lett. 58, 2486 (1987).

[5] E. M. Purcell, Phys. Rev. 69, 681 (1946).

[6] A. R. Parker *et al.*, Aphrodite's iridescence, *Nature* 409, 36 (2001).

[7] M. Ghulinyan *at al.*, Porous silicon free-standing coupled microcavity, *Appl. Phys. Lett.* 82, 1550 (2003).

[8] O. Bisi, S. Ossicini and L. Pavesi, Porous silicon: a quantum sponge structure for silicon based optoelectronics, *Surf. Sci. Rep.* 38, 1 (2000).

[9] E. Yablonovitch and T. J. Gmitter. Photonic band structure: the face-centered-cubic case. *Physical Review Letters*, 63(18):1950-1953, 1989.

[10] K. M. Leung and Y. F. Liu. Photonic band structures: The plane wave method. *Physical Review B*, 41(14):10188-10190, 1990.

[11] K. M. Ho, C. T. Chan, and C. M. Soukoulis. Existence of a photonic band gap in periodic dielectric structures. *Physical Review Letters*, 65(25):3152-3155, 1990.

[12] E. Yablonovitch, T. J. Gmitter, and K. M. Leung. Photonic band structure: the face-centered cubic case employing non spherical atoms. *Physical Review Letters*, 67(17):2295-2298, 1991.

[13] L. P. Bouckaert, R. Smoluchowski, and E. Wigner, *Theory of Brillouin zones and symmetry properties of wave functions in crystals*, Phys. Rev. 50, 58 (1936).

[14] H. Kogelnik and C. V. Shank, J. Appl. Phys. 43, 2327 (1972).

[15]H. Kogelnik and C. V. Shank, Appl. Phys. Lett. 18, 152 (1971).

[16] L. S. Goldberg, J. M. Schnur, U.S. Patent No. 3,771, 065 (1965)

[17] I.P. Il'Chishin, E. A Tikhonov, V. G. Tishchenko, M. T. Shpak, JETP Letters 32, 27 (1981)

[18] Yablonovitch, E. Inhibited spontaneous emission in solid-state physics and electronics. *Phys. Rev. Lett.* 58, 2059–2062 (1987).

[19] Joannopoulos, J. D., Villeneuve, P. R. & Fan, S. Photonic crystals: putting a new twist on light. *Nature* 386, 143–149 (1997).

[20] De Gennes, P. G. & Prost, J. *The Physics of Liquid Crystals* 2nd edn, Ch. 6 (Clarendon, Oxford, 1993).

[21] Kopp, V. I., Fan, B., Vithana, H. K. M. & Genack, A. Z., Low-threshold lasing at the edge of a photonic stop band in cholesteric liquid crystals. *Opt. Lett.* 23, 1707–1709 (1998).

[22] Song, M. H. *et al.* Effect of phase retardation on defect mode lasing in polymeric cholesteric liquid crystals. *Adv. Mater.* 16, 779–783 (2004).

[23] W. Cao, A. Munoz, P. Palffy-Muhoray and B. Taheri, Nature Mat. 1, 111 (2002).

[24] J. Schmidtke, W. Stille, H. Finkelmann and S. T. Kim, Adv. Mat. 14, 746 (2002).

[25] J. Schmidtke, W. Stille, eur. Phys. J. B 31, 179 (2003).

[26] V. I. Kopp, Z. Q. Zhang and A. Z. Genack, Phys. Rev. Lett. 86, 1753 (2001).

[27] C. F. Bohren and D. R. Huffman, "absorption and scattering of light by small particles" John Wiley & Sons, New York, (1983).

[28] H. C. van de Hulst, Light scattering by small particles, Dover, New York, (1981).

[29] A. F. Ioffe and A. R. Regel, Prog. Semicond. 4, 237 (1960).

[30] M. B. Van der Mark, Propagation of light in disordered media, PhD thesis (1990)

[31] A. Lagendijk, Bart A. van Tiggelen, Physics reports 270, (1996).

[32] M.P. van Albada and A. Lagendijk, Observation of Weak Localization of Light in a Random Medium, Phys. Rev. Lett. 55, 2692 (1985)

[33] P.E. Wolf and G. Maret, Weak Localization and Coherent Backscattering of Photons in Disordered Media, Phys. Rev. Lett. 55, 2696 (1985).

[34] A.Z. Genack and N. Garcia, Observation of photon localization in a threedimensional disordered system, Phys. Rev. Lett. 66, 2064 (1991)

[35] An introduction to electronic weak localization can be found at http://physics1.usc.edu/%7Ebergmann/.

[36] E.Abrahams, P.W.Anderson, D.C.Licciardello and T.V.Ramakrishnan, Scaling Theory of Localization: Absence of Quantum Di_usion in Two Dimensions, Phys. Rev. Lett. 42, 673 (1979)

[37] S. Chakravarty and A. Schmid, Weak localization: The quasiclassical theory of electrons in a random potential, Phys. Rep. 140 4, 193-236 (1986).

[38] D.S. Wiersma, M. P. van Albada, B. A. van Tiggelen, and Ad Lagendijk, Experimental Evidence for Recurrent Multiple Scattering Events of Light in Disordered Media, Phys. Rev. Lett. 74 4193 (1995).

[39] Y. Bidel, B. Klappauf, J. C. Bernard, D. Delande, G. Labeyrie, C. Miniatura, D. Wilkowski, and R. Kaiser Coherent Light Transport in a Cold Strontium Cloud, Phys. Rev. Lett. 88, 203902 (2002).

[40] I. Freund, M. Rosenbluh, R. Berkovits, and M. Kaveh Coherent Backscattering of Light in a Quasi-Two-Dimensional System, Phys. Rev. Lett. 61, 1214 (1988).

[41] D.S. Wiersma, M.P. van Albada, and A. Lagendijk, Coherent Backscattering of Light from Amplifying Random Media, Phys. Rev. Lett. 75, 1739 (1995).

[42] D.V. Vlasov, L.A. Zubkov, N.V. Orekhova, V.P. Romanov, Weak localization due to scattering of light in nonoriented liquid crystals, Pisma Zh. Eksp. Teor. Fiz. 48, 86 (1988) [JETP Lett. 48, 91 (1988)].

[43] J. de Rosny, A. Tourin, and M. Fink, Coherent Backscattering of an Elastic Wave in a Chaotic Cavity, Phys. Rev. Lett. 84, 1693 (2000).

[44] A.F. Koenderink, M. Megens, G. van Soest, W.L. Vos and A. Lagendijk Enhanced backscattering from photonic crystals, Phys. Lett. A. 268, 104-111 (2000).

[45] P. W. Anderson, Absence of diffusion in certain random lattices, *Phys. Rev.* **109**, 1492 (1958).

[46] N. Giordano, W. Gilson and D. E. Prober, Experimental study of Andersonn localization in thin wires, *Phys. Rev. Lett.* **43**, 725 (1979).

[47] D. Wiersma, P. Bartolini, A. Lagendijk and R. Righini, Localization of light in a disordered medium, *Nature* **390**, 671 (1997).

[48] N. F. Mott, Electrons in disordered structures, *Adv. Phys.* **16**, 49 (1967).

[49] D. S. Wiersma, A. Muzzi, M. Colocci, and R. Righini, Time-resolved experiments on light diffusion in anisotropic random media, *Phys. Rev. E* **62**, 6681 (2000).

[50] V.P. Romanov and A.N. Shalaginov, Opt. Spectrosc. 64, 774 (1988)

[51] A. Heiderich, R. Maynard, and B.A. van Tiggelen, Multiple light scattering in ordered nematic liquid crystals, J. Phys. II (France) 7, 765 (1997).

DFB Micro-cavity Lasers
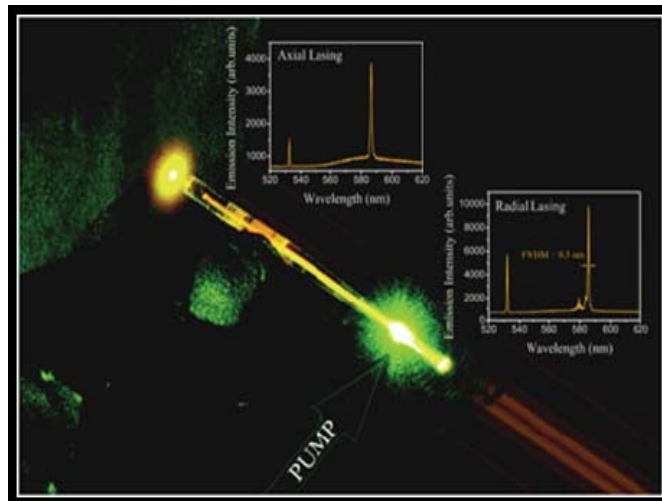
1.   Conventional Distributed Feedback Systems

The propagations of electromagnetic waves in dielectric periodic structures, represents a topic of great interest in various field of scientific research. Periodic structures, namely "photonic crystals" that strongly localize light, have recently attracted considerable attention because of their potential applications in display, telecommunications, and fiber optics technology[1,2]. One of the more attractive topic of photonic bandgap media has been the study of stimulated emission, with the purpose of realizing low threshold laser devices. In 1D structures, laser emission has been predicted at the photonic band edge,[3] and optically active chiral liquid crystals have recently been used to provide feedback for mirrorless organic lasers. The consideration of chiral liquid crystals as photonic gap medium has stimulated observation and investigation of lasing in cholesteric liquid crystals[4-6], lyotropic cholesteric LCs[7], ferroelectric chiral smectic C LCs[8,9],network polymers[10], elastomers[11] and blue phases[12].The idea of building organic mirrorless laser is not new, in fact several years ago Kogelnik and Shank [13] were the first to report laser action in periodic distributed feedback structures which do not utilize the conventional cavity mirrors but provide optical feedback via backward Bragg scattering, while laser action in chiral liquid crystals was proposed by Goldberg and Schnur in 1973[14].

Liquid crystals are promising photonic band gap materials. It is known that some of chiral liquid crystals such as cholesteric LCs naturally form helical structures with the helical pitch in the optical wavelength range[15]. Consequently, this periodicity gives rise to photonic band structures. The periodicity of the LC helix is very sensitive to its environment, such as the nature of the chiral dopant, temperature, mechanical stress and field conditions. This tunability of the photonic band is one of the remarkable features, that provide the possibility of controlling photonic phenomena.

Because of the birefringence and periodic structure, cholesteric liquid crystals are one dimensional photonic band gap materials. They possess a helical superstructure which provides a 1D spatial modulation of the refractive index giving rise to Bragg selective reflection for circularly polarized light having the same handedness as the LC structure. In PBG microstructures light can be confined and manipulated by engineering quasi-

ideal distributed feedback (DFB) micro-resonators [10]. In a CLC doped with fluorescent guest molecules, the spontaneous emission is suppressed for the reflection stop band and it is enhanced at the band edges where a series of narrow long-lived transmission modes are expected [16]. Within the bandgap, the wave is evanescent and decays exponentially, so that the density of states (DOS) within the gap vanishes in large structures. At the stop band edges the density of states is expected to diverge. The group velocity v_g is real, and at the photonic band edge tends to zero, while the photon dwell time is greatly increased, so that the gain is significantly enhanced at these spectral positions [17]. This gain enhancement together with distributed feedback mechanism can give rise to low threshold mirror-less lasing at the band edge in a variety of liquid crystal materials. In chiral liquid crystals the index modulation is relatively low so that sufficient feedback can be achieved by increasing the length of the resonant cavity. Thousands of periods are needed in order to obtain an optical cavity with a quite high quality factor, *Q* [18].

This chapter contain two big sections: in the first part we report the study of the light emission properties from novel fiber-like cylindrical microcavities hosting helixed liquid crystals doped with fluorescent guest molecules. In the second part we present a preliminary physical characterization of a novel array of organic distributed feedback microcavity lasers possessing a high ratio between the quality factor Q of the resonant cavity and its volume V. This optical microcavity was obtained by confining self-organized mesophases doped with fluorescent guest molecules into polarization holography patterned polymeric microchannels. The liquid crystal microchannels act as mirrorless cavity lasers, where the emitted laser light propagates along the liquid crystal helical axis behaving as Bragg resonator.

2.   Cylindrical Microcavity Lasers

Confinement of light in a small volumes has important implications for optical emission properties: it changes the probability of spontaneous emission from atoms, allowing both enhancement and inhibition[19]. In this section we present a study of the light emission properties from novel fiber like cylindrical microcavities hosting helixed liquid crystals doped with fluorescence guest molecules. The aim of this study is to gain

understandings about the role played by the number of helical periods, the influence of the CLC bulk volume and various surface treatments on the quality factor of the periodic mirrorless resonant system.

The cylindrical confinement of CLC ensures an increase of the axial resonant cavity length, while maintaining a small modal volume. Cylindrical geometry favors the existence of a very complex structure of the chiral liquid crystal as evidenced by optical and structural investigations which will be reported elsewhere[20]. The long-range periodicity guarantees the enhancement of distributed feedback mechanism in these systems which is behind the observed low-threshold tunable lasing action. The cylindrical microcavities are represented by capillary glass tubes with various diameter values ranging from 20 up to 200 µm(Fig. 1).
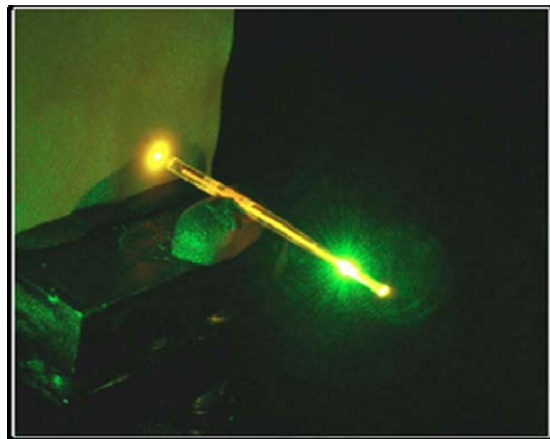
Fig.1: *Lasing action from optically pumped (532nm) cylindrical microcavity.*

2. 1 Experimental set-up

The geometry confinement used in these experiments is a cylindrical microcavities which are presented by capillary tubes. The diameter of these cylinder glass tubes ranging from 20 to 200µm. Several chemical treatments were applied to the inner surface of the cylindrical microcavities in order to induce a privileged molecular alignment for the liquid crystal. In this case the helical structure is oriented parallel to the cylindrical main axis.

Different chemical treatments used are mixtures of DMOAP (0.1% wt N,N-dimethyl-N-octadecyl-3- aminopropyltrimethoxysilyl chloride in isopropanol), orthochromic mixture (20% wt $K_2Cr_2O_7$ in H_2SO_4), ACM72 (0.1% wt in water), lecityne and polyimide which were used in different concentrations to induce axial alignment of the chiral liquid crystal helix in the proximity of the boundary surface. Experimental investigations show that polyimide treated cylindrical capillary tubes provide the strongest surface-liquid crystal interaction and alignment for the liquid crystal. The cylindrical tubes were filled by capillarity with a mixture M_1 of 99.7% BL094 right handed cholesteric liquid crystal (provided by merck) and 0.3% of Pyrromethene 597 (provided by exciton). The cholesteric liquid crystal used had a birefringence $\Delta n = 0.21$ and showed an optical band gap which spans from 525 to 585nm. The high efficiency region of the pyrromethene dye spectrum and the red-edge stop band of the cholesteric liquid crystal BL094 present very close spectral positions which maximizes the gain. The spectrum show an overlapping which could present the inconvenient of confusing the eventual amplified spontaneous emission effect with laser action, a second mixture M_2 was prepared by adding to M_1 a small percentage of BL001 nematic liquid crystal (Merck). As a result, the low-energy band edge red-shifted to 607 nm.

The cylindrical microcavity was optically pumped with 3 ns pulses produced by a frequency-doubled (532 nm) Nd YAG: yttrium-aluminum-garnet laser (NewWave, Tempest 20). The pump beam was focused by means of a cylindrical lens ($f =100$ mm) perpendicular to the axial sample direction. other optical instruments are used to select all the polarization states. The experimental setup is presented in figure 2. The light emission was collected within a restricted cone angle of 0.2 rad by using a multichannel charge-coupled device (CCD) (Jobin-Yvon, Micro-HR). By pumping the cylindrical tubes at low pump energy a dip in the spontaneous emission spectra occurred at the position of the stop band (Fig. 3). This indicate that PBG structure of the self-organized liquid crystal material severely modified the fluorescence spectrum of the laser dye molecules. By increasing the pump energy above a certain threshold value, a highly directional laser action was observed at the red edge of the stop band. The laser emissions were found to be circularly polarized, which indicates that distributed

feedback mechanisms take place through circular Bragg reflection. This level of confinement allows obtaining interesting emission properties: laser action is exhibited both in the axial and radial directions at different spectral positions indicating that waveguide effects are not responsible of the multidirectional emission. A striking point is represented by the spontaneous reconstruction of the helixed liquid crystal superstructural configuration inside the cylindrical microcavity, giving rise to a novel three-dimensional (3D) multidirectional lasing system. This complex system keeps the advantage of a 3D blue phase-like matrix while providing a wider thermal operating range and laser action wavelength tenability.
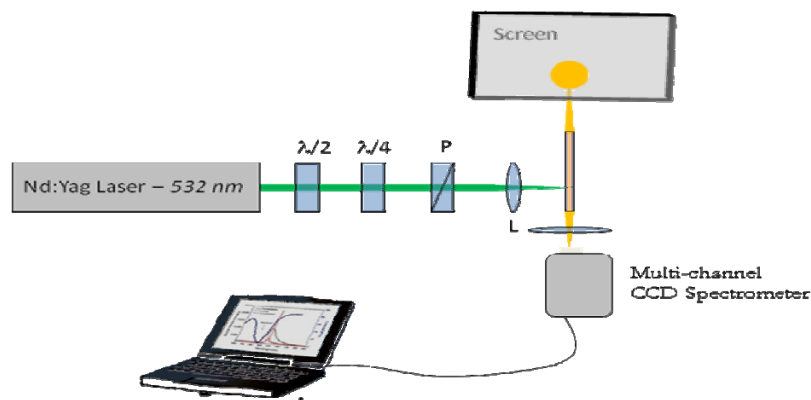
Fig. 2: *The experimental set-up. The samples were optically pumped with a Nd-Yag laser (532nm). The emission light was collected by a multichannel CCD spectrometer. Intense highly directional axial stimulated emission (at 587 nm) is observed on the background screen.*
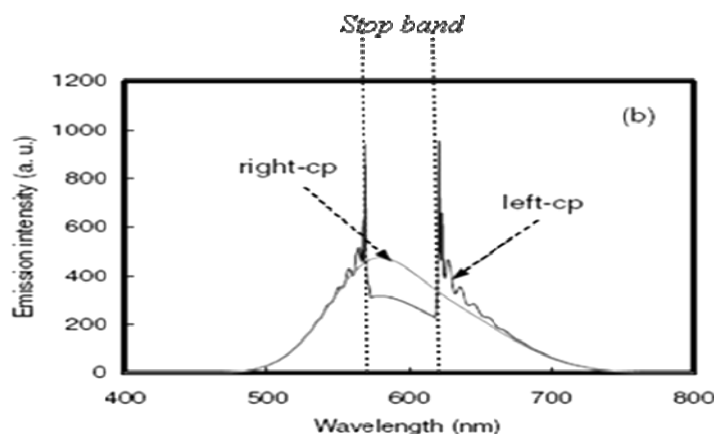
Fig. 3: *Modified fluorescence within the stop band.*

2. 2 Band edge and defect modes lasing

The LC micro-cylinder acts like a mirror-less cavity laser, where the emitted laser light propagates along the liquid crystal helical axis which behaves as a Bragg resonator. The experimental investigations show that radial and axial lasing spectra present slightly different wavelength positions and line widths (Fig. 4). The displayed lasing lines have a spectral position which correspond to the low-energy edge of the PBG and exhibit a very narrow stimulated emission peak of only 0.5 nm (limited by the resolution of the CCD spectrometer). The lowest measured lasing threshold was 250 nJ/ pulse for the radial direction and 500 nJ/ pulse for the axial one.
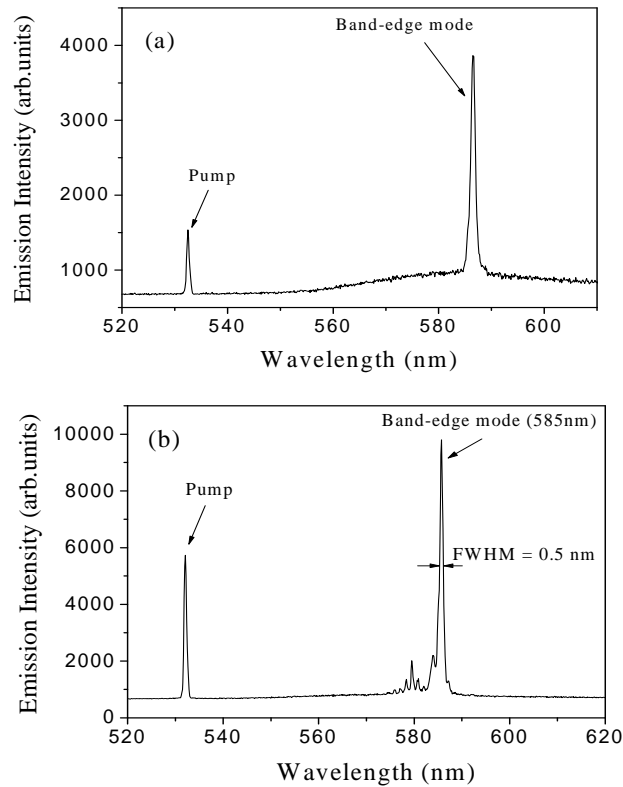
Fig. 4: *Axial (a) and radial (b) lasing spectra for a micro-cylinder, with r/p ≈250, show slightly different wavelength positions and line widths confirming the existence of two distinct micro-resonant superstructure configurations.*

To understand further this mechanism we experimentally defined that the ratio r / p, where r presents the internal radius of the cylinder and p being the pitch of the chiral liquid crystal, is the parameter which controls the arrangement of the helical superstructure. The simultaneous radial and axial lasing occurs when r / p < 50, indicating that the interplay of the strong boundary conditions and the symmetry of the micro cavity is responsible for the observed effect. In fact, the length ξ over which extends the influence of the surface depends on the inner alignment layer, and generally is about 1 μm which corresponds to a few pitch lengths. Therefore, the competition between the double-twist arrangement of the bulk region and the axial organization of the surface region finds a balance position for low r / p ratio.

In addition to the expected band edge lasing modes, low threshold defect lasing modes which usually occur within the selective reflection band gap have been observed. Introduction of a defect in photonic crystal can give rise to an additional resonant mode inside the photonic band gap[1,21]. Such defect modes are localized at the position of the defect and may be used for narrow band filters[22] and low threshold lasers. Recently Schmidtke and co-workers reported defect mode emission of a dye doped cholesteric polymer network by introduction of a phase jump in the cholesteric helix. They used two layers of a highly cross-linked CLC polymer film to create a phase jump of 90° in the cholesteric helix (Fig. 5). Lasing is facilitated at these wavelengths since the photon dwell time is enhanced, giving ample opportunity for amplification by stimulated emission since the excitation energy will not be drained by spontaneous emission into modes other than the lasing mode.

In the case of the presented cylindrical microstructure, the spontaneous rearrangement of the local director fields produces particular helical axis configurations which spans from planar (axial) to escaped twisted radial geometry. This structural organization materializes in the appearance of point defect modes. The local alteration of the sample which disrupts the periodicity of the structure leads to long-lived and, hence, spectrally narrow laser defect modes within the gap, observed both axially (Fig. 6a) and radially (Fig. 6b).
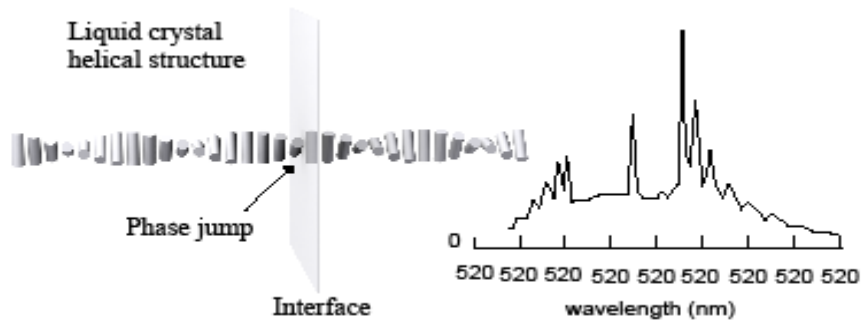
Fig. 5: a) *Sketch of the defect introduced in the cholesteric helix.b) Presence of the defect mode in the center of the stop band peaked at the location of the defect*

It is worth to notice that lasing wavelength on axial and radial defect modes are slightly different, since the resonant wavelength for the defect mode depends on the total phase slip which is given by the twist defect characteristics. Hence, the resonant wavelength undergoes important shift within the entire band gap by slightly changing either the defect layer thickness or the helical phase jump of the twist defect.
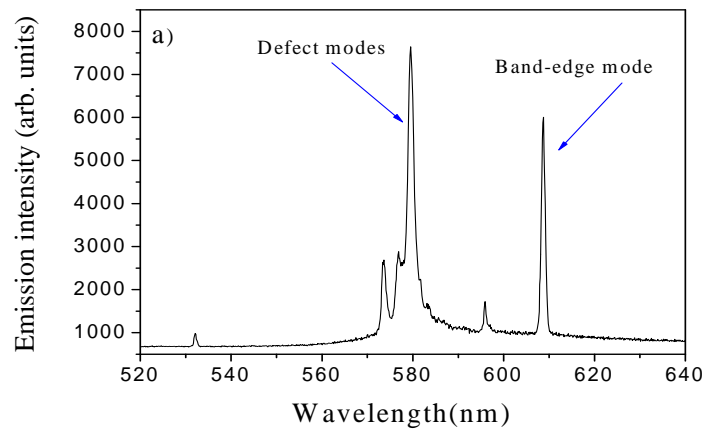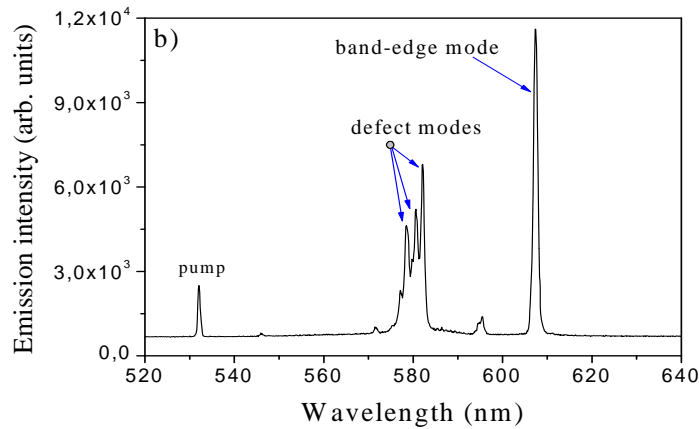
Fig. 6: *a) Axially and b) radially emitted narrow defect lasing modes within the stop band. The ratio r/p is about 50.*

2. 3 Thermal behavior

The most interesting aspect of the lasing in CLCs is that optical and geometrical parameters can be modified by applying weak external fields (temperature, electric field, mechanical stress, and optical field), resulting in a direct control of lasing features (wavelength, bandwidth, and emission intensity). These properties were found to be fully reversible.

The experimental evidence definitely proves that the distributed feedback mechanism, provided by the dielectric tensor modulation of the helixed liquid crystal, is behind the lasing process in these systems. By means of a miniature oven (CaLCTec S.r.l.) the system's temperature was varied from 25°C up to 50 °C allowing to obtain a fine-tuning of the laser emission wavelength. In fact the period of the chiral liquid crystal, the pitch p, changes with temperature variations [8]. The period of the helix increases by increasing the temperature, producing an overall displacement of the spectral region where the circular Bragg reflection takes place. As a result of the thermal elongation of the pitch, a shifting of the stop band edge where the laser action occurs is obtained.

Experimental measurements emphasize two different trends for lasing wavelength peak position in function of temperature for the radial and axial situations. A continuous temperature tuning of the lasing wavelength was obtained in the interval 585–595 nm by varying the temperature (Fig. 7). We recorded a linear increase of 0.3 nm/ °C for axial and 0.45 nm/ °C for radial stimulated emissions (Fig. 8). This dependence indicates that the axially oriented helical superstructure responds in a reduced way to an applied temperature gradient, with respect to the radial oriented helix. This different behavior is strongly related to the confinement, in other words the interfacial region offers a much stronger constraint at the helical superstructure than the free bulk region. Belyakov theoretically investigated the cholesteric pitch changing under the action of external perturbation. In particular he demonstrated the strong dependence of the anchoring energy on the structural behavior leading to a different response of the helical superstructure for interfacial and bulk regions of the cholesterics [23].
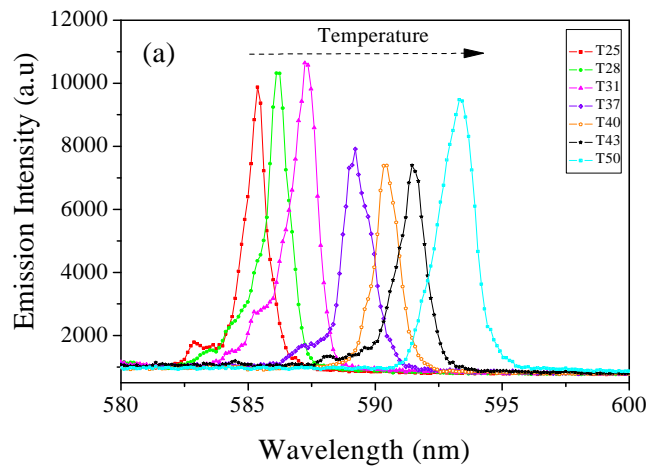
Fig. 7: *Stimulated emission spectra as function of temperature. A fine tuning of the lasing wavelength is achieved for both axial (0.3°C/nm) and radial(0.45°C/nm) emissions.*

Taking into account the experimental evidences and by analogy to what is reported in the study of the confinement of nematic liquid crystal in cylindrical cavities, we suggest a

model for this spontaneous rearrangement of helix of these systems in the cylindrical tubes (Fig. 9).
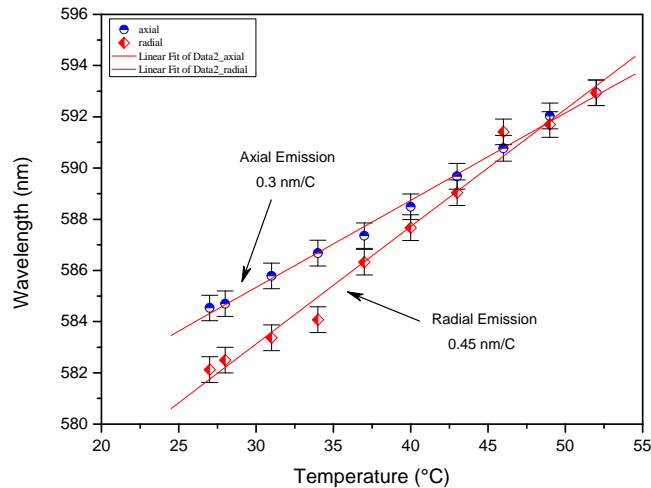
Fig. 8: *Temperature control of the lasing wavelength in self-organized helical mesophases confined in cylindrical microresonators. The different temperature dependence of the wavelength for the axial and radial stimulated emissions suggests the presence of two discrete DFB Bragg resonators.*

Due to the surface treatments we expected a preponderant orientation of the helical axis along the cylinder axis while in the bulk region the radial configuration is preferred due the big diameter of the cylinder. This spontaneous shift from planar to radial orientation gives rise to narrow defect layer which ensures this alignment passage. The formation of this layer is the responsible of the observed lasing defect modes. In the bulk region, because of the double-twist effect, a core interlinking zone has to be considered. Here, the local director is oriented along the cylindrical main axis, having a nematic-like structural configuration. This model is in good agreement with the experimental observations, explaining the existence of the two main DFB resonant configurations (axial and radial) and the presence of the defect modes lasing spectra within the stop band.
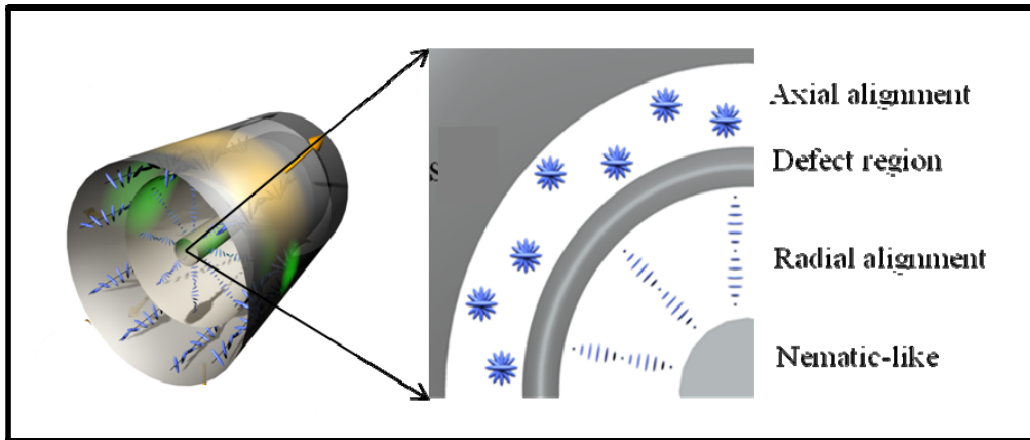
Fig. 9: *Schematic model of the chiral LC configuration inside the microcylinder. Axial organization of the helical structure in proximity of the boundary substrate is suggested, while in the bulk region a radial orientation is preponderant. The bulk organisation implies a double twist configuration together with a nematic-like order for the core region.*

We experimentally demonstrated that the confinement of dye doped helixed liquid crystal in cylindrical micro-cavities gives rise to a 3D periodical superstructure where the two naturally preferred helical directions (axial and radial) create spontaneously. Low-threshold highly directional laser action was observed both radially and axially. Along with the expected band edge mode we report the existence of long-lived spectrally narrow laser defect modes within the central region of the stop band. The defect modes are due to local dislocations of the chiral structure which yields optical phase jumps and weak light localization effects. Fine temperature tuning of the stimulated emission wavelength was achieved for both lasing situations. Experimental evidences suggest the existence of two main DFB resonant configurations (axial and radial) which are behind the demonstrated temperature tuneable multidirectional (3D) lasing system. Novel photonic architectures and optical devices could be engineered by using this level of confinement of periodic and quasi-periodic photonic crystals in order to minimized the scattering and increase the quality factor. In the following section we will report the

fabrication of periodic structure and the characterization of the laser action in these systems.

3.   Periodic Composite Micro-Structures

Kogelnik and Shank [13] were the first to report laser action in periodic DFB structures which do not utilize conventional cavity mirrors but provide optical feedback via backward Bragg scattering. Lasing has been demonstrated in dye-doped cholesteric liquid crystals [24], liquid crystals in polymer networks [25], and also in dye-doped helixed liquid crystals in holographically patterned polymeric microchannels (POLICRYPS)[26]. In order to gain further understanding on this work reported by Strangi and his group in 2005, we decided to continue within this approach by using a new micro-structuring techniques based on the combination of a dichroic photoinitiator and polarization holography and we reported also a study of the lasing emission properties in these systems. The orientation of the LC helix axis along these micro-structures offers several physical advantages: increase of the cavity length and thus the number of periods, small modal volume, directional control, improvement of the liquid crystal orientational order parameter, and wavelength tunability. The distributed feedback needed to obtain laser oscillations in the case of a small refractive index modulation requires thousands of periods in order to behave as an optical cavity with a quite high quality factor.

3.   1 Mono disperse membrane

Holography is a powerful technique, especially for the formation of gratings. It is defined as the transformation of an interference pattern of lasers in photo-sensitive films. In essence the process of creating holographic patterns consists of three steps:

- creating an interference pattern of coherent polarized light,

- capturing the interference pattern in a photo-sensitive film,

- reconstructing the hologram by diffraction of light from this film.

Holographic optical elements offer attractive properties for a variety of optical applications for their ability to control the direction and the wavelength of light with high efficiency, low absorption, and low levels of scattering[27,28]. They found a great

use in liquid crystal displays as filters, retarders and reflectors. In this chapter they have been thought as micro-cavities for lasing.

To prepare these holographic membranes for microcavity lasing we used NANO™ SU-8 (MicroChem Cop,Newton,MA) photoresist. SU-8 is a high contrast, negative, epoxy-based line of near-ultraviolet (UV) radiation-sensitive photoresists with suitable chemical and mechanical properties, capable of developing thick photoresist structures in a single photolithographic step [29].

The fabrication of these systems involves the exposure of a photosensitive material (photo-resist) to an interferometric pattern produced by a laser [30]. In general, two specific cases of interference patterns are distinguished : purely intensity-modulated interference patterns with constant polarization state known as intensity holography, which was used here to produce the holographic grating, and purely polarization-modulated interference patterns with constant intensity called also polarization holography. We will discuss further the later techniques in the next section. The interference pattern is constructed by two overlapping plane waves(coherent beams) with identical polarization sate. This pattern consists of a periodic sinusoidal intensity pattern as indicated in Fig. 11. If the beams (K_1 and K_2) are placed in the x,z-plane with an angle of θ and $-\theta$ from the z-axis respectively, the intensity will be independent of y and modulated in the x-direction with a periodicity determined by Bragg's Law:

$$\Lambda = \lambda \ / \ (2 \sin\theta)$$

Where Λ is the period and λ the wavelength of the light.
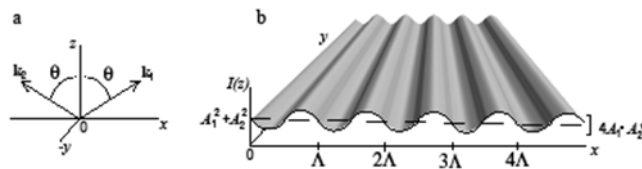
Fig. 10: *Interference pattern of 2 plane waves*

The SU-8 photo-resist was spin coated onto glass substrates of 2 by 2 cm in size, which were prepared in a clean room to ensure their purity. The cleaning process can be resumed in the following steps:

• Rinse the glass plates with demiwater

• Vibrate (ultra sonic bath) the glass plates for +/- 5 minutes in the "*Teepol*" (soap) solution

• Scrub the glass plates on both sides with a sponge and the *Teepol*-solution.

• Vibrate the glass plates again in the *Teepol* -solution

• Rinse the glass plates careful with demiwater

After that, a very thin layer of omnicoat^{TM} is coated on a clean glass plate. Next a uniform photo-resist layer is deposited by use of a spin coater. The rotation regime of this device and/or the mutual chemical concentration of the photo-resist and a solvent (thinner) can be varied allowing the precise "tuning" of the polymer layer thickness (Fig. 11). After evaporation of the solvent the sample is exposed with a holographic laser- writing set-up presented in Fig. 12.
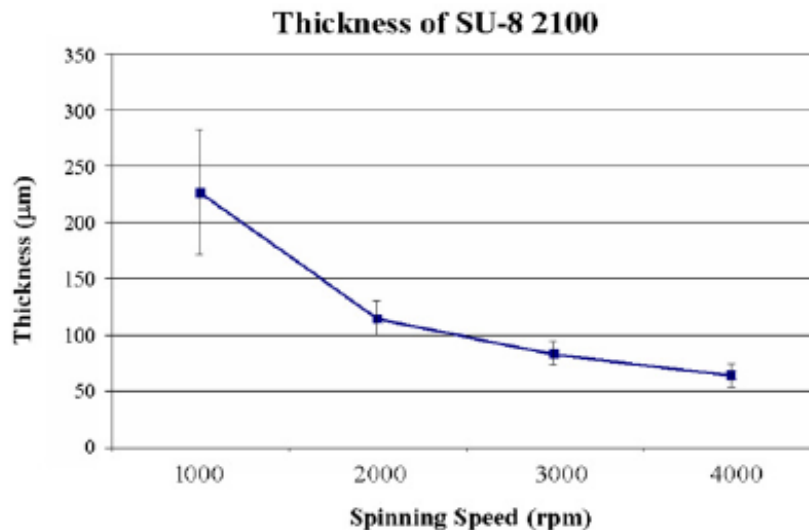
Fig. 11 : *Layer thickness as function of spinning speed.*
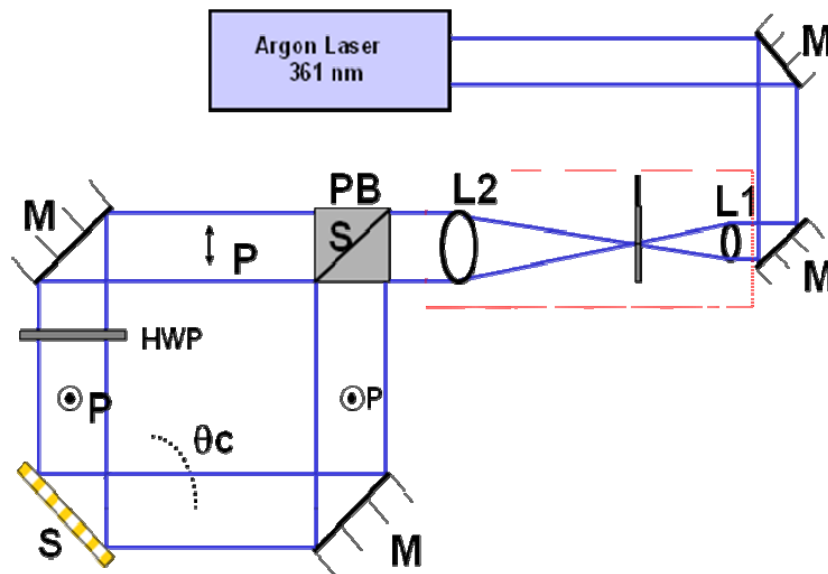
Fig. 12: *Optical setup for UV curing gratings; **M**, mirrors; **L1**, **L2**, lens; **I**, aperture; **PBS**, polariser beam splitter; **HWP**, half-wave plate; θc, curing angle; **S**, sample*

A single mode beam from an Ar-Ion laser operating at wavelength at 361 nm is broadened by a spatial filter (composed by two lens L1, L2, and a small aperture I) up to a diameter of about 30 mm. It is divided into two beams of nearly the same intensity by the polarizing beam splitter PBS. In order to have the same polarization of these two beams, a half-wave plate HWP has been adopted in one of the two arms of the interferometer system. These two beams intersect at the entrance plane of the sample S, giving rise to an interference pattern (Fig. 13)
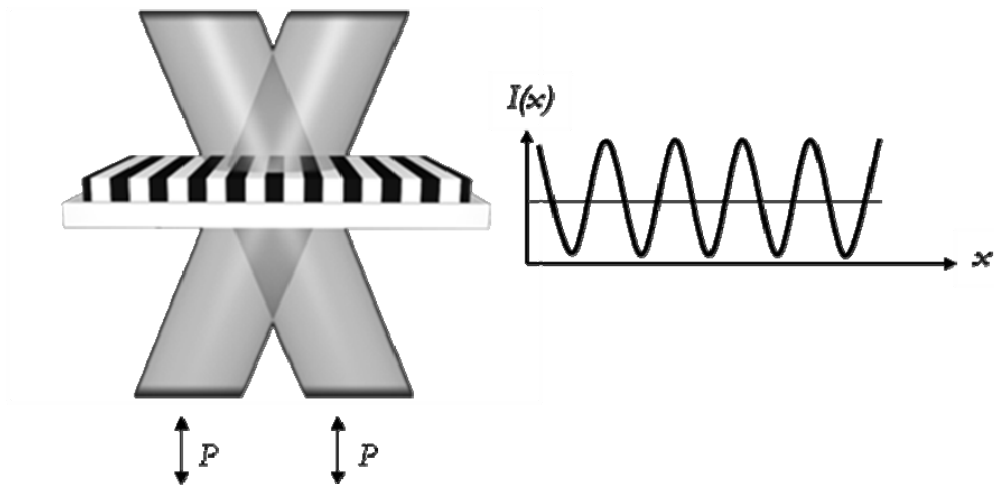
Fig. 13: *Interfering Laser beams' above the sample position and the interference intensity pattern below it*

After exposure, the sample is heated to crosslink the SU_8. The remaining non-cross linked and non exposed SU-8 is removed by SU-8 developer.

The whole process, for preparing grating structures, is represented in the following sketch(Fig. 14):
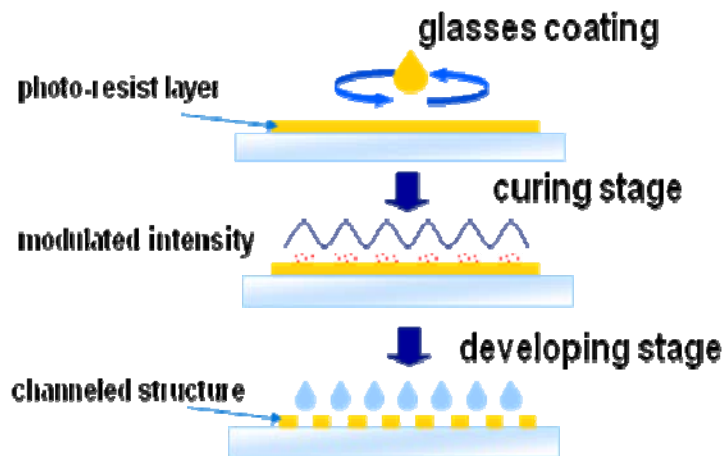
Fig. 14: *Sketch of the whole process for the realization of grating structures*

An important parameter in order to realize a periodic structure on a photosensitive material is the light absorbed by the photoresist during exposure, called photoresist dose. It is related to the curing time and curing power, namely:

$$[D]=[P]*[t]=watt*sec=joule$$

P is the curing power and *t* the curing time. By changing these two parameters it is possible to control the depth of the obtained grating. Depending on the dose, it is possible to obtain different morphology for the gratings.

By using the holography techniques and varying the angles between the exposures we can create different geometries of grating. If one time exposure is performed to the sample we obtain to regular line as shown in Fig. 15.
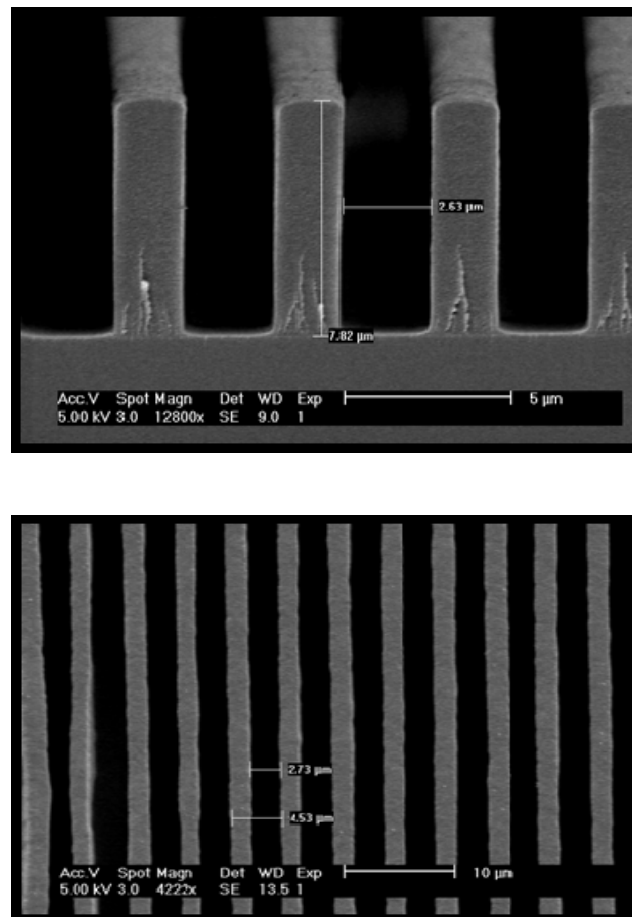
Fig. 15: *SEM picture of grating morphology obtained by using one time exposure*

If the angle between the first and the second exposure is 90° meaning circular pores are obtained in cubic packing (Fig.16).
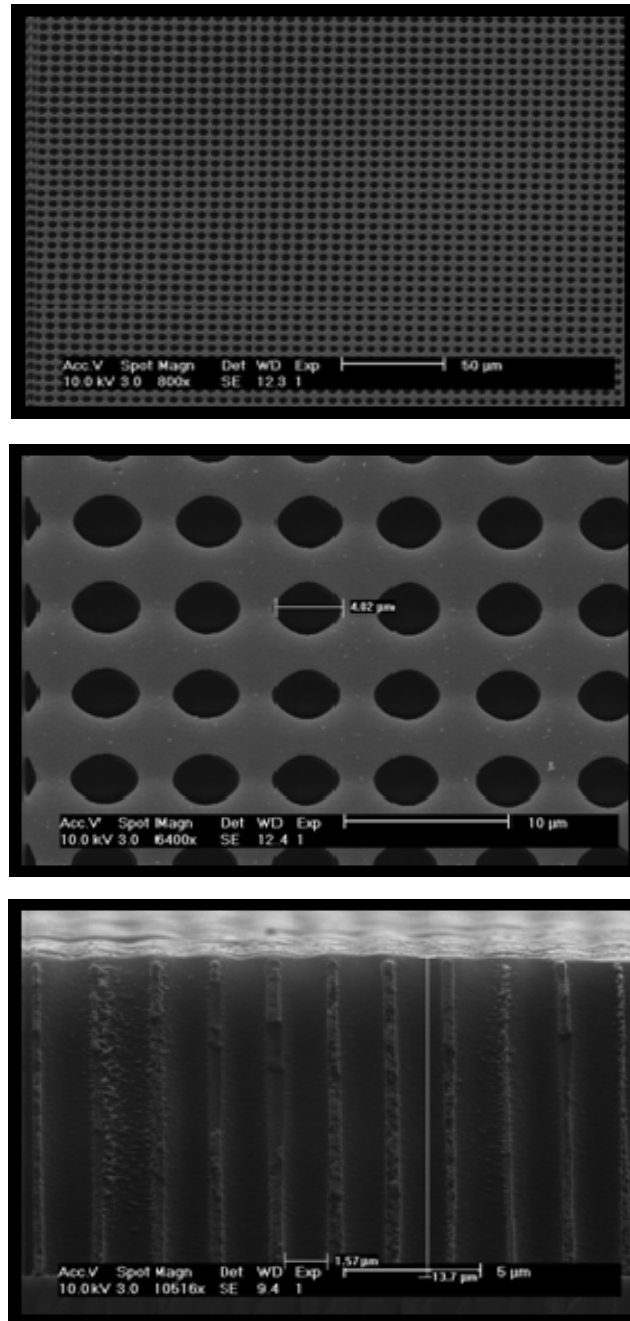
Fig. 16: *SEM picture of holographic membrane morphology obtained by using double-exposure time and the angle between the two exposures is 90°*

The double exposure at an angle about 60° we observed the following morphology presented in the Fig. 17
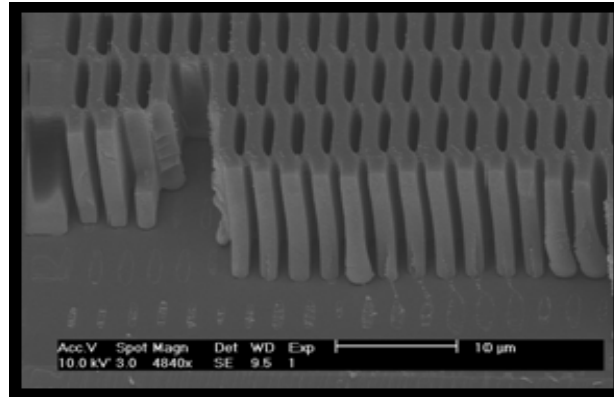
Fig. 17: : *SEM picture of hexagonal membrane morphology obtained by using double-exposure time and the angle between the two exposures is 60°*

And by changing the angle to180° we have planar channels as shown in Fig. 18
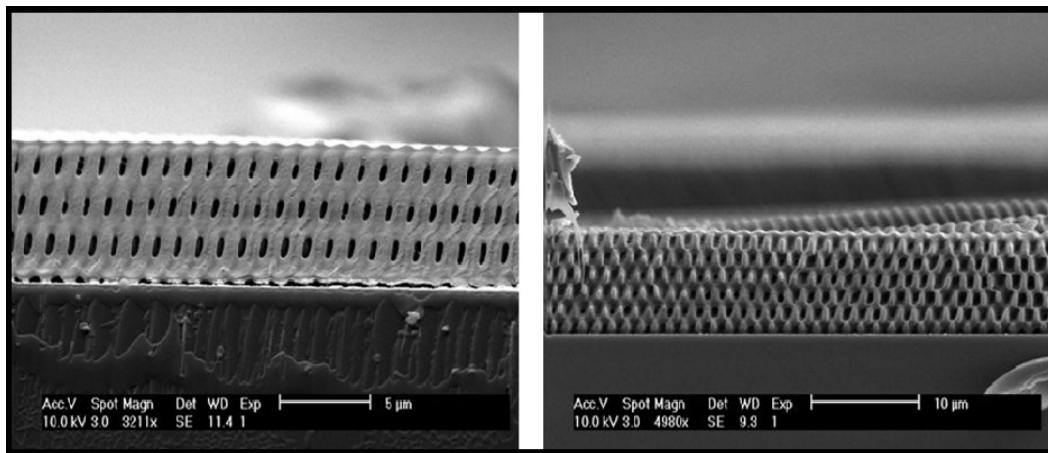
Fig.18: : *SEM picture of holographic membrane morphology obtained by using double-exposure time and the angle between the two exposures is 180°*

The microscope morphology of these microchannels filled by capillarity with a nematic liquid crystals is presented in Fig. 19.
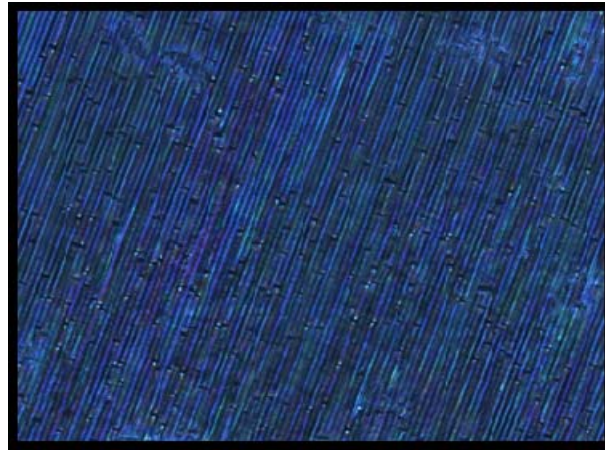
Fig. 19: *The microscope morphology of channels filled with NLC*

3. 2 High aspect ratio grating

Here we present a new micro-structuring technique based on the combination of a dichroic photoinitiator and polarization holography. Polarization holography has many similarities with classical intensity holography. Both are pattern transfer techniques that make use of the interference of coherent light. The period of the holographic structure is determined by the angle between the overlapping plane waves. To record the interference pattern, a light sensitive material is placed into the interference pattern and a corresponding pattern is somehow imprinted in the material. Depending on the material, several processing steps are required, including development, post-curing and desensitizing steps. As mentioned before intensity holography is the modulation of intensity generated by two plane waves with the same polarization. For polarization holography two plane waves interfere with orthogonal polarization states resulting in a modulation of the polarization state, while the intensity of light remains constant (Fig. 20).
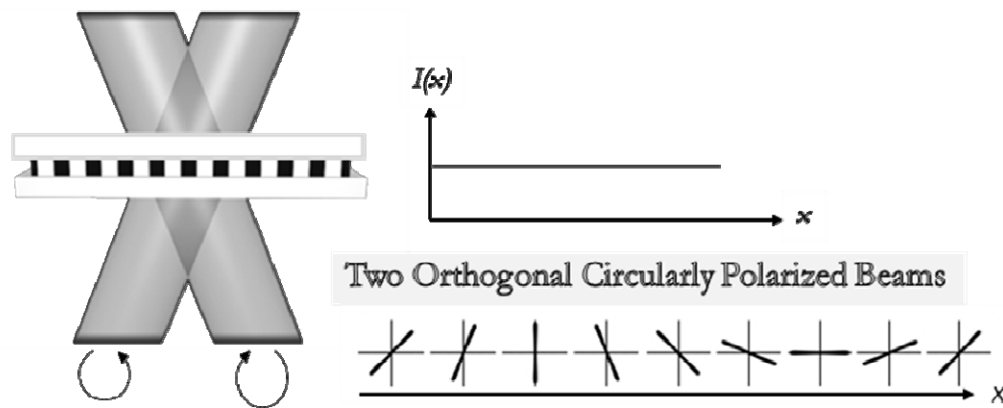
Fig. 20: *Polarization holography interference patterns created by two circularly polarized beams.*

In this work we combine the use of polarization holography with dichroic photoinitiator. The common photoinitiators are substances capable of initiating a polymerization reaction. Upon exposure to the proper wavelength, these materials dissociate, creating free radicals that initiate the polymerization reaction. The difference between the common photoinitiators and the dichroic one that the last have an additional property that the dissociation rate is orientation-dependent. Using polarized light, the dissociation of the dichroic photoinitiator occurs faster when the transition moment of the molecule is aligned in the direction of polarization, in fact an alignment of the photoinitiator is required. A macroscopic alignment of the dichroic photoinitiator is generated by blending a small amount into an anisotropic host such as a liquid crystal (LC) mixture. The alignment can then be manipulated by external stimuli such as electric or magnetic fields, alignment layers and surfactants.

The mixture used for the experiments contains approximately 30 % reactive LC (12% of C_6M and 18% C_3M) , 69 % non-reactive liquid crystal E7 and a small amount (1 %) of dichroic photoinitiator. All materials are kindly provided by Merck (Southampton, UK). This mixture is confined by capillarity in a sandwich cells which are manufactured by adhering two 2x2 cm glass plates separated by 5-10 μm spacers. The inner surfaces of the glasses are treated with a surfactant in order to introduce a privileged alignment. The cell was then exposed to linear polarized source and the curing process is performed by an Argon laser at the wavelength of 361nm. As the dissociation rate of dichroic

photoinitiators is orientation-dependent, the polymerization is preferentially initiated at the locations, where the photoinitiator is aligned parallel to the electrical field vector of the UV light. During this localized polymerization LC monomer is consumed and a concentration gradient is build up. This induces a diffusion of the LC monomer to the bright areas, where a relative fast polymerization occurs. Due to this polymerization, monomer is depleted and the non-reactive LC counter-diffuses to the more slow polymerizing regions. In this way we obtain a pattern of polymer LC lines separated by non-reactive LC rich regions. After exposure the etching process is performed by submerging the samples in THF solvent over night. The non reactive LC is removed and a polymer lines are observed in all the sample (Fig. 21).
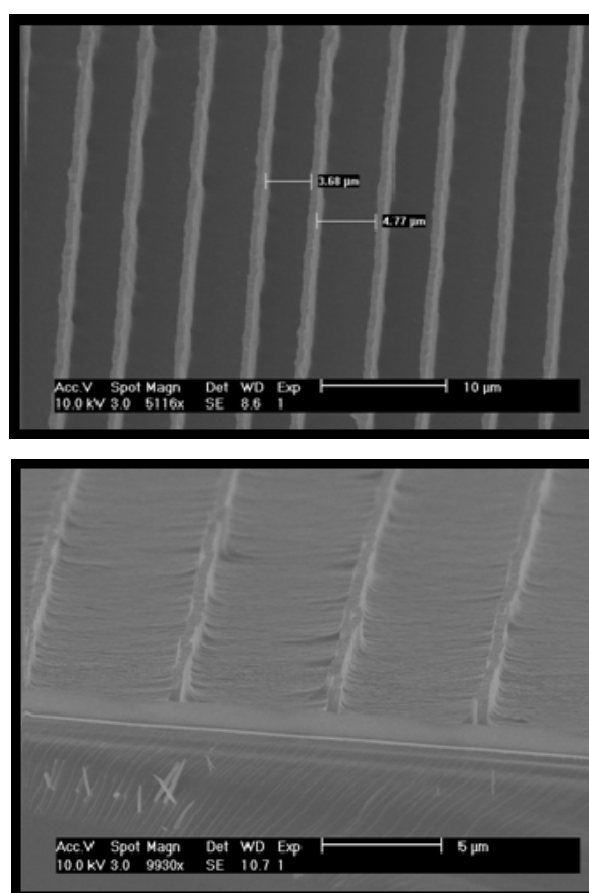
Fig. 21: *SEM images of a polymerized sample after etching process.*

For the reason that the dichroic photoinitiator is orientation dependent and during the exposure the LC director is orthogonal to the electric field of the light source, the

orientation of the molecules in the valleys is orthogonal to the orientation at the walls as shown in the sketch (Fig. 22).
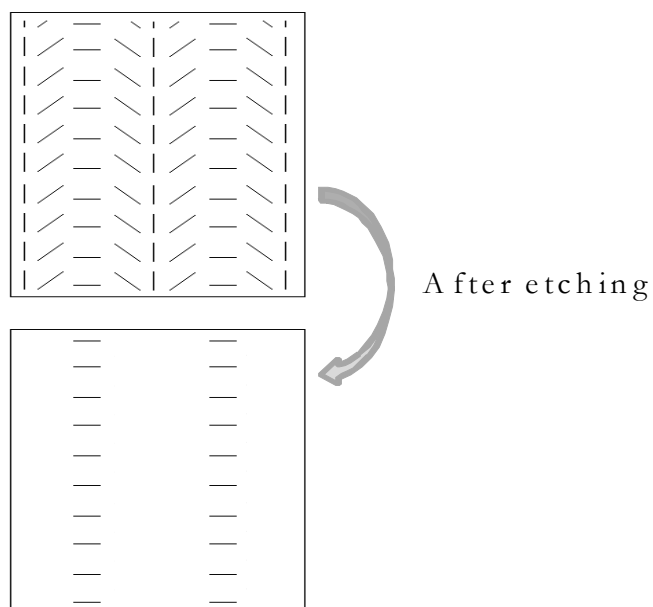
Fig. 22: *A Sketch of the polymerized sample before and after etching.*

The microscope analysis between crossed polarizer show the following sharp morphology (Fig. 23).
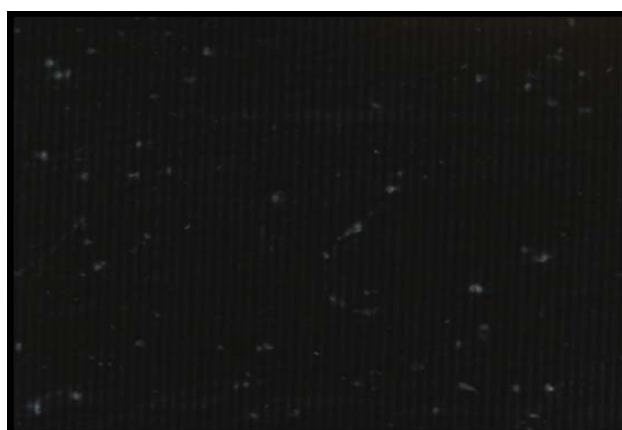
Fig. 23: *Microscope morphology of the TPH after etching*

3. 3 Laser action

Lasing in micro-channels containing chiral liquid crystal has been demonstrated by Strangi and co-workers[26]. Some experimental study shown the persistence of some monomer inside the LC channels. The monomer can distort the helical LC superstructure increasing the optical losses(Fig. 24). The aim of this work is to minimize the optical losses by constructing the micro channels as first step and then fill them with the active medium(dye doped cholesteric liquid crystal).
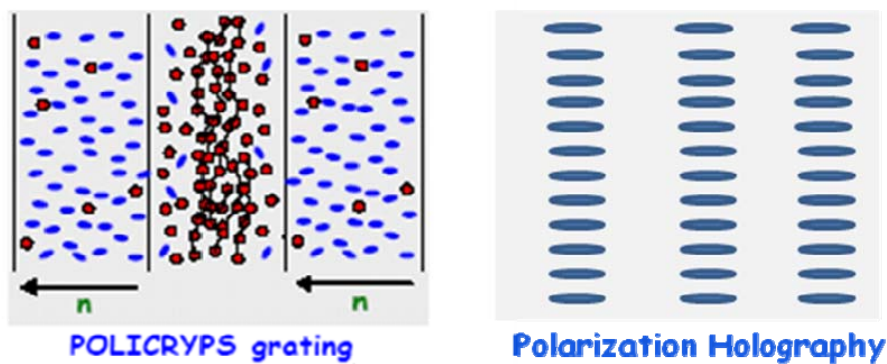
Fig. 24: *Sketch shown the difference between the POLICRYPS and the Polarization Holography structure.*

We adopted this systems to study the lasing in cholesteric liquid crystal infiltrated in predesigned microcavities. A series of significant physical advantages yield from adopting this type of configuration: increase of the optical cavity length, very small modal volume per each resonant micro-cavity (providing also minimization of the optical losses), directional control of the lasing emission, wavelength tunability and control over the emission intensity.

As reported also for POLICRYPS, the presented geometry allows to obtain a number of periods which is about 2 orders of magnitude larger than conventional systems because it exploits the entire length of the micro-channel in a waveguide regime instead of the sample thickness. In this way, each micro-channel becomes an optical mirror-less microcavity with a very small volume V of only a few cubic micrometers. This is highly

desirable since it enhances the factor of spontaneous emission and severely reduces the threshold of laser emission.

The microstructure was filled with cholesteric liquid crystal by capillarity at the isotropic phase and then cooling very slowly in order to get a homogeneous alignment of the helix. By cooling slowly the sample to room temperature (1°C /min) a self-organization process of the CLC helical occurs. The system tends to minimize its free energy by orienting the liquid crystal helices, on average, along the micro-channels. At the end of the whole process the helixed liquid crystal is oriented within the channels created by periodically separated polymer walls. The Mixture used is : 99.7% of BL094 (Merck) doped with 0.3% of PM dye (Merck). The sample was optically pumped with 3 ns pulses produced by a frequency-doubled (532 nm) Nd:YAG laser (NewWave, Tempest 20). The pump beam was focused onto the sample with a cylindrical lens ($f =$ 100 mm) producing an elliptical pro- file. The long axis of this beam profile was oriented perpendicularly to the micro-channels orientation so that several channels were simultaneously optically pumped. The PBG structure of the self-organized liquid crystal severely modified the fluorescence spectrum of the dye molecules: at low pump energies a dip in the emission occurred at the position of stop band (Fig. 25). This dip is the result of the localization of the emitted photons within the stop band, therefore it proves that a DFB mechanism is going on within our samples.
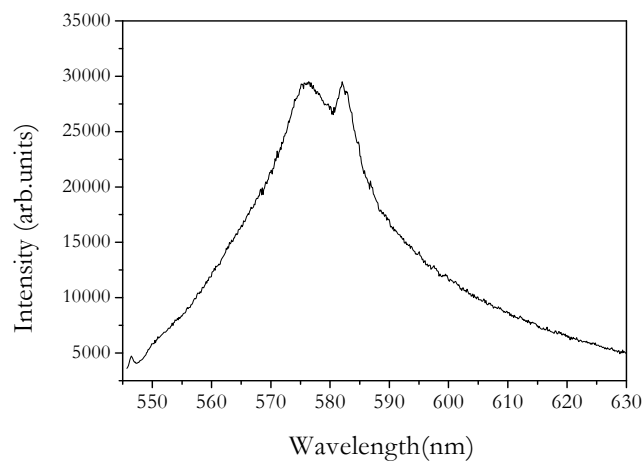
Fig. 25: *Modified fluorescence, a dip in the emission within the stop band.*

By increasing the pump energy above a given threshold value, laser action was observed along the micro-channels at the low-energy edge of the stop band, where the photonic density of the states diverges and the lasing is expected. The laser emissions emerging along the micro-channels direction were captured by using a multichannel CCD spectrometer (Jobin-Yvon). The line width of the laser emission is about 0.6 nm (Fig. 26). The laser emissions were found to be circularly polarized, indicating that distributed feedback mechanisms take place through circular Bragg reflection. The LC micro-channel behaves as a miniaturized mirror-less cavity laser, where the emitted laser light propagates in the waveguide defined by the chiral liquid crystal medium.
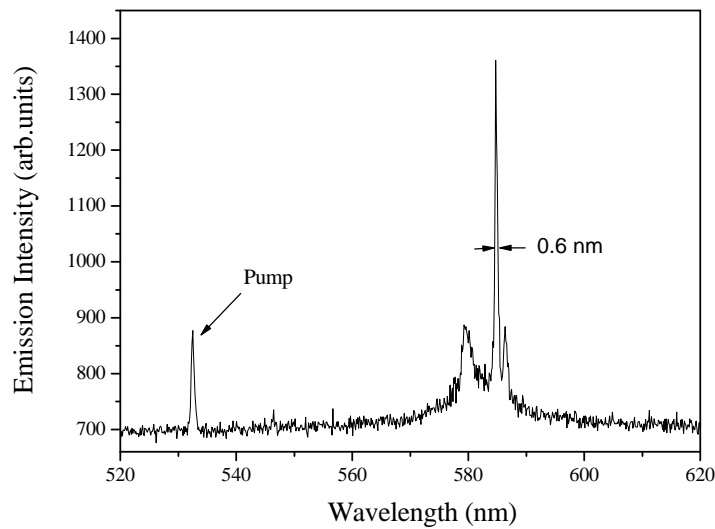
Fig. 26: *Above the threshold value a sharp lasing peak appears at the edge of the stop band.*

The sketch in figure 27 shows this lasing scenario of the microcavity laser. The emitted laser light propagates along the liquid crystal helical axis behaving as Bragg resonator.
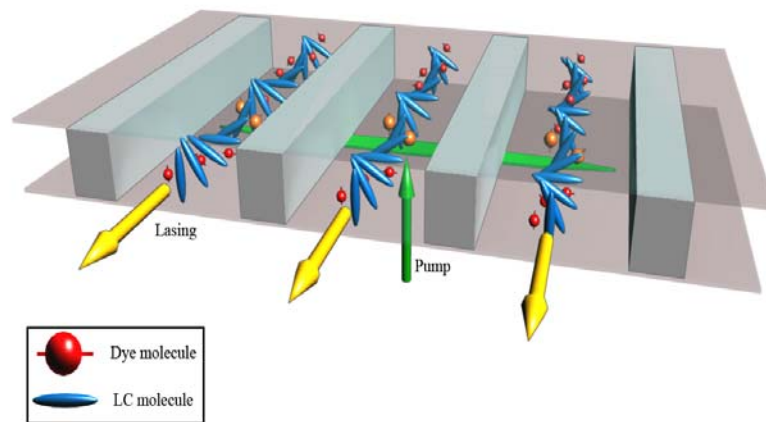
Fig. 27: *3D sketch describing the micro-laser array scenario. Highly directional and intense stimulated emission is achieved emerging from the microcavities in a direction parallel to the glass plates and along the microchannel structure.*

This systems are still the subject of extensive studies because of the tunability, resulting in a control of lasing wavelength, bandwidth and emission intensity, by applying a weak external fields (temperature, electric field, mechanical stress, and optical field). In fact, by varying the temperature of the system the wavelength of laser emission was observed to redshift (Fig. 27).
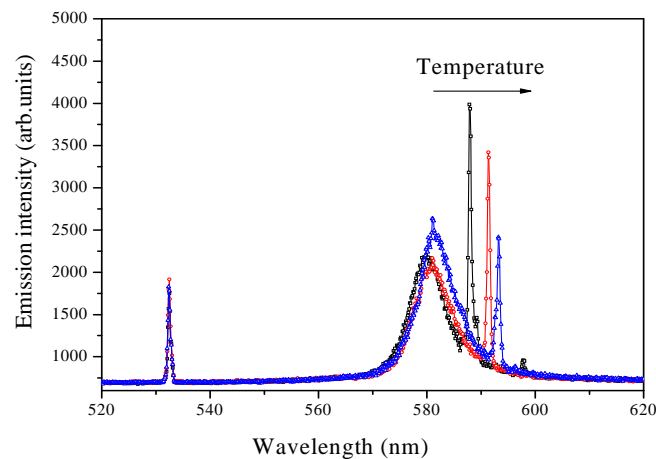
Fig. 27: *Temperature Dependence of Lasing Wavelength. A red-shift is observed by increasing the temperature.*

It is well known that the period of the helical superstructure, the pitch p, changes with varying temperature and so a shift of the spectral region where the circular Bragg reflection occurs. Thus, the thermal elongation of the pitch results in a shifting of the stop band edge where the laser actions is expected. This experimental evidence definitely proves that the distributed feedback mechanism, provided by the dielectric tensor modulation of the helixed liquid crystal, is behind the observed effect.

References:

[1] Joannopoulos et al "*Photonic crystals*", Princeton University Press : Princeton NJ,1995

[2] Sakoda et al "*Optical properties of Photonic Crystals*", Springer Verlag : Berlin, 2001

[3] J. P. Dowling et al, J. Appl. Phys. 75, 1896, 1994.

[4] V. I. kopp et al, Opt. Lett, 23, 1707, 1998.

[5] S. Furumi et al, App. Phys. Lett, 82, 16, 2003.

[6] F. Araoka et al, J. Appl. Phys, 94, 279, 2003.

[7] P. V. Shibaev et al, Macromolecules, 35, 3022, 2002.

[8] M. Ozaki et al , Adv. Mater, 14, 306, 2002.

[9] M. Ozaki et al , Adv. Mater, 15, 974, 2003.

[10] J. Schmidtke et al, Adv. Mater, 14, 746, 2002.

[11] J. Schmidtke et al, Phys. Rev. Lett, 90, 083902, 2003.

[12] H. Finkelmann et al, Adv. Mater, 13, 1069, 2001.

[13] H. Kogelnik and C. V. Shank, Appl. Phys. Lett. **18**, 152 (1971).

[14] L. S. Goldberg, J. M. Schnur, U.S. Patent No. 3,771,065 (1973).

[15] S. Chandrasekhar, "*Liquid Crystals*" (Chambridge University Press, Cambridge, (1992).

[16] R. C. McPhedran et al, Phy. Rev. E 69, 016609, 2004.

[17] V. I. kopp et al, Phys. Rev. Lett, 86, 1753, 2001.

[18] A. Yariv, "*Quantum Electronics*", CBS College Publishing, New York, 1985.

[19] D. Wiersma, Nature 406, 132, 2000.

[20] V. Barna et al, Appl. Phys. Lett. 87, 221108 (2005).

[21] E. Yablonovitch, Phys. Rev. Lett. **58**, 2059 (1987).

[22] I. J. Hodgkinson, Q. H. Wu, K. E. Thorn, A. Lakhtakia, and M.W. McCall, Opt. Commun. **184**, 57 (2000).

[23] V. A. Belyakov, Mol. Liq. Cryst. 410, 219 (2004).

[24] W. Cao, A. Munoz, P. Palffy-Muhoray, and B. Taheri, Nat. Mater. **1**, 111 (2002).

[25] P. A. Bermel and M. Warner, Phys. Rev. E **65**, 056614 (2002).

[26] Strangi. G et al, Phys. Rev. Lett. **94,** 063903 (2005).

[27] Y. Awatsuji et al, Appl. Phys. Lett. **85** 1069 (2004).

[28] A. Urbas et al, Adv. Mater **16** 1453 (2004).

[29] H. Lorenz et al, Sensors Actuators A 64 33–9 (1998).

Random Lasers and Weak Localization of Light in Nematic Liquid Crystals
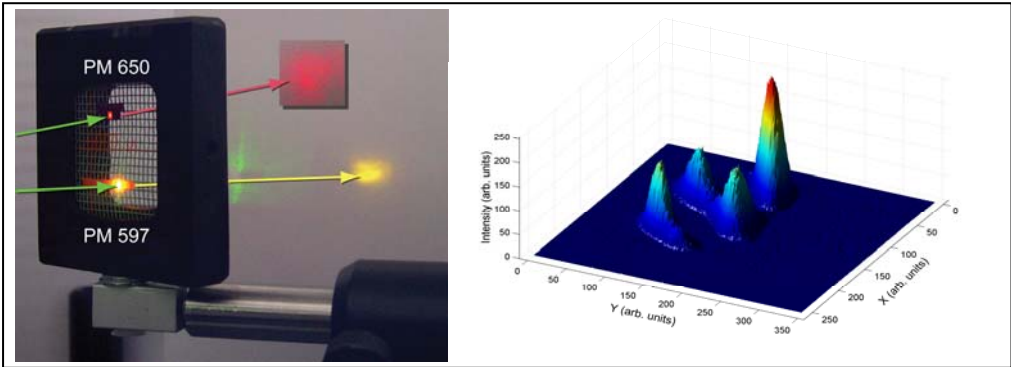
1.   History of random lasers

These days the laser is an essential tool in our society. It has found widespread use in industry, medicine and other areas of contemporary life. Besides the many applications that have been discovered since the first experimental demonstration, more than 50 years ago, in 1960 by Theodore Mainman, the laser itself has also been subject of intense scientific study.

The essential ingredients of a laser as mentioned in the previous chapter are a material that amplifies light through stimulated emission (the gain medium) and a cavity that traps light in the gain medium to enable more efficient amplification. The gain medium is pumped electrically or optically by another laser source. Fabry-Pérot is the most common laser cavity , made of two mirrors, one of which is partially transmitting, that face each other on either side of the gain medium. Light that is traveled back and forth between the mirrors is amplified each time it passes through the gain medium. Light can leave the cavity through the partially transmitting mirror. Light that remains in the cavity interferes constructively after traveling a round trip between the mirrors and returning to its original position. This means that the phase delay of a round trip must be equal to an integer multiple of 2π, a requirement that can be satisfied only at certain frequencies. The laser light transmitted through the partially reflecting mirror has well defined frequency, good directionality and a high degree of coherence. If however, there are scatterers inside the cavity, the light can be scattered in other directions, introducing additional loss and increasing the lasing threshold. This is why optical scattering is considered detrimental and why laser engineers work hard to minimize the amount of scattering in laser cavities.

What happens when the scattering is very strong? Surprisingly enough strong scattering can facilitate lasing action, and a disordered medium with gain light scattering turns out to have a positive effect on the laser process. Multiple scattering increases the time that light spends inside the sample and thus increases the dwell time of light enhancing light amplification. The combination of multiple scattering of light and gain are the essential ingredients of a random laser. In this scenario, we no longer need mirrors to trap the light in the gain medium since scattering can do the job on its own. Since strong light

scattering usually occurs in highly disordered media, the word "random" has been used to describe lasers that operate on the basis of these properties.

In 1966 a group led by laser pioneer and Nobel laureate *N. G.* Basov realized a new type of laser cavity that provided nonresonant feedback, by replacing one mirror of Fabry-Pérot with a scattering surface[1]. Light in the cavity undergoes multiple scattering. Since every time it is scattered its direction changed, it does not return to its original position after one round trip. In such a cavity, the spatial resonances of the electromagnetic field are absent and the dwell time of the light is not sensitive to frequency.

In 1968, Letokhov took the research further when he proposed self-generation of light in an active medium filled with scatterers. The photons spontaneously emitted by the excited atoms or molecules in the gain medium experience multiple scattering and undergo random walk before leaving the medium. As photons travel in the gain medium, they can induce the stimulated emission of additional photons.

Since the pioneering work of Letokhov and co-workers lasing in disordered media has been the subject of intense theoretical and experimental studies. It represents the process of light amplification by stimulated emission with feedback mediated by random fluctuation of the dielectric constant in space. Intense stimulated radiation was observed in a wide variety of laser crystal powders, semiconductor nanoparticles, ceramic powder to polymers, organic materials and biological tissues [2]. More recently in 1997 Wiersma and Lagendijk asked the question:"can we build a coherent random laser in which feedback is caused by interference in multiple scattering [3]. In the same line of reasoning Cao and coworkers state that there are two kinds of feedback: one is intensity or energy feedback, the other is field or amplitude feedback [4]. The field feedback is phase sensitive (i.e. coherent), and therefore frequency dependent (i.e. resonant). The intensity feedback is phase insensitive (i.e. incoherent) and frequency independent (i.e. non-resonant). Based on the feedback mechanisms, random lasers are classified into two categories: (i) random laser with incoherent and non-resonant feedback; (ii) random laser with coherent and resonant feedback [5,6]. The transition between coherent and incoherent random lasers is the transition between coherent feedback and amplified

spontaneous emission; according to Cao and coauthors ,the scattering strength of the sample, expressed by the transport mean free path of the sample, is the key parameter to distinguish between the different random lasers[5]. We will speak further about these different kinds of feedback later.

2. Random lasers

In the description of a conventional laser, scattering of light is regarded as loss and detrimental to the laser process. In contrast, in a disordered medium with gain light scattering turns out to have a positive effect on the laser process. Multiple scattering of light increases the time that light spends inside the sample and thus increases the time that the light will be amplified. The combination of multiple scattering of light and gain are the essential ingredients of a random laser. Due to their low threshold and their ease of manufacturing random lasers are expected to be applicable in many utilizations of our quotidian life.

Light diffusion and laser physics meet in the random laser: a multiply scattering medium that amplifies light. Optical scattering in a random medium may induce a phase transition in the photon transport behavior. When the scattering is weak, the propagation of light can be described by a normal diffusion process. By increasing the amount of scattering, recurrent light scattering events arise. Interference between the counter propagating waves gives rise to the enhanced backscattering, known as weak localization. Beyond a critical value of the amount of scattering, the system makes a transition into a localized state. Light propagation is inhibited due to interference in multiple scattering. Since Anderson localization is completely based on the interference effect, and interference is a common property of all wave phenomena, it is natural to extend electron localization to photon localization in disordered dielectric media.

In the case of strong scattering and gain, recurrent scattering events could provide coherent feedback and results in lasing [7,8]. When the scattering mean free path becomes equal to or less than the wavelength, light may return to a scatterer from which it was scattered before, and thereby forming closed loop paths. If the amplification along such a loop path exceeds the loss, laser oscillation could occur in the loop which serves as a laser resonator. The requirement of the phase shift along the loop being equal to a multiple of 2π determines the oscillation frequencies. Such a laser is called a "random laser".

There are two kinds of feedback for random lasing: Lasing with nonresonant feedback occurs in the diffusive regime. In a disordered medium, light is scattered and undergoes a random walk before leaving the medium. In the presence of gain, a photon may induce the stimulated emission of a second photon. When the gain length is equal to the average length of light path in the medium, the probability that a photon generates a second photon before leaving the gain medium approaches one. Thus the photon density increases. From the theoretical point of view, the solution to the diffusion equation, including optical gain, diverges. This phenomenon is similar to neutron scattering in combinations of nuclear fission. When optical scattering is strong, light may return to a scatterer from which it is scattered before forming a closed loop path. This is a random laser with coherent feedback. Of course, the picture of a closed loop is intuitive but naive. The light may come back to its original position through many different paths. All of the backscattered light waves interfere and determine the lasing frequencies. Thus, a random laser with coherent feedback is a randomly distributed feedback laser. The feedback in this case is provided by disorder induced scattering. This effect was evidenced by Lagendijk[9-14], Wiersma[15-17]and Cao [4,18-19]. Random laser was observed in a variety of materials: nanoparticle suspension of TiO_2 , laser crystals, Ti:Sa, ZnO powders for high scattering and gain and many others[12,20-24]. From the point of view of the random laser the crucial parameter is the transport mean free path, that is a measure of the scattering strength of the system. Most of the systems studied are in the diffusive regime, where $\lambda << l_t << L$.

Looking to the Figure 1 which shows the comparison between a "classic" laser and a random laser, one might question how laser action occurs in a disordered material, given that it lacks a real cavity? The answer is simple. The condition for lasing comes from a careful balance between gain and loss. The light is trapped inside the medium by multiple scattering and during the scattering it is amplified by the gain medium. The output radiation can be roughly monochromatic, but without coherence and it is emitted over the whole solid angle. The emission properties of random lasers are not so different from the traditional ones. In particular random laser exhibit a threshold behavior. When the gain overcomes the losses the system goes above threshold. The losses are proportional to the total sample surface and the gain to its volume, so the

threshold criterion can be expressed in terms of a critical volume V_{cr} above which the system lases [12]. The threshold of a laser depends on the balance between gain and loss of light in the system. A laser will lase when the loss inside the cavity equals the gain. The point at which the gain exactly compensates the loss is referred to as the threshold of the laser. In experiments this threshold can be observed for instance in the power out versus input graphs as we will demonstrate below as beta factor.
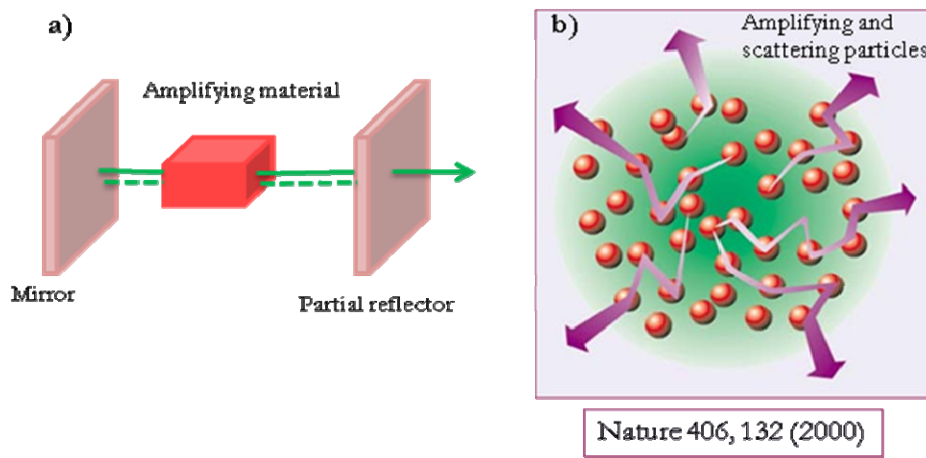
Fig. 1 : *(a) Traditional laser cavity. (b) Random laser; the light is retained in the sample by multiple scattering and it is amplified at the same time.*

2. 1 β factor

A quantitative description of a laser system is given in terms of rate equations. These equations describe the transport of laser light in a random laser:

$$\frac{\partial W_l}{\partial t} = D\nabla^2 W_l + \sigma_e c n_1 W_l + \frac{\beta}{\tau} n_1 \qquad (1)$$

$$\frac{\partial n_1}{\partial t} = \sigma_a c n_0 W_p - \sigma_e c n_1 W_l - \frac{1}{\tau} n_1 \qquad (2)$$

$W_{l,p}(z,t)$ are the laser and pump light densities, $n_{0,1}(z,t)$ is the density of dye molecules in the ground and excited states, with $n=n_0+n_1$ the total molecular density, c the speed of

light in the medium, $\sigma_{a,e}$ the molecular absorption and stimulated emission cross sections, and $D=1/\ 3cl$ is the diffusion coefficient for light. Further, l is the transport mean free path and τ is the excited state lifetime. Equations (1) and (2) are the random laser analog of the well-known kinematic rate equations describing the dynamics of conventional lasers [25]. In these equations one more parameter has been introduced: the b factor of a laser. By doing some mathematical calculations we can explain what b means in the equations (1) and how to obtain it.

To incorporate the spectral dependence we rewrite Eq(1) in terms of the specific energy density $W_l(\lambda)= W_l(l;\mathbf{r},t)$.

$$\frac{\partial}{\partial t}W_l\ (\lambda)\ d\lambda = D\nabla^2 W_l(\lambda)\,d\lambda + \sigma_e(\lambda)cn_1 W_l(\lambda)\ d\lambda + \frac{1}{\tau}n_1\ L(\lambda)M(\lambda)\,d\lambda$$

Integration over the entire spectrum yields Eq(1) from Eq. (3), where $L(\lambda)d\lambda$ is the spontaneous emission spectral density function and $M(\lambda)$ excludes spontaneous emission outside the lasing band from W_l, we get.

$$\frac{\partial}{\partial t}\int_{\lambda_l-\delta}^{\lambda_l+\delta} W_l\ (\lambda)\ d\lambda = D\nabla^2\int_{\lambda_l-\delta}^{\lambda_l+\delta} W_l(\lambda)\,d\lambda + \sigma_e(\lambda)cn_1\int_{\lambda_l-\delta}^{\lambda_l+\delta} W_l(\lambda)\ d\lambda$$
$$+\frac{1}{\tau}n_1\int_{\lambda_l-\delta}^{\lambda_l+\delta}\ L(\lambda)M(\lambda)\,d\lambda \tag{4}$$

so to equate Eqs. (1) and (4) we define:

$$\beta \equiv \int_{\lambda_l-\delta}^{\lambda_l+\delta}\ L(\lambda)\,M(\lambda)\,d\lambda$$

Spontaneous emission is usually the seed for lasing, both in cavity and in random lasers. However, not all spontaneous emission participates in the laser process. The fraction of spontaneous radiation that does contribute to lasing is called β. In the science of

conventional lasers this parameter is of great interest because of the promise of a "thresholdless laser" with $\beta=1$, in which all spontaneous emission is radiated into the lasing mode [26,27]. The "sharpness" of the laser threshold is governed by the value of β. Solving the laser rate equations with $\beta=0$ yields a sharp bend in the field energy density W as a function of pump rate r, a discontinuity in the derivative at the threshold r_{th} . Below threshold $W=0$ and above $W \propto r\text{-}r_{th}$. In the other limit, $\beta=1$, $W \propto r$. For $0<\beta<1$ there is a threshold, which becomes less sharp as β gets larger [25]. The behavior of a laser for the different limits of β is given in Fig 2.[28]
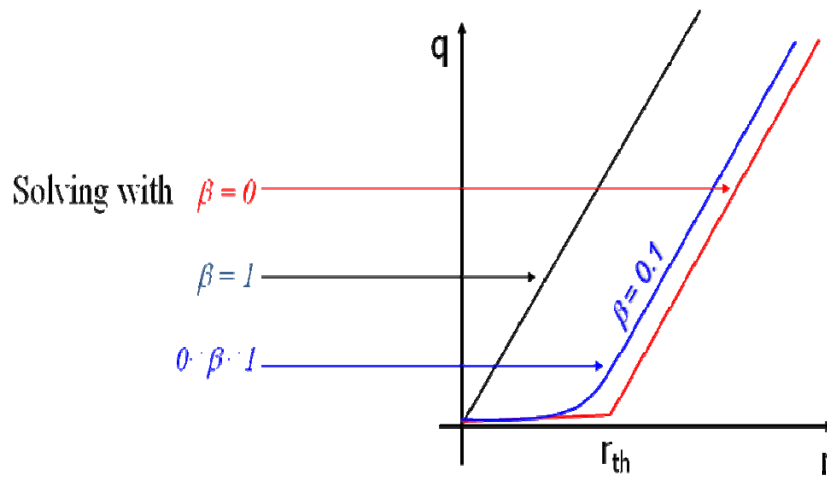
Fig . 2 : *B determines the sharpness of the laser threshold. The threshold is indicated by r_{th}. The abrupt bend for $\beta=0$ turns into a smoother transition for lager β, limited by the "thresholdless" for $\beta=1$.*

G. van Soest and Ad Lagendijk presented another method to determinate β. They construct β from the spectra as outlined in the Fig. 3.
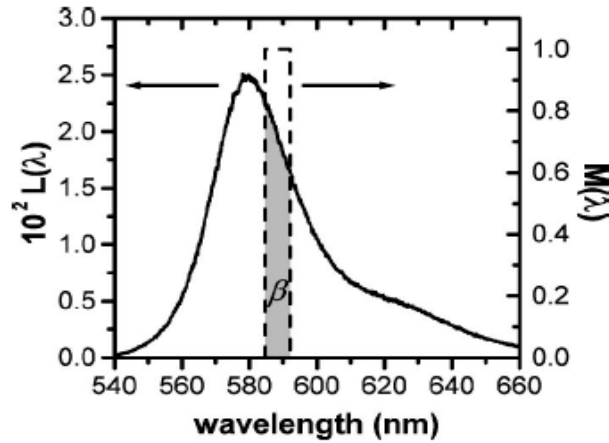
Fig. 3 : *Illustration of the construction of* $\beta \equiv \int_{\lambda_l - \delta}^{\lambda_l + \delta} L(\lambda) M(\lambda) d\lambda$ *, where L(λ)dl is the specific spontaneous emission spectral density (left axis) and M(λ) is the coupling to the random laser process (right axis)*

In the science of cavity laser this parameter is of great interest because of the information that provides.

3. Random lasing in confined dye doped nematics

The diffusion and transport of light waves in complex dielectric structures have spurred a vast range of experimental and theoretical work, revealing one of the most challenging and exciting scientific area of the past decade. The propagation of electromagnetic waves in periodically structured dielectric systems, i.e. photonic bandgap materials, and the linear and non linear optical phenomena in completely disordered systems doped with gain media represent two opposite sides of this promising scientific branch. The laser emission study in ordered and periodic systems has known an extraordinary revival in the last years; even because of the remarkable development of experimental techniques which allow scaling the photonic crystal structures down to the nanoscale with the aim to mould the flow of light [29]. Surprisingly, active random media repeatedly proved to be suitable for obtaining diffusive laser action, mainly based on the resonant feedback mechanisms in multiple scattering. Light localization and interference effects which survive to multiple scattering

events have been invoked to explain the random lasing observed in many exotic and complex systems [18,20,24,30-34]. In fact, when the diffusive photon transport in completely disordered systems encounters the condition $kl_t \sim 1$, being k is the magnitude of the local wave vector and l_t is the transport mean free path, an almost complete localization of light waves should occur. This effect is known as Anderson localization in analogy with the diffusion behaviour of electrons in some conductor lattices [35].

Weak localization of light waves is considered as a particular case of interference effects which were predicted and observed in random media and in partially ordered systems for $kl_t > 1$ [36-39].

The motivation of our study to random lasing in partially ordered systems is that a lot of work has been done in ordered systems as photonic crystals 1D, 2D and 3D exploiting photonic band gap and distributed feedback. A several investigations has been done also for totally disordered systems such as semiconductor powders and s.o exploiting the coherent back scattering and the interference effects that survive in this media but the area between this two extreme is still unexplored. Further, recently, Wiersma and his group demonstrate that coherent backscattering experiments performed with high accuracy apparatus manifested weak localization of light even in tensorial systems characterized by high optical anisotropy, like nematic liquid crystals [40]. These experiments show how the recurrent multiple scattering events exactly back enhance the scattered intensity giving rise to an anisotropic backscattering cone [41].

3. 1 Why nematic liquid crystals?

Nematic liquid crystals (NLC) are uniaxial fluids with rod-like molecules aligned on average along a local anisotropy axis which is represented by the unit vector *n(r,t)*, the molecular director. The spontaneous fluctuations of the director represented by $n(r,t) = n_0 + \delta n(r,t)$ leads to fluctuations in the local dielectric tensor $\varepsilon_{\alpha\beta} = \varepsilon_\perp \delta_{\alpha\beta} + (\varepsilon_{//} - \varepsilon_\perp) n_\alpha n_\beta$ which is the main effect responsible of the recurrent multiple scattering events as a light wave is propagating through the NLC medium. Nematics are turbid in appearance, the scattering of visible light by NLC is higher, by a

factor of the order of 10^6, than the scattering by conventional isotropic fluids [42]. This was in fact one of the things which cast doubt on the very existence of liquid crystals in the early years; it was tempting to assume that they were made of suspension of small crystallites in a fluid phase, with crystallite dimensions comparable to an optical wavelength. However it became clear that the high scattering power was in fact the intrinsic property of well defined nematic phases. The first experimental studies in this field has been reported by P. Chatelain[43], they give us a very direct probe of the spontaneous fluctuations of the alignment in a nematic medium.

The fluctuations of the local dielectric tensor $\varepsilon_{\alpha\beta}$ come from two different sources: (1) fluctuations in $\varepsilon_\perp$ and $\varepsilon_{//}$ due to small, local, changes in the density, temperature, etc.; (2) fluctuations in the orientation of $\boldsymbol{n}$, this is the dominant effect which is specific of nematic liquid crystals. When the scattering is increased beyond a critical value, the system makes a transition in a localized state, where light propagation is inhibited owing to interference in multiple scattering. The weak localization of light in an amplifying scattering medium supports stimulated emission through resonant and nonresonant optical feedback. Such laser action is usually called diffusive or random lasing.

In this study, we mainly consider the multiple scattering of spontaneously emitted photons within the gain medium. These photons are characterized by different initial states of polarization which does not depend on the excitation polarization. The polarization of the excitation pulses and the scattering intensity is considered only in terms of quantum yields and photons available to be radiated into the lasing modes.

In this chapter we report the first experimental observation of random laser action in a partially ordered and highly anisotropic NLC doped with fluorescent guest molecules. The study of laser emission in such system emphasizes the peculiar behaviour of diffusive laser action, randomness of laser emission was observed in time, space and frequency. In fact, the spatial distribution of the emitted light is speckle-like accompanied by strong intensity fluctuations and slight shifts of the resonant peaks occur for each pump pulse. The random laser relevant length scales, i.e. the scattering mean path length l, the gain length l_g, and the sample size are found to be in good

agreement with the random laser theory. In fact, the gain length at the onset of lasing is $l_g \sim V^{2/3} / l \sim 3.5 \times 10^{-2}$ mm, is in reasonable agreement with the value found experimentally at the lasing threshold pump intensity (4.4×10^{-2} mm). In addition, the scattering mean path length was measured to be about an order of magnitude longer than the gain length providing ample opportunities to trigger the lasing effect.

Fig. 4 : *Schematic representation of a random walk in an anisotropic nematic liquid crystal medium. The pump light is diffusively scattered in the system and creates the gain region . When a photon travels inside the gain region it is amplified, while outside it is only scattered.*

A schematic view of the random laser action is shown in Fig. 4. The absorption of the pump beam follows the Beer law

$$I(z) = I(z = 0) \exp(-k_{abs}z)$$

where $k_{abs} = 1/l_{abs}$ is the absorption coefficient. This means that after a distance equivalent to l_{abs} the light intensity that enters the sample is reduced by a factor e^{-1}. Pump light is absorbed and part of the system becomes amplifying. Emitted photons are amplified while they travel into the gain region. Outside the gain region only scattering takes place, but photons have also the chance to enter again into the gain region and to be amplified again. Gain in a diffusive medium mainly amplifies long light

path, just like absorption attenuates them. In a diffusive random laser the spatial selectively of a cavity, which is essential in concentrating the stored energy in few modes, does not exist. The only selection mechanism is the wavelength dependence of the gain. Said otherwise, the electromagnetic modes of the system are broad (because of large losses) and strongly overlapped. A system that provides very strong scattering could decouple the modes of the system. This is called "random laser with resonant feedback" due to the supposed formation of random cavities in the Anderson localization regime [4].

3. 2 Experimental set-up

The nematic liquid crystals used in this experimental studies are: BL001 provided by Merck, having the following bulk phase sequence *Cr. – -10°C – Nematic – 63°C – iso.* The nematic liquid crystals was doped with 0.3 wt% of dye molecules(in this work we used more than one dye: the Pyrromethene 597, Pyrromethene 650 and the DCM. These dyes are provided by Exciton). The mixtures were bounded in several confinement geometries in order to investigate the role of the shape and the size of the confining system.

The first experiments were performed by confining the mixture (nematic liquid crystal and 0.3% of dye) in a wedge cell constituted by two glass-ITO plates separated by Mylar spacers, with a thickness of 150 μm at one edge and 2 μm at the other one. The inner side of the plates were covered with rubbed polyimide alignment layers in order to induce a homogeneous alignment of the NLC molecules at the interface.

The empty wedge cells has been checked by measuring the transmission and reflection spectra collected by using a high sensitivity spectrophotometer (UV-visible-near-infrared Cary 500 by Varian) in order to rule out any cavity effect due to multiple reflected light waves at the boundaries. Indeed, the experiments revealed the absence of constructive interference in these cells. In addition, the free spectral range was calculated by assuming a cavity effect and it was found to be absolutely incompatible with the wavelength of the lasing modes and with the spectral spacing of the modes.

The wedge cell was filled by capillarity the flow was directed along the rubbing direction and normal with respect to the wedge. Upon observing the sample under a

polarized microscope, it shows a planar alignment with the optical axis which lies in the plane of the cell parallel to the rubbing direction. The dye molecules dissolved in the NLC at very low concentration (0.3-0.5% by wt), proved to be completely miscible as evidenced by the almost complete absence of micro-droplets of dye embedded in the nematic phase. The wedge sample was optically pumped with 3-5 ns pulses produced by a frequency-doubled (532 nm) Nd:YAG laser (NewWave, Tempest 20). The pump beam was focused onto the thick region of the sample (about 150 μm) with a spherical lens (f = 100 mm) yielding a beam waist of about 30 μm at the focus position(see Fig. 5).
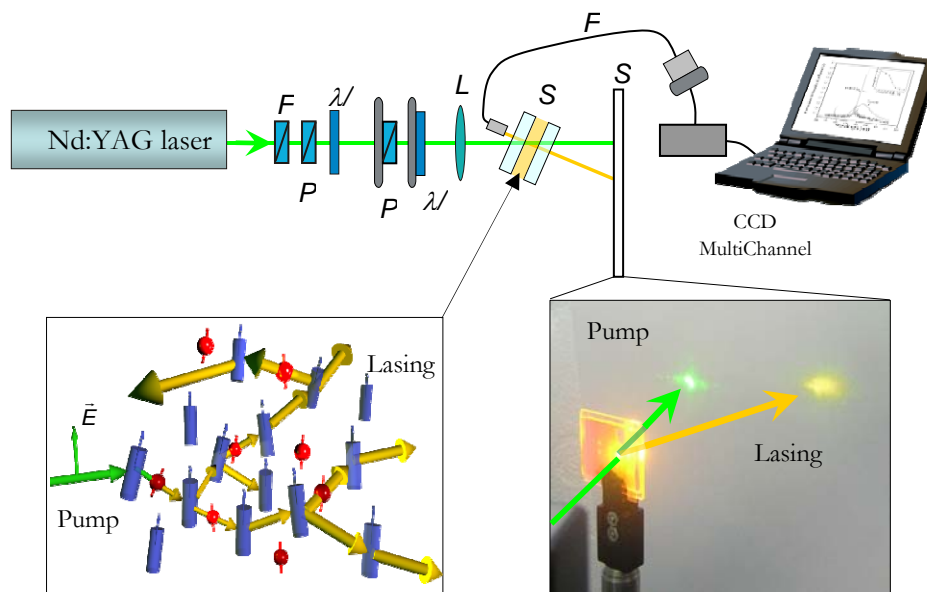
Fig. 5 : *Experimental apparatus for measuring the emission features of a random laser in nematic liquid crystal sample. The laser was a frequency doubled (λ = 532 nm) Nd:YAG. It operated at 20 Hz repetition rate and had a pulse width of 5 ns. The emitted light was collected by a spectrometer that allowed a resolution of 0.5 nm. The pump beam was focused on the sample, resulting in a spot size of 40mm of diameter.*

The experimental set-up presents a combination of optical elements (quarter-wave plates, half-wave plates and Glan-Thompson polarizers) in order to select all the states of polarization of the pump beam. A multichannel CCD spectrometer with a high spectral resolution (0.5 nm) and with a fiber termination was used to capture the emission spectra within a limited cone angle of 0.05 rad. The speckle-like pattern of the

emission spot was imaged on a screen while simultaneously the emission spectrum was captured by means of the CCD spectrometer.

The same mixture was confined also in cylindrical capillaries see Fig. 6, without any surface treatment, having inner sections of 0.2 mm and 0.5 mm. These capillary tubes were checked also experimentally to rule out the existence of Whispering Gallery Modes (WGM) which occur at particular resonant wavelengths related to the index refraction and size of the cavity. In fact, the inner surface of these cylindrical cavities have been covered with a thin film of dye doped nematic liquid crystal, under optical excitation, the emitted light presented just the typical spontaneous emission curve of the dye molecules. These systems have been characterized with the some experimental setup as the wedge cells.
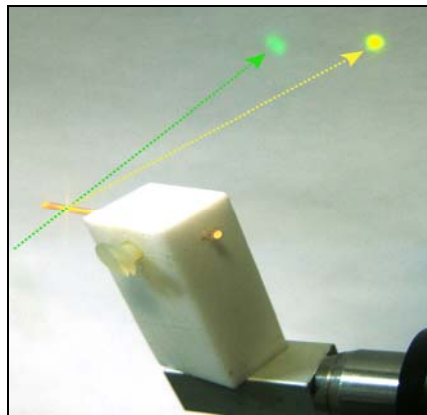
Fig. 6 : _Picture of diffusive lasing from optically pumped cylindrical capillary_

As mentioned before the emitted light was collected and spectrally analyzed using a high resolution optical multichannel charge coupled device (CCD) spectrometer (Jobin-Yvon). The input pump energy was varied, an example of an emission spectrum is shown in Fig. 7. At low pump power, the emission spectra show the typical spontaneous emission curve of dye molecules, indicating that NLC does not

considerably modify the fluorescence spectrum . Upon increasing the pump power above a given threshold value discrete sharp peaks emerge from the residual fluorescent spectrum. The line width of these sharp peaks were less than 0.5 nm, yielding a quality factor Q of this random cavities larger than 1000. The narrow peaks denotes a decrease of the width of the spectrum of the emitted light triggered by the increase of the pump energy. A measure for the gain narrowing is the narrowing factor NF, defined as the full width half maximum (FWHM) of the emitted light below threshold (FWHM$_{below}$) divided by the FWHM of the emission spectrum of the random laser above threshold (FWHM$_{above}$)

$$NF \equiv \frac{FWHM_{below}}{FWHM_{above}}$$

In the case of the Fig . 7, the narrowing factor (NF) is: 50
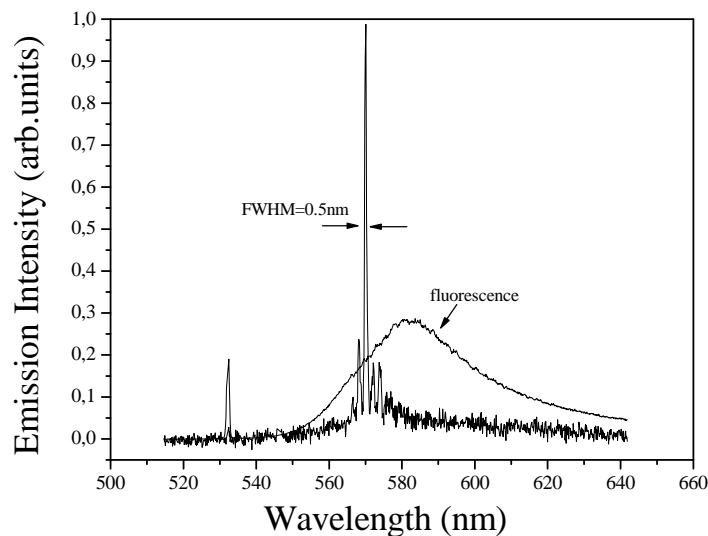
Fig . 7 : *Fluorescence and lasing spectra are reported. Discrete sharp peaks emerge from the residual spontaneous emission for pump energy of about 1.2 μJ/pulse.*

Going further in the details, by increasing the pump energy below a threshold value 600 nJ/pulse, the emission spectra show an amplified spontaneous emission of the dye used (Fig. 8a). Upon reach a given threshold value, about 960 nJ/pulse discrete sharp

peak appear (Fig. 8b). Increasing further the pump energy more sharp peaks emerge and the output energy was found to be about 150 nJ/pulse at room temperature (Fig. 8c). When the incident pump energy exceeds the threshold value, the peak intensity increases much more rapidly with the pump power and more sharp peaks appear, because now the balance gain-loss of these lossiest modes become positive. As the optical gain increase, the lasing peaks become narrower. We noted also that the number of lasing modes increases with the pumping intensity(Fig. 8d). Eventually the spectral density of lasing peaks becomes saturated, the number of lasing modes increases linearly with the sample volume.

The figure 7 present a blue shift of the laser emission with respect to the fluorescence maximum. This is due to that the lasing frequencies are determined by phase relationship of the counter-propagating scattered light waves. In fact, the weak localization of light waves owing to the strong optical scattering gives rise to reciprocal paths within the gain medium. When the phase accumulation in reciprocal path is equal, constructive interference occurs among the backscattered amplitudes. Therefore, it was believed the blue shift is determined by interference effects which introduce coherence and feedback, leading to lasing action.
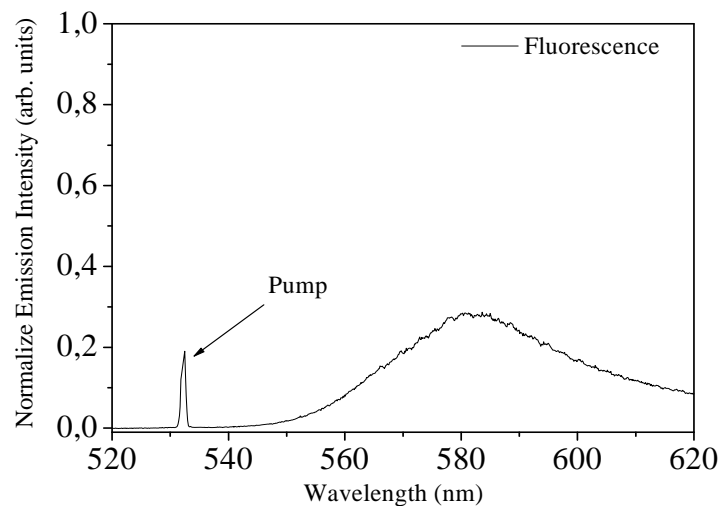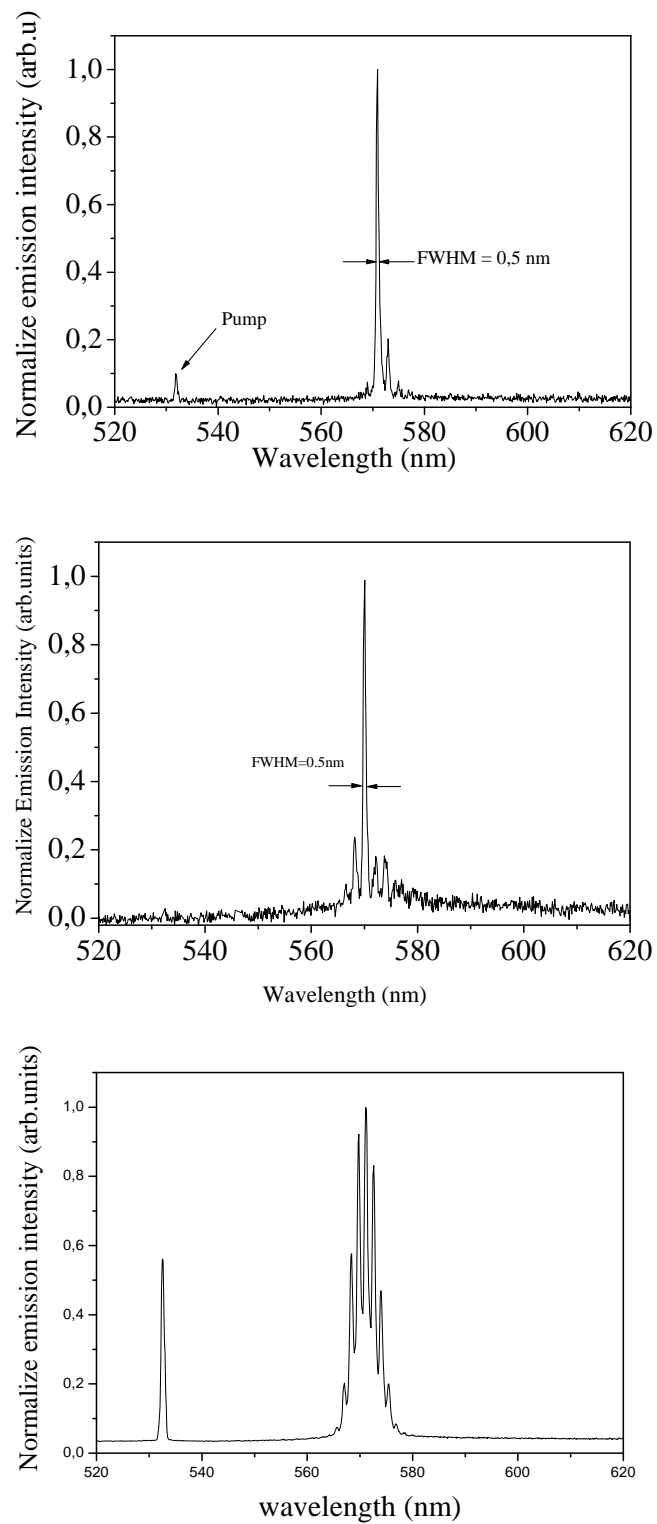
Fig. 8 : *(a) A typical spontaneous emission curve of the PM597 dye, (b,c,d) Lasing spectra increasing the pump energy.*

A variety of characterization studies have been performed after this first observation of random lasing in partially ordered nematic liquid crystals, such as the polarization dependence of lasing intensity and polarized fluorescence.

The Fig. 9 shows the dependence of lasing intensity as a function of the orientation of the linear state of polarization of the pump beam. The lasing intensity undergoes a five-fold lowering when the pump light is polarized perpendicularly to the NLC director (*o*-wave) compared with the light polarized parallel to the director (*e*-wave). The polarization dependence of the scattering intensity and the coupling of the optical field with the gain medium have to be taken into account for the observed anisotropy. The former effect is mainly due to polarization dependence of the diffusion constant D for the emitted photons, indeed a larger diffusion constant for the e-wave compared to the o-wave is generally measured.

Fig. 9 : (a)T*he dependence of the lasing intensity on the angle* θ *between the linearly polarized light and the local nematic director orientation.(b) Lasing spectra for parallel and perpendicular polarisation.*

The latter aspect can be analyzed by considering the *Fermi's Golden Rule* which clearly states that the molecular transitions and the rate of emission strongly depend by the coupling of the pump electric field $\boldsymbol{E}$ and the transition dipole moment $\boldsymbol{d}$ of the dye

molecules. Thus, these processes are governed by the projection $\boldsymbol{E} \cdot \boldsymbol{d}$. In addition, the experimental results emphasize that the fluorescent molecules adopt to some degree the local nematic order of the liquid crystal solvent, which results in an anisotropic orientational distribution of the transition dipole moment (see Fig. 10).
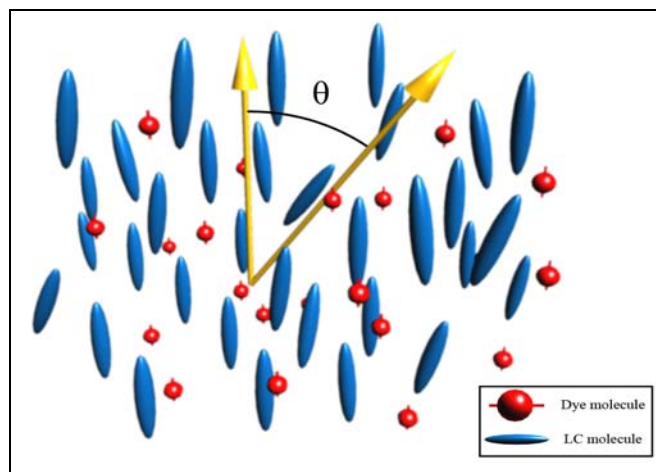
Fig. 10 : *Schematic showing the proposed preferential orientation of the dye molecules inside a wedge cell. θ is the angle between the direction of the local molecular director and the input polarization direction of the pump beam.*

In fact, polarized fluorescence measurements emphasize a strong dependence of the emission intensity on the pump polarization, as it is shown in the polar plot of figure. 11
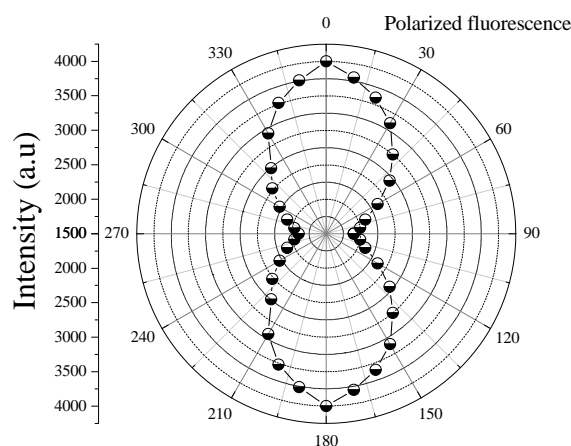
Fig. 11 : *Polar plot of the polarized fluorescence of the dye doped nematic sample. It is obtained by measuring the fluorescence intensity by analyzing the polarized emission at different angles about the local nematic director*

It is worth to point out that the maximum of the lasing intensity was obtained for linearly polarized pump pulses with E oriented along the local director $(\theta = 0°)$, being in good agreement with the polarized fluorescence results as well as the polarization dependence of the scattering intensity. This indicates that the dye molecules possess an anisotropic orientational distribution of the transition dipole moments along the local nematic director, with a dye order parameter $S_D = 0.2$ calculated as follows [44]:

$$S_D = \frac{\left(\dfrac{F_{//}}{F_{\perp}}\right)^{1/2} - 1}{\left(\dfrac{F_{//}}{F_{\perp}}\right)^{1/2} + 2}$$

Here $F_{//}$ and $F_{\perp}$ are fluorescence intensities polarized parallel and perpendicular to the NLC director, respectively. Therefore, this confirms that the dipolar coupling modifies the quantum yield for fluorescence and plays an important role for the light amplification process; some states of polarization of the pump pulses provide a larger number of spontaneously emitted photons which are radiated in the lasing modes.

Another interesting characterization for a random laser is the study of β factor. When you speak about diffusive lasing you have to introduce this factor. Hence, in order to gain further understanding on the diffusive laser action observed in this partially ordered system, a comparative study of the emission properties of systems with different order degree was performed. The input-output characteristics was investigated and the β-factor of the following systems was evaluated (Fig. 12): 1) self-ordered dye doped helixed liquid crystals confined in conventional sandwich cell [45-48]; 2) laser dye solution containing TiO_2 nanoparticles [49]; 3) dye doped nematic liquid crystal confined in a wedge cell. While the first two systems have been widely investigated showing a lasing action with a well known input-output behaviour, the unexplored presented system presents a peculiar intermediate behaviour. In a conventional laser, β is defined as the ratio of the rate of spontaneous emission into the lasing modes to the total rate of spontaneous emission $(0 \leq \beta \leq 1)$, and determines the sharpness of the laser threshold [28]. In the science of cavity laser this parameter is of great interest

because of the promise of "thresholdless laser" with β=1, in which all the spontaneous emission is radiated into the lasing modes.

Fig. 12 : *Light input-output curves for systems with different order degree are reported. The emission rate of ordered dye doped cholesterics with a periodic helical structure, disordered nanoparticles of TiO$_2$ dissolved in methanol solution and partially ordered nematic liquid crystals are compared.*

In figure 12 is reported the integrated emission intensity in function of the pump energy for the investigated systems characterized by different order degree. Unlike the sharpness of the lasing threshold observed in the self-ordered cholesteric cells ($\beta \sim 0.01$), in which a super-linear increase of the emission intensity is measured above the threshold, the input-output curve measured in the random medium shows a stretched-exponential behaviour characterized by $\beta \sim 0.2$. The partially ordered nematic sample shows behaviour intermediate between these two extremes. In fact, the output energy increases almost exponentially with the pump power ($\beta \sim 0.08$). The presented behaviour suggests that a large part of the spontaneous emission is radiated into the lasing modes by of the optical feedback provided by the anisotropic coherent backscattering.

Diffusive lasing in partially ordered liquid crystal has been observed also in other nematics doped with guest molecules such as the MBBA and ZHK650, the Fig. 13

shows the emitted light from these systems. Due to the weak temperature transition of the MBBA and the cumulating heating of the sample from the pump beam, lasing in MBBA was not stable and the signal vanish as soon as the sample resent the pump beam. For this raison we choice to work with BL001because the life time of the signal is much larger than the MBBA and ZKH650.
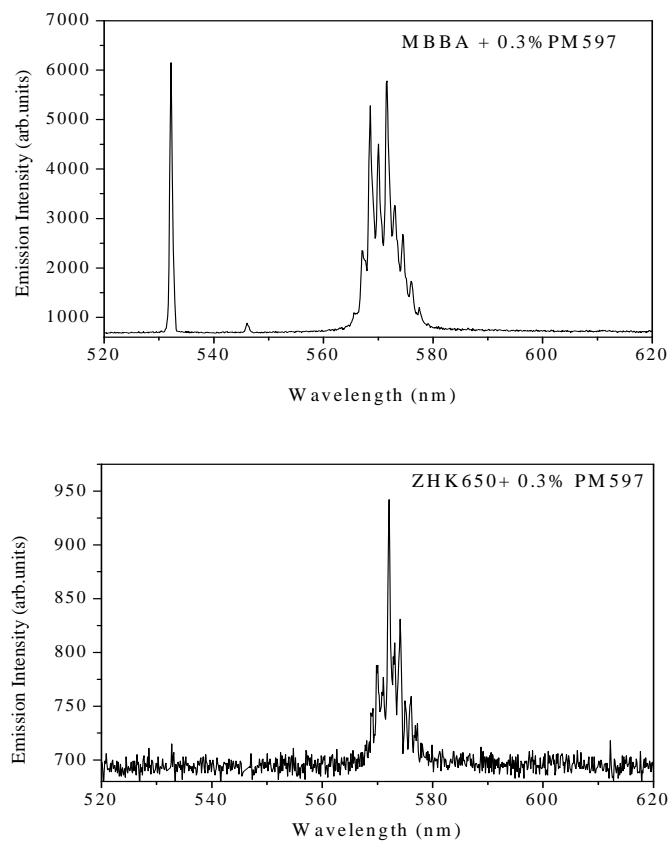
Fig. 13 : *lasing spectra in the case of a wedge cell for different type of liquid crystal*

Further varying the nematic liquid crystals, we used several dyes: DCM, Pyrromethene 597 and Pyrromethene 650. The some concentration of dye was added each time to the nematic choice. The figure 13 shows that lasing is still present for each dye with almost the same line width. The experimental studies show that the Pyrromethene 597 is more efficient than Pyrromethene 650 (Fig. 14).
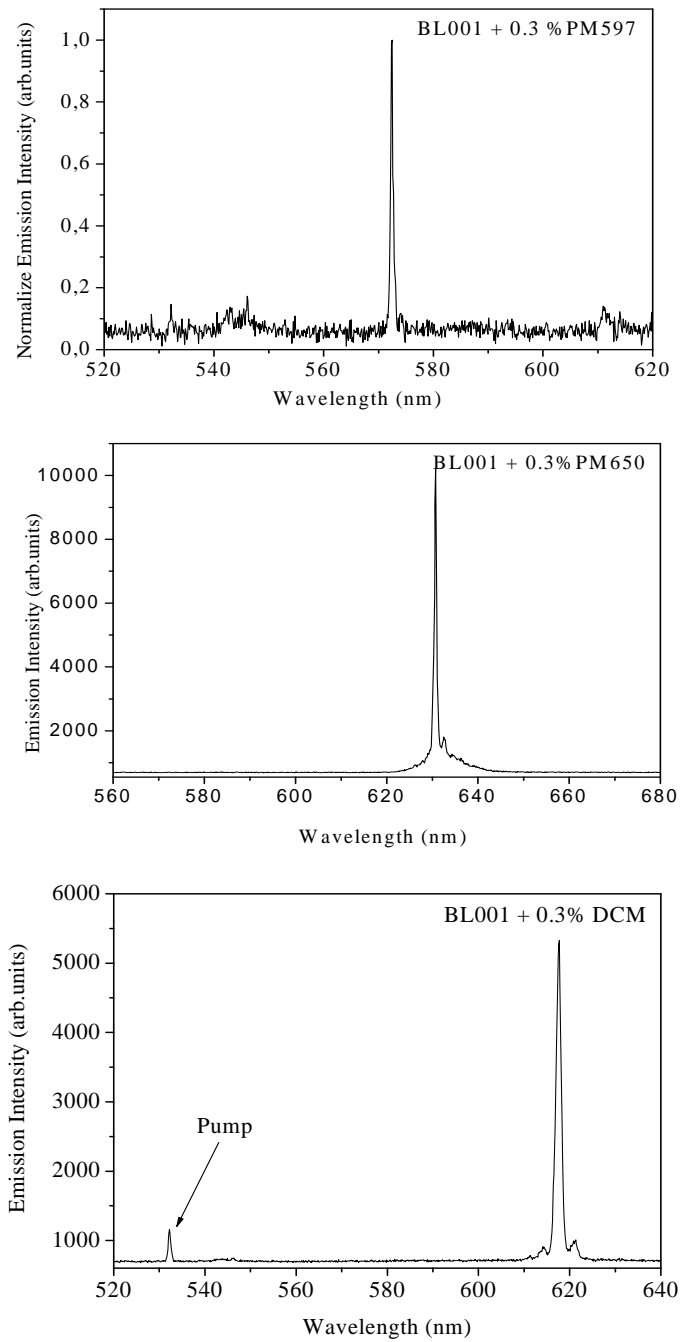
Fig. 14 : *lasing spectra in the case of a wedge cell for different type of dye.*

After presenting this characterizations of diffusive lasing in partially ordered nematic liquid crystal confined in wedge cells, one may ask are you sure that the bulk play the main role in the lasing process.

To answer to this question we approached two strategies:

1-   Quenching the fluctuations of the nematic director by polymerizing the gain medium. We prepared a mixture of 50 % of BL001 and 50% of active liquid crystal (C6M[RM82; EMD], C3M [RM257 (4-(3-Acryloyloxypropyloxy)-benzoic acid 2-methyl-1,4-phynyleneester; Merck] and dichroic photo initiator [BDH1468, Merck]). We add to the mixture 0,3wt% of PM597 and infiltrated it by capillarity in wedge cell. We characterized spectrally the sample before polymerizing it, we noted that the signal is still present. However after an exposure of 20 minutes at a UV lamp, the mixture is polymerized the fluctuations are quenched and the diffusive lasing is vanished. We observed just an amplified spontaneous emission typical of the PM597. This can be a good validation that the bulk play the mean role in the lasing process

2-   Going further in this direction (to check the origin of the lasing process) we decide to change the confinement geometries.

We report here a comparison study between wedge cell and capillary tube. The both geometries are filled with the same mixture. The cylindrical cavities were used without any orientation treatment. The emitted light was spectrally analyzed for both geometries, as shown in Fig. 15 possessing almost the same line with. The measured sharp peaks prove that the effect does not depend on the size and the geometry of the boundary conditions, but the key role is played by bulky dye doped nematics.
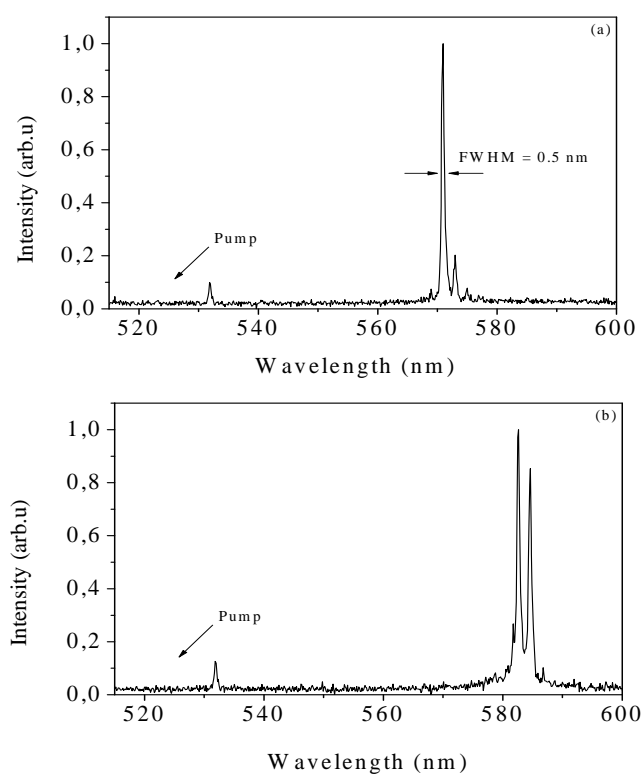
Fig. 15 : *(a)* *Wedge cell and* *(b)* *Capillary tube lasing spectra show different wavelength positions and number of lasing modes.*

A comparative study demonstrated that the emitted light by the cylindrical capillary was redshifted with respect to the wedge, this is due to phase relationships which depend on the boundary constraints. Also looking to the polarized fluorescence measurements presented in Fig. 16 one can observe a pronounced anisotropy for the wedge cell however a quasi circular profile for the capillaries. This clearly indicates that the dye molecules adopt to some degree the higher order parameter and the alignment of the nematic phase confined in the wedge cell with respect to the degenerate alignment within the untreated cylindrical capillary. Upon increasing the pump intensity, more sharp peaks appeared and the peak intensity increased more rapidly. Since the condition for lasing comes from a careful balance between gain and losses, where the gain becomes larger than the losses the system starts to lase.
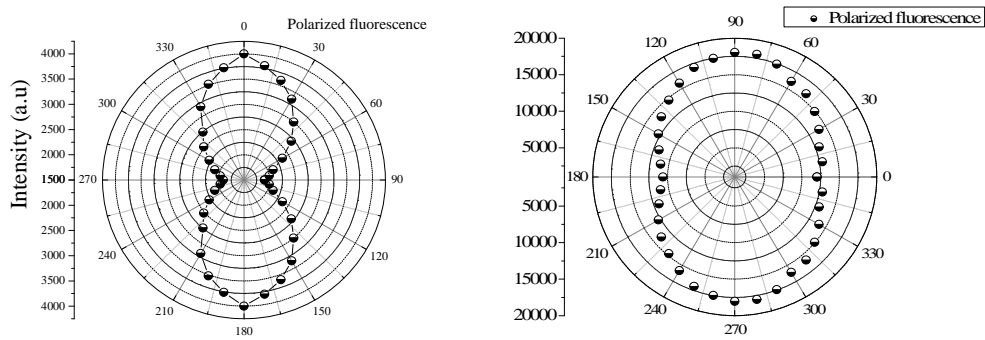
Fig. 16 : *Polar plot for a wedge (a) and capillary (b) dye doped nematic sample showing the dependence of the polarized fluorescence emission on the angle θ between the linearly polarized light and the local nematic director orientation. A significant lowering of the intensity is obtained when the pump light is polarized parallel and perpendicular with respect to the nematic director.*

In order to understand the underlying mechanisms responsible for the observed excitation threshold behavior, we investigated the input-output characteristics of both systems. The figure 17 shows that the lasing threshold for the two types of confinement is quite different. The experimental study of the output vs input shows that the lasing threshold is lower for the wedge cell than in the case of the micro cylinder.
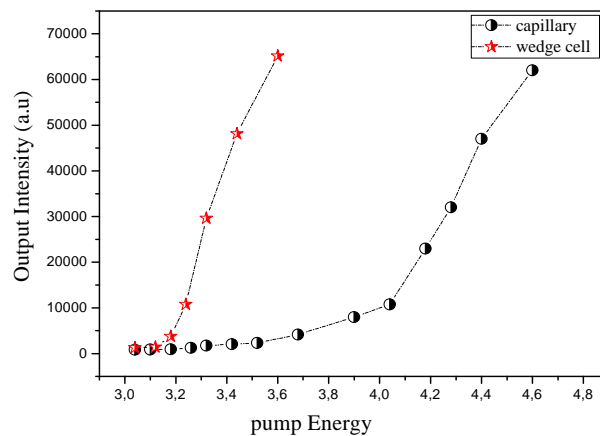
Fig . 17 : *Emission intensity vs pump energy for the wedge cell and capillary glass microtube. The two confining geometries present different threshold values of the input pump energy above which random lasing is obtained.*

4.   Freely suspended liquid crystal random laser

Multiple scattering and amplification of the light are the mechanisms that govern the random laser action. In our case due to fluctuations of the nematic directors, light is trapped inside the gain medium long enough to be amplified before escapes through the sample surface. The overall gain depends on the excitation and on how strongly the materials scatters light. The more the material scatters light the longer the light is kept inside and the larger the overall gain can grow.

In this section, by employing a novel geometry, the idea was to create the condition of almost complete absence of boundaries for a dye doped nematic liquid crystal film in order to study how the partial order of unbounded organized fluids can play the role of random resonators leading to a multi-mode laser. The motivation of this work finds its important support in the opportunity to investigate the mechanisms of amplification and localization and their interplay in such complex system in absence of confinement. Upon freely suspending organized fluids is possible to exploit the unique optical properties of these materials which can be modified by several external parameters, i.e. magnetic, electric, thermal, and mechanical stimuli. The visco-elastic properties and the surface tension mainly determine the profile of the free standing films, in case of high viscosity liquid crystalline materials (smectic phase) was possible to obtain very thin films, only few smectic layers thick (tens of nanometers). The mismatching of refractive indices, the irregular shape of the air-liquid crystal interface and the scattering cross sections are some of the parameters accounted to study the reported effect. Several systems have been investigated by changing the dye laser (PM597, PM650, DCM ..) and the geometry to suspend the gain complex fluid, with the aim to study how the menisci and liquid crystal-air interfaces modify the emission properties.

The mixtures, consist of a nematic liquid crystal BL001 (Merck) doped with dye molecules, were freely suspended by means of a fluid spreader on a PVC net creating squared comb (800 μm x 800 μm) having a thickness of about 300 μm (Fig. 18). The suspended films observed at the optical microscope show a poly-domains structure where the single domain possesses a residual birefringence. Both mixtures show a high

degree of miscibility of the dye laser in the liquid crystalline solvent, in fact was not found evidence of dye micro-droplets phase separated by the liquid crystalline phase. In addition, the spectro-photometric measurement reveals that the absorbance curve is only slightly modified with respect to usual dye solutions of isopropanol or other pure solvents. The PVC net was cleaned with usual solvents, dried in an oven at 50 °C for 1 hour without any treatment to align the liquid crystal molecules. Nevertheless, a partially ordered medium was obtained due to the flow induced by the spreading process over the comb. The profile of menisci driven by competitive forces (gravity, viscosity and surface tension) across the medium present a thinner region of about 300-350 µm.
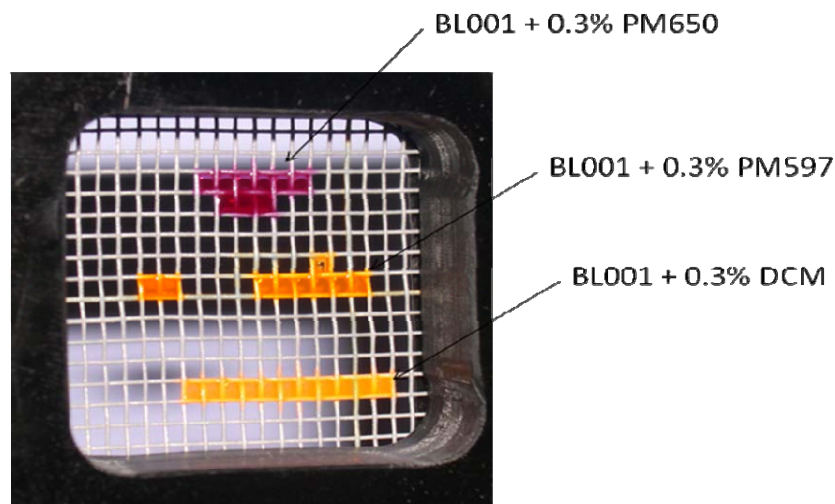
Fig. 18 : *Network containing several freely suspended thin film of dye doped nematic liquid crystal*

The system has been optically pumped with 532nm produced by a frequency-doubled Nd:YAG laser (NewWave, Tempest 20). The pump light consisted of a train of twenty 3-ns pulses focused into a 50-µm spot by means of a spherical lens and circularly polarized by means a quarter-wave plates in order to maximize the excitation cross section(Fig . 19).
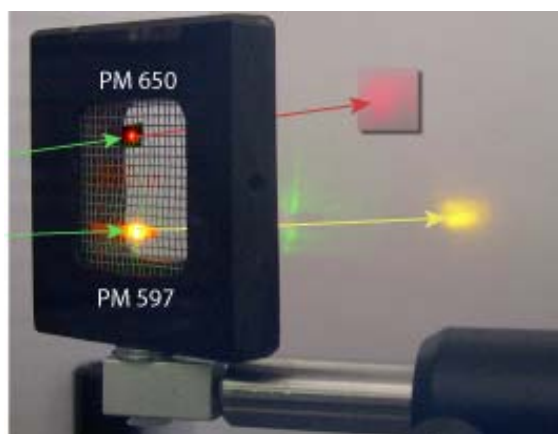
Fig .19 : *Image of the diffusive lasing by optically pumping the samples freely suspended. Intense stimulated emission is observed on the background screen for two different dyes.*

At low pump energy a strongly diffuse isotropic signal of fluorescence was observed. Upon increasing the pump energy above a given threshold, the emitted light appears focalized along the excitation volume. This effect is spectrally accompanied by the collapse of the fluorescence emission and the appearance of sharp bright tiny spots in a wide cone about the excitation volume. The spectral and spatial study of the emission patterns clearly revealed a random lasing behaviour characterized by narrow banded (FWHM = 0,5 nm) brilliant spikes which rapidly fluctuate in frequency and space (Fig. 20).
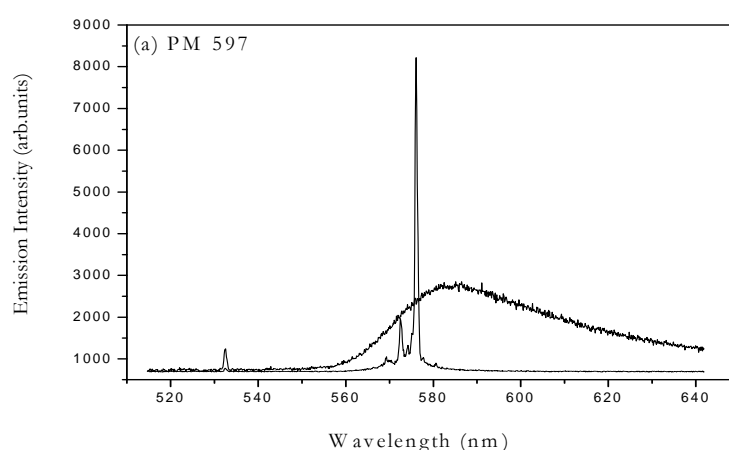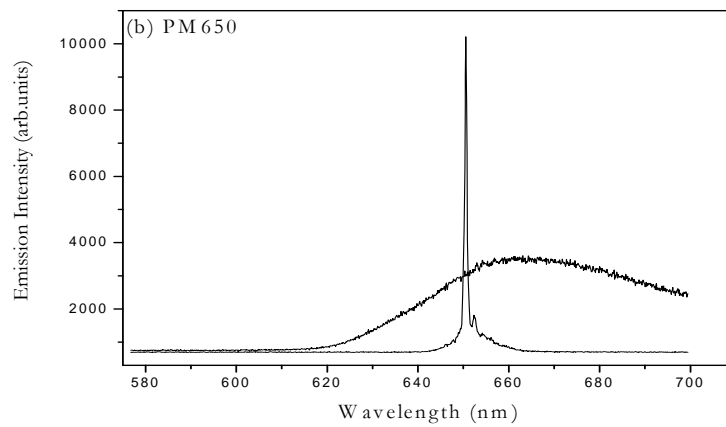
Fig. 20 : *Fluorescence and lasing spectra in thin films freely suspended nematic liquid crystal doped with PM597(a) and PM650 (b).*

In order to understand the mechanisms behind this effect we performed a study by varying the geometry and to identify the role of each material several mixture were prepared. The first experiments were carried out in the suspended on the squared plastic network, the sample was optically pumped with an appropriate laser pulses train.

Additionally, other experiments performed on dye doped liquid crystal drops controlled in diameter by means of a special syringe evidenced a richer spectrum and emphasized the mode dependence of geometry and size of the system.. The drop is standing by gravitational strength from a syringe (Fig. 21). The diameter of the drop is about 2 mm. The green pumping beam was focused in this drop by a spherical lens. Like in the other geometries almost the same threshold behavior has been observed. Above a critical value the system starts to lase.
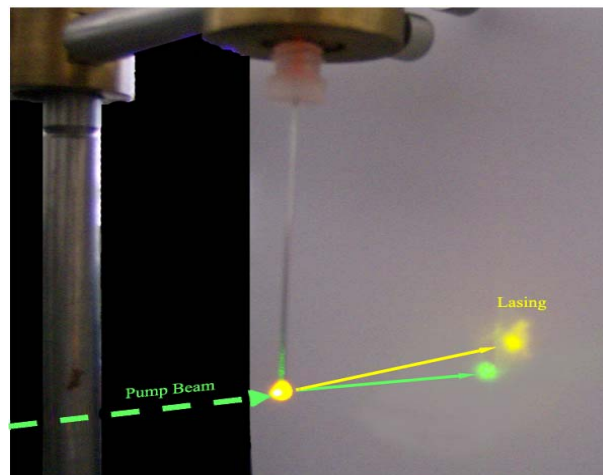
Fig. 21 : *A picture illustrating the random lasing phenomenon in a dye doped nematic liquid crystal droplet.*

Indeed upon optical pumping the system lases and an intermittent speckle like pattern of granular aspect is obtained on the background screen. By investigating the emission spectra we can clearly recognize that random lasing occurs above a given pump energy threshold value for which the coherent backscattering is sufficient enough to promote the gain inside the active material. Measured spectral line widths results to be about 0.6 nm, as shown in the Fig . 22.
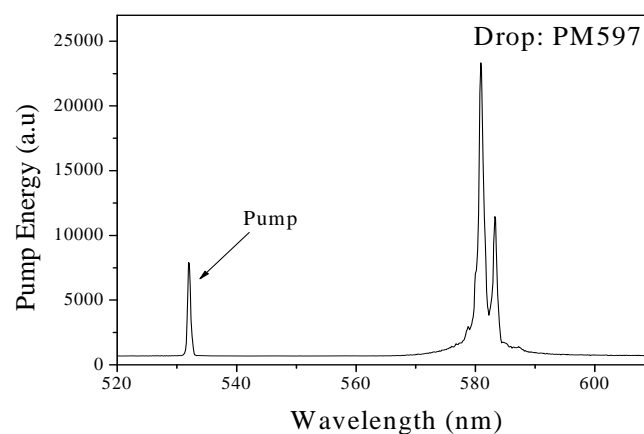
Fig . 22 : *Lasing spectrum of a free standing dye doped nematic liquid crystal.*

By freely suspending these fluidic gain media on a squared plastic net realizes a new approach to study the generation of random laser light. Additionally, this approach assumes an important technological valence being a complex system but extremely easy to prepare and study. Spatially fluctuating narrow banded lasing peaks occur as the pump energy exceeds a few microjoule/pulse realizing a random laser with a relatively low lasing threshold. The threshold lowering is due to the absence of boundaries which reduce the optical losses (absorbance, guided modes).

5. Fluctuations of emitted light: spectral, spatial and temporal

In order to gain further understanding on the diffusive laser action observed in partially ordered system, the far field spatial distribution of the emitted light was analyzed. Lasing emission was captured in a limited cone angle ($\theta \cong 0.1$rad) by means of a high resolution and sensitivity CCD camera (1390 X 1024 12bit PixelFlyQe by PCO). After elaborate the image with a Matlab program we observed that the intensity profile is formed by a series of bright tiny spots spatially overlapped which create a richly structured pattern typical of diffusive lasing. Figure 23 depicts the interesting scenario of the random lasing emission pattern from dye doped nematic liquid crystals confined in a wedge geometry pumping shot by shot the sample. The sequence of images was obtained for four successive pump pulses and we can clearly observe that random lasing changes both spatially and in terms of intensity. This emission mechanism is based on the diffusive process of spontaneously emitted photons by fluorescent guest molecules launched at random directions from random positions. These photons are involved in a weak localization process within the gain medium because of recurrent multiple scattering. Since the condition for lasing comes from a careful balance between gain and loss, it is clear that in this case not for every pump pulse the random walk inside the anisotropic medium gathers enough gain for the system to lase.
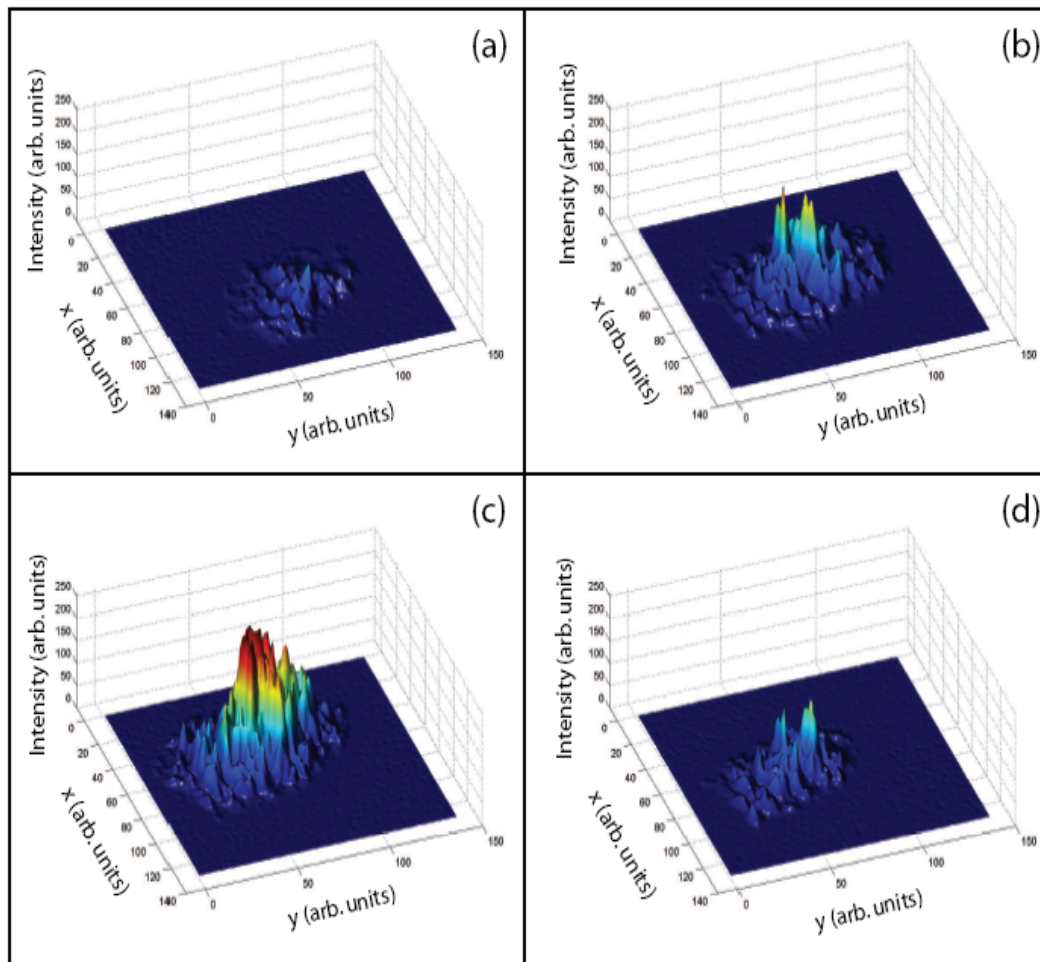
Fig. 23 : *Far field spatial distribution of the emission intensity profile in a wedge NLC sample in the case of four successive (a,b,c,d) pump beam pulses present an irregular intermittent behavior, both spatial and temporal, of the emission.*

The same spatial fluctuation mechanism has been noted for the other confinement geometries. Fig . 24 reports the spatial far field of emitted light measurements for the freely suspended film captured with a high sensitivity and resolution CCD camera (Pixel-Fly-QE by PCO).
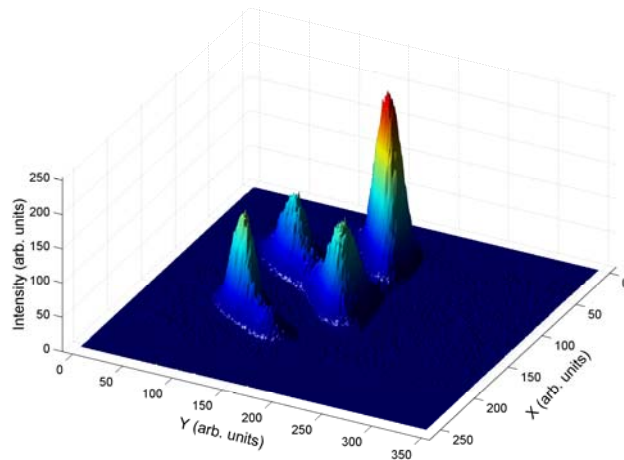
Fig. 24 : *Far field spatial distribution of the emission intensity profile in a freely suspended dye doped nematic liquid crystal film.*

In addition, the figure 25 present a comparison of the far filed spatial distrubution between an ordered system(cholesteric sample) and partially ordered system (nematic sample). In the case of cholesteric sample we observed an expected pseudo-Gaussian lasing profile obtained for a well ordered systems unlike in the nematic liquid crystal sample.
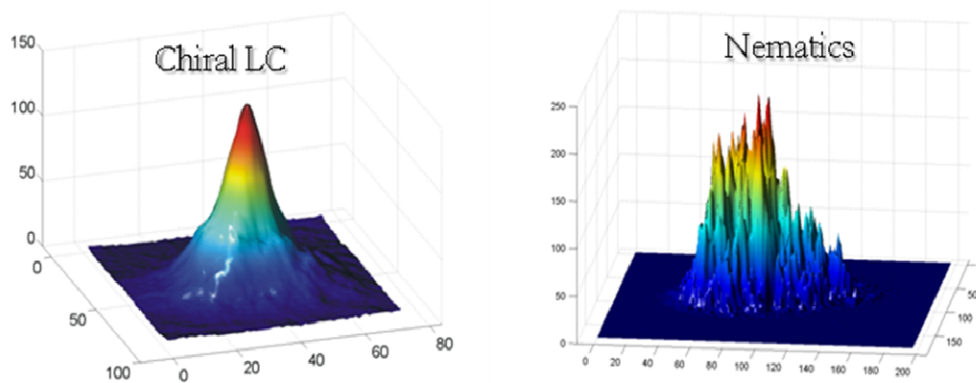
Fig. 25 : *Intensity spatial distribution showing a Pseudo-Gaussian profile obtained for a well ordered helixed liquid crystal sample (top) is compared with (bottom) the laser emisssion for a dye doped NLC wedge cell. Bright tiny spots spatially overlapp describing a richly structured emission pattern typical of diffusive laser action.*

Further experiments haves been carried out for investigating the multiple scattering mechanism as the study of time dependent behavior of the lasing emission intensity. For this purpose, we collected the emitted light by means of a fast photodiode which was simultaneously triggered by the pump pulse. The signal was then sent to an oscilloscope and analyzed. Figure 26 shows the temporal behavior of laser action in the case of highly ordered cholesteric and partially ordered nematic samples doped with fluorescent guest molecules. For a fixed pump power the cholesteric system shows very small variations in the lasing output intensity (the pump energy was kept fixed above the lasing threshold). Essentially, for each shot of the pump beam the system was in the "on" state. A totally different situation is revealed in the case of the nematic dye doped system: strong fluctuations of the emission intensity are measured for pump power above the lasing threshold. Irregular intermittent sequences of "on" and "off" states demonstrate a characteristic behavior for a diffusive laser.
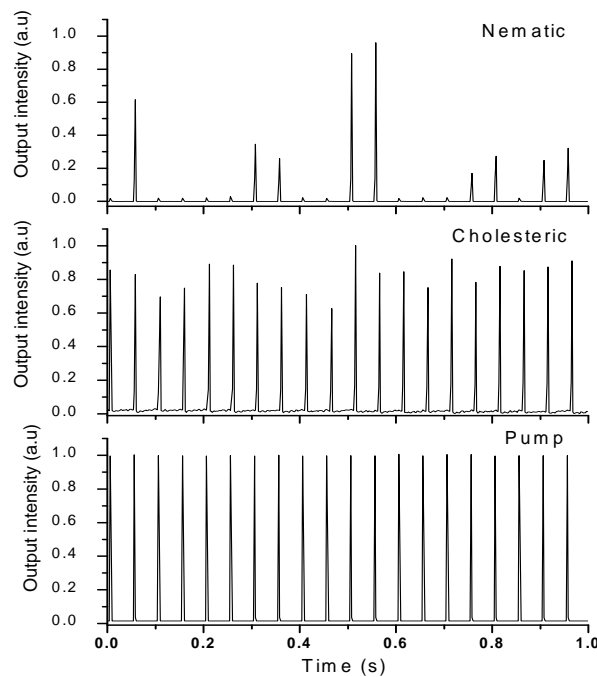
Fig. 26 : *Pump and output emission intensities from both dye doped cholesteric and dye doped nematic samples as function of time.*

6.   The thermal behavior

By using liquid crystal as a scattering medium, we can have an external control over the diffusion constants [50]. Liquid crystals go through partially ordered phases when heated, each liquid-crystal phase has a different refractive index and therefore different scattering properties. In fact diffusion constant has a strongly temperature dependence.

Interestingly, upon increasing the temperature of the dye doped nematic liquid crystal sample, the diminished nematic order parameter results in a smoother lasing threshold, approaching the threshold behavior of the fully disordered nano-powdered (presented in section mmm) system. The thermally induced disorder comes from an enhancement of the director fluctuations and strong gradients of concentration of the cyanobiphenyl components of the E7 mixture.[42] The enhanced scattering shifts the balance gain loss because a larger number of spontaneously emitted photons are needed to act as seeds for the stimulated emission process. Thus, increasing the temperature results in having a lasing threshold behavior similar to the typical stretched exponential curve of nano-powdered dye solutions (fig. 27).
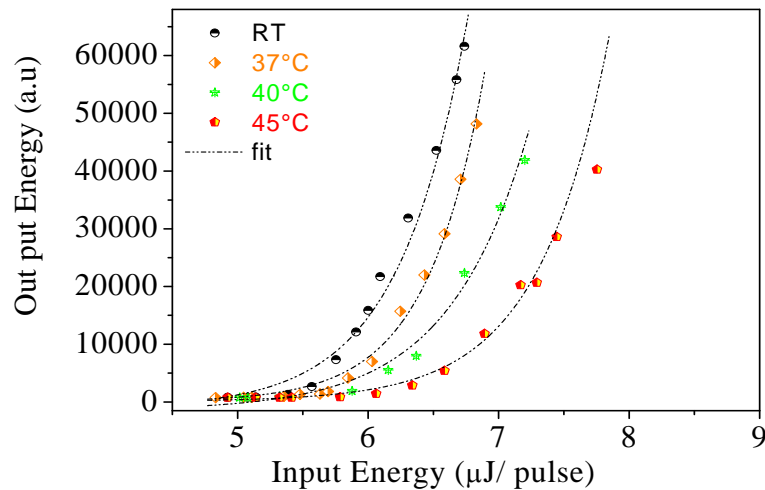
Fig. 27 : *β-factor thermal behaviour of the nematic liquid crystal sample: Upon increasing the temperature above RT, β approaches the behaviour found for a random system indicating that the randomness drives the amount of spontaneous emission radiated into the lasing modes.*

 Interestingly, upon increasing the temperature of the sample and collecting the emitted light with a fast photodiode(as done in the section 5 for a comparative study between nematic and cholesteric liquid crystal), the system tends to present the off state more frequently (fig 28). By increasing the temperature, the total scattering intensity slightly increases but the coherent backscattering cone is lowered emphasizing that the incoherent scattering component increases within the medium. The enhancement of incoherent scattering lowers the gain inside the system and decreases the probability of having lasing modes in this situation, since a larger number of spontaneously emitted photons are needed for the stimulated emission process.
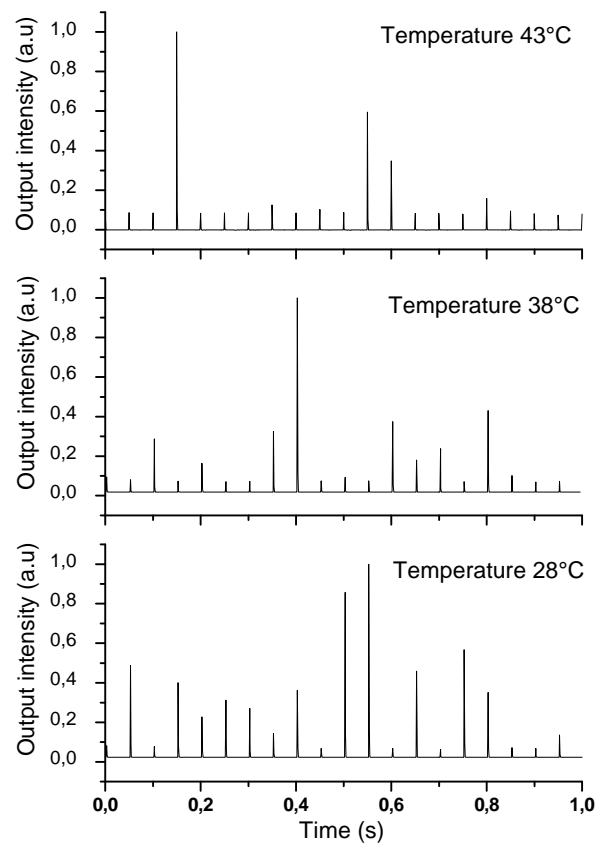
Fig. 28 : *The intensity lasing peak's dependence on the temperature of the system for a dye doped NLC sample.*

By increasing the temperature of our sample from room temperature, the emitted light drops off as the temperature approaches 50 °C and reappears in the proximity of nematic-isotropic transition (about 56 °C). The mixture used in these experiments is the BL001 doped with 0.3% of PM597 dye, which has the following temperature sequence: Cr. – *-10°C* – Nematic – *63°C* – Iso. This effect is accompanied by a strong scattering of the pump beam during the temperature range over which the lasing is absent, indicating that a cascade of scattering regimes occurs as the temperature varies upward and downward the nematic phase.

Here we report just a simple observation of this phenomenon, which is noted for a wedge cell (Fig. 29)and capillary tube (Fig. 30).
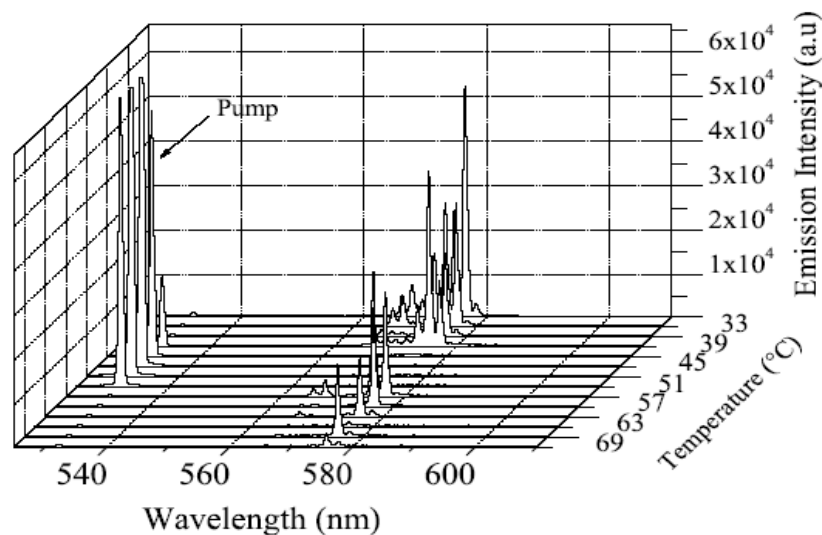
Fig . 29 :*Temperature dependence of the random lasing emission spectra for the wedge sample. The graphic shows an unexpected behaviour; the emitted light intensity drops off as the temperature reaches 50°C but it reappears in the proximity of nematic-isotropic transition (around 57°C).*
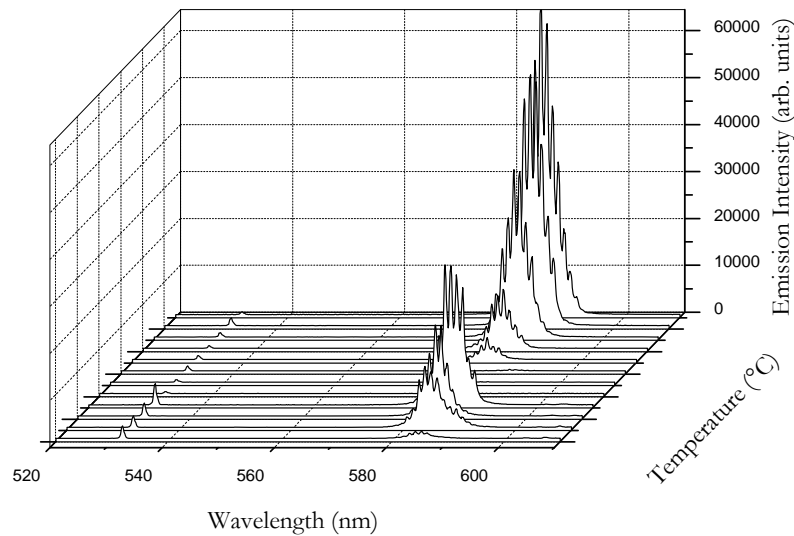
Fig . 30 :*Temperature dependence of the random lasing emission spectra for the capillary tube. The graphic shows an unexpected behaviour; the emitted light intensity drops off as the temperature reaches 48°C but it reappears in the proximity of nematic-isotropic transition (around 58°C).*

As conclusion the mode selection mechanisms in these systems imply important interference effects, enhanced by the presence of the gain medium, and related to the random walk of multiple scattered light waves. The huge number of localized modes dispersed along the visible spectrum is sustained by multiple scattering processes. The experimental study is performed by a theoretical and statistical study reported in the next chapter.

References

[1] R. V. Ambartsumyan et al., in Progress in Quantum Electronics, J. H. Sanders and K. W. H. Stevens, eds., Vol. 1, (Pergamon Press, London, 1970).

[2] Randal C. Polson and Z. Valy Vardenya), Apl. Phys. Lett **85**, N7 (2004).

[3] D. Wiersma and A. Lagendijk, *Laser action in very white paint*, Physics World 33–37 (1997) p.34.

[4] Cao H, Ling Y, Xu J Y, Cao C Q and Kumar P *Phys. Rev. Lett.* **86** 4524 (2001)

[5] Cao H, Xu J Y, Chang S-H and Ho , *Phys. Rev.* E **61 (**1985)

[6] Cao H, Xu J Y, Ling Y, Burin A L, Seelig E W, Liu X and Chang R P H *IEEE J. Select. Top. Quantum Electron.* **9** 111(2003).

[7]A. Mitra and R. K. Thareja, J. Appl. Phys. 89, 2025 (2001).

[8] G. Van Soest. Experiments on random lasers, PhD thesis, University of Amsterdam (2001).

[9]A. Langendijk, Bart A. Van Tiggelen, Physics Reports 270, (1996).

[10] M. P. Van Albada, B. A. Van Tiggelen, A. Langendijk, and A. Tip, Phys. Rev. Lett 66, 3132-3135 (1991).

[11] D. S. Wiersma, P. Bartolini, A. Lagendijk and R. Righini, Nature 390, 671 (1997).

[12] D. S. Wiersma, M. P. Van Albada and A. Lagendijk, Phys. Rev. Lett. 75, 1739 (1995).

[13]G. Van Soest, F. J. Poelwijk, R. Sprik and A. Lagendijk, Phys. Rev. Lett. 86, 1522 (2001).

[14]G. Van Soest, M. Tomita and A. Lagendijk, Opt. Lett. 24, 306 (1999).

[15] D. S. Wiersma et al, Phys. Rev. Lett. 74, 4193 (1995).

[16] D. S. Wiersma et al, Phys. Rev. Lett. 83, 4321 (1999).

[17] D. S. Wiersma, Nature 406, 132 (2000).

[18] H. Cao et al, Phys. Rev. Lett. 82, 2278 (1999).

[19] H. Cao et al, Phys. Rev. E. 66, R25601 (2002).

[20] V. S. Letokhov, Sov, Phys. JETP 26, 835 (1968).

[21] W. L. Sha, C. H. Lui and R.R.Alfano, Opt. Lett. 19, 1922 (1994).

[22] M. Siddique, R.R.Alfano, G. A. Berger, M. Kempe and A. Z Genack, Opt. Lett. 21,

450 (1996).

[23]P. C. de Oliveira, A. E. Perkins, and N. M. Lawandy, Opt. Lett. 21, 1685 (1996).

[24]D. S. Wiersma, Nature 414, 709 (2001)

[25] A. E. Siegman, *Lasers* (University Science Books, Mill Valley, 1986), Secs. 13.2 and

13.3.

[26] Yamamoto and R. E. Slusher, Phys. Today **46**(6), 66 (1993).

[27] Y. Yamamoto, S. Machida, and G. Bjo¨rk, Phys. Rev. A **44**, 657 (1991).

[28] G. Van Soest, and A. Lagendijk, Phys. Rev. E. 65, 47601 (2002).

[29] J. D. Joannopoulos, R. D. Meade, and J. N.Winn, Photonic Crystals: "*Moulding the*

Flow of Light" (Princeton University Press, Princeton, NJ, 1995).

[30] A. Z. Genack and J. M. Drake, Nature **368**, 400 (1994).

[31] V. M. Markushev, V. F. Zolin and Ch. M. Briskina Sov. J. Quantum Electron. **16**,

281 (1986).

[32] C. Gouedard, D. Husson, C. Sauteret, F. Auzel and A. Migus, J. Opt. Soc. Am. B **10**, 2358 (1993).

[33] M. A. Noginov, N. E. Noginov, H. J. Caulfield, P. Venkateswarlu, T. Thompson, M. Mahdi, and V. Ostroumov, J. Opt. Soc. Am. B **13**, 2024 (1996).

[34] D. S. Wiersma and A. Lagendijk, Phys. Rev. E **54**, 4256 (1997).

[35] P.W. Anderson, Phys. Rev. **109**, 1492 (1958).

[36] V. P. Romanov and A. N. Shalaginov, Opt. Sectrosc.(Trans. of Opt. Spektrosk.) **64**, 774 (1988).

[37] M. H. Kao, K. A. Jeter, A. G. Yodh, P. J. Colling, Phys. Rev. Lett. **77**, 2233 (1996).

[38] H. Stark Holger Stark, Ming H. Kao, Kristen A. Jester, T. C. Lubensky, Arjun G. Yodh, and Peter J. Collings, J. Opt. Soc. Am. A **14**, 156 (1997).

[39] P.M. Johnson, B. J. Bret, J. G. Rivas, J. J. Kelly, and Ad. Langendijk, Phys. Rev. Lett. **89**, 243901 (2002).

[40] H. K. Vithana, L. Asfaw, and D. L. Johnson, Phys. Rev. Lett. **70**, 3561 (1993).

[41] R. Sapienza, S. Mujumdar, C. Cheung, A. G. Yodh, D. Wiersma, Phys. Rev. Lett. **92**, 033903(2005).

[42] P. G. deGennes, "*The Physics of the Liquid Crystals*" (Oxford University Press, New York, 1974).

[43] chatelin

[44] S. T. Wu and D.K. Yang, "*Reflective Liquid Crystal Displays*" (John Wiley & Sons, Chichester, 2001).

[45] V. I. Kopp, B. Fan, H. K.M. Vithana, and A. Z. Genack, Opt. Lett. **23**, 1707 (1998).

[46] W. Cao, A. Munoz, P. Palffy-Muhoray, and B. Taheri, Nature Materials **1**, 111 (2002).

[47] J. Schmidtke, W. Stille, H. Finkelmann, and S.T. Kim, Adv. Mater. **14**, 746 (2002).

[48] G. Strangi, V. Barna, R. Caputo, A. De Luca, G. N. Price, C. Versace, N. Scaramuzza, C. Umeton, and R. Bartolino, Phys. Rev. Lett. **94**, 063903 (2005). (Editor's choice for the 2005 Virtual J. Nanoscale Sci. Technol., 11 (8), 2005).

[49] H. Cao, J. Y. Xu, E. W. Seelig, and R. P. H. Chang, Appl. Phys. Lett., **76**, 2997 (2000).

 [50] D. S. Wiersma, M. Colocci, R. Righini and F. Aliev Phys. Rev. B 64, 144208-1 144208-6 (2001).

Statistical analysis of random lasing emission properties in nematic liquid crystals

Since the pioneering work of Ambartsumyan et al [1], lasing in disordered media has been the subject of intense theoretical and experimental studies [2]. The random laser represents a non conventional laser whose feedback is mediated by random fluctuations of the dielectric constant in the space. The propagation of the light waves inside disordered dielectric systems shows several analogies with electron transport. In such materials light is multiply scattered and also amplified. The diffusion process traps light long enough inside the sample to reach an overall gain larger than the losses. The formation of resonant lasing modes relies on the interference of scattered waves that return to the coherence volume via different closed paths. When light is trapped inside the gain medium long enough, the amplification along such a loop path can exceed the optical loss and the system starts to lase. As the pump energy is further increased, the balance between gain and loss becomes positive and narrow peaks appear in the emission spectrum. The coherence interference effect selects the lasing frequencies, leading to discrete narrow peaks in lasing spectrum.

In 1996, Wiersma's group performed scattering experiments on fully and partially disordered systems, demonstrating that interference effects manage to survive the scattering regime and give rise to enhancement of the light intensity in the backscattered direction, namely the cone of coherent backscattering [3]. Recently, Strangi et.al [4] reported the first observations of random laser action in a partially ordered dye-doped nematic liquid crystals systems presenting various confining geometries. The gain medium consists of a nematic liquid crystal mixture (BL001 by Merck) doped with 0.3%wt of Pyrromethene 597 dye (Exciton). The experimental set-up and other details were presented in the chapter 4.

In order to gain further understanding about the multiple scattering mechanism,in these systems, and its time and temperature dependent behavior we statistically analyzed the emission intensity fluctuations. For this purpose, we collected the emitted light by

means of a fast photodiode which was simultaneously triggered by the pump pulse. The signal was then sent to an oscilloscope and analyzed. Figure 1 depicts the temporal behaviour of laser action in the case of highly ordered cholesteric and partially ordered nematic samples doped with fluorescent guest molecules. For a fixed pump power the cholesteric system shows very small variations in the lasing output intensity (the pump energy was kept fixed above the lasing threshold). Essentially, for each shot of the pump beam the system was in the "on" state. A totally different scenario is revealed in the case of the nematic dye doped system: strong fluctuations of the emission intensity are measured for pump power above the lasing threshold. Irregular intermittent sequences of "on" and "off" states demonstrate a characteristic behavior for a random laser. Since the condition for lasing comes from a careful balance between gain and loss, it is clear that in this case not for every pump pulse the random walk inside the anisotropic medium gathers enough gain for the system to lase. Interestingly, by increasing the temperature of the sample the system tends to present the off state more frequently. By increasing the temperature, the total scattering intensity slightly increases but the coherent backscattering cone is lowered emphasizing that the incoherent scattering component increases within the medium. The enhancement of incoherent scattering lowers the gain inside the system and decreases the probability of having lasing modes in this situation, since a larger number of spontaneously emitted photons are needed to act as seeds for the stimulated emission process.
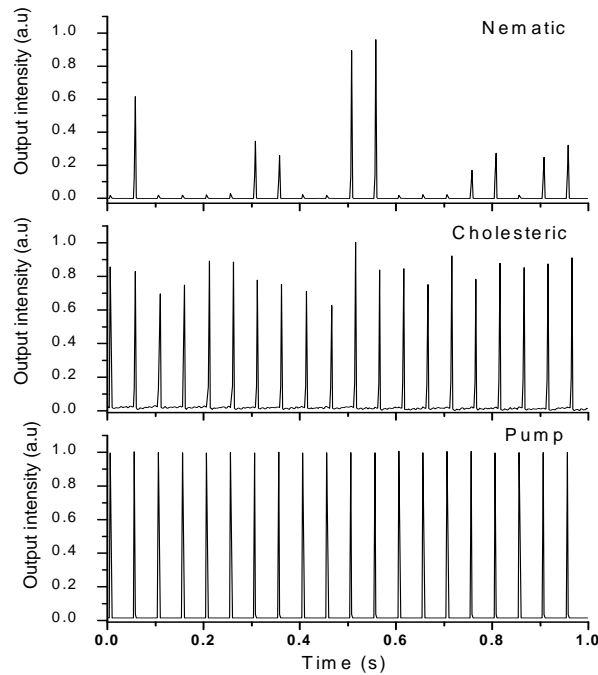
Fig. 1: *Pump and output emission intensities from both dye doped cholesteric and dye doped nematic samples as function of time.*

1.   Statistical study

To better understand the driving mechanisms within these systems, a statistical study has been performed. In particular, we used two different statistical tools, already adopted in other contexts, to characterize the possible presence of memory in the system. As can be clearly seen by a look at Figure 2, and as we have already mentioned, the diffusive laser action in dye doped NLC is rather irregular. It seems thus natural to investigate whether such irregularity is the result of a completely random process, or if, instead, some form of correlation is present, indicating the existence of an underlying mechanism in the system. The statistical description of the irregularity properties of the system could give useful information on several aspects, as for example the temperature dependence mentioned above.
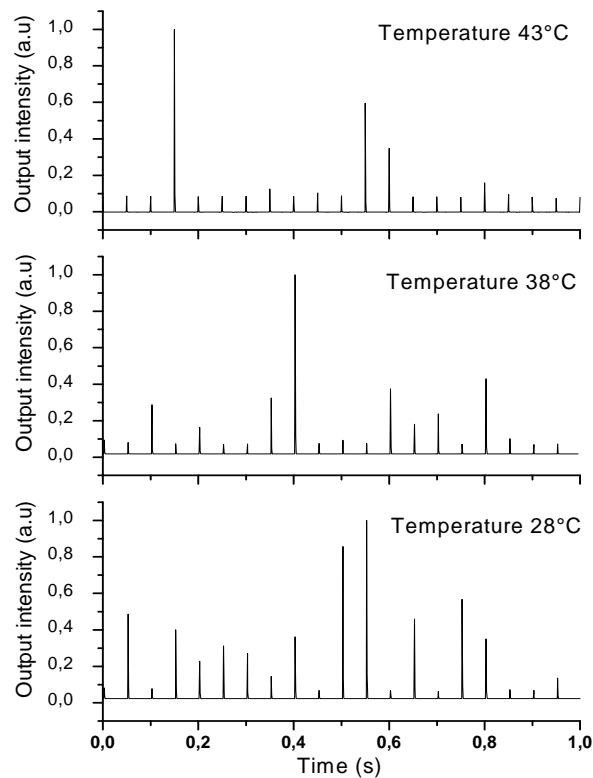
Fig. 2: *The intensity lasing peak's dependence on the temperature of the system for a dye doped NLC sample.*

Since, in this section, we are interested in the irregularly alternating status of lasing (lasing or non-lasing in response to the pump), we chose to identify an "event" with the total intensity emitted by the system, as observed in correspondence with the pump pulse. Then, we set a threshold, right above the noise level of the recorded signal and the pump level, to separate the "non-lasing" events from the "lasing" ones. The result of such process is a signal, made of "on" and "off" digits, indicating the status of emission of the system at each pump pulse. The presence of correlations, and thus of memory effect, corresponds to evidence of some degree of regularities in the signal obtained through this procedure.

2. The Shannon entropy

Let us now introduce the first statistical tool used in this work, known in literature as Shannon (or information) entropy [5,6]. The regularity of a sequence of $N - 1$ symbols (as, for example, a word of binary digits), produced by any source, can be characterized through the ability in predicting the N-th symbol. In our case, the possible symbols are limited to the "on" and "off" states, so that the binary digits "0" and "1" are only needed to describe the sequence. We will give a brief description of the Shannon entropy in this case, reminding that the theory can be extended to an arbitrary number of different symbols. Given a sequence of N binary digits $s(i)(i = 1, ...,N)$, we introduce the probability $P(C_n)$ (namely the occurrence rate within the sequence) of a particular "word" $C_n = (s(1), s(2), . . . , s(n))$ of length n. Then, the entropy associated to a generic n-digits word can be defined as $H_n = -P\{C_n\} P(C_n) \log P(C_n)$, where the sum is computed over all the possible combinations of length n. The quantity $h_n = H_{n+1} - H_n$, indicated as differential entropy, thus represents the average information provided by the (n+1)-th digit, once the previous n digits are known. For a stationary source, the Shannon entropy can finally be defined as the limit for large values of n

$$h_{sh} \approx \lim_{n\to\infty} h_n \approx \lim_{n\to\infty} \frac{H_n}{n} \tag{1}$$

This quantity is a measure of the regularity of the sequence. For example, for a given regular (say periodic) sequence, the information carried by the next digit after one period is zero, since the full knowledge of the sequence in contained into the first period. The predictability of such a sequence is then trivially high, and the signal is completely correlated with long range memory. On the contrary, if the sequence is chaotic, the information provided by the knowledge of each digit can be high. For example, for a random realization, namely if all digits have the same chance to be "0" or "1", any next digit carries with it the same amount of information as the previous ones. Such a sequence is completely unpredictable, and neither memory nor correlations are present. In this case the limit (1) can be easily shown to be $h_{sh} = \log 2$. Thus, the quantities defined so far represent a tool to describe the complexity of the source, through the regularities of the emitted sequences. Note that although the theoretical

Shannon entropy is defined as the limit to infinity of the word length, in the real experiments the convergence of the limit (1) is normally already obtained for small values n < 10.

Let us now consider our dataset. In this work we focused on six data-set obtained by performing the same experiment at different values of the temperature, in the interval between 26∘C and 41∘C. The experimental data have been reduced to 6 sequences of 2000 digits, each corresponding to the output state (lasing, that is "on", or non-lasing, that is "off") as response to the excitation pulses.

Table 1: For each temperature, the sequences size, the fraction of "on" states (in %), and the Shannon entropy are reported.

T(°C)	N of events	N of "1" enevts (%)	H_{sh}
26	2000	78%	0.54
29	1999	71%	0.60
32	1999	65%	0.64
35	1854	39%	0.67
38	1896	26%	0.58
41	1971	14%	0.42

We underline that the choice of the threshold is not relevant. In fact, different realizations of the analysis obtained with reasonable variations of the threshold gave the same results, so that we do not need to discuss it here. For each sequence, made of "0" and "1" digits (see Table1), we have then computed the quantities defined above, namely the entropy H_n, the differential entropy h_n and the Shannon entropy h_{sh}, using words of length up to n = 18. The results are collected in Figures 3 and 4. For comparison, on the same figures are reported, together with the 6 realizations at different temperatures, the results obtained using two artificial datasets. The first one is a regular sequence of alternating "0" and "1", while the second one is a completely random realization. Both sequences include 2000 digits, as for the observed strings. Looking at the top panel of Figure 3, it is possible to observe that, for the regular string, there is no increase of information when the number n of digit of the words increases. This corresponds, as expected, to a vanishing differential entropy (bottom panel of

Figure 3) leading to $h_{sh} \sim 0$. The random case, conversely, displays a constant growth of entropy H_n with the number of digits, indicating that all of them bring the same amount of information (top panel of Figure 3). This correspond to a constant differential entropy h_n (bottom panel of Figure 3). In order to obtain a value of the Shannon entropy, we observe that a saturation of H_n, and consequently a vanishing trend for h_n, is reached for n > 5, due to the finite size of our sequence. Thus, we can assume that the Shannon entropy is well represented by the constant region of the differential entropy h_n, with n < 5. We decide, thereafter, to use the first value reported in the plot, namely h_2, as a proxy for the Shannon entropy. The values of our estimates are displayed in Figure 32. For the random case, the expected value $h_{sh} = \log 2$ is obtained. The experimental sequences, obtained from the different datasets, show clear temperature dependence, accordingly to the probability variations reported in Table 1. At low temperature, at which the string is mainly composed by "on" digits (see Table 1), the entropy curve indicate that the system is chaotic, but with some degree of regularity. This is evidenced by the fact that the information entropy H_n grows more slowly than for the random case (Figure 3). Moreover, the values of the Shannon entropy are somewhat smaller than the upper value $h_{sh} = \log 2$ (see Figure 4). Thus, the amount of information carried by each digit is small. As the temperature is increased, the number of "on" and "off" digits becomes comparable, so that for T = 35∘C the Shannon entropy reaches its maximum value $h_{sh} = 0.67$, very close to the completely chaotic value. For higher temperatures, the trend is reversed, and long "0" series are interrupted by sporadic "1" digits. Both the high temperature and the low temperature configurations, which are almost undistinguishable as far as Shannon entropy is concerned, imply the presence of recurrent words of the same state (e.g. 000. . .0) that makes the system more predictable, the information carried by each digit smaller, so that the Shannon entropy decreases.

Fig. 3 : *The values of the entropy H_n (top panel) and of the differential entropy h_n (bottom panel) as a function of the words length n. Different colours refer to the different dataset (the corresponding temperatures are indicated in the legend). For both panels, the black dotted lines represent the results obtained using the completely ordered artificial dataset (the bottom curve) and the completely random realization (top curve).*

The indication of high chaoticity is anyway still valid. It should be noted that the number of the "on" states decreases very smoothly (indeed almost linearly) with the temperature, varying from a mainly-on configuration to a mainly-off one. The dominating state changes from "on" to "off" at some point between 32∘C and 35∘C (see figure 4). By comparing the slopes before and after the inversion of the Shannon entropy trends, we notice that it decreases more rapidly with respect to the rise phase. It means that by increasing the temperature the number of excitation pulses, that actually create the conditions to have lasing, reduce more rapidly after the inversion point. In order to shed light on this point, a series of experiments have been planned in which we

intend to use pure LC and compare with mixtures where some phase-separations could occur producing a rapid increase of the intensity of the incoherent scattering component.

3.   The local-Poisson test

As we have seen, the Shannon entropy analysis provides the useful information that the system under study is highly chaotic, especially at intermediate temperatures. At high and low temperatures, there is the indication of presence of regularity of the gain mechanisms behind the laser spiking, mainly due to the occurrence of long periods of stable state. One further information is that the system chaoticity changes smoothly with the temperature.
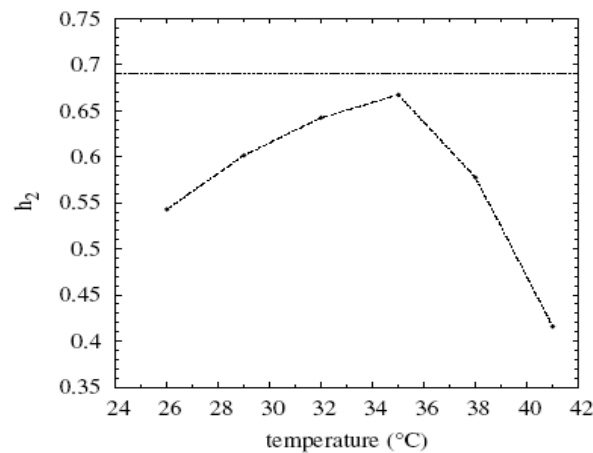
Fig. 4 : *the value of the differential entropy h_2 as a proxy for the Shannon entropy, measured at different temperatures. the dotted line shows the completely random value $H_2 = 0.69$*

However, it is desirable to gain more insight on the system and in particular on the specific features of chaos. This can be obtained, for example, by looking at correlations of the emitted pulses. Correlations are indeed related to some underlying mechanism, so that their presence in a signal indicates the non-stochasticity of the phenomenon. Let us now consider our experimental data as a succession of words made of the same digit. This corresponds to transform the strings in series of "0"-only or "1"-only words of variable length η, this last being defined as the number of consecutive identical digits.

Thus, the persistence of the system in a given state (lasing or non-lasing) is concerned here. In order to investigate the presence of correlations in the system, the probability distribution function (PDFs) of the persistence lengths can be studied. Indeed, for a completely random process, such distributions are expected to be exponential. The presence of correlations, conversely, produces long-range power-law PDFs. This is an easy test to perform on our data. Figure 33 displays the distribution functions $P(\eta)$ obtained for three values of the temperature. PDFs are approximately power-laws, indicating that the system is correlated not only at the border temperatures (T = 26∘C and T = 41∘C), but also at intermediate ones (T = 35∘C).

Because of the limited size of the datasets, the PDFs shown in Figure 33 might suffer of some uncertainties. We then performed a further analysis, which is less sensitive to the sample size. Such analysis has been introduced some years ago in cosmology [7], and used more recently in astrophysical [6,8-9], geophysical [10] and econophysics [11]context.

Consider the sequence of *m* words, identified as the consecutive sets of identical symbol within the original binary sequence, as described above. The separation points between two successive words can be labeled with an index i, and identified as an event. The events are thus defined as the change of state of the system from lasing to non-lasing and vice-versa. For each event i, we use the length of the following or preceding next and second next words, that we call $L_1(i)$ and $L_2(i)$ respectively. The choice between the pair of word following the event i, and the pair preceding the same event, is made in order to have the smallest $L_1(i)$. $L_1(i)$ and $L_2(i)$ are then the lengths of the two word following or proceeding a given state change i. We then introduce a quantity, which we denote by q, which is nothing but the suitably normalized local word length

$$h\big(L_1(i), L_2(i)\big) \approx \frac{2L_1(i)}{2L_1(i) + L_2(i)} \tag{2}$$

If the words lengths are randomly distributed, it can be shown that the probability density function P(q) of the stochastic variable q defined above is uniformly distributed

in q ∈ [0, 1]. This correspond to have a linear decrease for the surviving function of P(q), namely

$$P(q \geq Q) \approx \int\limits_{Q}^{\infty} P(q)dq \approx 1 - Q$$

To better understand the meaning of this tool, note that in a process where $L_2(i)$ are systematically smaller than $2L_1(i)$, clusters of state changes are present and the average value of q is greater than $1/2$. On the contrary, when the process is characterized by increasing persistence of state, the average value of q is less than $1/2$. Both cases indicate the presence of correlations in the signal. The test described above is thus an useful tool to discriminate between a sequence of random words and a sequence of correlated ones. From the experimental strings, it is straightforward to calculate the surviving function $P(q \geq Q)$ and the test is easily performed. Figure 5 shows the surviving functions computed for the same three cases as $P(\eta)$. The stepwise shape of the surviving function is due to the discrete nature of the sequence and to the relatively small set of possible values of the lengths η. This results confirm that at all temperatures there is a relevant deviation from stochasticity, so that the presence of correlations is strong.

Fig. 5 : *Top panel: the PDF of the lengths η of words made of "1" only for three different values of the temperature. A power- law is also plotted for reference. Bottom panel: the surviving function of the variable q (see text) for the same temperatures. The thin straight line 1−x represents the Poisson-like, decorrelated case.*

References

[1] R. V. Ambartsumyan, N. G. Basov, P. G. Kryukov, and V. S. Letokhov, IEEE J. Quantum Electron. QE-2, 442 (1966).

[2] H. Cao, Waves Random Media 13, R1 (2003).

[3] R. Sapienza and S. Mujumdar and C. Cheung and A. G. Yodh and D. Wiersma, Phys. Rev. Lett., 92 (2005) 033903

[4] G. Strangi and S. Ferjani and V. Barna and A. De Luca and C. Versace and N. Scaramuzza and R. Bartolino, Optics Express, 14 (2006) 7737

[5] C.E. Shannon, A mathematical theory of communication, edited by The Bell System Technical J., Vol. 27 1948, p. 379432, 623656.

[6] G. Boffetta et al., Physics Reports, 356 (2002) 367

[7] H. Bi and G. Corner and Y. Chu, Astron. Astrophys, 218 (1989) 19

[8] G. Boffetta et al., Phys. Rev. Lett., 83 (1999) 4662

[9] F. Lepreti and V. Carbone and P. Veltri, Astrophys. J., 555 (2001) L133

[10] V. Carbone and L. Sorriso-Valvo and A. Vecchio and F. Le preti and P. veltri and P. Harabaglia and I. Guerra, Phys. Rev. Lett. , 96 (2006) 128501

[11] A. Greco and V. Carbone and L. Sorriso-Valvo, Physica A , 376 (2007) 480

Conclusions

Lasers were invented some 40 years ago and are now used in a plethora of applications. Stable liquid crystals were discovered at about the same time and are now the basis of a large display industry. Both technologies involve photonics, the former in the creation and use of light and the latter in the control and manipulation of light. However, it is only recently that these mature technologies have been combined to form liquid-crystal lasers, heralding a new era for these photonic materials and the potential for novel applications. We have summarized in this doctoral thesis the characteristics of liquid crystals that lead to laser devices, the wide diversity of possible laser systems, and the properties of the light produced. In particular, this work focused on the study of three type of LC lasers, the LC band-edge laser, the defect-mode laser and the random laser. A relatively wide series of soft matter systems have been investigated allowing us to span from periodic to random, the modulation of the degree of order through structuring techniques and external stimuli allowed us to learn how important is the molecular organization in this field. The combination of optical feedback and amplification processes are behind the laser action observed in the various samples presented here. The most important section has been dedicated to random lasing in dye doped nematic liquid crystals, either confined in different geometries (cylindrical capillary tube, sandwich and wedge cells) and freely suspended. The interplay between weak light localization and gain underline the random lasing in such materials. The nematic liquid crystals proved to be partially ordered materials able to localize the light through recurrent multiple scattering. The occurrence of interference effects in weakly scattering nematics provide fascinating physics where interestingly several effects combine and compete to give rise to the most complicate kind of laser. This doctoral thesis has not the ambitions to be conclusive, by the way we do believe that most of the

results reported here are only the first steps moved within a complex scenario where interdisciplinary efforts will be needed to gain further understandings.

The LC laser appears to have a great future. Their small size, with length scales of the order of tens to hundreds of microns, and high versatility enable them to operate as light sources that are tunable from ultraviolet wavelengths, through the visible range, to infrared wavelengths. The material properties of the LC host can be manipulated not only to vary the laser threshold energy and slope efficiency but also to provide alternative laser device designs. For example, polymerization of an LC laser gives rise to a flexible laser device. The performance of these lasers is continually improving. Recent reports have achieved optical slope efficiencies in the range of 20% and 30% by improving the dye/LC host combination or the LC host molecular structure. Such efficiencies are comparable to more conventional solid-state microlaser sources when operated in similar wavelength regions.

Potential applications for this technology include labs-on-a-chip, spectroscopy, displays, and a wide variety of medical applications. In addition, recent work has demonstrated the use of an LC laser as an electro-tunable optical diode. Currently, however, it is necessary to optically pump these systems with pulsed lasers, which restricts their range of potential applications. To achieve continuous wave operation of LC lasers, it will be necessary to reduce the threshold through material design taking into account the LC properties discussed above, minimize internal cavity losses resulting from absorption, and optimize the LC cavity design. A significant reduction in the threshold would increase the number of potential pumping mechanisms that might be available for use, such as a light-emitting diode or white light source. This will, in turn, increase the potential applications for these highly versatile, soft-matter microlasers.

Pubblications

[1] V. Barna, S. Ferjani, A. De Luca, R. Caputo, N. Scaramuzza, C. Versace, and G. Strangi **"Multidirectional Laser Action Due to Confinement of Helixed Liquid Crystals in Cylindrical Microcavities"** Applied Physics Letters **87,** 221108 (2005).

[2] G. Strangi, S. Ferjani, V. Barna, A. De Luca, C. Versace, N. Scaramuzza and R. Bartolino "**Random Lasing and Weak Localization of Light in Nematic Liquid Crystals**" Vol. 14, No. 17 Optics Express 7737(2006)

[3] S. Ferjani, V. Barna, A. De Luca, C. Versace, N. Scaramuzza, R. Bartolino and G. Strangi "**Thermal Behaviour of Random Lasing in Dye Doped Nematic Liquid Crystals**" Applied Physics Letters **89,** 1 (2005).

[4] G. Strangi, S. Ferjani, V. Barna, A. De Luca, C. Versace, N. Scaramuzza and R. Bartolino **" Random lasing in dye doped nematic liquid crystals: the role of confinement geometry" Proc. SPIE** Vol. 6587, 6587 0P (May. 9, 2007).

[5] S. Ferjani, V. Barna, A. De Luca C. Versace and G. Strangi, "**Random lasing in freely suspended dye doped complex fluids**" submitted to APL.

[6] S. Ferjani, L. Sorriso-Valvo, A. De Luca, V. Barna, R. DeMarco and G. Strangi **"Statistical analysis of random lasing emission properties in nematicliquid crystals"** (submitted to PRE).

Awards

- Italian Workshop on "Optics and Photonics", 2006, 5-7 July, Ancona, Italy (Best paper by Optical Society of America).

PAPERS

Band edge and defect modes lasing due to confinement of helixed liquid crystals in cylindrical microcavities

V. Barna, S. Ferjani, A. De Luca, R. Caputo, N. Scaramuzza, C. Versace, and G. Strangi[a)]
*LICRYL-INFM and Center of Excellence CEMIF.CAL, Department of Physics, University of Calabria,
I-87036 Rende (CS), Italy*

Peculiar light emission properties have been observed in cylindrical microcavity hosting dye-doped helixed liquid crystals, which behaves as a fiber-like multidirectional distributed feedback laser. Experimental studies performed for this level of confinement show that laser action is exhibited both axially and radially, indicating a self-organized three-dimensional blue phase-like configuration. Thermal wavelength tunability was observed for both orientations emphasizing two different linear behaviors. The distributed feedback mechanism and the Q factor of the mirrorless resonant cavity result enhanced for axial stimulated emission because of the significant increase in the number of helical periods. In addition, long-lived spectrally narrow defect modes appear within the photonic band gap owing to optical phase jumps which take place in local structural defects. © *2005 American Institute of Physics.* [DOI: 10.1063/1.2137458]

The concept of wave transport in complex media, in particular the propagation of electromagnetic waves in dielectric periodic structures, represents a topic of great interest in various fields of scientific research. Periodic structured materials, namely "photonic crystals" that strongly localize light, are finding applications in many technological areas, providing an intriguing stage for controlling radiation fields.

Photonic crystals introduced by Yablonovitch[1] and John,[2] have attracted great interest for the great potentiality they express in fundamental physics and emerging applications.[3–6]

Helixed liquid crystals materials are self-organized mesophases which possess all the peculiar optical properties for achieving organic mirrorless optical resonant cavities.

Due to their birefringence and natural ability to form periodic structures, chiral liquid crystals are interesting one-dimensional photonic band gap materials.[7] In a matrix of CLC doped with fluorescent guest molecules, the spontaneous emission is suppressed in the reflection band gap and it is enhanced at the band edges where a series of narrow long-lived transmission modes are expected.[8,9] At the band edges the density of states is expected to diverge.[10–13]

Kogelnik and Shank[14] were the first to report laser action in periodic DFB structures which do not utilize conventional cavity mirrors but provide optical feedback via backward Bragg scattering, while laser action in chiral liquid crystals was proposed by Goldberg and Schnur[15] in 1973.

Here, we report the study of the light emission properties from novel fiber-like cylindrical microcavities hosting helixed liquid crystals doped with fluorescent guest molecules. The level of confinement ensures an increase of the axial resonant cavity length, while maintaining a small modal volume. Cylindrical geometry favors the existence of a very complex structure of the chiral liquid crystal as evidenced by optical and structural investigations which will be reported elsewhere. The long-range periodicity guarantees the enhancement of distributed feedback mechanism which is be-

hind the observed axial and radial low-threshold tunable lasing action. The aim of this study was to gain understandings about the role played by the number of helical periods, the influence of the CLC bulk volume and various surface treatments on the quality factor of the periodic mirrorless resonant system. This level of confinement allows obtaining interesting emission properties: laser action is exhibited both in the axial and radial directions at different spectral positions indicating that waveguide effects are not responsible of the multidirectional emission. A striking point is represented by the spontaneous reconstruction of the helixed liquid crystal superstructural configuration inside the cylindrical microcavity, giving rise to a novel three-dimensional (3D) multidirectional lasing system. This complex system keeps the advantage of a 3D blue phase-like matrix[16] while providing a wider thermal operating range and laser action wavelength tunability.

The hosting cylindrical microcavities are represented by capillary tubes with various diameter values ranging from 15 up to 200 μm. Several treatments were applied to the inner surface of the cylindrical microcavities in order to induce a privileged molecular alignment. The presented results have been obtained by performing investigations on 20 μm diameter polyimide treated cylindrical capillary tubes, since they showed the strongest surface-liquid crystal interaction.

The microstructure was filled by capillarity with a mixture ($M1$) of 99.7 wt % BL094 right handed cholesteric liquid crystal (Merck) and 0.3 wt % of PM-597 Pyrromethene dye (Exciton). The confined cholesteric liquid crystal had a birefringence $\Delta n = 0.21$ and showed an optical bandgap which spans from 525 to 585 nm. The high efficiency region of the dye fluorescence spectrum and the red-edge stop band of BL094 present very close spectral positions (580 and 585 nm) which maximizes the gain. Since this spectral overlapping could present the inconvenient of confusing the eventual amplified spontaneous emission effect with laser action, a second mixture ($M2$) was prepared by adding a small percentage of BL001 nematic liquid crystal (Merck). As a result, the low-energy band edge redshifted to 607 nm. The cylindrical microcavity was optically pumped (Fig. 1) with

---

[a)]Author to whom correspondence should be addressed; electronic mail: strangi@fis.unical.it
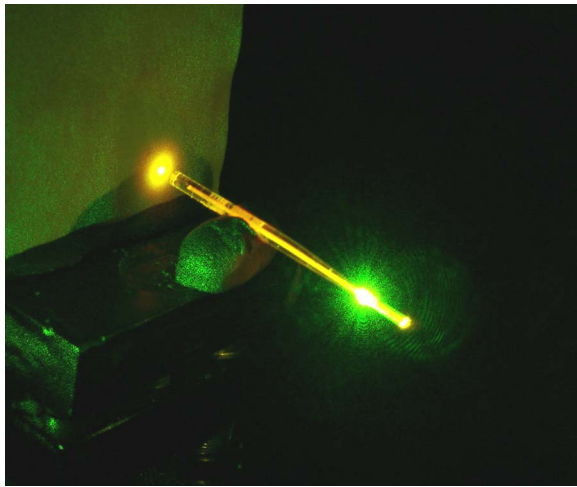
FIG. 1. (Color online) Lasing action from optically pumped cylindrical microcavity. Intense highly directional axial stimulated emission (at 587 nm) is observed on the background screen.

3 ns pulses produced by a frequency-doubled (532 nm) Nd: yttrium-aluminum-garnet laser (NewWave, Tempest 20). The pump beam was focused by means of a spherical lens ($f = 100$ mm) perpendicular to the axial sample direction. The radial and axial emission were collected within a restricted cone angle of ~ 0.15 rad by using a multichannel charge-coupled device (CCD) (Jobin-Yvon, Micro-HR). By increasing the pump energy above a certain threshold value, a highly directional laser action was observed at the red edge of the stop band both axially and radially. The laser emissions were found to be circularly polarized, which indicates that distributed feedback mechanisms take place through circular Bragg reflection.

The LC microcylinder acts like a miniaturized mirrorless cavity laser, where the emitted laser light propagates along the liquid crystal helical axis which behaves as a Bragg resonator. Recorded radial and axial lasing spectra present slightly different wavelength positions and linewidths full width at half maximum (Fig. 2). The displayed lasing lines have a spectral position which correspond to the low-energy edge of the PBG and exhibit a very narrow stimulated emission peak of only 0.5 nm (limited by the resolution of the CCD spectrometer). The lowest measured lasing threshold was 250 nJ/pulse for the radial direction and 500 nJ/pulse for the axial one. We experimentally found that the ratio r/p, with r as the internal radius of the cylinder and p as the pitch of the chiral liquid crystal, is the parameter which controls the arrangement of the helical superstructure. The simultaneous radial and axial lasing indeed occurs when $r/p \leqslant 50$, indicating that the interplay of the strong boundary conditions and the symmetry of the microcavity is responsible for the observed effect.

In addition to the expected band edge lasing modes, low-threshold defect lasing modes which occur within the selective reflection band gap have been observed (Fig. 3). Defect mode laser action has been previously mentioned in layered chiral liquid crystal polymer networks as a consequence of the induced phase jump in the optical field or dislocations, being responsible for opening spectrally narrow transmission modes within the stop band.[17] Lasing is facilitated at these wavelengths since the photon dwell time is enhanced, giving ample opportunity for amplification by stimulated emission,
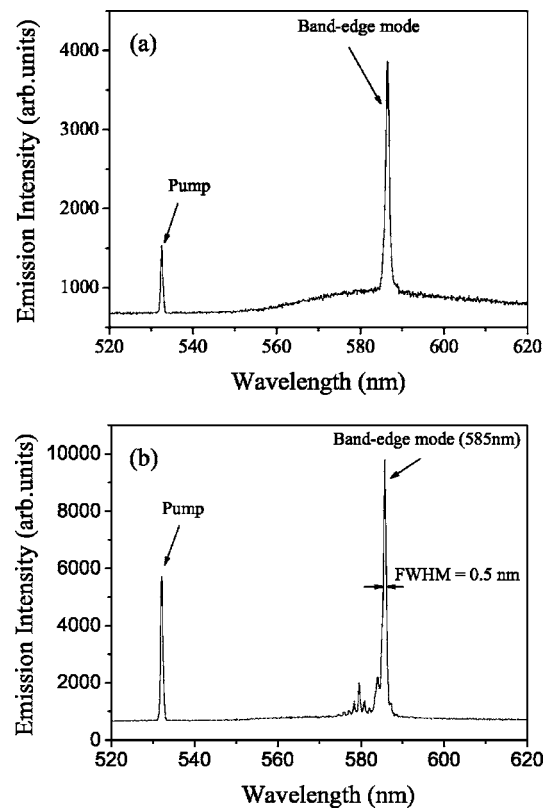
FIG. 2. Axial (a) and radial (b) lasing spectra show slightly different wavelength positions and linewidths confirming the existence of two distinct microresonant superstructure configurations.
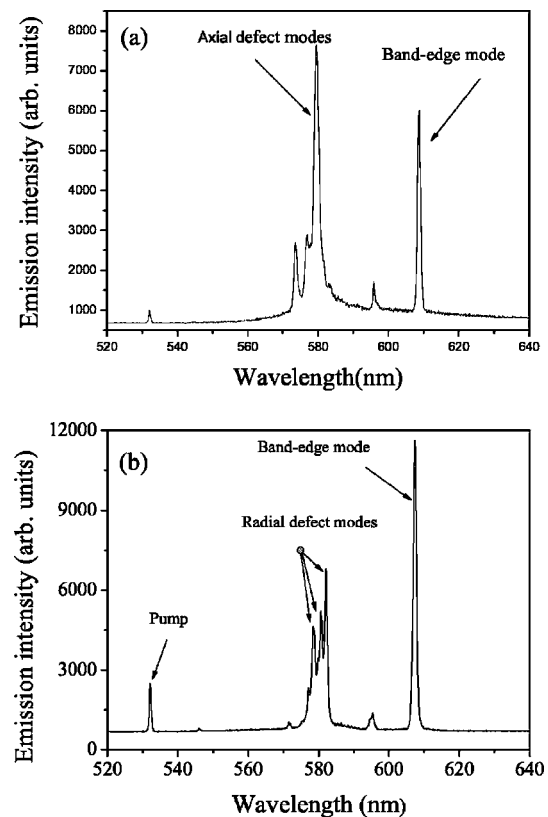

FIG. 3. Axially (a) and radially (b) spectrally narrow laser defect modes are present within the band gap central region. $M2$ mixture is used, thus the lasing action occurs at 609 and 607 nm for, respectively, axially and radially recorded stimulated emissions.
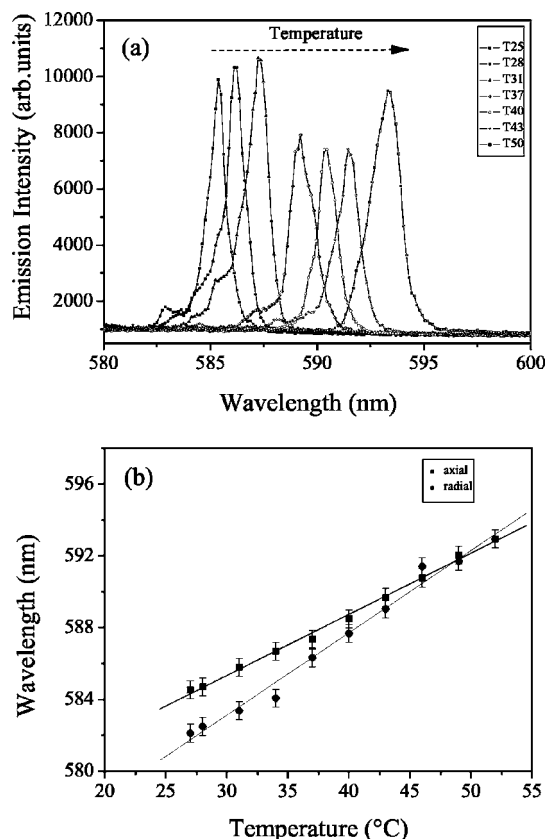
FIG. 4. Temperature control of the lasing wavelength in self-organized helical mesophases confined in cylindrical microresonators. (a) A redshift of 0.3 nm/ °C for axial and 0.45 nm/ °C for radial stimulated emissions were recorded by increasing the temperature from 25 up to 50 °C resulting in a fine tuning of the lasing action. (b) The different temperature dependence of the wavelength for the axial and radial stimulated emissions suggests the presence of two discrete DFB Bragg resonators.

as predicted by Kopp[18] and Yablonovitch.[1] In the case of the presented cylindrical microstructure, the spontaneous rearrangement of the local director fields produces particular helical axis configurations which spans from planar (axial) to escaped twisted radial geometry. This structural organization materializes in the appearance of point defect modes.[19] The local alteration of the sample which disrupts the periodicity of the structure leads to long-lived and, hence, spectrally narrow laser defect modes within the gap, observed both axially [Fig. 3(a)] and radially [Fig. 3(b)]. It is worth to notice that lasing wavelength on axial and radial defect modes are slightly different, since the resonant wavelength for the defect mode depends on the total phase slip which is given by the twist defect characteristics.

An important feature of the system is represented by the possibility of temperature tuning process of the lasing wavelength for the band edge modes. This effect is completely reversible. The period of the helix increases by increasing temperature, producing an overall displacement of the spectral region where the circular Bragg reflection takes place.[10] As a result of the thermal elongation of the pitch, a shifting of the stop band edge where the laser action occurs is obtained. Experimental measurements emphasize two different trends for lasing wavelength peak position in function of temperature for the radial and axial situations. A continuous temperature tuning of the lasing wavelength was obtained in the interval 585–595 nm by varying the temperature from 25 up to 50 °C [Fig. 4(a)]. We recorded a linear increase of

0.3 nm/ °C for axial and 0.45 nm/ °C for radial stimulated emissions [Fig. 4(b)].

This dependence indicates that the axially oriented helical superstructure responds in a reduced way to an applied temperature gradient, with respect to the radial oriented helix. This different behavior is strongly related to the confinement, in other words the interfacial region offers a much stronger constraint at the helical superstructure than the free bulk region. Belyakov theoretically investigated the cholesteric pitch changing under the action of external perturbation, in particular which has been shown the strong dependence of the anchoring energy on the structural behavior leading to a different response of the helical superstructure for interfacial and bulk regions of the cholesterics.[20]

In conclusion, the confinement of dye doped helixed liquid crystal in cylindrical microcavities gives rise to a 3D periodical superstructure where the two naturally preferred helical directions (axial and radial) create spontaneously. Low-threshold highly directional laser action was demonstrated both radially and axially. Along with the expected band edge mode we report the existence of long-lived spectrally narrow laser defect modes within the central region of the stop band. Fine temperature tuning of the stimulated emission wavelength was achieved for both lasing situations. Experimental evidences suggest the existence of two main DFB resonant configurations (axial and radial) which are behind the demonstrated temperature tunable multidirectional (3D) lasing system. Novel photonic architectures and optical devices could be engineered by using this level of confinement of periodic and quasiperiodic photonic crystals.

[1] E. Yablonovitch, Phys. Rev. Lett. **58**, 2059 (1987).
[2] S. John, Phys. Rev. Lett. **58**, 2486 (1987).
[3] J. D. Joannopoulos, R. D. Meade, and J. N. Winn, *Photonic Crystals: Molding the Flow of Light* (Princeton University Press, Princeton, 1995).
[4] D. Kleppner, Phys. Rev. Lett. **47**, 233 (1981).
[5] D. Wiersma, Nature (London) **406**, 132 (2000).
[6] J. S. Foresi, P. R. Villeneuve, J. Ferrera, E. R. Thoen, G. Steinmeyer, S. Fan, J. D. Joannopoulos, L. C. Kimerling, H. I. Smith, and E. P. Ippen, Nature Lett. **390**, 143 (1997); H. Finkelmann, S. T. Kim, A. Munoz, P. Palffy-Muhoray, and B. Taheri, Adv. Mater. (Weinheim, Ger.) **13**, 1069 (2001); J. Schmidtke, W. Stille, H. Finkelmann, and S. T. Kim, Adv. Mater. (Weinheim, Ger.) **14**, 746 (2002).
[7] P. G. de Gennes, *The Physics of Liquid Crystals* (Oxford University Press, Oxford, 1974).
[8] V. I. Kopp, B. Fan, H. K. M. Vithana, and A. Z. Genack, Opt. Lett. **23**, 1707 (1998).
[9] J. P. Dowling, M. Scalora, M. J. Bloemer, and C. M. Bowden, J. Appl. Phys. **75**, 189 (1994).
[10] G. Strangi, V. Barna, R. Caputo, A. De Luca, G. Price, C. Versace, N. Scaramuzza, C. Umeton, and R. Bartolino, Phys. Rev. Lett. **94**, 063903 (2005).
[11] J. Schmidtke and W. Stille, Eur. Phys. J. B **31**, 179 (2003).
[12] R. C. McPhedran, L. C. Botten, J. McOrist, A. A. Asatryan, C. M. de Sterke, and N. A. Nivorovici, Phys. Rev. E **69**, 016609 (2004).
[13] V. I. Kopp, Z. Q. Zhang, and A. Z. Genack, Phys. Rev. Lett. **86**, 1753 (2001).
[14] H. Kogelnik and C. V. Shank, Appl. Phys. Lett. **18**, 152 (1971).
[15] L. S. Goldberg, J. M. Schnur, U.S. Patent No. 3,771,065 (1973).
[16] W. Cao, A. Munoz, P. Palffy-Muhoray, and B. Taheri, Nat. Mater. **1**, 111 (2002).
[17] J. Schmidtke, W. Stille, and H. Finkelmann, Phys. Rev. Lett. **90**, 083902 (2003).
[18] V. I. Kopp and A. Z. Genack, Phys. Rev. Lett. **89**, 033901 (2002).
[19] H. S. Kitzerow, B. Liu, F. Xu, and P. P. Crooker, Phys. Rev. E **54**, 568 (1996).
[20] V. A. Belyakov, Mol. Cryst. Liq. Cryst. **410**, 219 (2004).

Random lasing and weak localization of light in dye-doped nematic liquid crystals

G. Strangi, S. Ferjani, V. Barna, A. De Luca, C. Versace, N. Scaramuzza, and R. Bartolino

LICRYL (CNR-INFM) and Center of Excellence CEMIF.CAL
Department of Physics, University of Calabria, I-87036 Rende (CS), Italy.
strangi@fis.unical.it

Abstract: The first observation of random laser action in a partially ordered, optically anisotropic nematic liquid crystal with long-range dielectric tensor fluctuations is reported. Above a given pump power the fluorescence curve collapses and the typical narrowing and explosion effect leads to discrete sharp peaks. The unexpected surviving of interference effects in recurrent multiple scattering provide the required optical feedback for lasing in nematics. Coherent backscattering of light waves in orientationally ordered nematic liquid crystals manifests a weak localization of light which strongly supports diffusive laser action in presence of gain medium. Intensity fluctuations of the speckle–like emission pattern indicate the typical spatio-temporal randomness of diffusive laser emission. A comparison of the laser action is reported for systems with different order degree: fully disordered semiconductor powders, self-ordered cholesterics and partially ordered nematic liquid crystals.

OCIS codes: (230.3720) Liquid crystal devices; (290.13500) Back scattering; (999.9999) Random lasing.

References

1. J. D. Joannopoulos, R. D. Meade, and J. N.Winn, Photonic Crystals: "*Moulding the Flow of Light*" (Princeton University Press, Princeton, NJ, 1995).
2. V. S. Letokhov, "Quantum statistics of multiple- mode emission of an atomic ensemble," Sov. Phys.–JETP **26,** 1246 (1968).
3. A. Z. Genack and J. M. Drake, "Scattering for super-radiation," Nature **368**, 400 (1994).
4. V. M. Markushev, V. F. Zolin and Ch. M. Briskina "Luminescence and stimulated emission of neodymium in sodium lanthanum molybdate powders," Sov. J. Quantum Electron. **16**, 281 (1986).
5. C. Gouedard, D. Husson, C. Sauteret, F. Auzel and A. Migus, "Generation of spatially incoherent short pulses in laser-pumped neodymium stoichiometric crystals and powders," J. Opt. Soc. Am. B **10**, 2358 (1993).
6. M. A. Noginov, N. E. Noginov, H. J. Caulfield, P. Venkateswarlu, T. Thompson, M. Mahdi, and V. Ostroumov, "Short-pulsed stimulated emission in the powders of NdAl3(BO3)4, NdSc3(BO3)4, and Nd:Sr5(PO4)3F laser crystals,", J. Opt. Soc. Am. B **13**, 2024 (1996).
7. D. S. Wiersma and A. Lagendijk,"Light diffusion with gain and random lasers," Phys. Rev. E **54**, 4256 (1997).
8. H. Cao, Y. G. Zhao, S. T. Ho, E. W. Seelig, Q. H. Wang, and R. P. H. Chang, "Random Laser Action in Semiconductor Powder," Phys. Rev. Lett. **82**, 2278 (1999).
9. D. Wiersma and S. Cavalieri, "A temperature tunable random laser," Nature **414**, 708 (2001).
10. P.W. Anderson, "Absence of Diffusion in Certain Random Lattices," Phys. Rev. **109**, 1492 (1958).
11. V. P. Romanov and A. N. Shalaginov, Opt. Sectrosc.(Trans. of Opt. Spektrosk.) **64**, 774 (1988);
12. B. A. van Tiggelen, R. Maynard, and A. Heiderich, "Anisotropic Light Diffusion in Oriented Nematic Liquid Crystals," Phys. Rev. Lett. **77**, 639 (1996).
13. H. Stark and T. C. Lubensky, "Multiple Light Scattering in Nematic Liquid Crystals," Phys. Rev. Lett. **77**, 2229 (1996).
14. M. H. Kao, K. A. Jeter, A. G. Yodh, P. J. Colling, "Observation of Light Diffusion and Correlation Transport in Nematic Liquid Crystals," Phys. Rev. Lett. **77**, 2233 (1996).
15. H. Stark Holger Stark, Ming H. Kao, Kristen A. Jester, T. C. Lubensky, Arjun G. Yodh, and Peter J. Collings, "Light diffusion and diffusing-wave spectroscopy in nematic liquid crystals," J. Opt. Soc. Am. A **14**, 156 (1997).

16. D. S. Wiersma, A. Muzzi, M. Colocci, R. Righini, "Time-Resolved Anisotropic Multiple Light Scattering in Nematic Liquid Crystals," Phys. Rev. Lett. **83**, 4321 (1999).
17. P.M. Johnson, B. J. Bret, J. G. Rivas, J. J. Kelly, and Ad. Langendijk, "Anisotropic Diffusion of Light in a Strongly Scattering Material," Phys. Rev. Lett. **89**, 243901 (2002).
18. H. K. Vithana, L. Asfaw, and D. L. Johnson, "Coherent backscattering of light in a nematic liquid crystal," Phys. Rev. Lett. **70**, 3561 (1993).
19. R. Sapienza, S. Mujumdar, C. Cheung, A. G. Yodh, D. Wiersma, "Anisotropic Weak Localization of Light," Phys. Rev. Lett. **92**, 033903 (2005).
20. P. G. deGennes, "*The Physics of the Liquid Crystals*" (Oxford University Press, New York, 1974).
21. S. T. Wu and D.K. Yang, "*Reflective Liquid Crystal Displays*" (John Wiley & Sons, Chichester, 2001).
22. V. I. Kopp, B. Fan, H. K.M. Vithana, and A. Z. Genack, "Low-threshold lasing at the edge of a photonic stop band in cholesteric liquid crystals," Opt. Lett. **23**, 1707 (1998).
23. W. Cao, A. Munoz, P. Palffy-Muhoray, and B. Taheri, "Lasing in a three-dimensional photonic crystal of the liquid crystal blue phase II," Nature Materials **1**, 111 (2002).
24. J. Schmidtke, W. Stille, H. Finkelmann, and S.T. Kim, "Laser Emission in a Dye Doped Cholesteric Polymer Network," Adv. Mater. **14**, 746 (2002).
25. M. Ozaki, M. Kasano, D. Ganzke, W. Haase, and K. Yoshino, "Mirrorless Lasing in a Dye-Doped Ferroelectric Liquid Crystal," Adv. Mater. **14**, 306 (2002).
26. G. Strangi, V. Barna, R. Caputo, A. De Luca, G. N. Price, C. Versace, N. Scaramuzza, C. Umeton, and R. Bartolino, "Color-Tunable Organic Microcavity Laser Array Using Distributed Feedback," Phys. Rev. Lett. **94**, 063903 (2005). (Editor's choice for the 2005 Virtual J. Nanoscale Sci. Technol., 11 (8), 2005).
27. H. Cao, J. Y. Xu, E. W. Seelig, and R. P. H. Chang, "Microlaser made of disordered media," Appl. Phys. Lett., **76**, 2997 (2000).
28. G. V. Soest and Ad Lagendijk; "β factor in a random laser," Phys. Rev. E, **65**, 047601 (2002).

1. Introduction

The diffusion and transport of light waves in complex dielectric structures have spurred a vast range of experimental and theoretical work, revealing one of the most challenging and exciting scientific area of the past decade. The propagation of electromagnetic waves in periodically structured dielectric systems, i.e. photonic bandgap materials, and the linear and non linear optical phenomena in completely disordered systems doped with gain media represent two opposite sides of this promising scientific branch. The literature demonstrates that much has been done in these extreme areas, but the huge intermediate world constituted by the partially ordered systems still remains almost unexplored. The laser emission study in ordered and periodic systems has known an extraordinary revival in the last years; even because of the remarkable development of experimental techniques which allow to scale the photonic crystal structures down to the nanoscale with the aim to mould the flow of light [1]. Surprisingly, active random media repeatedly proved to be suitable for obtaining diffusive laser action, mainly based on the resonant feedback mechanisms in multiple scattering. Light localization and interference effects which survive to multiple scattering events have been invoked to explain the random lasing observed in many exotic and complex systems [2-9]. In fact, when the diffusive photon transport in completely disordered systems encounters the condition $kl_t \sim 1$, being k is the magnitude of the local wave vector and l_t is the transport mean free path, an almost complete localization of light waves should occur. This effect is known as Anderson localization in analogy with the diffusion behaviour of electrons in some conductor lattices [10].

Weak localization of light waves is considered as a particular case of interference effects which were predicted and observed in random media and in partially ordered systems for $kl_t > 1$ [11-17]. Recently, coherent backscattering experiments performed with high accuracy apparatus manifested weak localization of light even in tensorial systems characterized by high optical anisotropy, like nematic liquid crystals [18]. These experiments show how the recurrent multiple scattering events exactly back enhance the scattered intensity giving rise to an anisotropic backscattering cone [19].

Nematic liquid crystals (NLC) are uniaxial fluids with rod-like molecules aligned on average along a local anisotropy axis which is represented by the unit vector $n(r,t)$, the molecular director.

The spontaneous fluctuations of the director represented by $n(r,t) = n_0 + \delta n(r,t)$ leads to fluctuations in the local dielectric tensor $\varepsilon_{\alpha\beta} = \varepsilon_\perp \delta_{\alpha\beta} + (\varepsilon_{//} - \varepsilon_\perp) n_\alpha n_\beta$ which is the main effect responsible of the recurrent multiple scattering events as a light wave is propagating through the NLC medium. The scattering of visible light by NLC is higher, by a factor of the order of 10^6, than the scattering by conventional isotropic fluids [20]. The fluctuations of $\varepsilon_{\alpha\beta}$ come from two different sources: (1) fluctuations in $\varepsilon_\perp$ and $\varepsilon_{//}$ due to small, local, changes in the density, temperature, etc.; (2) fluctuations in the orientation of n, this is the dominant effect which is specific of nematic liquid crystals. When the scattering is increased beyond a critical value, the system makes a transition in a localized state, where light propagation is inhibited owing to interference in multiple scattering. The weak localization of light in an amplifying scattering medium supports stimulated emission through resonant and nonresonant optical feedback. Such laser action is usually called diffusive or random lasing. In this letter, we mainly consider the multiple scattering of spontaneously emitted photons within the gain medium. These photons are characterized by different initial states of polarization which does not depend on the excitation polarization. The polarization of the excitation pulses and the scattering intensity is considered only in terms of quantum yields and photons available to be radiated into the lasing modes.

Here we report the first experimental observation of random laser action in a partially ordered and highly anisotropic NLC doped with fluorescent guest molecules. The study of laser emission in such system emphasizes the peculiar behaviour of diffusive laser action, randomness of laser emission was observed in time, space and frequency. In fact, the spatial distribution of the emitted light is speckle-like accompanied by strong intensity fluctuations and slight shifts of the resonant peaks occur for each pump pulse. The random laser relevant length scales, i.e. the scattering mean path length l, the gain length lg, and the sample size are found to be in good agreement with the random laser theory. In fact, the gain length at the onset of lasing is $lg \sim V^{2/3}/l \sim 3.5 \times 10^{-2}$ mm, is in reasonable agreement with the value found experimentally at the lasing threshold pump intensity (4.4×10^{-2} mm). In addition, the scattering mean path length was measured to be about an order of magnitude longer than the gain length providing ample opportunities to trigger the lasing effect.

2. Experimental

The nematic liquid crystal, BL001 provided by Merck, having the following bulk phase sequence *Cr. – -10°C – Nematic – 63°C – Iso* was doped with 0.3 wt% of Pyrromethene 597 dye (Exciton). The mixture was confined in a wedge cell constituted by two glass-ITO plates separated by Mylar spacers, with a thickness of 100 µm at one edge and 1.5 µm at the other one. The inner side of the plates were covered with rubbed polyimide alignment layers in order to induce a homogeneous alignment of the NLC molecules at the interface. Then, the wedge cell was filled by capillarity with the flow direction along the rubbing direction and normal with respect to the wedge. Upon observing the sample under a polarized microscope, it shows a planar alignment with the optical axis which lies in the plane of the cell parallel to the rubbing direction. The pyrromethene dye molecules dissolved in the NLC at very low concentration (0.3-0.5% by wt), proved to be completely miscible as evidenced by the almost complete absence of micro-droplets of dye embedded in the nematic phase. The wedge sample was optically pumped with 3-5 ns pulses produced by a frequency-doubled (532 nm) Nd:YAG laser (NewWave, Tempest 20). The pump beam was focused onto the thick region of the sample (about 100 µm) with a spherical lens (f = 100 mm) yielding a beam waist of about 30 µm at the focus position. The experimental set-up (see Fig. 1) presents a combination of optical elements (quarter-wave plates, half-wave plates and Glan-Thompson polarizers) in order to select all the states of polarization of the pump beam. A multichannel CCD spectrometer with a high spectral resolution (0.5 nm) and with a fiber termination was used to capture the emission spectra within a limited cone angle of 0.05 rad. The speckle-like pattern

of the emission spot was imaged on a screen while simultaneously the emission spectrum was captured by means of the CCD spectrometer (see Fig. 1).

At low pump power, the emission spectra show the typical spontaneous emission curve of pyrromethene dye, indicating that NLC does not considerably modify the fluorescence spectrum (Fig. 2). Upon increasing the pump power above a given threshold value (about 900 nJ/pulse), discrete sharp peaks emerge from the residual fluorescent spectrum and the output energy was found to be about 150 nJ/pulse at room temperature. The line width of these sharp peaks were less than 0.5 nm, yielding a quality factor Q of this random cavities larger than 1000. When the incident pump energy exceeds the threshold value, the peak intensity increases much more rapidly with the pump power and more sharp peaks appear, because now the balance gain-loss of these lossiest modes become positive (see Fig. 2). Hence, diffusive lasing occurs in dye doped nematics by recurrent light scattering and the lasing frequencies are determined by phase relationship of the counter-propagating scattered light waves. In fact, the weak localization of light waves owing to the strong optical scattering gives rise to reciprocal paths within the gain medium.
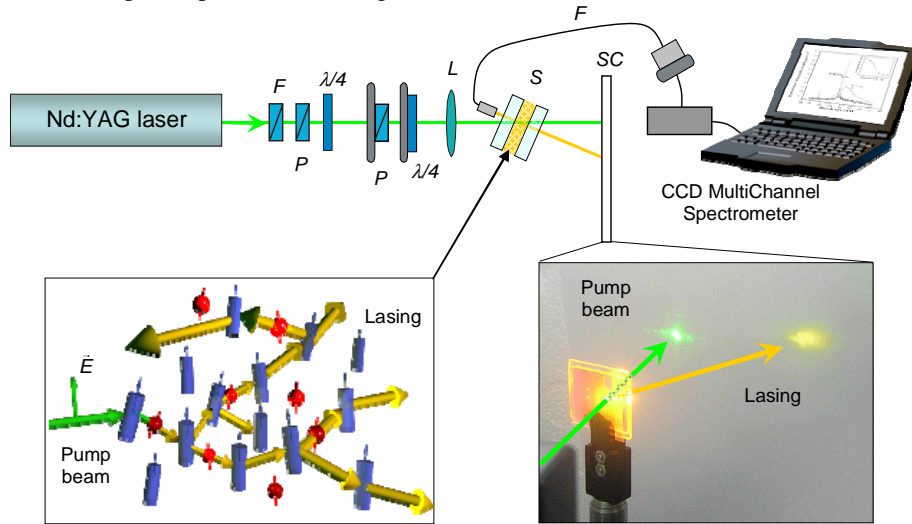
Fig. 1. Schematic diagram of the experimental set-up: the picture shows the pump beam and the diffusive laser emission projected on the screen. Recurrent multiple light scattering in dye doped nematics provides the feedback for laser oscillations.

When the phase accumulation in reciprocal path is equal, constructive interference occurs among the backscattered amplitudes. Therefore, we do believe that blue shift of the laser emission with respect to the fluorescence maximum is determined by interference effects which introduce coherence and feedback, leading to lasing action.

The inset of Fig. 2 shows the dependence of lasing intensity as a function of the orientation of the linear state of polarization of the pump beam. The lasing intensity undergoes a five-fold lowering when the pump light is polarized perpendicularly to the NLC director (o-wave) compared with the light polarized parallel to the director (e-wave). The polarization dependence of the scattering intensity and the coupling of the optical field with the gain medium have to be taken into account for the observed anisotropy. The former effect is mainly due to polarization dependence of the diffusion constant D for the emitted photons, indeed a larger diffusion constant for the e-wave compared to the o-wave is generally measured. The latter aspect can be analyzed by considering the *Fermi's Golden Rule* which

clearly states that the molecular transitions and the rate of emission strongly depend by the coupling of the pump electric field E and the transition dipole moment d of the dye molecules.

Fig. 2. Fluorescence and lasing spectra are reported. Discrete sharp peaks emerge from the residual spontaneous emission for pump energy of about 1.2 μJ/pulse. The inset shows the dependence of the lasing intensity on the angle θ between the linearly polarized light and the local nematic director orientation.

Thus, these processes are governed by the projection $E \circ d$. In addition, the experimental results emphasize that the fluorescent molecules adopt to some degree the local nematic order of the liquid crystal solvent, which results in an anisotropic orientational distribution of the transition dipole moment. In fact, polarized fluorescence measurements emphasize a strong dependence of the emission intensity on the pump polarization, as it is shown in the polar plot of Fig. 3.

It is worth to point out that the maximum of the lasing intensity was obtained for linearly polarized pump pulses with E oriented along the local director ($\theta = 0°$), being in good agreement with the polarized fluorescence results as well as the polarization dependence of the scattering intensity. This indicates that the dye molecules possess an anisotropic orientational distribution of the transition dipole moments along the local nematic director, with a dye order parameter $S_D = 0.2$ calculated as follows [21]:

$$S_D = \frac{\left(\dfrac{F_{//}}{F_{\perp}}\right)^{1/2} - 1}{\left(\dfrac{F_{//}}{F_{\perp}}\right)^{1/2} + 2}$$

Here $F_{//}$ and $F_{\perp}$ are fluorescence intensities polarized parallel and perpendicular to the NLC director, respectively. Therefore, this confirms that the dipolar coupling modifies the quantum yield for fluorescence and plays an important role for the light amplification process; some states of polarization of the pump pulses provide a larger number of spontaneously emitted photons which are radiated in the lasing modes.

Fig. 3. Polar plot of the polarized fluorescence of the dye doped nematic sample. It is obtained by measuring the fluorescence intensity by analyzing the polarized emission at different angles about the local nematic director.

Finally, in order to gain further understanding on the diffusive laser action observed in this partially ordered system, a 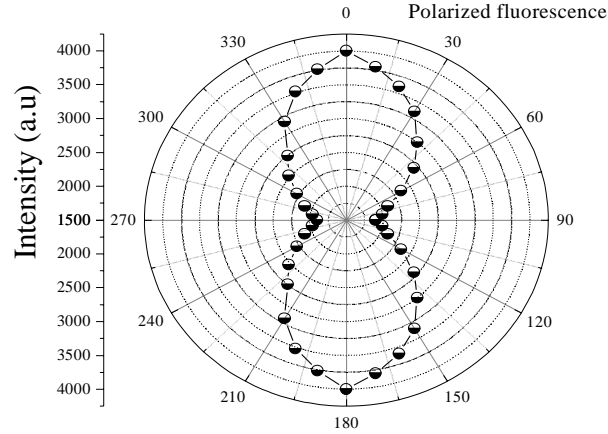comparative study of the emission properties of systems with different order degree was performed. We investigated the input-output characteristics and evaluated the β-factor of the following systems: 1) self-ordered dye doped helixed liquid crystals confined in conventional sandwich cell [22-26]; 2) laser dye solution containing ZnO nanoparticles [27]; 3) dye doped nematic liquid crystal confined in a wedge cell. While the first two systems have been widely investigated showing a lasing action with a well known input-output behaviour, the unexplored presented system presents a peculiar intermediate behaviour. In a conventional laser, β is defined as the ratio of the rate of spontaneous emission into the lasing modes to the total rate of spontaneous emission $(0 \leq \beta \leq 1)$, and determines the sharpness of the laser threshold [28]. In the science of cavity laser this parameter is of great interest because of the promise of "thresholdless laser" with $\beta=1$, in which all the spontaneous emission is radiated into the lasing modes. In figure 4 is reported the integrated emission intensity in function of the pump energy for the investigated systems characterized by different order degree. Unlike the sharpness of the lasing threshold observed in the self-ordered cholesteric cells $(\beta \sim 0.01)$, in which a super-linear increase of the emission intensity is measured above the threshold, the input-output curve measured in the random medium shows a stretched-exponential behaviour characterized by $\beta \sim 0.2$. The partially ordered nematic sample shows a behaviour intermediate between these two extremes. In fact, the output energy increases almost exponentially with the pump power $(\beta \sim 0.08)$. The presented behaviour suggests that a large part of the spontaneous emission is radiated into the lasing modes by of the optical feedback provided by the anisotropic coherent backscattering. Interestingly, upon increasing the temperature of the sample, the diminished nematic order parameter results in a smoother lasing threshold, approaching indeed the random system behaviour. Anyway, a detailed study of the aforementioned effect will be reported elsewhere.
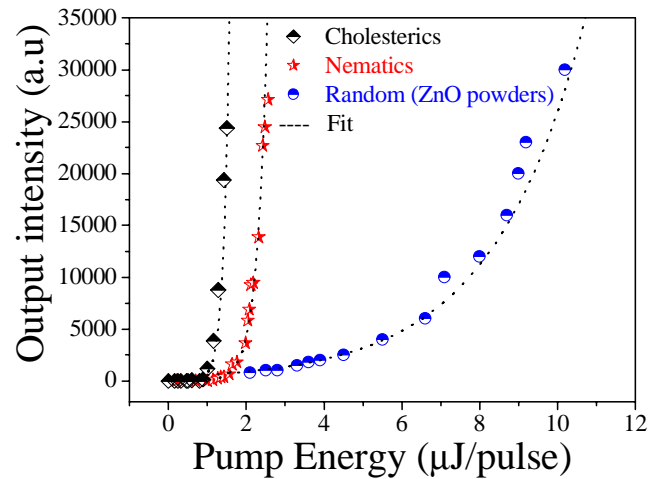
Fig. 4. Light input-output curves for systems with different order degree are reported. The emission rate of ordered dye doped cholesterics with a periodic helical structure, disordered nanoparticles of ZnO dissolved in methanol solution and partially ordered nematic liquid crystals are compared.

3. Conclusion

In conclusion, random laser action in highly anisotropic and partially ordered NLC has been observed. The underlying mechanism is mainly based on interference effects which survive to recurrent multiple scattering driven by nematic director fluctuations. Coherent backscattering experiments performed on similar systems have already proven that interference effects leads to weak localization of light waves [14]. Weakly localized light waves into dye doped nematic sample are responsible for amplification while the resonance frequencies are selected through interference phenomena of the counter-propagating light waves within the localized loops. For the sake of simplify, photons spontaneously emitted by the fluorescent guest molecules are launched at random directions from random positions within the excited volume. Because of the recurrent multiple scattering the probability to trace reciprocal paths by these photons is not null, as demonstrated by coherent backscattering experiments, thus resulting in equal phase accumulation during these open loops. Being the gain length comparable with the transport mean free path the emission of other photons is stimulated before the recurrently scattered photons leave the sample, triggering a coherent chain reaction. When the balance gain-loss becomes positive the optically excited dye doped nematic start to lase. Unlike distributed feedback mirror-less laser, this system can be considered as a cavity-less microlaser where the disorder unexpectedly plays the most important role, behaving as randomly distributed feedback laser. We found that the dye transition dipole moments adopt in some degree the orientational order parameter of the nematic director, resulting in a control of the emission intensity by varying the polarization of the pump beam. In addition, the evaluated β-factor for the presented system yields an intermediate value with respect to the random and fully ordered systems, suggesting that the order parameter drives the amount of spontaneous emission radiated into the lasing modes. Many further studies will be needed in order to gain full understandings of the diffusive laser action in nematic samples, indeed a wide series of experiments, simulations and extensive investigations have been planned. The aim of this letter is to report the experimental evidence of random lasing in nematics in order to enlighten the intriguing world of the partially ordered systems, and its peculiar emission properties when doped with gain media. Clearly, this could represent an exceptionally promising route for fundamental prospective studies with strong technological implications for integrated optical systems, nanophotonic and optoelectronic fields.

Acknowledgments

Thermal behavior of random lasing in dye doped nematic liquid crystals

S. Ferjani, V. Barna, A. De Luca, C. Versace, N. Scaramuzza,
R. Bartolino, and G. Strangi[a]
*LICRYL (INFM-CNR) and Center of Excellence CEMIF.CAL, Department of Physics,
University of Calabria, I-87036 Rende (CS), Italy*

The role of the thermally modulated order parameter in the diffusive laser action observed in dye doped nematic liquid crystals was investigated. Above a given pump energy a randomly distributed series of bright tiny spots appear, giving rise to a strongly fluctuating emission pattern. The spectral analysis reveals discrete sharp peaks (about 0.5 nm) slightly blueshifted with respect to the highest efficiency region of the gain medium. A comparative study was performed in systems having different sizes and confining geometries, corroborating the idea that the random lasing observed in dye doped nematic phase is fluctuation driven through a recurrent multiple scattering process. © 2006 American Institute of Physics. [DOI: 10.1063/1.2356087]

Since the first appearance of experimental evidences of random laser action in fully disordered gain media a huge number of exotic systems have been investigated in order to understand the mechanisms behind this interesting phenomenon.[1–8] The study of laser action ranges from periodically highly ordered materials, i.e., photonic crystals, to completely disordered systems such as powders, suspensions of microspheres, or strongly scattering materials. In fact, light propagation in complex dielectric materials is a rich and fascinating area of research and one of the fastest growing subjects in modern physics. Since first proposed by Letokhov in 1967, random lasers have been intensively studied, both experimentally and theoretically.[1] In random lasers, strong optical scattering in the gain medium provides for stimulated emission feedback, thus eliminating the need for an external cavity, like in regular lasers. This phenomenon has been observed in experiments on strongly scattering powders. The emission from such systems was shown to become narrow banded above a threshold and to exhibit laser spiking. This observable fact, also known as diffusive random lasing, has been demonstrated in a variety of materials such as powdered laser crystals,[9] microparticles in laser dye solution,[10] and liquid crystal-dye infiltrated porous glass.[8] Recurrent multiple scattering was repeatedly invoked as the source of the optical feedback for stimulated emission. The random walk of light waves results in the retention of light within the material long enough for the amplification to become efficient. Letokhov predicted that the combination of multiple scattering and light amplification would lead to a form of laser. Indeed, coherent backscattering experiments performed on fully and partially disordered systems demonstrated that interference effects survive this scattering regime, manifested as an enhancement of light intensity in the backscattering direction. This substantial enhancement is called the cone of coherent backscattering and represents a marker for the fascinating effect of weak localization of light.[11,12]

In this letter we report the thermal behavior of random lasing in a partially ordered dye doped nematic liquid crystal in various confining geometries and volumes. Liquid crystals in the nematic phase (NLC) are optically anisotropic strongly scattering materials, exhibiting turbidity and coherent backscattering. They differ fundamentally from common isotropic media being uniaxial fluids with rodlike molecules aligned on average along a local anisotropy axis which is represented by the unit vector $n(r,t)$, the molecular director. The spontaneous fluctuations of the director represented by $n(r,t)=n_0+\delta n(r,t)$ leads to fluctuations in the local dielectric tensor $\varepsilon_{\alpha\beta}=\varepsilon_\perp \delta_{\alpha\beta}+(\varepsilon_\parallel-\varepsilon_\perp)n_\alpha n_\beta$, which is the main effect responsible of the recurrent multiple scattering events as a light wave is propagating through the NLC medium. The scattering of visible light by NLC is higher, by a factor of the order of 10^6, than the scattering by conventional isotropic fluids.[13] In our experiments the gain medium consisted of a nematic liquid crystal mixture (BL001 by Merck) doped with 0.3% by weight of pyrromethene 597 dye (Exciton). The liquid crystal bulk phase sequence is as followes: crystal −10 °C—nematic 63 °C—isotropic. Dye doped nematics were confined in two different geometries: wedge cells and cylindrical capillaries. The wedge cells were constituted by two glass indium tin oxide plates separated by Mylar spacers having a thickness of 2 μm at one side and 200 μm at the other one. The plates were covered with rubbed polyimide alignment layers in order to induce a homogeneous alignment of the NLC molecules at the interface. The pyrromethene dye molecules dissolved in the NLC at very low concentration (0.3%–0.5% by weight) proved to be completely miscible as evidenced by the almost complete absence of microdroplets of dye embedded in the nematic phase. The same mixture was confined also in cylindrical capillaries, without any surface treatment, having inner diameters of 0.2 and 0.5 mm. These systems were investigated with 532 nm light from a frequency-doubled neodymium doped yttrium aluminum garnet laser (NewWave, Tempest 20). The pump light consisted of a train of twenty 3 ns pulses focused into a 50 μm spot. The input pump energy was varied, and we spectrally analyzed the resulting emission, using a high resolution optical multi channel charge coupled device (CCD) spectrometer (Jobin-Yvon).

Experiments have been performed on empty cells (both geometries) by checking the transmission and reflection spectra collected by using a high sensitivity spectrophotometer (UV-visible-near-infrared Cary 500 by Varian) in order to rule out any cavity effect due to multiple reflected light

---

[a]Author to whom correspondence should be addressed; electronic mail: strangi@fis.unical.it
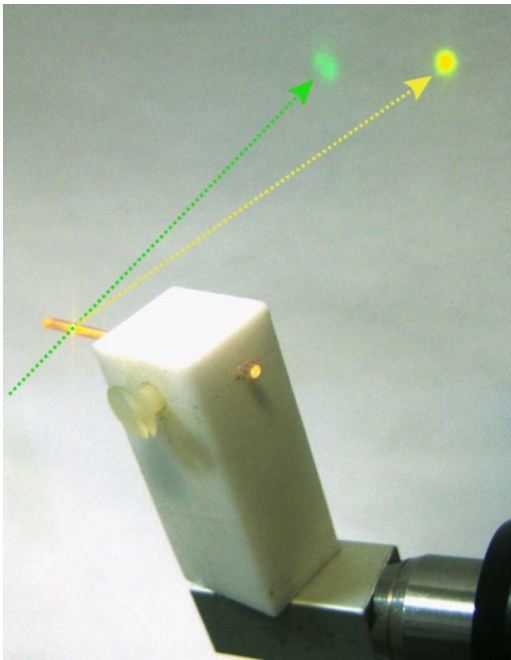
FIG. 1. (Color online) Image of diffusive lasing from optically pumped cylindrical capillary. Intense stimulated emission is observed on the background screen.

FIG. 2. (a) Wedge cell and (b) capillary tube emission spectra show different lasing wavelengths and numbers of lasing modes. The insets show the dependence of the polarized fluorescence on the angle θ between the linearly polarized light and the local nematic director orientation for the two confining geometries.

waves at the boundaries. In addition, we calculated the free spectral range by assuming a cavity effect and it was found to be absolutely incompatible with the wavelength region of the lasing modes and with the spectral spacing of the modes.

At the low power pump the emission spectra show the typical spontaneous emission curve of pyrromethene dye. Upon increasing the pump energy above a given threshold value (about 1 μJ/pulse) discrete sharp peaks appear (full width at half maximum ~0.5 nm). The spatial distribution of the emission shows brilliant tiny spots randomly distributed as a speckle, thus fluctuating in time and space (see Fig. 1). The emitted light was spectrally analyzed for both geometries, as shown in Fig. 2, the measured sharp peaks prove that the effect does not depend on the size and the geometry of the boundary conditions, but the key role is played by bulky dye doped nematics. In addition Fig. 2(b) shows that the emitted light by the cylindrical capillary was redshifted with respect to the wedge, this is due to phase relationships which depend on the boundary constraints. Polarized fluorescence measurements (insets of Fig. 2) show a pronounced anisotropy for the wedge cell. This clearly indicates that the dye molecules adopt to some degree the higher order parameter and the alignment of the nematic phase confined in the wedge cell with respect to the degenerate alignment within the untreated cylindrical capillary. Upon increasing the pump intensity, more sharp peaks appeared and the peak intensity increased more rapidly. Since the condition for lasing comes from a careful balance between gain and loss, where the gain becomes larger than the loss the system starts to lase.[14] In order to understand the underlying mechanisms responsible for the observed excitation threshold behavior, we investigated the input-output characteristics of systems with diverse order degree. The emission intensity was measured as function of the pump energy for fully disordered nanopowder dye solution,[15] self-ordered dye doped helixed liquid crystal sample (cholesteric phase),[16] and a partially ordered dye doped nematic sample [see Fig. 3(a)]. While the first two

systems have been widely investigated showing a lasing action with a well known input-output behavior, the unexplored presented system presents a peculiar intermediate behavior. The sharpness of the lasing threshold is determined by the β factor, defined as the ratio of the rate of spontaneous emission into the lasing modes to the total rate of spontaneous

FIG. 3. (Color online) (a) Input-output energy curves for systems with different order degrees are reported (chiral LC, nematic LC, and nanopowdered dye solution). (b) Thermal behavior of β factor for the nematic liquid crystal sample. Upon increasing the temperature β factor approaches the values yielded for a fully disordered system (TiO nanopowders).
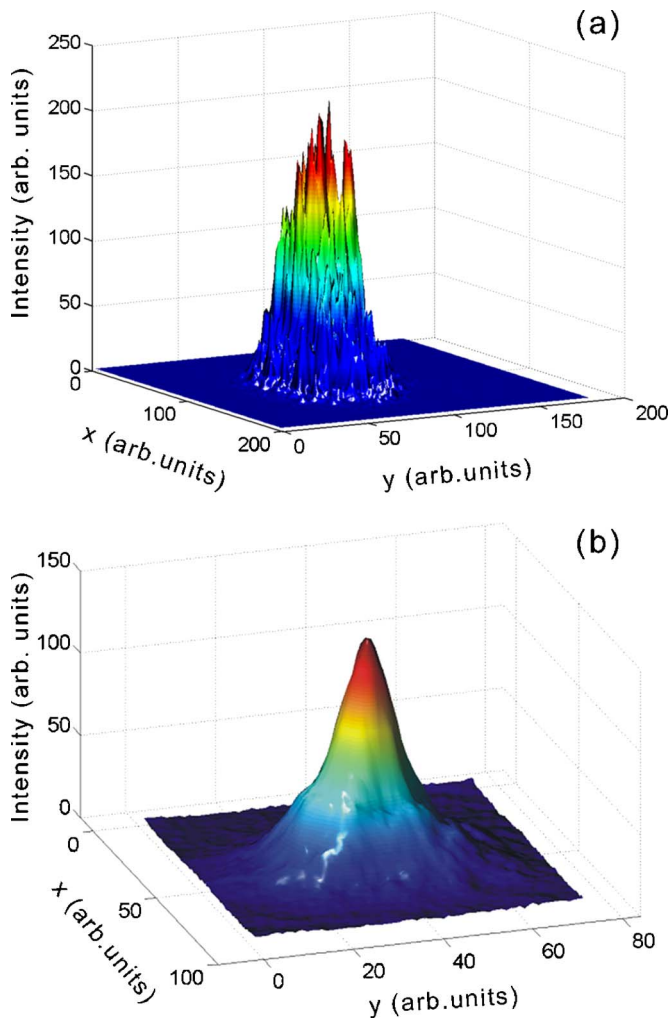
FIG. 4. (Color online) (a) Intensity spatial distribution obtained for a dye doped NLC cell is compared with the (b) expected pseudo-Gaussian profile obtained by a well ordered helixed liquid crystal sample. Bright tiny spots spatially overlapped show a richly structured emission pattern typical of diffusive laser action.

emission.[17] The exponential increase of the output as function of the input energy for the nematic sample is characterized by $\beta \sim 0.08$, representing the fraction of spontaneous emission which is radiated into the lasing modes. This radiative transfer is regulated by the order of the system, as clearly evidenced by the curves reported in Fig. 3(b) for the nematic sample. Interestingly, upon increasing the temperature of the sample, the diminished nematic order parameter results in a smoother lasing threshold, approaching the threshold behavior of the fully disordered nanopowdered system. The th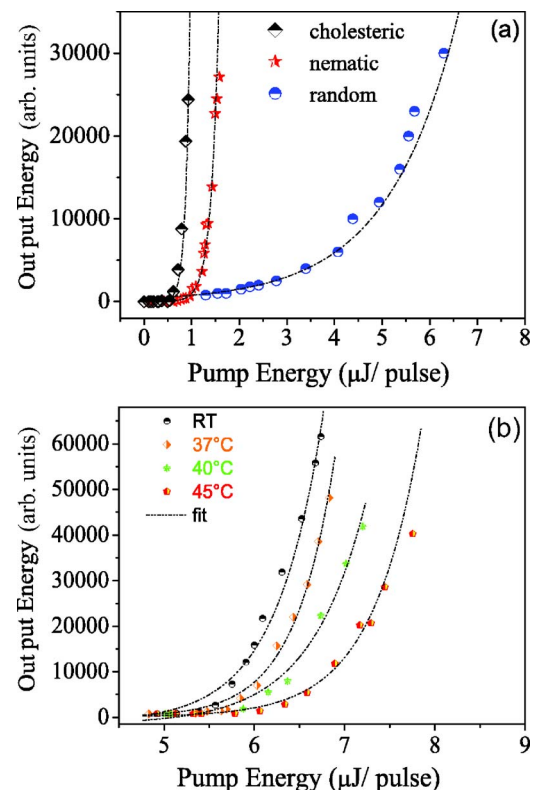ermally induced disorder comes from an enhancement of the director fluctuations and strong gradients of concentration of the cyanobiphenyl components of the E7 mixture.[13] The enhanced scattering shifts the balance gain-loss because a larger number of spontaneously emitted photons are needed to act as seeds for the stimulated emission process. Thus, increasing the temperature results in having a lasing threshold behavior similar to the typical stretched exponential curve of nanopowdered dye solutions. In addition, the thermal analysis of the emission spectra reveals an unexpected behavior; the emitted light drops off as the tempera-ture approaches 50 °C and reappears in the proximity of nematic-isotropic transition (about 63 °C). This effect is accompanied by a strong scattering of the pump beam during the temperature range over which the lasing is absent, indicating that a cascade of scattering regimes occurs as the temperature varies upward and downward the nematic phase.

Finally, the far field spatial distribution of the emitted light was captured by a high resolution CCD camera in a limited cone angle (~ 0.1 rad). It reveals a series of bright tiny spots spatially overlapped creating a richly structured pattern. In Fig. 4 this spatial distribution is compared with the expected pseudo-Gaussian profile obtained for a well ordered helixed liquid crystal creating a one-dimensional photonic band gap structure. This emission mechanism is based on the diffusive process of spontaneously emitted photons by fluorescent guest molecules launched at random directions from random positions. These photons are involved in a weak localization process within the gain medium because of recurrent multiple scattering. The entrapment of the emitted photons for enough time gives rise to reciprocal paths providing the optical feedback. In fact, the reciprocal paths are responsible of interference effects which survive in multiple scattering, because generally the phase accumulates equally in such paths. In conclusion, we demonstrated random laser action in dye doped nematics confined with diverse boundary conditions (i.e., geometry, size, and surface treatment). The thermal behavior of laser action points out the importance of the order of the system by evidencing that the mechanisms which are behind this optical feedback have nothing to do with distributed feedback or any other resonant regime due to a passive cavity.

[1] V. S. Letokhov, Sov. Phys. JETP **26**, 1246 (1968).
[2] A. Z. Genack and J. M. Drake, Nature (London) **368**, 400 (1994).
[3] V. M. Markushev, V. F. Zolin, and Ch. M. Briskina, Sov. J. Quantum Electron. **16**, 281 (1986).
[4] C. Gouedard, D. Husson, C. Sauteret, F. Auzel, and A. Migus, J. Opt. Soc. Am. B **10**, 2358 (1993).
[5] M. A. Noginov, N. E. Noginova, H. J. Caulfield, P. Venkateswarlu, T. Thompson, M. Mahdi, and V. Ostroumov, J. Opt. Soc. Am. B **13**, 2024 (1996).
[6] D. S. Wiersma and A. Lagendijk, Phys. Rev. E **54**, 4256 (1997).
[7] H. Cao, Y. G. Zhao, S. T. Ho, E. W. Seelig, Q. H. Wang, and R. P. H. Chang, Phys. Rev. Lett. **82**, 2278 (1999).
[8] D. Wiersma and S. Cavalieri, Nature (London) **414**, 708 (2001).
[9] V. M. Markushev, V. F. Zolin, and Ch. M. Briskina, Zh. Prikl. Spektrosk. **45**, 847 (1986); N. E. Ter-Garielyan, V. M. Markushev, V. R. Belan, Ch. M. Briskina, O. V. Dimitrova, V. F. Zolin, and A. V. Lavrov, Sov. J. Quantum Electron. **21**, 840 (1991).
[10] N. M. Lawandy, R. M. Balachandran, A. S. L. Gomes, and E. Sauvain, Nature (London) **368**, 436 (1994); D. S. Wiersma, M. P. van Albada, and A. Lagendijk, *ibid.* **373**, 204 (1995); W. L. Sha, C. H. Liu, and R. R. Alfano, Opt. Lett. **19**, 1922 (1994).
[11] P. W. Anderson, Phys. Rev. **109**, 1492 (1958).
[12] R. Sapienza, S. Mujumdar, C. Cheung, A. G. Yodh, and D. Wiersma, Phys. Rev. Lett. **92**, 033903 (2005).
[13] P. G. deGennes and J. Prost, *The Physics of the Liquid Crystals* (Clarendon, Oxford, 1993), p. 139.
[14] D. S. Wiersma, Nature (London) **406**, 132 (2000).
[15] H. Cao, J. Y. Xu, E. W. Seelig, and R. P. H. Chang, Appl. Phys. Lett. **76**, 2997 (2000).
[16] G. Strangi, V. Barna, R. Caputo, A. De Luca, G. N. Price, C. Versace, N. Scaramuzza, C. Umeton, and R. Bartolino, Phys. Rev. Lett. **94**, 063903 (2005).
[17] G. van Soest and A. Lagendijk, Phys. Rev. E **65**, 047601 (2002).

Random lasing in dye doped nematic liquid crystals: the role of confinement geometry

G. Strangi[a], S. Ferjani[a], V. Barna[a], A. De Luca[a], C. Versace[a]
N. Scaramuzza[a] and R. Bartolino[a]

[a]LICRYL CNR-INFM and Center of Excellence CEMIF.CAL
Department of Physics, University of Calabria, I-87036 Rende (CS), Italy

ABSTRACT

The first experimental evidence of random laser action in a partially ordered, dye doped nematic liquid crystal with long-range dielectric tensor fluctuations is reported. Above a given pump power the fluorescence curve collapses and discrete sharp peaks emerge above the residual spontaneous emission spectrum. The spectral linewidth of these emission peaks is narrow banded, typically around $0.5nm$. The unexpected surviving of interference effects in recurrent multiple scattering of the emitted photons provide the required optical feedback for lasing in nematic liquid crystalline materials. Light waves coherent backscattering in orientationally ordered nematics manifests a weak localization, strongly supporting the diffusive laser action phenomenon in the presence of a gain medium. Unlike distributed feedback mirror-less laser, this system can be considered as a cavity-less microlaser where the disorder unexpectedly plays the most important role, behaving as randomly distributed feedback laser. The far field spatial distribution of the emission intensity shows a huge number of bright tiny spots spatially overlapped and the intensity of each pulse strongly fluctuates in time and space. Here, we report the main characteristics of this novel systems for various confinement geometries and under different conditions. A brief presentation of boundary-less systems such as free standing and freely suspended dye doped nematic films and droplets is also introduced, revealing unique emission features because of the complete absence of confining borders.

Keywords: Random Lasing, Nematic Liquid Crystals, Multiple Scattering, Confinement Geometries

1. INTRODUCTION

The diffusion and transport of light waves in complex dielectric structures have encouraged a wide series of experimental and theoretical investigations, revealing one of the most challenging and exciting scientific area of the past decade. The propagation of electromagnetic waves in periodically structured dielectric systems and the linear and non linear optical phenomena in completely disordered systems doped with gain media represent two opposite sides of this promising scientific branch. The literature demonstrates that much has been done in these extreme areas, but the huge intermediate world constituted by the partially ordered systems still remains almost unexplored. The study of laser emission properties in ordered and periodic systems has known an extraordinary revival in the last years; even because of the remarkable development of experimental techniques which allow the design of photonic crystal structures as low as nanoscale ranges.[1] Surprisingly, active random media repeatedly demonstrated to be suitable candidates for obtaining diffusive laser action, mainly based on the resonant feedback mechanisms in multiple scattering, thus eliminating the need for an external cavity, like in the case of regular lasers. Light localization and interference effects which survive the multiple scattering events have been invoked to explain the random lasing observed in many exotic and complex systems.[2-8] The study of laser action extends from periodically highly ordered materials (i.e. photonic crystals) to completely disordered systems such as powders, suspensions of microspheres, or strongly scattering materials. Since firstly proposed by Letokhov[9] in 1968, random lasers have been intensively studied, both theoretically and experimentally. The arbitrary walk of light waves inside random media results in the confinement of light within the material long enough for the amplification to become efficient. Letokhov predicted that the combination of multiple scattering and light

amplification would lead to a form of laser. In fact, when the diffusive photon transport in completely disordered systems encounters the condition $kl_t \sim 1$ (where k is the magnitude of the local wave vector and l_t is the transport mean free path) an almost complete localization of light waves should occur. This effect is known as Anderson localization, by analogy to the electronic model proposed by Philip W. Anderson in 1958 in the famous article 'Absence of diffusion in certain random lattices'.[10] He described the vanishing of electron propagation in the regime of very strong multiple scattering due to the interference effects in electronic lattices where disorder was introduced as impurities and this concept served as a model for metal-insulator transitions. On the other hand, weak localization of light waves is considered to be a particular case of interference effects, predicted and observed in random media and in partially ordered systems for $kl_t > 1$ (the Ioffe-Regel criterion for localization).[11–15] Indeed, the performed coherent backscattering experiments demonstrated that interference effects survive the scattering regime and an enhancement of the light intensity in the back direction is observed. This enhancement is called the cone of coherent backscattering and denotes a marker for the fascinating effect of weak localization of light.[10, 16] Nematic liquid crystals (NLC) are uniaxial fluids with rod-like molecules aligned on average along a local anisotropy axis called molecular director, $n(r, t)$. The spontaneous fluctuations of the director, represented by $n(r, t) = n_0 + \delta n(r, t)$, lead to fluctuations in the local dielectric tensor, $\varepsilon_{\alpha\beta} = \varepsilon_\perp \delta_{\alpha\beta} + (\varepsilon_\parallel - \varepsilon_\perp) n_\alpha n_\beta$ being the main responsible effect for the recurrent multiple scattering events that a light wave experiences while propagating through the NLC medium. The scattering of visible light by a NLC is higher, by a factor of the order of 10^6, than the scattering by conventional isotropic fluids.[17] The fluctuations in the dielectric tensor come from two different sources: (i) fluctuations in $\varepsilon_\perp$ and $\varepsilon_\parallel$ due to small, local changes in the density, temperature, etc.; (ii) fluctuations in the orientation of n, this being the dominant effect, which is specific for nematic liquid crystalline materials. When the scattering is increased beyond a threshold value, the system makes a transition into a localized state, where light propagation is inhibited owing to interference in multiple scattering. The weak localization of light in an amplifying scattering medium supports stimulated emission through resonant and nonresonant optical feedback. Such laser action is usually called diffusive or random lasing. A review of the main characteristics for the emission properties in systems consisting of partially ordered and highly anisotropic confined nematic liquid crystals doped with fluorescent guest molecules, for which we recently reported the first experimental observations of random laser action,[18, 19] is the main objective of this paper. Here, we primarily consider the multiple scattering of spontaneously emitted photons within the gain medium. These photons are characterized by different initial states of polarization which does not depend on the excitation polarization. The polarization of the excitation pulses and the scattering intensity is considered only in terms of quantum yields and photons available to be radiated into the lasing modes. The study of the emission properties for the above mentioned systems emphasizes the peculiar behaviour of the diffusive laser action, in particular randomness of laser emission was observed in time, space and frequency. The spatial distribution of the emitted light assumes a speckle-like profile accompanied by strong intensity fluctuations and slight shifts of the resonant peaks occur for each pump pulse. The random laser relevant length scales (i.e. the scattering mean path length l_t, the gain length l_g and the sample size) were found to be in good agreement with the random laser theory.

2. EXPERIMENTAL SETUP AND CONFINEMENT GEOMETRIES

In our experiments we have employed two different types of confining geometries, mainly wedge cells and cylindrical glass capillaries. These systems were filled by capillarity with a mixture made of nematic liquid crystal (BL001 - provided by Merck), having the following bulk phase sequence $Cr. - (-10°C) - Nematic - 63°C - Iso$ doped with 0.3 wt % of Pyrromethene 597 dye (from Exciton). The wedge cell was constituted by two glass-ITO plates separated by Mylar spacers, having a thickness of $100\mu m$ at one edge and $1.5\mu m$ at the other one. The inner side of the plates was covered with a rubbed polyimide thin film for inducing a homogeneous (planar) alignment of the NLC molecules at the interfaces. The cell was then filled allowing for the flow direction to be along the rubbing direction and normal with respect to the wedge. Upon observing the sample under a polarized microscope it shows a planar alignment, with the optical axis sitting in the plane of the cell and parallel to the rubbing direction. The pyrromethene dye molecules dissolved in the NLC at very low concentration $(0.3 - 0.5wt.\%)$, proved to be completely miscible as evidenced by the almost complete absence of micro droplets of dye embedded in the nematic phase. The same mixture was also confined into micro cylindrical capillaries, with inner diameters between 50 and $250\mu m$, but without any preliminary surface treatment. The samples were optically pumped with 3-5 ns pulses produced by a frequency-doubled ($532nm$) Nd:YAG laser (NewWave,
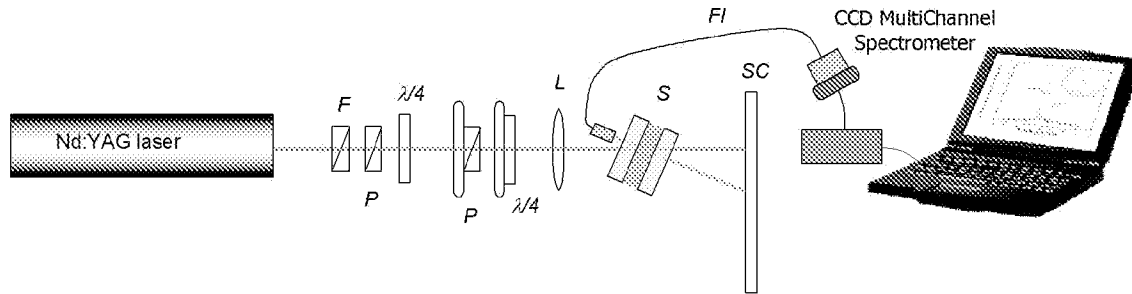
Figure 1. Diagram of the experimental setup line.

Tempest 20). The pump beam was focused onto the sample by means of a spherical lens ($f = 100mm$), yielding a beam waist of about $30\mu m$ at the focus position. The experimental set-up (Fig. 1) shows a combination of several optical elements (quarter-wave plates, half-wave plates and Glan-Thompson polarizers) used for selecting all the polarization states for the pump beam. A multichannel CCD spectrometer with a high spectral resolution ($0.5nm$) and a fiber termination (FI) was employed for acquiring the emission spectra within a limited cone angle of approximately $0.05rad$. Preliminary measurements were performed on empty samples by checking the transmission and reflection spectra (UV-visible-near-infrared Cary 500 Spectrophotometer by Varian) in order to rule out any possible cavity effects due to the multiple reflections at the boundaries. Furthermore, by assuming the existence of a potential cavity effect and calculating the free spectral range, it was found to be entirely incompatible with the wavelength region of the lasing modes and with their spectral line spacing.

3. EXPERIMENTAL RESULTS AND DISCUSSION

When optically pumping the systems and increasing the input energy above a certain threshold value, a fluctuating speckle-like spot, typical of random lasers, appears on the background screen (Fig. 2). We spectrally
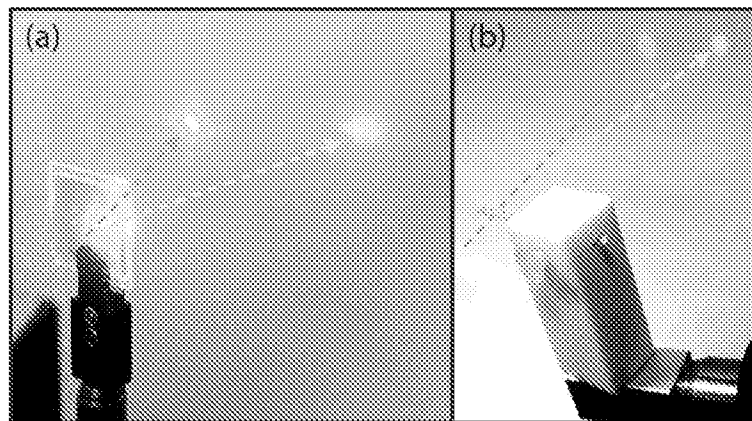
Figure 2. Image of diffusive lasing from optically pumped wedge cell (a) and cylindrical capillary (b). Intense stimulated emission is observed on the background screen.

analyzed the resulting emission, using the high resolution optical multi channel charge coupled device (CCD) spectrometer (Jobin-Yvon). At low pump energy regimes, the emission spectra show the typical spontaneous emission curve of the pyrromethene dye, indicating that NLC does not considerably modify the fluorescence spectrum (Fig. 3a). Upon increasing the pump power above a given threshold value (about $900nJ/pulse$ in the case of a wedge cell), discrete sharp peaks emerge from the residual fluorescence spectrum, while the output energy was found to be about $150nJ/pulse$ at room temperature (Fig. 3b). The line width of these sharp peaks
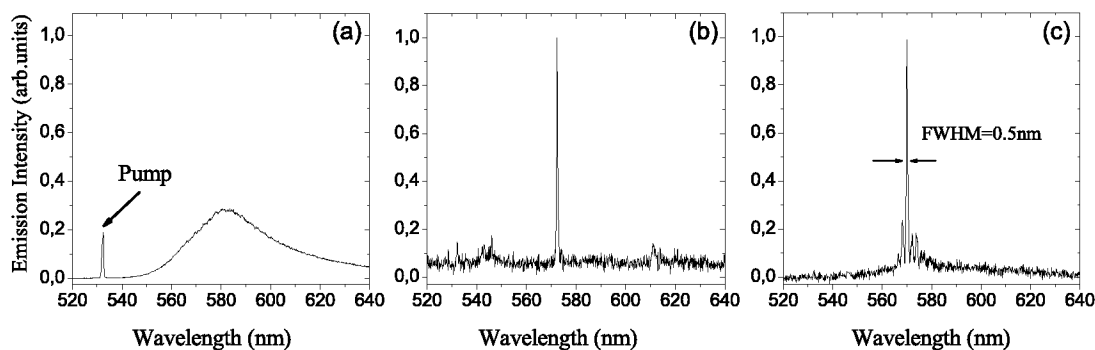
Figure 3. Fluorescence (a) and random lasing spectra (b,c) in the case of a wedge cell upon increasing the pump energy. Discrete sharp peaks emerge from the residual spontaneous emission for pump energy of about $900nJ/pulse$.

was measured to be less than $0.5nm$, limited by the spectral resolution of the CCD. When the incident pump energy exceeds the threshold value, the peak intensity increases much more rapidly with the pump power and more sharp peaks appear, because now the balance gain-loss of these lossiest modes become positive (Fig. 3c).

Diffusive random lasing occurs in dye doped nematics by recurrent light scattering and the lasing frequencies are determined by phase relationship of the counter-propagating scattered light waves. The weak localization of light owing to the strong optical scattering gives rise to reciprocal paths within the gain medium. When the phase accumulation in reciprocal path is equal, constructive interference occurs among the backscattered amplitudes. Therefore, it is believed that the observed spectral blue shift of the lasing peaks with respect to the fluorescence maximum is mainly due to the interference effects which introduce coherence and feedback, leading
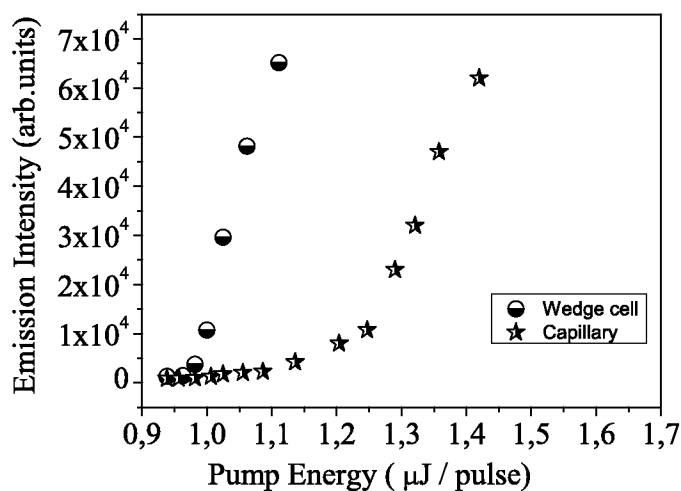
Figure 4. Emission intensity vs pump energy for the wedge cell and capillary glass microtube. The two confining geometries present different threshold values of the input pump energy above which random lasing is obtained.
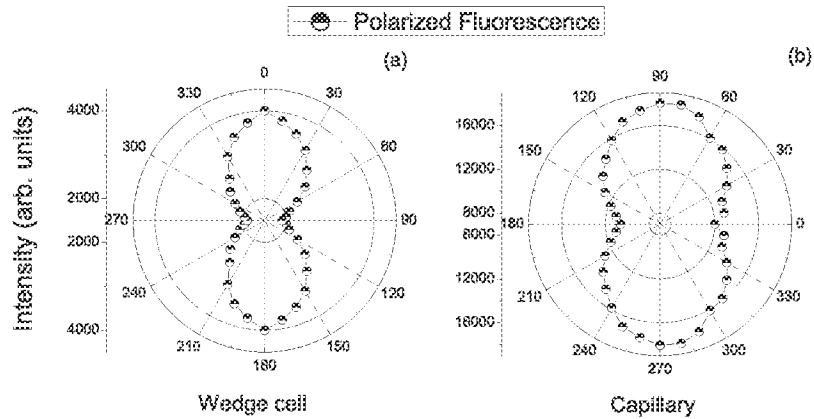
Figure 5. Polar plot for a wedge (a) and capillary (b) dye doped nematic sample showing the dependence of the polarized fluorescence emission on the angle θ between the linearly polarized light and the local nematic director orientation. A significant lowering of the intensity is obtained when the pump light is polarized parallel and perpendicular with respect to the nematic director.

to lasing action. The stimulated emission sharp peaks prove that lasing effect does not depend strongly on the sample size, but the key role is played by the bulky dye doped nematics. A small difference can be noticed however, in terms of the random lasing pump energy threshold, for the two confining geometries (Fig. 4). The distinct order degrees encountered for these systems makes probably the difference; we obtain a $1.2 \mu J/pulse$ value of the lasing energy threshold in the case of cylindrical confinement. Furthermore, in the case of the micro capillary tubes, the random lasing peak wavelengths tend to be lightly redshifted with respect to the wedge cell confinement, owing to the phase relationships which depend somehow on the boundary constraints. In the science of cavity laser a parameter of great interest because of the promise of 'thresholdless laser' is the β factor. For a conventional laser, this is defined as the ratio of the rate of spontaneous emission into the lasing modes to the total rate of spontaneous emission ($0 = \beta = 1$) and determines the sharpness of the laser threshold ($\beta = 1$ when all the spontaneous emission is radiated into the lasing modes).[20] In the case of our wedge sample, the output energy increases almost exponentially with the pump power and from calculations we obtained a value for $\beta \sim 0.08$. The presented behaviour suggests that a large part of the spontaneous emission is radiated into the lasing modes because of the sufficient optical feedback provided by the anisotropic coherent backscattering medium. This radiative transfer is regulated by the order of the system meaning that the order parameter drives the amount of spontaneous emission radiated into the lasing modes. This can explain the higher value of the threshold pump energy in the case of the micro capillary sample, due to the lower alignment order. Figure 5a shows that the fluorescence emission intensity undergoes a significant lowering when the pump light is polarized perpendicularly to the NLC director (o-wave) compared with the light polarized parallel to the director (e-wave). The polarization dependence of the scattering intensity and the coupling of the optical field with the gain medium have to be taken into account for the observed anisotropy. The former effect is mainly due to polarization dependence of the diffusion constant D for the emitted photons. A larger diffusion constant for the e-wave compared to the o-wave is generally measured. The latter aspect can be analyzed by considering the Fermi's Golden Rule which clearly states that the molecular transitions and the rate of emission strongly depend by the coupling of the pump electric field E and the transition dipole moment d of the dye molecules. Therefore, these processes are governed by the projection $E \cdot d$. The experimental results also emphasize that the fluorescent molecules adopt to some degree the local nematic order of the liquid crystal, which results in an anisotropic orientational distribution of the transition dipole moment. From figure 5 we can notice that polarized fluorescence measurements show a more pronounced anisotropy for the wedge sample. This is an expected result when comparing the better nematic alignment of the wedge cell with respect to the degenerate one within the
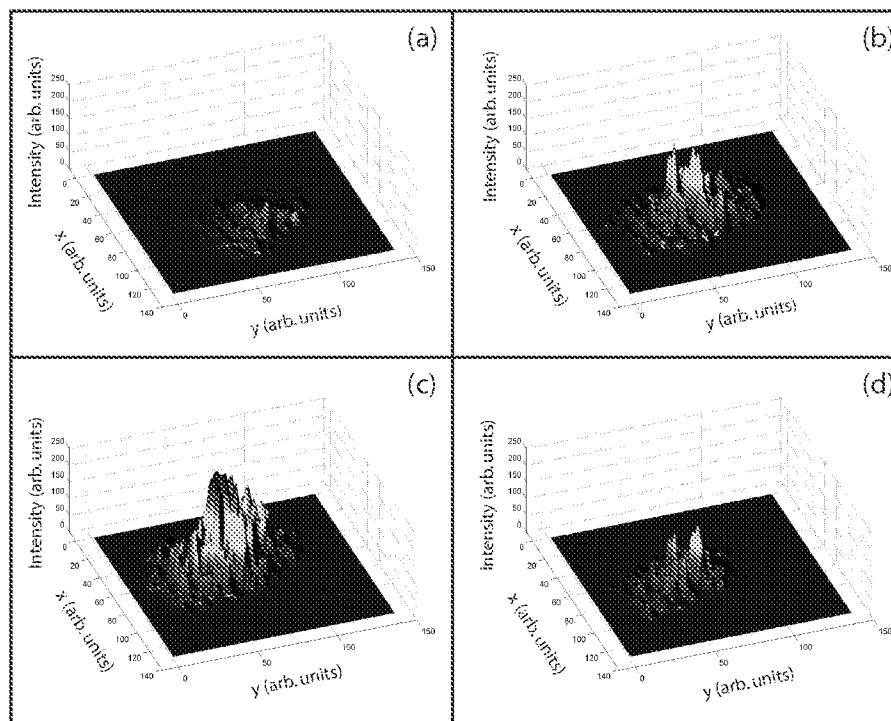
Figure 6. Far field spatial distribution of the emission intensity profile in a wedge NLC sample in the case of four successive (a,b,c,d) pump beam pulses (f = 10Hz) present an irregular intermittent behaviour, both spatial and temporal, of the emission.

untreated cylindrical capillary. This result once again confirms that the dipolar coupling modifies the quantum yield for fluorescence and plays an important role for the light amplification process; some states of polarization of the pump pulses provide a larger number of spontaneously emitted photons which are radiated in the lasing modes. It is worth pointing out that the maximum for the lasing intensity was obtained for linearly polarized pump pulses with E oriented along the local director ($\theta = 0°$), being in good agreement with the polarized fluorescence results as well as the polarization dependence of the scattering intensity. In order to gain further understanding on the diffusive laser action observed in partially ordered system, the far field spatial distribution of the emitted light was analyzed. Lasing emission was captured in a limited cone angle ($\sim 0.1 rad$) by means of a high resolution and sensitivity CCD camera (1390 X 1024 12bit PixelFlyQe by PCO). Figure 6 depicts an interesting scenario of the random lasing emission pattern from dye doped nematic liquid crystals confined in a wedge geometry. The intensity profile is formed by a series of bright tiny spots spatially overlapped which create a richly structured pattern. The sequence of images was obtained for four successive pump pulses and we can clearly observe that random lasing changes both spatially and in terms of intensity. This emission mechanism is based on the diffusive process of spontaneously emitted photons by fluorescent guest molecules launched at random directions from random positions. These photons are involved in a weak localization process within the gain medium because of recurrent multiple scattering. Since the condition for lasing comes from a careful balance between gain and loss, it is clear that in this case not for every pump pulse the random walk inside the anisotropic medium gathers enough gain for the system to lase. Further experiments for investigating the multiple scattering mechanism consisted in the study of time and temperature dependent behaviour of the lasing emission intensity. For this purpose, we collected the emitted light by means of a fast photodiode which was simultaneously triggered by the pump pulse. The signal was then sent to an oscilloscope and analyzed. Figure 7 depicts the temporal behaviour of laser action in the case of partially ordered nematic samples doped with fluorescent guest molecules.

As previously seen from the far field spatial distribution analysis, the obtained results show strong fluctuations
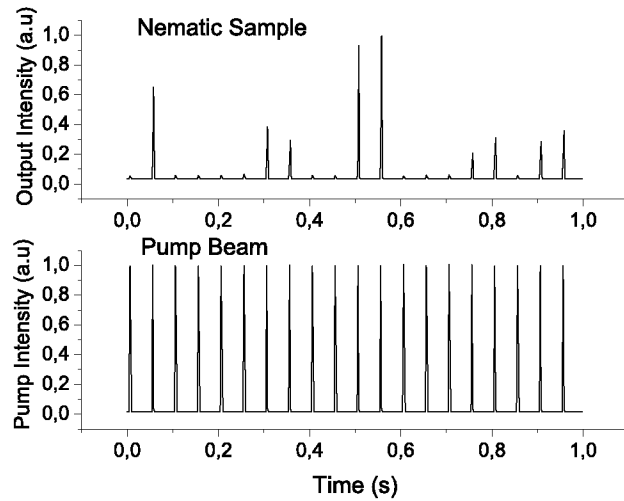
Figure 7. Output emission intensity dependence in a wedge sample illustrating the high temporal fluctuations, for a fixed value of the pump energy.
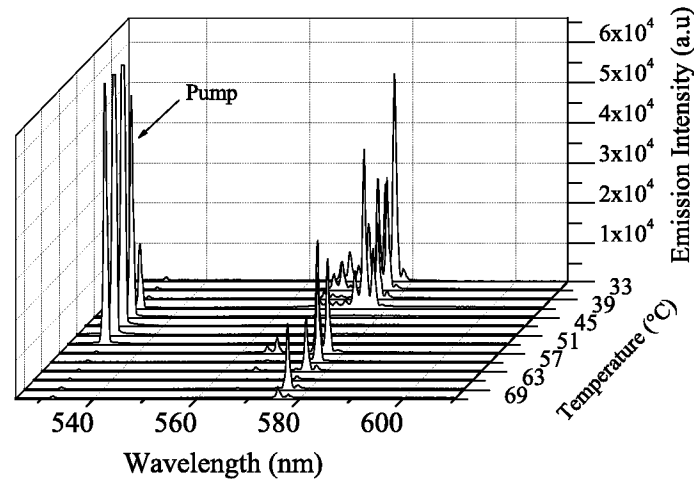
Figure 8. Temperature dependence of the random lasing emission spectra for the wedge sample. The graphic shows an unexpected behaviour; the emitted light intensity drops off as the temperature reaches $50°C$ but it reappears in the proximity of nematic-isotropic transition (around $60°C$).

in the emission intensity even in the case of a fixed pump energy value above the lasing threshold. Irregular intermittent sequences of 'on' and 'off' states demonstrate a characteristic behaviour for a random laser. In addition, the thermal analysis of the emission spectra reveals an unexpected behaviour in our systems (Fig. 8); the emitted light intensity drops off as the temperature approaches $50°C$ but it reappears in the proximity of nematic-isotropic transition (around $60°C$). By increasing the temperature, the incoherent scattering level within the medium is also amplified; the enhancement of incoherent scattering lowers the gain inside the system
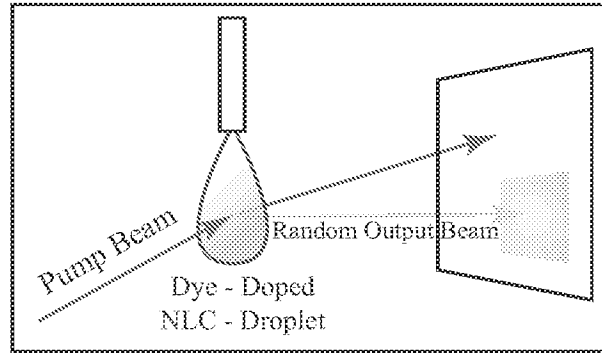
Figure 9. Schematic diagram illustrating the random lasing phenomenon in a dye doped nematic liquid crystal droplet.

and decreases the probability of having lasing modes in this situation, because a larger number of spontaneously emitted photons are needed to act as seeds for the stimulated emission process. This anomalous behaviour is accompanied by a strong scattering of the pump beam during the temperature range over which the lasing is absent, indicating that a cascade of scattering regimes occur as the temperature varies upward and downward the nematic phase. A detailed statistical characterization of the random lasing emission properties in function of the system temperature will be reported elsewhere. Recent experiments exploit the possibility of obtaining random laser action in freely suspended films and droplets of dye doped nematic liquid crystalline materials. With great enthusiasm we found out that these systems lase when optically pumped with an excitation laser. One of the proposed geometries is depicted in figure 9 and consists in a freely suspended dye doped NLC droplet with maximum diameter of about $1,5mm$. Upon optical pumping the system lases and an intermittent speckle like pattern of granular aspect is obtained on the background screen. By investigating the emission spectra we can clearly acknowledge that random lasing occurs above a given pump energy threshold value for which the coherent backscattering is sufficient enough to promote the gain inside the active material. Measured spectral line widths are about $0.5nm$, limited by the resolution of the CCD detector. Detailed future investigations were planned for fully characterizing these novel lasing systems.

4. CONCLUSIONS

For the first time it was observed and characterized the process of random laser action in confined dye doped nematics, for the case of various boundary conditions (i.e. confinement geometry, bulk volume and surface treatment) and external field constraints (i.e. pumping conditions, temperature gradient). The underlying mechanism is mainly based on interference effects which survive to recurrent multiple scattering driven by nematic director fluctuations. Weakly localized light waves into dye doped nematic sample are responsible for amplification while the resonance frequencies are selected through interference phenomena of the counter-propagating light waves within the localized loops. For simplicity, photons spontaneously emitted by the fluorescent guest molecules are launched at random directions from random positions within the excited volume. Because of the recurrent multiple scattering the probability to trace reciprocal paths by these photons is not null, as demonstrated by coherent backscattering experiments, thus resulting in equal phase accumulation during these open loops. While the gain length is comparable with the transport mean free path the emission of other photons is stimulated before the recurrently scattered photons leave the sample, triggering a coherent chain reaction. When the balance gain-loss becomes positive the optically excited dye doped nematic starts to lase. Unlike distributed feedback mirror-less laser, this system can be considered as a cavity-less microlaser where the disorder unexpectedly plays the most important role, behaving as randomly distributed feedback laser. We found that the random lasing peaks are extremely narrow banded $(0.5nm)$ and also that dye transition dipole moments adopt to some degree the orientational order parameter of the nematic director, resulting in a control of the emission intensity by varying the polarization of the input pump beam. The lasing emission intensity can also be manipulated by applying an external gradient of temperature while a completely switched off status is obtained for a certain interval $(42 - 55°C)$. Both confined systems (wedge and capillary) posses the characteristics of a random laser and a

detailed analysis of the far field modal profile for the emission intensity illustrate a series of spatially overlapped tiny spots creating a richly structured pattern which varies in time and position. Many other new geometries for the lasing systems are being designed and investigated, such as freely standing and freely suspended dye doped NLC droplets and thin films. Further studies will be needed in order to gain full understandings of the diffusive laser action in nematic samples and a wide series of experiments, simulations and extensive investigations are being considered.

REFERENCES

1. J. D. Joannopoulos, R. D. Meade, and J. N.Winn, "Photonic Crystals: Moulding the Flow of Light", Princeton, NJ, 1995.
2. G. Strangi, V. Barna, R. Caputo, A. De Luca, C. Versace, N. Scaramuzza, C. Umeton, R. Bartolino, and G.Price, "Color tunable distributed feedback organic micro-cavity laser," *Phys. Rev. Lett.* **94**, 2005.
3. V. Barna, S. Ferjani, A. De Luca, R. Caputo, N. Scaramuzza, C. Versace, and G. Strangi, "Band-edge and defect modes lasing due to confinement of helixed liquid crystals in cylindrical microcavities," *Appl. Phys. Lett.* **87**, 2005.
4. D. Wiersma and S. Cavalieri, "A temperature tunable random laser," *Nature* **414**, 2001.
5. V. M. Markushev, V. F. Zolin, and C. M. Briskina, "Luminescence and stimulated emission of neodymium in sodium lanthanum molybdate powders," *Sov. J. Quantum Electron.* **16**, 1986.
6. C. Gouedard, D. Husson, C. Sauteret, F. Auzel, and A. Migus, "Generation of spatially incoherent short pulses in laser-pumped neodymium stoichiometric crystals and powders," *J. Opt. Soc. Am. B* **10**, 1993.
7. M. A. Noginov, N. E. Noginov, H. J. Caulfield, P. Venkateswarlu, T. Thompson, M. Mahdi, and V.Ostroumov, "Short-pulsed stimulated emission in the powders of ndal3(bo3)4, ndsc3(bo3)4, and nd:sr5(po4)3f laser crystals," *J. Opt. Soc. Am. B* **13**, 1996.
8. H. Cao, Y. G. Zhao, S. T. Ho, E. W. Seelig, Q. H. Wang, and R. P. H. Chang, "Random laser action in semiconductor powder," *Phys. Rev. Lett.* **82**, 1999.
9. V. S. Letokhov, "Quantum statistics of multiple-mode emission of an atomic ensemble," *Sov. Phys. JETP* **26**, 1968.
10. P. Anderson, "Absence of diffusion in certain random lattices," *Phys. Rev.* **109**, 1958.
11. A. Ioffe and A. Regel *Prog. Semicond.* **4**, 1960.
12. B. A. van Tiggelen, R. Maynard, and A. Heiderich, "Anisotropic light diffusion in oriented nematic liquid crystals," *Phys. Rev. Lett.* **77**, 1996.
13. H. Stark and T. C. Lubensky, "Multiple light scattering in nematic liquid crystals," *Phys. Rev. Lett.* **77**, 1996.
14. M. H. Kao, K. A. Jeter, A. G. Yodh, and P. J. Colling, "Observation of light diffusion and correlation transport in nematic liquid crystals," *Phys. Rev. Lett.* **77**, 1996.
15. P. Johnson, B. J. Bret, J. G. Rivas, J. J. Kelly, and A. Langendijk, "Anisotropic diffusion of light in a strongly scattering material," *Sov. Phys. JETP* **89**, 2002.
16. R. Sapienza, S. Mujumdar, C. Cheung, A. G. Yodh, and D. Wiersma, "Anisotropic weak localization of light," *Phys. Rev. Lett.* **92**, 2005.
17. P. G. deGennes and J. Prost, "The Physics of the Liquid Crystals", Oxford, 1993.
18. G. Strangi, S. Ferjani, V. Barna, A. De Luca, N. Scaramuzza, C. Versace, C. Umeton, and R. Bartolino, "Random lasing and weak localization of light in dye-doped nematic liquid crystals," *Opt. Express* **14**, 2006.
19. S. Ferjani, V. Barna, A. De Luca, N. Scaramuzza, C. Versace, C. Umeton, R. Bartolino, and G. Strangi, "Thermal behavior of random lasing in dye doped nematic liquid crystals," *Appl. Phys. Lett.* **89**, 2006.
20. G. V. Soest and A. Lagendijk, "β factor in a random laser," *Phys. Rev. E* **65**, 2002.

Statistical analysis of random lasing emission properties in nematic liquid crystals

Sameh Ferjani[1,2,3], Luca Sorriso-Valvo[2], Antonio De Luca[1,2,3],

Valentin Barna[1,2,3], Rossana De Marco[1], Giuseppe Strangi[1,2,3]

[1] *Dipartimento di Fisica, Università della Calabria, and*

CNISM – Unità di Cosenza, Ponte P. Bucci, Cubo 31C, 87036 Rende (CS), Italy

[2] *Regional Laboratory LICRYL - INFM/CNR, Ponte P. Bucci, Cubo 33B, 87036 Rende (CS), Italy and*

[3] *Center of Excellence CEMIF.CAL, 87036 Rende (CS), Italy*

(Dated: September 5, 2007)

A statistical analysis of random lasing events observed in dye doped nematic liquid crystal (NLC) films is reported. The occurrence of random laser action in such complex fluids is due to residual resonances in the multiple scattering of spontaneously emitted photons. The Shannon entropy and a local-Poisson test are used here in order to quantitatively characterize the chaotic behavior of laser spikes and gain further understandings of the mechanisms underlying the lasing effect in strongly scattering organized fluids arising by an unexpected interplay of localization and amplification.

I. INTRODUCTION

Since firstly proposed by Letokhov in 1968, which predicted that the combination of multiple scattering and light amplification would lead to a form of laser, lasing in disordered media has been a subject of intense theoretical and experimental studies [1, 2]. Multiple scattering phenomena have been observed in various systems such as powdered laser crystals, micro and nano particles in laser dye solutions and liquid crystal-dye infiltrated porous glasses. In these cases, the emission was shown to become narrow banded above a given pump energy threshold [3]. The physical mechanism behind random lasing can be explained by making an analogy to the electronic model proposed by Philip W. Anderson in 1958 in the famous article "Absence of diffusion in certain random lattices" [4]. He described the vanishing of electron propagation in the regime of very strong multiple scattering due to interference in lattices where disorder was introduced as impurities. This concept served as a model for metal-insulator transitions. In an active random media, when the scattering is weak, the emission is spontaneous. When light scattering is enhanced above a critical value, recurrent light scattering events arise and the Ioffe-Regel criterion for localization, $kl_t < 1$ ($k = 2p/\lambda$ is the wave vector and l_t is the scattering mean free path), is met. The dwell time of light photons in such media can be increased, so that light is amplified by walking a longer random path inside the system. In the strong multiple scattering regime, the system makes a transition into a localized state where light propagation is inhibited owing to survival of interference effects. In random lasers, it is exactly this strong multiple scattering inside the gain medium that provides the means for stimulated emission feedback. In 1996, Wiersma's group performed scattering experiments on fully and partially disordered systems, demonstrating that interference effects manage to survive the scattering regime and give rise to enhancement of the light intensity in the backscattered direction,

namely the cone of coherent backscattering [5]. When optical scattering is strong, light may return to a scatterer from which it was scattered before, and thereby forms a closed loop path that serves as a "random cavity". When light is trapped inside the gain medium long enough, the amplification along such a loop path can exceed the optical loss and the system starts to lase. As the pump energy is further increased, the balance between gain and loss becomes positive and additional narrow peaks appear in the emission spectrum. Such laser action is called diffusive or random lasing. Because random lasing modes come from the eigenstates of disordered systems, random lasers open a special door to study the interplay between localization and amplification. Recently, Strangi et.al [6] reported the first observations of random laser action in a partially ordered dye-doped nematic liquid crystals systems presenting various confining geometries. In this letter, we investigate the random lasing emission properties in dye doped nematic liquid crystals for different temperatures, below the nematic-isotropic transition. In particular, a statistical study of the emitted photons is reported and a model is intended to explain the temperature (vs. time) dependent behaviour of the speckle-like emission.

II. EXPERIMENTAL

The gain medium consists of a nematic liquid crystal mixture (BL001 by Merck) doped with $0.3\%wt$ of Pyrromethene 597 dye (Exciton). The liquid crystal bulk phase sequence is Cr. $-10°C$ Nematic $63°C$ Iso. The mixture was confined in a wedge cell constituted by two glass-ITO plates separated by Mylar spacers, with a thickness of $2\mu m$ at one side and $0.2mm$ at the other one. The glasses were treated with polyimide in order to induce a homogeneous alignment of the NLC molecules. The system was then optically pumped with $532nm$ light from a frequency-doubled Nd:YAG laser (NewWave,

Tempest 20). The pump light consisted of a train of twenty $3ns$ pulses focused into a $50\mu m$ spot by means of a spherical lens. The emission properties were spectrally analyzed by means of a high-resolution optical multichannel CCD spectrometer (Jobin Yvon, Micro-HR). For low pump energy, the emission spectrum shows the typical spontaneous emission curve of the pyrromethene dye. When the pump intensity exceeds a certain threshold, several sharp lasing peaks emerge (Fig. 1a). The far field spatial distribution of the emitted light was captured with a high sensitivity and resolution CCD camera (PixelFlyQE by PCO) and it shows a series of spatially overlapped bright tiny spots which create a richly structured pattern typical of random lasers (Fig. 1b).
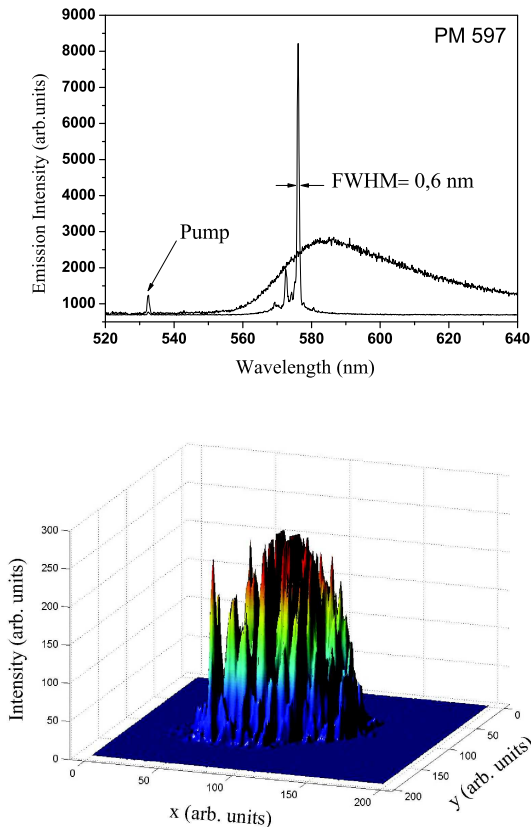

FIG. 1: a) Fluorescence and lasing spectra in partially ordered dye doped nematic liquid crystal confined in a wedge cell. Above a given threshold pump energy, discrete sharp peaks emerge from the residual spontaneous emission. b) Far-field spatial distribution of the emission intensity shows a multitude of spatially overlapped lasing peaks.

In order to gain further understanding about the multiple scattering mechanism and its time and temperature dependent behaviour we statistically analyzed the emission intensity fluctuations. For this purpose, we collected the emitted light by means of a fast photodiode which was simultaneously triggered by the pump pulse. The signal was then sent to an oscilloscope and analyzed. Figure 2a depicts the temporal behaviour of laser action in the case of highly ordered cholesteric and partially ordered nematic samples doped with fluorescent guest molecules. For a fixed pump power the cholesteric system shows very small variations in the lasing output intensity (the pump energy was kept fixed above the lasing threshold). Essentially, for each shot of the pump beam the system was in the "on" state. A totally different scenario is revealed in the case of the nematic dye doped system: strong fluctuations of the emission intensity are measured for pump power above the lasing threshold. Irregular intermittent sequences of "on" and "off" states demonstrate a characteristic behaviour for a random laser. Since the condition for lasing comes from a careful balance between gain and loss, it is clear that in this case not for every pump pulse the random walk inside the anisotropic medium gathers enough gain for the system to lase. Interestingly, upon increasing the temperature of the sample the system tends to present the off state more frequently. By increasing the temperature, the total scattering intensity slightly increases but the coherent backscattering cone is lowered emphasizing that the incoherent scattering component increases within the medium. The enhancement of incoherent scattering lowers the gain inside the system and decreases the probability of having lasing modes in this situation, since a larger number of spontaneously emitted photons are needed to act as seeds for the stimulated emission process.

III. CHARACTERIZATION: LOOKING FOR CORRELATIONS

To better understand the driving mechanisms within these systems, a statistical study has been performed. In particular, we used two different statistical tools, already adopted in other contexts, to characterize the possible presence of memory in the system. As can be clearly seen by a look at Figure 2b, and as we have already mentioned, the diffusive laser action in dye doped NLC is rather irregular. It seems thus natural to investigate whether such irregularity is the result of a completely random process, or if, instead, some form of correlation is present, indicating the existence of an underlying mechanism in the system. The statistical description of the irregularity properties of the system could give useful information on several aspects, as for example the temperature dependence mentioned above. Since, in this paper, we are interested in the irregularly alternating status of lasing (lasing or non-lasing in response to the pump), we chose to identify an "event" with the total intensity emitted by the system, as observed in correspondence with the pump pulse. Then, we set a threshold, right above the noise level of the recorded signal and the pump level, to separate the "non-lasing" events from the "lasing" ones. The result of such process is a signal, made of "on" and "off" digits, indicating the status of emission of the system at each pump pulse. The presence of correlations,
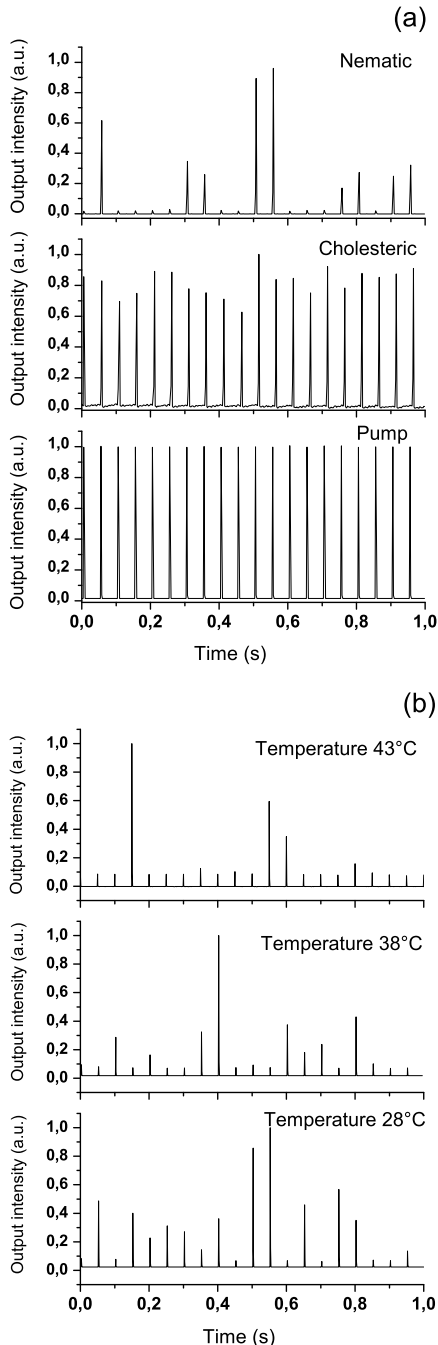
FIG. 2: a) Pump and output emission intensities from both dye doped cholesteric and dye doped nematic samples as function of time. b) The temporal emission intensity dependence on system temperature for a dye doped NLC sample.

and thus of memory effect, corresponds to evidence of some degree of regularities in the signal obtained through this procedure.

A. The Shannon entropy

Let us now introduce the first statistical tool used in this work, known in literature as Shannon (or information) entropy [7, 9]. The regularity of a sequence of $N-1$ symbols (as, for example, a word of binary digits), produced by any source, can be characterized through the ability in predicting the N-th symbol. In our case, the possible symbols are limited to the "on" and "off" states, so that the binary digits "0" and "1" are only needed to describe the sequence. We will give a brief description of the Shannon entropy in this case, reminding that the theory can be extended to an arbitrary number of different symbols. Given a sequence of N binary digits $s(i)(i = 1, ..., N)$, we introduce the probability $P(C_n)$ (namely the occurrence rate within the sequence) of a particular "word" $C_n = (s(1), s(2), \dots, s(n))$ of length n. Then, the entropy associated to a generic n-digits word can be defined as $H_n = -\sum_{\{C_n\}} P(C_n) \log P(C_n)$, where the sum is computed over all the possible combinations of length n. The quantity $h_n = H_{n+1} - H_n$, indicated as differential entropy, thus represents the average information provided by the $(n + 1)$-th digit, once the previous n digits are known. For a stationary source, the Shannon entropy can finally be defined as the limit for large values of n

$$h_{sh} = \lim_{n \to \infty} h_n = \lim_{n \to \infty} \frac{H_n}{n}. \qquad (1)$$

This quantity is a measure of the regularity of the sequence. For example, for a given regular (say periodic) sequence, the information carried by the next digit after one period is zero, since the full knowledge of the sequence in contained into the first period. The predictability of such a sequence is then trivially high, and the signal is completely correlated with long range memory. On the contrary, if the sequence is chaotic, the information provided by the knowledge of each digit can be high. For example, for a random realization, namely if all digits have the same chance to be "0" or "1", any next digit carries with it the same amount of information as the previous ones. Such a sequence is completely unpredictable, and neither memory nor correlations are present. In this case the limit (1) can be easily shown to be $h_{sh} = \log 2$. Thus, the quantities defined so far represent a tool to describe the complexity of the source, through the regularities of the emitted sequences. Note that although the theoretical Shannon entropy is defined as the limit to infinity of the word length, in the real experiments the convergence of the limit (1) is normally already obtained for small values $n < 10$.

Let us now consider our dataset. In this work we focused on six data-set obtained by performing the same experiment at different values of the temperature, in the interval between 26°C and 41°C. The experimental data have been reduced to 6 sequences of 2000 digits, each corresponding to the output state (lasing, that is "on", or non-lasing, that is "off") as response to the excitation

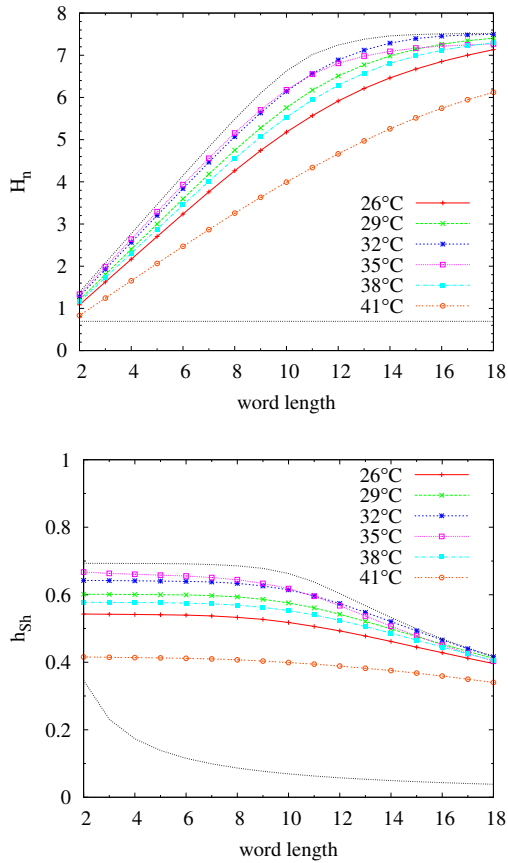| T ($\circ$ C)	n of events	n of "1" events (%)	h_{sh}
26	2000	78%	0.54
29	1999	71%	0.60
32	1999	65%	0.64
35	1854	39%	0.67
38	1896	26%	0.58
41	1971	14%	0.42

FIG. 3: The values of the entropy H_n (top panel) and of the differential entropy h_n (bottom panel) as a function of the words length n. Different colours refer to the different dataset (the corresponding temperatures are indicated in the legend). For both panels, the black dotted lines represent the results obtained using the completely ordered artificial dataset (the bottom curve) and the completely random realization (top curve).

pulses. We underline that the choice of the threshold is not relevant. In fact, different realizations of the analysis obtained with reasonable variations of the threshold gave the same results, so that we do not need to discuss it here. For each sequence, made of "0" and "1" digits (see Table III A), we have then computed the quantities defined above, namely the entropy H_n, the differential entropy h_n and the Shannon entropy h_{sh}, using words of length up to $n = 18$. The results are collected in Figures 3 and 4. For comparison, on the same figures are reported, together with the 6 realizations at different temperatures, the results obtained using two artificial datasets. The first one is a regular sequence of alternating "0" and "1", while the second one is a completely random realization. Both sequences include 2000 digits, as for the observed strings. Looking at the top panel of Figure 3, it is possible to observe that, for the regular string, there is no increase of information when the number n of digit of the words increases. This corresponds, as expected, to a vanishing

differential entropy (bottom panel of Figure 3) leading to $h_{sh} \sim 0$. The random case, conversely, displays a constant growth of entropy H_n with the number of digits, indicating that all of them bring the same amount of information (top panel of Figure 3). This correspond to a constant differential entropy h_n (bottom panel of Figure 3). In order to obtain a value of the Shannon entropy, we observe that a saturation of H_n, and consequently a vanishing trend for h_n, is reached for $n > 5$, due to the finite size of our sequence. Thus, we can assume that the Shannon entropy is well represented by the constant region of the differential entropy h_n, with $n < 5$. We decide, thereafter, to use the first value reported in the plot, namely h_2, as a proxy for the Shannon entropy. The values of our estimates are displayed in Figure 4. For the random case, the expected value $h_{sh} = \log 2$ is obtained.

The experimental sequences, obtained from the different datasets, show clear temperature dependence, accordingly to the probability variations reported in Table III A. At low temperature, at which the string is mainly composed by "on" digits (see Table III A), the entropy curve indicate that the system is chaotic, but with some degree of regularity. This is evidenced by the fact that the information entropy H_n grows more slowly than for the random case (Figure 3). Moreover, the values of the Shannon entropy are somewhat smaller than the upper value $h_{sh} = \log 2$ (see Figure 4). Thus, the amount of information carried by each digit is small. As the temperature is increased, the number of "on" and "off" digits becomes comparable, so that for $T = 35°C$ the Shannon entropy reaches its maximum value $h_{sh} = 0.67$, very close to the completely chaotic value. For higher temperatures, the trend is reversed, and long "0" series are interrupted by sporadic "1" digits. Both the high temperature and the low temperature configurations, which are almost undistinguishable as far as Shannon entropy is concerned, imply the presence of recurrent words of the same state (e.g. 000...0) that makes the system more predictable, the information carried by each digit smaller, so that the Shannon entropy decreases. The indication of high chaoticity is anyway still valid. It should be noted that the number of the "on" states decreases very smoothly (indeed almost linearly) with the temperature, varying from a mainly-on configuration to a mainly-off one. The dominating state changes from "on"

to "off" at some point between 32°C and 35°C (see figure 4). By comparing the slopes before and after the inversion of the Shannon entropy trends, we notice that it decreases more rapidly with respect to the rise phase. It means that by increasing the temperature the number of excitation pulses, that actually create the conditions to have lasing, reduce more rapidly after the inversion point. In order to shine light on this point, a series of experiments have been planned in which we intend to use pure LC and compare with mixtures where some phase-separations could occur producing a rapid increase of the intensity of the incoherent scattering component.
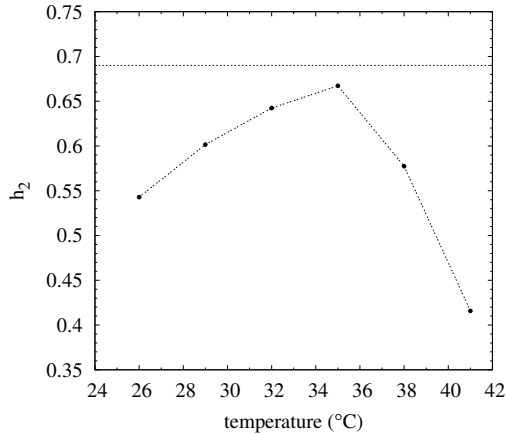

FIG. 4: The values of the differential entropy h_2 as a proxy for the Shannon entropy, measured at different temperatures. The dotted line shows the completely random value $H_2 = 0.69$.

B. The local-Poisson test

As we have seen, the Shannon entropy analysis provides the useful information that the system under study is highly chaotic, especially at intermediate temperatures. At high and low temperatures, there is the indication of presence of regularity of the gain mechanisms behind the laser spiking, mainly due to the occurrence of long periods of stable state. One further information is that the system chaoticity changes smoothly with the temperature. However, it is desirable to gain more insigth on the system and in particular on the specific features of chaos. This can be obtained, for example, by looking at correlations of the emitted pulses. Correlations are indeed related to some underlying mechanism, so that their presence in a signal indicates the non-stochasticity of the phenomenon. Let us now consider our experimental data as a succession of words made of the same digit. This corresponds to transform the strings in series of "0"-only or "1"-only words of variable length η, this last being defined as the number of consecutive identical digits. Thus, the persistence of the system in a given state (lasing or non-lasing) is concerned here. In

order to investigate the presence of correlations in the system, the probability distribution function (PDFs) of the persistence lengths can be studied. Indeed, for a completely random process, such distributions are expected to be exponential. The presence of correlations, conversely, produces long-range power-law PDFs. This is an easy test to perform on our data. Figure 5 displays the distribution functions $P(\eta)$ obtained for three values of the temperature. PDFs are approximately power-laws, indicating that the system is correlated not only at the border temperatures ($T = 26°C$ and $T = 41°C$), but also at intermediate ones ($T = 35°C$).
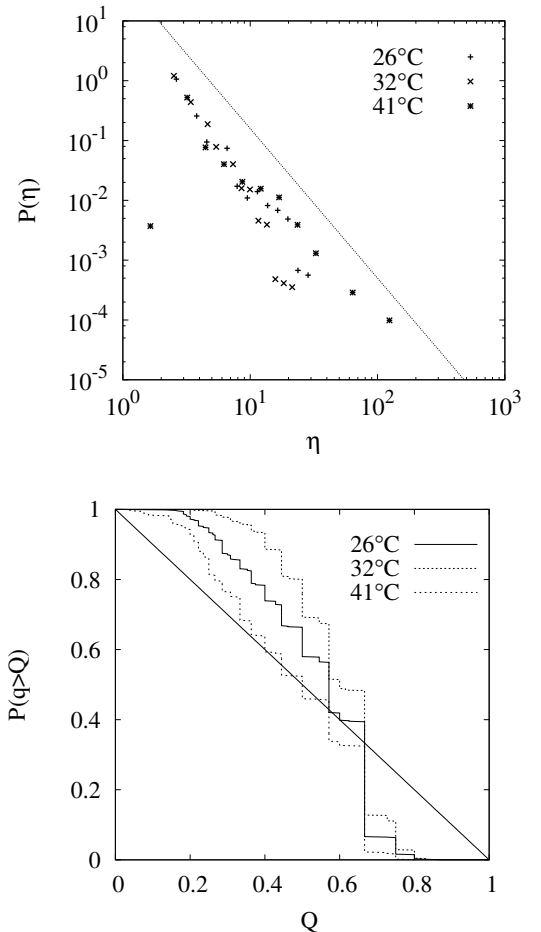
FIG. 5: Top panel: the PDF of the lengths η of words made of "1" only for three different values of the temperature. A power-law is also plotted for reference. Bottom panel: the surviving function of the variable q (see text) for the same temperatures. The thin streigth line $1 - x$ represents the Poissonian, decorrelated case.

Because of the limited size of the datasets, the PDFs shown in Figure 5 might suffer of some uncertainties. We then performed a further analysis, which is less sensitive to the sample size. Such analysis has been introduced some years ago in cosmology [8], and used more recently in astrophysical [9–11], geophysical [12] and econo-

physics [13] context.

Consider the sequence of m words, identified as the consecutive sets of identical symbol within the original binary sequence, as described above. The separation points between two successive words can be labeled with an index i, and identified as an event. The events are thus defined as the change of state of the system from lasing to non-lasing and vice-versa. For each event i, we use the length of the following or preceding next and second next words, that we call $L_1(i)$ and $L_2(i)$ respectively. The choice between the pair of word following the event i, and the pair preceding the same event, is made in order to have the smallest $L_1(i)$. $L_1(i)$ and $L_2(i)$ are then the lengths of the two word following or preceeding a given state change i. We then introduce a quantity, which we denote by q, which is nothing but the suitably normalized local word length

$$h(L_1(i), L_2(i)) = \frac{2L_1(i)}{2L_1(i) + L_2(i)} \qquad (2)$$

If the words lengths are randomly distributed, it can be shown that the probability density function $P(q)$ of the stochastic variable q defined above is uniformly distributed in $q \in [0, 1]$. This correspond to have a linear decrease for the surviving function of $P(q)$, namely $P(q \geq Q) = \int_Q^\infty P(q)dq = 1 - Q$. To better understand the meaning of this tool, note that in a process where $L_2(i)$ are systematically smaller than $2L_1(i)$, clusters of state changes are present and the average value of q is greater than $1/2$. On the contrary, when the process is characterized by increasing persistence of state, the average value of q is less than $1/2$. Both cases indicate the presence of correlations in the signal. The test described above is thus an useful tool to discriminate between a sequence of random words and a sequence of correlated ones.

From the experimental strings, it is straightforward to calculate the surviving function $P(q \geq Q)$ and the test is easily performed. Figure 5 shows the surviving functions computed for the same three cases as $P(\eta)$. The stepwise shape of the surviving function is due to the discrete nature of the sequence and to the relatively small set of possible values of the lengths η. This results confirm that at all temperatures there is a relevant deviation from stochasticity, so that the presence of correlations is strong.

IV. CONCLUSIONS

The chaos of the amplification mechanism in dye doped complex fluids has been quantitatively described through the Shannon entropy. The results have shown that it is highly chaotic, and that a peculiar dependence on the temperature is present. In particular, we have shown that chaoticity level increases when temperature is increased, then reaches a peak at intermediate temperature, and finally decreases faster than in the growing regime. This could be due to the smooth changes in relative number of lasing and non-lasing states in the signal. We have then performed a test to verify the presence of correlations between the successive states of the random lasing. The results show clearly that correlations are observed in the emission properties of the dye doped liquid crystal. On the other hand in the presented system has already been observed through backscattering experiments unexpected coherence effects responsible of the optical feedback [5]. The correlations found in the lasing spikes could be related to the amplification mechanisms through the coherent scattering component that can present important fluctuations with long range correlations. Our results suggest that for a better understanding of the basic physical mechanisms of our systems, other tailored dye doped complex fluids need to be explored. The comparison of statistical characteristics could reveal the entity of coherence effects in light localization processes.

[1] H. Cao, Y. G. Zhao, S. T. Ho, E. W. Seelig, Q. H. Wang & R. P. H. Chang, Phys. Rev. Lett., **82**, 2278 (1999).
[2] D. Wiersma & S. Cavalieri, Nature **414**, 708 (2001).
[3] H. Cao, J. Y. Xu, E. W. Seelig & R. P. H. Chang, Appl. Phys. Lett. **76**, 2997 (2000).
[4] P.W. Anderson, Phys. Rev. **109**, 1492 (1958).
[5] R. Sapienza, S. Mujumdar, C. Cheung, A. G. Yodh & D. Wiersma, Phys. Rev. Lett. **92**, 033903 (2005).
[6] G. Strangi, S. Ferjani, V. Barna, A. De Luca, C. Versace, N. Scaramuzza & R. Bartolino, Optics Express **14**, 7737 (2006).
[7] C.E. Shannon, *A mathematical theory of communication*, (The Bell System Technical J. Vol. 27, 379432–623656, 1948).
[8] H. Bi, G. Corner & Y. Chu, Astron. Astrophys **218**, 19 (1989).
[9] G. Boffetta et al., Physics Reports **356**, 367 (2002).
[10] G. Boffetta et al., Phys. Rev. Lett. **83**, 4662 (1999).
[11] F. Lepreti, V. Carbone & P. Veltri, Astrophys. J. **555**, L133 (2001).
[12] V. Carbone, L. Sorriso-Valvo, A. Vecchio, F. Le preti, P. veltri, P. Harabaglia & I. Guerra, Phys. Rev. Lett. **96**, 128501 (2006).
[13] A. Greco, V. Carbone & L. Sorriso-Valvo, Physica A **376**, 480 (2007).

Random Lasing in Freely Suspended Dye Doped Nematic Liquid Crystals

S. Ferjani[1], V. Barna[1,2], A. De Luca[1,2], C. Versace[1] and G. Strangi[1]

[1] *Licryl CNR-INFM and Cemif. Cal (Center of Excellence MIUR), Department of Physics, University of Calabria, I-87036 Rende (CS), Italy*

[2] *Liquid Crystals and Complex Fluids Laboratory, Department of Physics, Case Western Reserve University Cleveland, Ohio 44106 USA.*

Author for correspondence: Strangi@fis.unical.it

Random lasing in fully disordered systems having organic and inorganic nature has been the subject of extensive studies since the beginning of last decade. The interest mainly emerges from the unexpected role played by disorder in the laser action. The disorder was considered detrimental for the optical feedback in cavity laser, until was demonstrated that multiple scattering materials including a gain medium act as random laser. Here, a completely new approach is reported, where freely suspended complex fluid films doped with fluorescent molecules under optical excitation generate narrow banded lasing peaks. The constellation of localized modes is selected by properly choosing the gain profile. The idea to have laser action in absence of mirrors and boundaries realizes an unparalleled tunable and mouldable laser source.

Since the first appearance of random lasing in nano-powdered inorganic systems enormous interest has been focused in trying to understand the mechanisms driving this interesting and unexpected phenomenon[1]. Random laser action in fully disordered organic and inorganic systems (nanopowdered dye solutions, colloidal suspensions, etc.) has been widely investigated paving the way to an entirely new research field with important scientific and technological implications[2-4]. In particular, random laser have relevant impact and applications in the physics of soft-matter and biological tissues[5-6]. Light localization through strong multiple scattering and residual effect of coherence have been invoked as the main responsible of the feedback mechanism driving the coherent light generation in a fully or quasi-disordered system doped with guest fluorescent molecules. The surviving of interference effects in multiple scattering evidenced by coherent backscattering experiments[7-8], motivated the studies about the interplay between localization and amplification, predicted by Lethokov[1] almost four decades ago. The coupling of strongly scattering and gain media can generate random lasing, through an unexpected modes selection mechanism. In cavity-less disordered media the entrapment of spontaneously emitted photons within reciprocal paths, because of recurrent multiple scattering, give rise to phase relationships, providing the coherent optical feedback which triggers the lasing effect. The emission properties of this kind of laser present peculiar characteristics emphasized by strong intensity fluctuations varying spatially and spectrally producing a continuously changing emission pattern. In fact, by capturing the emission pattern by a high speed CCD camera usually shows a sequence of different spots characterized by several intense little spots spatially overlapped. The lifetime of these random modes generally spans from tens of picoseconds up to few nanoseconds leading to random emission patterns. There are several experimental evidences of absolutely non-trivial dynamics and statistics of random laser systems[9]. The random lasing can be assimilated to amplification processes triggered by stochastic resonators which randomly create the conditions to lase, since a disordered medium sustains a large number of modes with overlapping resonances. The constellation of modes which appears during the lasing process are mainly due to the rapid variation of the phases and slow changes of the

amplitudes of the optically localized field. Furthermore, it can be considered as a multimode-laser with some renormalized coefficient in standard Lamb theory, but still lack a fully solvable analytical model.

In this work, by employing a novel geometry, we make a critical step of demonstrating random laser action in freely suspended liquid crystal films. The idea was to create the condition of almost complete absence of boundaries for a dye doped nematic liquid crystal film in order to study how the partial order of unbounded organized fluids can play the role of random resonators leading to a multi-mode laser. The motivation of this work finds its important support in the opportunity to investigate the mechanisms of amplification and localization and their interplay in such complex system in absence of confinement. Upon freely suspending organized fluids is possible to exploit the unique optical properties of these materials which can be modified by several external parameters, i.e. magnetic, electric, thermal, and mechanical stimuli. The visco-elastic properties and the surface tension mainly determine the profile of the free standing films, in case of high viscosity liquid crystalline materials (smectics) was possible to obtain very thin films (tens of nanometers) only few smectic layers thick[10]. The mismatching of refractive indices, the irregular shape of the air-liquid crystal interface and the scattering cross sections are some of the parameters accounted to study the reported effect. Several systems have been investigated by changing the dye laser and the geometry to suspend the gain complex fluid, with the aim to study how the menisci and liquid crystal-air interfaces modify the emission properties. The gain media consist of a nematic liquid crystal mixtures (BL001 by Merck) doped with 0.3 wt% of Pyrromethene PM 597 and 650 dyes (Exciton). These dyes are based on the fluoroboration (BF_2 complex) of two pyrrole rings linked by a conjugated π-system chain, giving the dipyrromethene-BF_2 (PM) complexes, which can also be described as cyclic cyanine dyes. These green-yellow and red dyes have interesting photo-physical properties with a fluorescence quantum yield which can be close to 1. Dipyrromethene BF_2 complexes can lase more efficiently than rhodamines (the most commonly used laser dyes in the visible part of the electromagnetic spectrum), with a lasing efficiency as high as 85% of the pumping power. The high laser efficiency of PM dyes is based not only on the high fluorescent capacity but also on the low T-T absorption capacity over the lasing spectral region[11].

In addition, these dyes present a high photostability, increasing the lifetime of laser action. The liquid crystal bulk phase sequence is (-10°C) Crystal - Nematic (63°C) Nematic -Isotropic. The mixtures were freely suspended by means of a fluid spreader on a PVC net creating squared comb (800 μm x 800 μm) having a thickness of about 300 μm (see Figure 1). The suspended films observed at the optical microscope show a poly-domains structure where the single domain possesses a residual birefringence. Both mixtures show a high degree of miscibility of the dye laser in the liquid crystalline solvent, in fact was not found evidence of dye micro-droplets phase separated by the liquid crystalline phase. In addition, the spectro-photometric measurement reveals that the absorbance curve is only slightly modified with respect to usual dye solutions of isopropanol or other pure solvents. The PVC net was cleaned with usual solvents, dried in an oven at 50 °C for 1 hour without any treatment to align the liquid crystal molecules. Nevertheless, a partially ordered medium was obtained due to the flow induced by the spreading process over the comb. The profile of menisci driven by competitive forces (gravity, viscosity and surface tension) across the medium present a thinner central region of about 300-350 μm. The system was then optically pumped with 532-nm light from a frequency-doubled Nd:YAG laser (NewWave, Tempest 20). The pump light consisted of a train of twenty 3-ns pulses per second, focused into a 50-μm spot by a spherical lens and circularly polarized using a quarter-wave plate in order to maximize the excitation cross section. The emitted light was spectrally analyzed by means of a high-resolution optical multi-channel CCD spectrometer (Jobin Yvon, Micro-HR). At low pump energy a strongly diffuse isotropic signal of fluorescence was observed. Upon increasing the pump energy above a given threshold, the emitted light appeared focalized along the excitation volume. This effect is spectrally accompanied by the collapse of the fluorescence emission and the appearance of sharp bright tiny spots in a wide cone about the excitation volume[12]. The spectral and spatial study of the emission patterns clearly revealed a random lasing behaviour characterized by narrow banded (FWHM = 0,5 nm) brilliant spikes which rapidly fluctuate in frequency and space (Fig. 2). In figure 3 the emission spectra for both samples are reported, where it is possible to emphasize the presence of sharp lateral peaks

which anomalously occurs at different spectral position about the main lasing peak. The most intense peaks arise at 578 nm and 652 nm in the case of the PM597 and PM650 mixture respectively.

A dye doped complex fluid spatially suspended which generates spectrally sharp peaks represents an innovative system to study the random emission properties. In order to understand the mechanisms behind this effect we performed a study by varying the geometry (diameter controlled drops and free standing thin films), and to identify the role of each material several mixture were prepared. The experiments have been performed in the mixture of BL001 doped with pyrromethene 597 0.3 wt% and suspended on the squared plastic network, the sample was optically pumped with an appropriate laser pulses train (λ_{exc}= 532nm; rep.rate = 20Hz). The far field spatial distribution of the emitted light was captured with a high sensitivity and resolution CCD camera (Pixel-Fly-QE by PCO) and it shows a series of spatially overlapped bright tiny spots which create a richly structured pattern typical of random lasers (Fig. 2b). The spectral study performed in both mixtures shows that lasing modes have been generated at spectral location which mainly depends on the gain profile of the dye. The narrow lines (FWHM ~ 0.6 nm) are always accompanied by lateral wider modes which fluctuate shot by shot corroborating the idea of an intrinsically stochastic process. The statistics of the emission properties of our system have been studied and will be reported elsewhere. The mode selection mechanisms imply important interference effects, enhanced by the presence of the gain medium, and related to the random walk of multiple scattered light waves. The huge number of localized modes dispersed along the visible spectrum is sustained by multiple scattering processes. Soukoulis modeled a simplistic mono-dimensional dye doped random media by FDTD method, predicting that localized and extended modes are expected[13]. The former might be invoked as the only responsible of random lasing with so high quality factor of the "cavity".

Additionally, other experiments performed on dye doped liquid crystal drops controlled in diameter by means of a special syringe evidenced a richer spectrum and emphasized the mode dependence of geometry and size of the system. In conclusions, multimode random lasing in free standing liquid crystal films doped with fluorescent molecules is reported, the almost complete absence of rigid

boundaries give rise to a laser source having unique characteristics. By freely suspending these fluidic gain media on a squared plastic net realizes a new approach to study the generation of random laser light. Additionally, this approach assumes an important technological valence being a complex system but extremely easy to prepare and study. Spatially fluctuating narrow banded lasing peaks occur as the pump energy exceeds a few microJoule/pulse realizing a random laser with a relatively low lasing threshold. The threshold lowering is due to the absence of boundaries which reduce the optical losses (absorbance, guided modes).

REFERENCES

1. V.S. Letokhov, *Sov. Phys. JETP* 26, 835 (1968);

2. N.M. Lawandy, R.M. Balachandran, S.S. Gomers, and E. Sauvain, *Nature* (London) 368, 436 (1994);

3. D. S. Wiersma, M. P. van Albada, and A. Lagendijk, *Nature* (London) 373, 203 (1995);

4. H. Cao, *Waves Random Media* 13, R1 (2003);

5. M. Siddique, Li Yang, Q. Z.. Wang, R. R. Alfano, *Opt. Comm.* 117, 475 (1995);

6. R. C. Polson and Z. V. Vardeny Appl. Phys. Lett. 85, 1289 (2004);

7. H. K. Vithana, L. Asfaw, and D. L. Johnson, *Phys. Rev. Lett.* 70, 3561 (1993);

8. R. Sapienza, S. Mujumdar, C. Cheung, A. G. Yodh, D. Wiersma, *Phys. Rev. Lett.* 92, 033903 (2005);

9. S. Mujumdar, M. Ricci, R. Torre, D. Wiersma, *Phys. Rev. Lett.* 93, 053903 (2004);

10. D. R. Link, J. E. Maclennan, and N. A. Clark, *Phys. Rev. Lett.* 77, 2237 (1996);

11. E. Yariv *, R. Reisfeld, *Optical Materials* 13, 49 (1999);

12. G. Strangi, S. Ferjani, V. Barna, A. De Luca, C. Versace, N. Scaramazza and R. Bartolino, *Opt. Express* 14, 7737 (2006);

13. X. Jiang and C. M. Soukoulis *Phys. Rev. E*, 65, 025601 (2002);

FIGURE CAPTIONS

Figure 1: (Color on-line only) Experimental set-up schematic. Inset digital photo shows the dye doped sample freely suspended by means of a squared-comb PVC net.

Figure 2: (Color on-line only) a) The picture shows the lasing emission spots of the two freely suspended mixture films; b) Spatial distribution of the lasing peaks which stochastically changes for each pump pulse.

Figure 3: Lasing emission spectra for the liquid crystalline compound (BL001) doped with PM597 and PM650. For each mixture the fluorescence curves are reported together with the narrow-banded laser lines (FWHM ~ 0.6 nm).